Dynamic Behavior of Slender Footbridges Due to Human-Induced Vibrations

Sousamli Marianthi

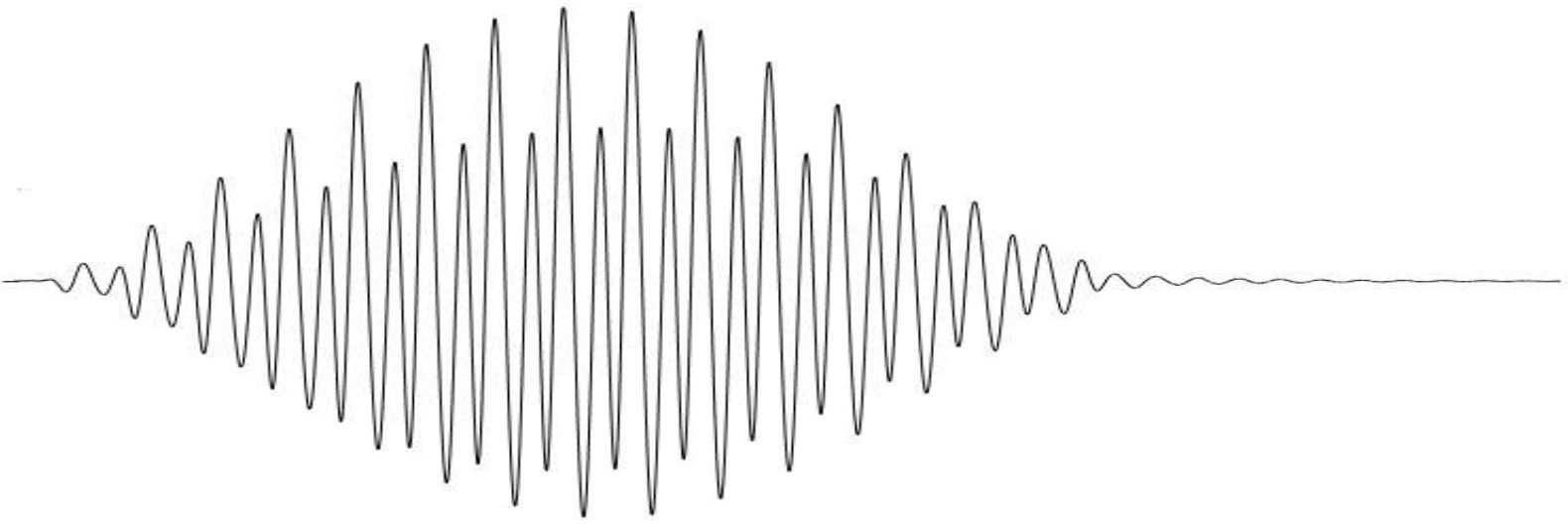

TU Delft

Gemeente Rotterdam

Dynamic Behavior of Slender Footbridges Due to Human-Induced Vibrations

Sousamli Marianthi

Supervisor:
Prof.dr.ir D.A. Hordijk - TU Delft
Dr.ir. C.B.M. Blom - TU Delft
Dr.ir. C. van der Veen - TU Delft
Dr.ir. K.N. van Dalen - TU Delft

Faculty of Civil Engineering and Geosciences
Section of Structural Engineering
&
Municipality of Rotterdam
General Department of City Development

In partial fulfillment of the requirements for the degree of
Master of Science
in Civil Engineering
Specialization: Concrete Structures
December 2016

Acknowledgements

This thesis was written as part of the Civil Engineering curriculum at the Delft University of Technology, for the master track of Structural Engineering with a specialization in Concrete Structures. The research was carried out in cooperation with Gemeente Rotterdam (Municipality of Rotterdam), at the General Department of City Development from March to December of 2016.

I would like to express my appreciation to all those who contributed in the fulfillment of my master thesis.

Firstly, I want to thank my committee and especially my daily supervisor at the Municipality of Rotterdam, Kees Blom, for providing me with the opportunity to perform my research in such a positive environment and for being always so enthusiastic about my research. The time spent talking and your guidance are irreplaceable and the feedback and comments I received always helped me to improve the quality of my work. I learned a lot from you both as a student and as an engineer and I'm very grateful for that.

A person is nothing without his friends and for that reason I would like to thank all of my friends in Delft for making these two and a half years so unforgettable. Meeting and interacting with so many people from all around the world was the greatest experience and the biggest lesson I've learned in Delft. Special thanks to my friends: Georgia, Stefanos, Arsha, Karan, Dani, Aivaras and Clara for helping me with my experiments and for being there for me throughout the year. Without you the experiments wouldn't run so smoothly and for sure they wouldn't be as fun to perform. Additionally, many thanks to my roommate Apostolis, for always being there to discuss about the progress of my research and providing me with feedback. As for my friends back home, Giorgina, Christina and Dimitris, the distance might be great but your support is always by my side.

To my big fat greek family, thank you for always believing in me, even when I would doubt or stop believing in myself. I wouldn't be the person I am today if it weren't for you. Everything I am and everything I do, I owe it to you. Finally, I would like to thank my loving César for putting up with my mood swings and complaints throughout these years and for making my days happier.

Abstract

The rapid technological breakthroughs in the engineering world have enabled the construction of slender and lightweight structures, causing a reduction in their mass and their stiffness. In bridge engineering, slender structures like this have lower frequencies and are more susceptible to human-induced vibrations. This arises concern about the level of comfort and safety that the pedestrians experience that can become a significant issue for the Serviceability Limit State (SLS) of the footbridge.

Currently, the design of the footbridges is carried out according to the modern eurocode regulations and guidelines, which propose simple load models to simulate the pedestrian loading and additionally they introduce acceleration limits to reassure that the comfort of the pedestrians is satisfied. Nonetheless, the acceleration limits proposed are unjustifiably low, with no further explanation on how they were chosen, while on the other hand the load models proposed do not cover the case of vandal loading.

From the literature study conducted it was clear that the perception of vibrations of the pedestrians is a complicated term, not easy to be measured since it is dependent on many factors, a few of which are the posture of the human body, the age and the gender of the pedestrians, the site usage of the bridge, the dynamic characteristics of the bridge and its appearance. Moreover, parameters such as the structural damping and the synchronization between the pedestrians have a great effect on the response of the structure and should be investigated in greater depth.

Due to the complexity in expressing the perception of vibrations and the discomfort of the pedestrians it was considered too conservative to incorporate in a single value of acceleration all the factors that influence the comfort limit. Therefore, it was decided to investigate which ranges of accelerations and displacements correspond to different comfort levels for active and passive pedestrians. For that reason experiments were performed on three footbridges, where the accelerations and the displacements produced due to human-induced vibrations were recorded and the pedestrians graded the level of comfort they experienced for the different experiments. These experiments were followed by the simulation of one of the tested footbridges in a Finite Element Analysis program and the application of the theoretical pedestrian load models proposed by the bibliography. The response of the structure that

was derived by the model was compared with the real response of the structure and hence it was possible to define which load models describe more accurately the cases of walking, running and jumping. Subsequently, these more realistic load models were applied on a slender footbridge from Ultra High Performance Fibre Reinforced Concrete. For the SLS the accelerations and the displacements were determined for different step frequencies and different degrees of synchronization, to examine the effect of these parameters on the final response of the structure. Furthermore, a comparison was made between the responses and the comfort classifications resulting from the application of the codes. For the Ultimate Limit State (ULS), the vandal load proposed by Bachmann is applied. The analyses performed shed light on the effect that have on the maximum developed bending moments and forces the following parameters: a) the number of people acting on the bridge, b) the degree of synchronization between the vandals, c) the degree of synchronization between the vandals and the footbridge and d) the structural damping.

The first important observation of this study is that the limits that describe the comfort of the active pedestrians are higher than the limits that correspond to the passive pedestrians, proving that standing people are more sensitive to vibrations than those moving. In addition to that, the derived limits of the maximum accelerations that describe the comfort level of the active pedestrians are higher than the equivalent limits proposed by the regulations, whereas the corresponding acceleration limits for the passive pedestrians are very similar to the limits proposed by the regulations.

Secondly, the load models proposed by Bachmann to describe the walking, running and jumping loads lead to very realistic responses of the footbridge. The proximity of the step frequency of the pedestrians to the natural frequency of the footbridge has a great effect on the response of the structure. However, even a small divergence between the step frequency of the pedestrians and the natural frequency of the bridge can reduce the amplitude of the accelerations and displacements significantly. Respectively, a small degree of asynchronism between the pedestrians leads to much lower responses.

Additionally, when it comes to the application of the vandal loading, apart from the effect of synchronization, the structural damping is playing a great role in the capacity of the structure to withstand vandal loading. Furthermore, from the experiments it was observed that the damping increases in the case of jumping (vandal loading).

Finally, it can be concluded that it is more realistic to design a footbridge by applying the theoretical load models and to verify its serviceability by comparing the maximum calculated accelerations with the derived acceleration limits for the comfort of the active pedestrians, than to design the footbridge according to the available codes and guidelines, the limits of which are more conservative.

Contents

Chapter 1

Introduction

1.1 Problem definition

As technology progresses engineers strive to build even more slender and structurally challenging structures. This is the outcome of the better understanding of the structural behavior of constructions, the use of innovative materials with improved properties and the use of more accurate design and simulation methods. As a result, the structures tend to be lighter and slenderer and to have reduced stiffness and mass. When it comes to pedestrian bridges, those traits have the nefarious effect of reducing their natural frequency. If the natural frequencies of the bridges coincide or are close to the dominant frequencies of the pedestrian-induced loads, the bridges will be prone to excessive and complex vibrations caused by the pedestrians. Therefore, in cases like this, the dynamic loading of the structure could be proven to be the governing design loading, either in order to satisfy the comfortability of the pedestrians or to prevent the collapse of the pedestrian bridge due to accidental loading, like vandal loading.

There have been several recorded cases in which pedestrian-induced loading has caused excessive resonance of the bridges, such as the Millennium bridge in London and the Solferino bridge in France. High amplitude vibrations interfere with the activities of the pedestrians and can often cause a feeling of unsafety and panic. For such reasons, a number of studies has been carried out to shed light on the behavior of slender footbridges under pedestrian loading, the human-structure interaction, the sensitivity of humans to vibrations and the comfort criteria.

The modern design codes, in their attempt to ensure the safety and the comfort of the users, have set some limits for the accelerations caused by human-induced loads. Nevertheless, the method of calculating the accelerations of the structure, the loads imposed on the structure and even the acceleration limits vary, with some codes being more conservative than others. Most of these limits were set when the construction of slender and lightweight bridges was

still a novelty and since then they have not been reviewed, with the exception of the Setra and EUR23984 recommendations. For the case of Setra and EUR23984 the acceleration limits were chosen with regard to four comfort classes following experiments conducted on Solferino footbridge and on an experimental platform. The British standards adopted the limits proposed by Blanchard, while the British National Annex for the Eurocode proposes the use of a limit that depends on parameters that influence the human perception of the vibrations, however a fixed upper limit is always set. Unfortunately, details about the conditions under which these limits were chosen, such as the type of the experiments performed to deduce the limits are not disclosed. Moreover, the proposed limits for comfort criteria are quite low. This could lead to footbridges being designed with regard to the serviceability limit state, having as a consequence larger dimensions and more expensive designs that will not take full advantage of the improved properties of the new materials and make their implementation harder and less desirable. Another limitation of the available codes is that although vandal loading is acknowledged as a dangerous source of loading that could cause serious damage to the bridge, not only at the serviceability but especially at the ultimate state, none of the codes proposes a load model to describe vandal loading neither addresses ways to overcome a possible problem.

1.2 Problem statement

In today's regulatory framework we are faced with the following problem definition:

"The available codes and guidelines for the design of footbridges under human-induced vibration are not sufficient for the design of lightweight, slender footbridges from UHPFRC. The acceleration limits proposed appear to be unjustifiably low, whereas there are no available models for vandal loading. For the promotion and broader use of new materials in structural engineering, it is of great significance the availability of better defined comfortability limits and more complete load models, that will take into consideration the human-structure interaction that appears in lightweight footbridges."

1.3 Research goal

The goal of this graduation thesis is to

1. evaluate the stringency of the comfort limits proposed by the codes and to propose new comfort limits that will correspond to the real behavior of a lightweight, slender bridge, by taking into account the human-structure interaction and the human perception of the vibrations,
2. design and perform a dynamic analysis of a lightweight footbridge from UHPFRC, in which the above findings will be implemented.

Through this thesis the following research questions will be investigated:

1. Are the recommended acceleration limits conservative?
2. Should more factors be taken into account during the definition of these limits, and if so which factors?
3. How do pedestrians perceive and interpret the accelerations? Are the accelerations they feel the same as the ones affecting the bridge?
4. Since standing, walking or jogging influences the perception of vibrations, should the design criteria be based on the comfort levels of people standing, walking or jogging?
5. Are there cases when the acceleration limits might be exceeded but the pedestrians do not feel discomfort?

6. How should the vandal loading be confronted? What is an appropriate way to model it? And, should the comfort limits for vandal loading (that is an extreme load) remain the same as for walking (or running), or be more flexible and mainly guarantee the safety of the structure and the humans and not the comfort criteria?

7. Is measuring the acceleration the ideal way to assess the comfort limits? Could the displacement be a complementary way of evaluation?

1.4 Report outline

The work developed during this project as an internship in the Municipality of Rotterdam, is presented in the following chapters. In chapter 2 an overview of the literature concerning the dynamic behavior of pedestrian footbridges due to pedestrian loading, the comfort limits and the load models proposed by the codes is presented. Chapter 3 is about the properties of Ultra High Performance Fibre Reinforced Concrete (UHPFRC), a relatively new material that is used in the design of slender and lightweight structures. Chapter 4 describes the tests performed to re-define the comfort and safety limits with respect to accelerations and displacements as perceived by the pedestrians. Chapter 5 compares the measured dynamic response of a tested footbridge with the dynamic response that results from the application of pedestrian loads on the Finite Element Model of the fore-mentioned footbridge. Finally, in chapters 6 and 7 the dynamic behavior of a slender footbridge from UHPFRC is described, according not only to the available codes and guidelines for the serviceability limit state, but also according to some more realistic load models both for the serviceability limit state and the ultimate limit state (due to vandal loading). The conclusions and the recommendations of this research are summarized in chapter 8.

Chapter 2

Dynamic of Footbridges

2.1 Equation of motion of structures

A bridge that is under a dynamic load can be described as an oscillator. An oscillator consists of a mass m, a spring k that provides stiffness to the system and a viscous damper c that dissipates vibrational energy of the system. The equation of motion of such a single degree of freedom system is given by equation 2.1:

$$m\ddot{u}(t) + c\dot{u}(t) + ku(t) = F(t) \tag{2.1}$$

where *u(t)* is the relative displacement or deformation of the structure and *F(t)* is the dynamic load acting on the structure, that may consist of a harmonic excitation, a pulse or a random vibration [12].

For multiple degrees of freedom systems (MDOF), the equation of motion now takes the form of 2.2:

$$\mathbf{M}\ddot{u}(t) + \mathbf{C}\dot{u}(t) + \mathbf{K}u(t) = \mathbf{F}(t) \tag{2.2}$$

Where $\boldsymbol{M}$, $\boldsymbol{K}$ and $\boldsymbol{C}$ are the mass, stiffness and damping matrices respectively. These matrices are of order $n \times n$ where n is the number of degrees of freedom of the structure. The acceleration $\ddot{u}(t)$, velocity $\dot{u}(t)$ and displacement *u(t)* , as well as the external load $\boldsymbol{F(t)}$ are vectors with dimensions $n \times 1$. Usually, the mass and the stiffness matrices are calculated by the Finite Element Method (FEM). This implies that a real structure is discretized in smaller elements that are interconnected at a finite number of nodes. Each one of those elements has its own stiffness and mass matrices, which combined in the proper way lead from the local matrices to the global mass and stiffness matrices [55]. The system of equations given by 2.5 is coupled and the most common and easy way to uncouple them is to apply the

modal analysis. In that way it is possible to get uncoupled equations such that each equation describes a *SDOF* system, with its own modal mass and stiffness. By solving these *SDOF* equations the modes of a structure and its eigen frequencies can be found.

2.1.1 Influencing Parameters

Mass

Mass is dependent on the geometry of the structure (cross sectional area A) and on the material properties (the mass density ρ) and is often expressed as mass over length *[kg/m]*.

Stiffness

Stiffness depends on the geometry of the structure (moment of inertia I and length of members l) and on the material properties (modulus of elasticity E). The stiffness is strongly influenced by the boundary conditions of the structure, but the influence they have on the stiffness other uncertain parameters should also be considered. Such parameters are: the non-structural elements (e.g. handrails), the dynamic modulus of elasticity of concrete, as well as the stiffness of a cracked concrete cross section and the stiffness of the supports [55].

Damping

As it has been already stated, the damping represents the energy dissipation of a structure [12]. The loss of energy during the motion is mostly caused by three main sources: nonlinearity of members, energy radiation and inherent damping [3]. In-structure damping consists mainly of three categories:

- Material-Internal damping
  This type of damping originates from energy dissipation that is caused by a complex molecular interaction within the material. Consequently, material damping depends in the type of the material, the manufacturing methods and the final finishing processes.[28] Some resulting defects caused by the micro-structural interaction are: dislocations in the grain lamina, grain boundaries and thermal effects caused locally by temperature gradients. [40]

- Structural damping
  Structural damping is caused mainly from rubbing friction or contact among the different components of a structure. The most important form of structural damping is

the slip damping, that is caused by Coulomb friction at a structural joint and depends on the surface properties and the joint forces [33]. Usually, the structural damping of a fully built up system is found to be larger than the material damping, at least by an order of magnitude. [40].

- Fluid viscous damping
  This emerges from the drag force that is created by the relative motion between a fluid and the material that is immersed into that fluid. [33]

In general, it is quite hard to model mathematically the damping mechanisms of the structure. The most commonly used damping model is the viscous damping because of its simplicity. For MDOF systems, viscous damping is usually expressed in its modal form by using the damping ratios ζ, that are defined individually for each mode [55]. More information about the way the damping matrix of MDOF systems is formed, can be found in Appendix C.

Natural frequencies and natural modes of vibration

Each characteristic deflected shape in which the structure vibrates is called a natural mode of vibration of the system [12]. The natural frequency f_n of a natural mode n of a system is the number of cycles of simple harmonic motion that occur during a time period equal to one second. By knowing the natural frequencies of a footbridge, it can be evaluated if the footbridge will be susceptible to human-induced-vibrations or not. The natural frequencies of a pedestrian bridge, with a constant mass and stiffness over the bridge length, can be calculated by the equation 2.3

$$f_n = \frac{1}{2\pi}\sqrt{\frac{K_n^*}{M_n^*}} = \frac{C}{2\pi}\sqrt{\frac{EI}{\rho A L^4}} \tag{2.3}$$

Where K_n^* and M_n^* are the modal stiffness and modal mass respectively and factor C represents the support conditions of the structure. Figure 2.1 presents the five lowest principal modes of a beam with constant $\frac{EI}{\rho A}$ for different boundary conditions [48].

2.2 Pedestrian-induced vibrations

The vibrations produced by human-induced loads are usually a serviceability rather than a safety issue. The reason behind this is the ability of the human body to sense vibrations with amplitudes of displacements as low as 0.001mm. Nevertheless, the reaction to vibrations

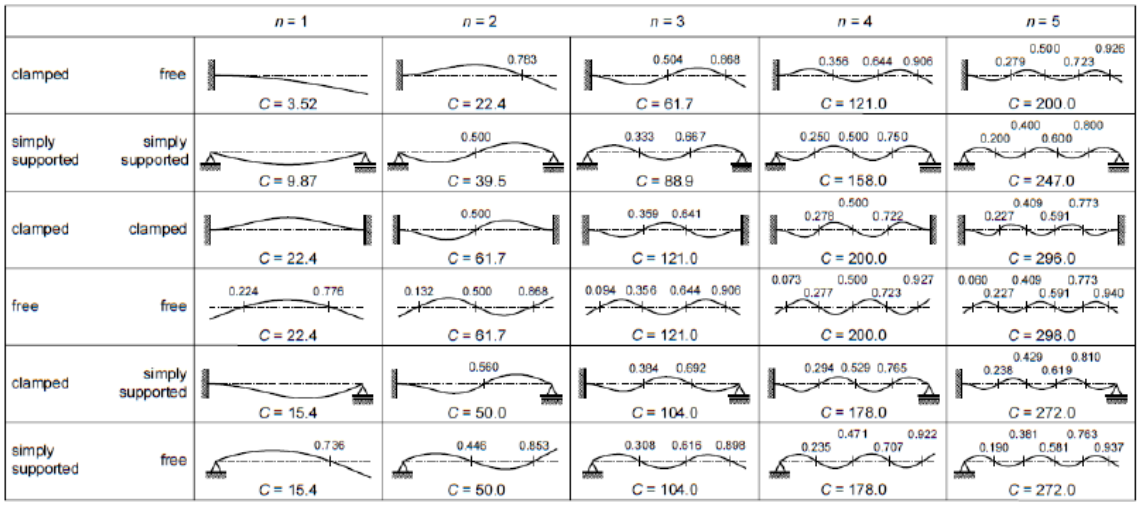

Figure 2.1 Natural modes of beams with different supports. [48]

depends a lot on the circumstances and on personal attitudes [6]. This high sensitivity makes the problem of the vibration serviceability critical much before the vibration levels are sufficiently strong to cause damage of the structure itself. [55]. The human-induced dynamic loading can be categorized in 5 categories: 1) walking, 2) running, 3) vandal loading, 4) crowd loading and 5) special events. The forces that act on the footbridge due to the pedestrian's actions are described below.

2.2.1 Types of human-induced loading

Single pedestrian loading walking

When walking, a pedestrian produces a dynamic force that varies with time and that has components in all three directions: vertical, horizontal-longitudinal and horizontal-lateral [55].The vertical component is up to 40% of the body weight, while the longitudinal and lateral are considerably smaller. [43]. In Figure 2.2 are presented the shapes of the walking forces in the 3 dimensions as they were calculated by Andriacchi et all. It was also observed that increasing walking velocity led to an increasing step length and peak force magnitude, which means that the dynamic effect of the forces was dependent on the walking speed [4].

The vertical walking force has the shape of a saddle, two peaks and a trough. The first peak represents the effect of the footfall, (i.e. the heel touching the ground) and the second peak represents the push off. It should be noted that while walking at least one foot is in contact with the ground, while there is also observed an overlap due to the period of time that both the feet are on the ground (during the lifting of the toe of the one foot, the heel of

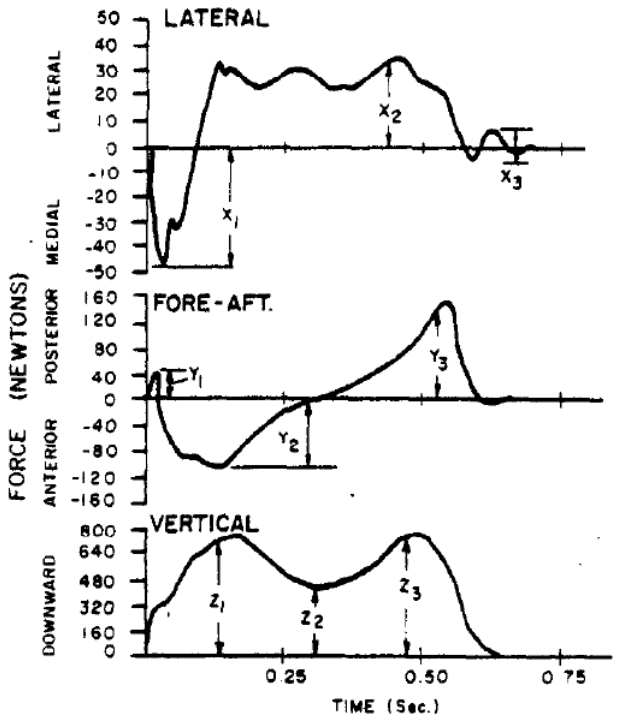

Figure 2.2 Illustration of the walking force in lateral (top), longitudinal (middle) and vertical (bottom) direction. [4]

the other foot touches the ground), as can be seen on Figure 2.3 [22]. In Figure 2.4 different types of human activities and their typical force patterns are presented [52]. It can easily be observed that the amplitude of the force in the case of slow walk and brisk walk is higher than for normal walk and it is maximum in the case of running.
The walking frequency of pedestrians has been found to be between 1.7-2.3 Hz according to Leonard and in between 1.6-2.4 Hz according to Bachmann et al. [30] [7]

In order to apply the measured dynamic forces in the design it is necessary to model them analytically. There are two types of such models, time-domain and frequency-domain and they are both quite complicated to model since the forces that are about to be modelled are influenced by many parameters like the variability in time and space, the number of persons and the degree of synchronization and the interaction between the pedestrians and the structure [55].

- Time domain force models
  Time domain models are used more frequently and they can be either deterministic or probabilistic. The deterministic model aims to establish one general force model for each type of human activity, whereas the probabilistic model intends to take into account also other influencing parameters, like the body weight of the pedestrians and

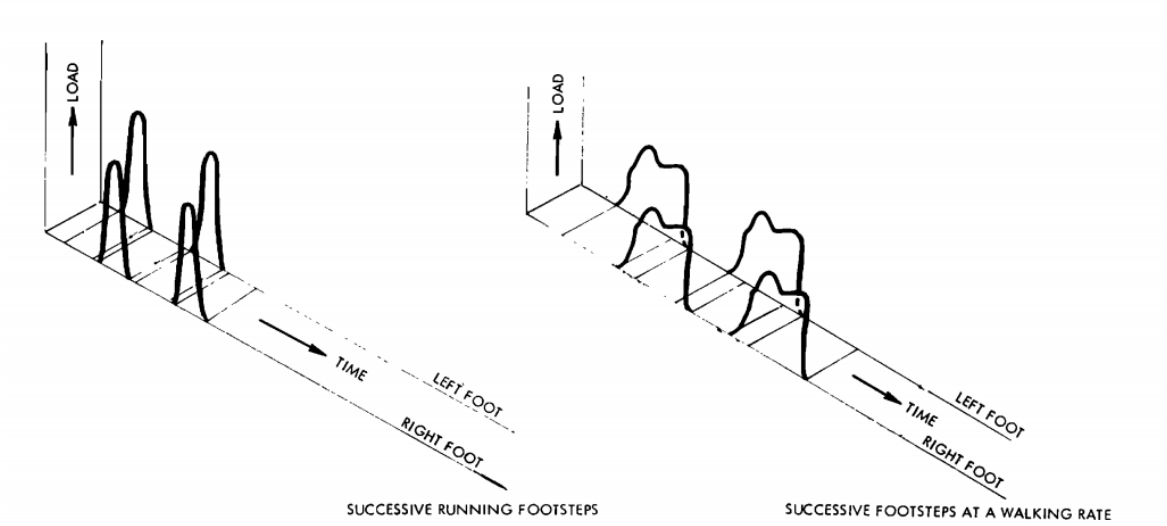

Figure 2.3 : Typical pattern of combination of successive footsteps for running and walking. [22]

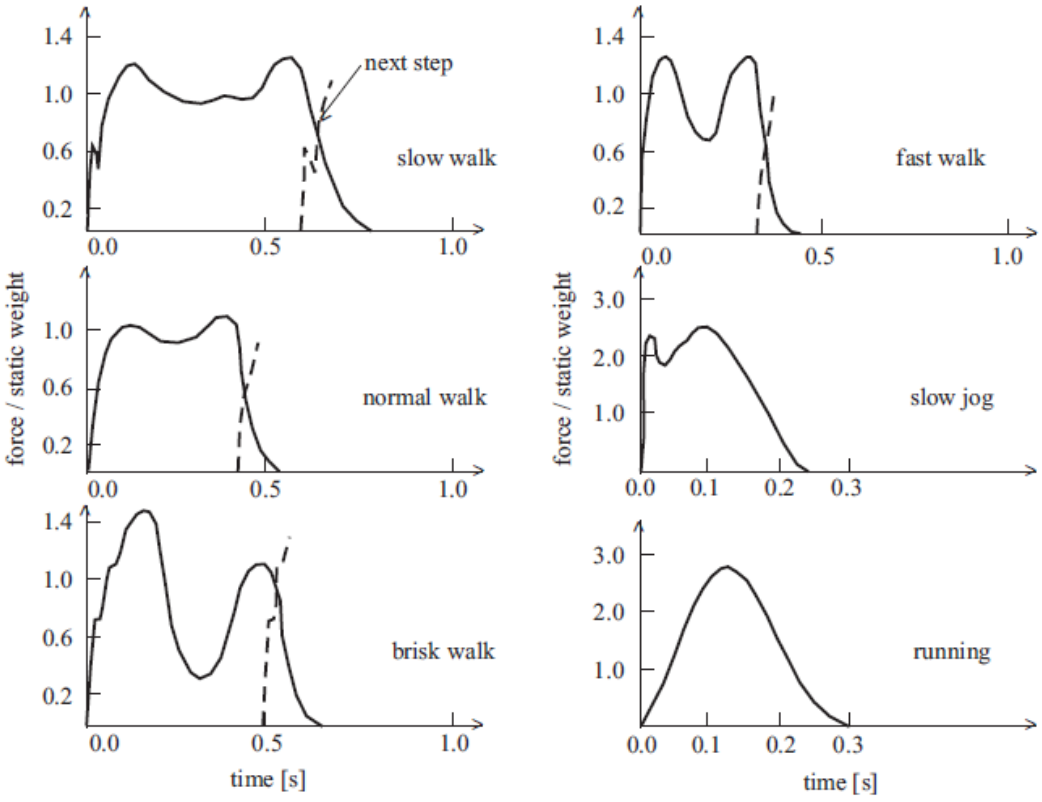

Figure 2.4 Typical patterns for vertical force for different types of human activities [52]

the different frequencies in each activity, as random variables. In both cases however, it is considered that both the left and the right feet produce the same force and the force produced is periodic.

- Deterministic force models
  A periodic force $F_p(t)$ with a frequency f_p can be represented by a Fourier series:

$$F_p(t) = G + \sum_{i=1}^{n} G\alpha_i \sin(2\pi f_p t - \phi_i) \tag{2.4}$$

  where G is the weight of the pedestrian (N) , i is the number of the order of the harmonic, α_i is the Fourier coefficient of the harmonic (a dynamics load factor), f_p is the frequency of the activity (Hz) , ϕ_i is the phase shift of the i^th harmonic and n is the total number of contributing harmonics. Živanović et al gathered the Dynamic Load Factors (DLF) proposed by many researches for different types of activities in a table 2.1.

- Probabilistic force models
  According to a probabilistic model, the force of a single pedestrian, even though it is periodic, is taking into account the randomness, that is inserted in the analysis through probability distributions of the pedestrian's weight, the pace of walking, the time delay between the different people walking and so on.

Running loads

The running load differs from the walking load in a number of things. Firstly, the frequency of running is higher than the walking frequency, and according to Bachmann et al. ranges between 2-3.5 Hz. Secondly, as it can be observed in Figure 2.2, there is a time that the jogger isn't in contact with the ground, consequently there is no step overlap as in the case of walking. Finally, the force induced by joggers has a higher amplitude than the force induced by walkers. Usually, Equation 2.4 is also adopted for running loads by most of the code proposals and researches. However, it does not take into account the discontinuous nature of the running load. In their study, Occhiuzzi et all, propose a different running model that takes into account the no contact period [35]. A comparison of the widely used model and the proposed model can be seen in Figure 2.5, where the thin line represents the load proposed by Bachmann and the thick line the model proposed by Occhiuzzi.

For the formation of the analytical model, each period T is divided into a contact period (Δt_c) and a no contact period (Δt_{nc}). For an ordinary running activity, it can be assumed

Table 2.1 : DLFs for single person force models after different authors [55]

Author(s)	DLFs for considered harmonics	Comment	Type of activity and its direction
Blanchard et al. [34]	$\alpha_1 = 0.257$	DLF is lessen for frequencies from 4 to 5 Hz	Walking—vertical
Bachmann and Ammann [14]	$\alpha_1 = 0.4 - 0.5$ $\alpha_2 = \alpha_3 = 0.1$	Between 2.0 and 2.4 Hz At approximately 2.0 Hz	Walking—vertical
Schulze (after Bachmann and Ammann [14])	$\alpha_1 = 0.37$, $\alpha_2 = 0.10$, $\alpha_3 = 0.12$, $\alpha_4 = 0.04$, $\alpha_5 = 0.08$	At 2.0 Hz	Walking—vertical
	$\alpha_1 = 0.039$, $\alpha_2 = 0.01$, $\alpha_3 = 0.043$, $\alpha_4 = 0.012$, $\alpha_5 = 0.015$	At 2.0 Hz	Walking—lateral
	$\alpha_{1/2} = 0.037$, $\alpha_1 = 0.204$, $\alpha_{3/2} = 0.026$, $\alpha_2 = 0.083$, $\alpha_{5/2} = 0.024$	At 2.0 Hz	Walking—longitudinal
Rainer et al. [42]	α_1, α_2, α_3 and α_4	DLFs are frequency dependent (Fig. 10)	Walking, running, jumping—vertical
Bachmann et al. [48]	$\alpha_1 = 0.4/0.5$, $\alpha_2 = \alpha_3 = 0.1/-$	At 2.0/2.4 Hz	Walking—vertical
	$\alpha_1 = \alpha_3 = 0.1$	At 2.0 Hz	Walking—lateral
	$\alpha_{1/2} = 0.1$, $\alpha_1 = 0.2$ $\alpha_2 = 0.1$	At 2.0 Hz	Walking—longitudinal
	$\alpha_1 = 1.6, \alpha_2 = 0.7$, $\alpha_3 = 0.2$	At 2.0–3.0 Hz	Running—vertical
Kerr [36]	α_1, $\alpha_2 = 0.07$, $\alpha_3 \approx 0.06$	$\alpha_1$is frequency dependent (Fig. 11)	Walking—vertical
Young [56]	$\alpha_1 = 0.37(f - 0.95) \leqslant 0.5$ $\alpha_2 = 0.054 + 0.0044f$ $\alpha_3 = 0.026 + 0.0050f$ $\alpha_4 = 0.010 + 0.0051f$	These are mean values for DLFs	Walking—vertical
Bachmann et al. [48]	$\alpha_1 = 1.8/1.7$, $\alpha_2 = 1.3/1.1$, $\alpha_3 = 0.7/0.5$	Normal jump at 2.0/3.0 Hz	Jumping—vertical
	$\alpha_1 = 1.9/1.8$, $\alpha_2 = 1.6/1.3$, $\alpha_3 = 1.1/0.8$	High jump at 2.0/3.0 Hz	Jumping—vertical
	$\alpha_1 = 0.17/0.38$, $\alpha_2 = 0.10/0.12$, $\alpha_3 = 0.04/0.02$	At 1.6/2.4 Hz	Bouncing—vertical
	$\alpha_1 = 0.5$	At 0.6 Hz	Body swaying while standing—lateral
Yao et al. [52]	$\alpha_1 = 0.7$, $\alpha_2 = 0.25$	Free bouncing on a flexible platform with natural frequency of 2.0 Hz	Bouncing—vertical

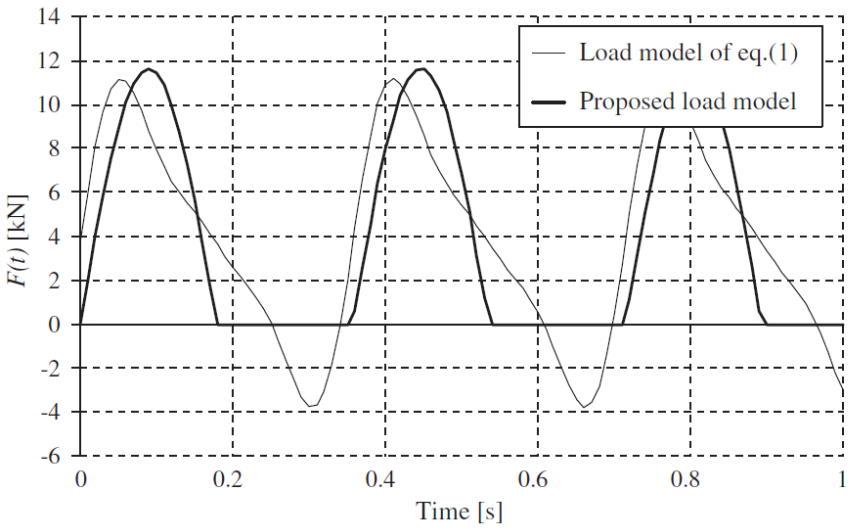

Figure 2.5 Comparison of running load models for joggers [35]

that the contact and no contact periods are equal to half the period $(\Delta t_c = \Delta t_{nc} = T/2)$. However, in general if (Δt_c) is expressed as $\Delta t_c = kT$ for $k < 1$, then the no contact time will be expressed as $\Delta t_{nc} = (1-k)T$. The vertical component of the jogging load is given by Equation 2.5 [35].

$$\begin{aligned} F(t) &= Amg\sin(\frac{\pi f}{k}t) \quad for \quad iT < t \leq (i+k)T \\ F(t) &= 0 \qquad\quad for \quad (i+k)T < t \leq (i+1)T \end{aligned} \tag{2.5}$$

where i represents the step number and A is an amplification factor, similar to the DLF of Equation 2.4, that is given by $A = \frac{\pi}{2k}$.

Vandal loading

As quoted by Schwartz et all: "Vandalism is coined as a specific kind of footbridge loading characterized by the intentional and well-coordinated action of one or several persons, moving their own body with the sole aim to increase the structural vibration level to a maximum value" [46]. There is a number of induced vibrations that can deliberately cause excitation to resonance of a pedestrian bridge: vertical bending, lateral or torsional. The easiest way to induce resonance through vertical vibrations is jumping. Another way is bobbing (i.e. bending-knees excitation). In that case, both the feet of the pedestrian are in contact with the ground and the amplitude of the induced force is generally lower than in the case of jumping. However, the degree of synchronization among a group of pedestrians is higher for

bobbing [9]. Another mean of vandal loading can be considered to be swaying of the body, that causes mostly lateral vibrations. Jumping forces can be modeled by using the Fourier series in a similar way as the running loads, with the difference that the jumping loads don't move across the structure. Like in the case of running, during one cycle of jumping there is a period that the feet are in contact with the structure and a period that there is no contact [55]. According to Bachmann et al. jumping requires more harmonics in order to be described accurately, in comparison with walking [6] The DLF and the frequencies that are given by many researches can be found in Table 2.1.

Crowd loading

A crowd is considered as a group of randomly walking pedestrians, each one having his own pace, velocity, weight and phase. The force that acts on the bridge due to the group of pedestrians is not equal to the number of pedestrians multiplied by the load of a single pedestrian, but the amplitude of the force is usually reduced by a factor that takes into account the synchronization between the pedestrians. This reduction factor is usually expressed as an equivalent number of people and its expression varies for the different codes and for different authors. For example, according to Matsumoto this factor is taken as $\sqrt{N}$, where N is the number of pedestrians [34].

When in large crowds, the people can adjust their walking behavior in accordance with the movement of the other pedestrians, a fact more probable to happen in denser crowds. By changing their velocity and walking frequency, in addition to the synchronization of the pedestrians among themselves, there can be also synchronization with the bridge vibrations, this is called lock-in effect and is a a phenomenon noticed mostly in the lateral direction. Synchronization between the crowd and the bridge movement is much less likely [[55],[54]. According to Bachmann and Ammann however, vertical synchronization could occur for amplitudes larger than 10mm [6].

Special events

Special events are another type of crowd loading that is expected to occur on footbridges. Usually, these events occur only a few times during the lifespan of a bridge. Such events might be the inauguration of a new bridge, a marathon, a parade, etc. In these cases, the crowd is expected to be denser than usual and the synchronization of the pedestrians can also be triggered by external incentives, like music. It is very probable that panic and anxiety could occur due to the extensive vibrations of the bridge [42].

2.2.2 Human-Structure Interaction (HSI)

When designing slender structures occupied by people and dynamically excited by them, the term of human-structure-interaction arises, to refer to the effect that human activities have on the motion of the bridge and how the pedestrians are affected by this motion of the bridge. In the past, the interaction was neglected, but as structures become more slender it is becoming more common than not, to not be neglected. There are two main aspects of this phenomenon. The first one is the change that is observed in the dynamic properties of the pedestrian bridge, due to the presence of humans. The change in the dynamic properties often includes a slight decrease of the natural frequency of the footbridge and/or an increase if the damping [55]. The second aspect concerns the human-structure synchronization in the vertical and lateral direction. If a certain critical value of the amplitude of the vibration is exceeded, the pedestrians are affected by the motion of the footbridge and tend to adjust their walking frequency and phase, resulting in a synchronization between the walking of the pedestrians and the motion of the structure [41].

The human-structure interaction has its origins on the contact between the structure and the humans. When the crowd is active (jumping, running, walking) the contact is not maintained. Consequently, only the passive humans or those in contact with the structure interact with it. The effects of the human-structure interaction are more frequent in long span, unsupported structures of lightweight material, that have low range of natural frequencies [44].

Dynamic properties of footbridges due to human-structure interaction

The presence of a stationary (standing or sitting) person, influences the dynamic properties of the occupied structure, with the most important outcome being the increase in the damping of the human-structure-dynamic system in comparison with the damping of an empty structure. This effect is amplified with the presence of more people. It can, consequently, be concluded that the human body behaves like a damped dynamic system attached to the main structural system. According to biomechanics, humans can be treated as a system of actuators and dampers [55] [41]. In this section, the studies performed by many researchers about the effects of human-structure interaction on the dynamic properties of footbridges will be presented.

In their study Georgakis and Jørgensen [23] tried to evaluate the change in mass and damping of vertically vibrating footbridges due to pedestrians. By exciting initially an empty footbridge, they determined its characteristics (eigenmodes, frequencies, modal mass and damping). Next, a hydraulic actuator was attached at the midspan of the footbridge in order

to ensure the frequency and amplitude-controlled excitation, without changing the dynamic properties of the bridge. After that, pedestrians were asked to walk on the bridge with varying flow rates. The observed frequency shift was attributed to the change of the structural mass and/or a change in the damping.
The new modal mass due to the traversing pedestrians is found to be:

$$m' = m\frac{\omega_D^2(1-\xi'^2)}{\omega_D'^2(1-\xi^2)} \tag{2.6}$$

where m is the modal mass of the empty bridge,ω_D and ω_D' are the damped circular frequencies of the empty bridge and of the occupied bridge respectively and ξ and ξ' are the viscous damping of the empty and occupied bridge respectively, for the first eigenmode.
The modified footbridge damping, is then found as:

$$\xi' = \frac{E_D}{2\pi m'\omega_D' X^2} \tag{2.7}$$

where $E_D = \int_0^T F(t)v(t)dt$ is the energy dissipated per cycle by the footbridge, expressed as a function of the load imparted by the actuator and the velocity of the pedestrian bridge where the load is applied, and X is the maximum displacement at the mid-span. It is obvious that in order to calculate the modified modal mass of the footbridge, an iterative approach need to be applied [23].

From the experiments held by Georgakis and Jørgensen, it was found that both the modal frequency and the damping were dependent of the vibration amplitude. When it comes to the first natural frequency, the larger the displacement, the smaller the frequency, whereas the damping increased with increasing amplitude up to a certain displacement (5mm) and then it started decreasing again but in a slower rate. It was also found that the average added mass per pedestrian is 102% of the pedestrian's mass. Finally, it was observed that the damping of the pedestrians diminishes for increasing amplitude of vibration, which indicates that there is a modification in the way the pedestrians interact with a footbridge for higher vibrations [23].

Another similar study was performed by Pedersen [38] in order to evaluate the damping effect of humans in the structures. However, instead of using a mechanical device to excite the floor, he measured the accelerations that were produced by the rhythmic activities of active humans, in the case of a floor with and without passive humans. The experiments showed that the presence of passive persons with a total mass equal to only 0.4% of the modal mass of the floor and positioned close to the midpoint of the floor resulted in reduced acceleration levels generated by the jumping of the active humans, by 55%. When comparing the experimental results with the theoretical results, it was noticed that the damping effect of humans suggested by the experimental results was much higher than the one found by the

theoretical model. The most probable explanation for this seems to be the inability of humans to maintain the same excitation during the performed test. It is suggested that "a short period of off-resonant excitation could bring down acceleration levels, and optimal synchronization between jumpers might have failed, during some sequences of the test." Another factor that is also questioned is the effect of the visual contact between the passive and active humans. It is observed that when less passive humans were present, the coordination of the jumpers was improved and higher accelerations were reached [38].
Capellini et al. [10] performed an experimental and numerical study on the effect of humans on the modal parameters of a structure. By experiments on a steel staircase, it was observed a small decrease of the frequency when the staircase was occupied by people. Moreover, the damping ratio in the cases of the occupied staircase was higher than in the case of an empty stair, by 4 times for 40 people and 2 times for 20 people. It is worth mentioning that the biggest change was noticed in the first and second modes [10].

A full-scale measurement system was used by Zuo et al. to monitor the vibrations of a full-scale bridge due to pedestrian excitation. The measurements taken while the bridge was empty and those taken when it was occupied by a crowd of pedestrians were analyzed and their results showed that indeed the walking pedestrians on the bridge affect the vibration frequency of the bridge by adding mass to the system and that a significant level of synchronization of the pedestrian footfalls is achieved when the bridge is packed with pedestrians, something that leads to noteworthy vibrations [56].

Experiments conducted by Salyards & Firman [44] to investigate the effects of the crowd characteristics to the human-structure interaction, confirmed that an increasing crowd size and its corresponding mass ratio decrease the natural frequency of the combined structure and cause an increase in the system's damping ratio.
Regarding the effects of the posture of the human body, three different postures were examined: standing with straight knees, standing with bending knees and sitting. It was observed that the standing crowd with straight knees had a bigger impact on the natural frequency, followed by the seated crowd that also had a notable decrease in the natural frequency. When it comes to the effect of the postures on the damping of the system, it was noticed that the damping of the combined system was approximately 20 times higher when the structure was occupied by crowds standing with straight knees or sitting, while the bending knees posture had a less significant increase in the damping [44].

On a research performed later, it was observed that the passive human has indeed a mitigating effect on the structural vibrations. However, "the damping effect of a passive person on structural vibrations" is not a unique property but it depends on the acceleration

properties that are chosen for consideration. In addition to this, a walking pedestrian and a standing person, will not perceive the same accelerations at their feet [39].

When it comes to the walking pedestrians, an interaction model was developed by Qin et al. to shed light on the influence the structural vibrations have on the walking behavior of the pedestrian and the way the pedestrian responds to those vibrations to maintain a steady pace. It was concluded that the leg stiffness has a notable effect on the dynamic response of the structure, when the step frequency is close to the natural frequency of the structure. Moreover, it was found that when the attach angle of the foot increases, the peak accelerations of the footbridge decrease and that the human-structure dynamic interaction increases with an increasing vibration level of the structure. The latter was observed by the increase in the interacting force between the human and the structure while the pedestrian was reaching the mid-span of the footbridge. The reason behind that is that at the mid-span the acceleration and displacement is much larger and therefore more external energy should be input to maintain steady walking [41].

An extensive study on the human-structure dynamic interaction was performed on 3 footbridges by Živanović et al. In all cases it was observed an inability of the pedestrian to keep walking on a steady pace while feeling strong vibrations. This phenomenon applies both to the case of walking with the help of a metronome and walking freely. Due to this effect, there were differences between the amplitudes of the simulated models and the measured amplitudes of the real bridges. The differences were even larger in the case of walking without metronome since in that case it is easier to lose a steady step. "The time instant when differences in the simulated and measured responses start occurring was adopted as the moment when a pedestrian loses his steady step during walking." The level of vibration felt by the pedestrian in that moment, named "disturbing vibration level", can then be calculated in terms of accelerations. This level was found to be approximately 50% lower than the recommended values of the British footbridge design code. In order to take into account the inability to maintain a steady step, either footbridge damping can be increased while keeping constant harmonic excitation force, or the harmonic force should be modified while keeping the damping constant [54].

Synchronization between pedestrians

The phenomenon of synchronization between pedestrians depends on a great degree on the density of the crowd occupying footbridge. When the density of the crowd walking on a bridge deck is low, the pedestrians are free to walk in their own pace, without any obstacles that could modify their walking gait. However, when the crowd becomes denser, the humans need to adjust their walking frequency and velocity according to the surroundings. Hence, the

velocity of the pedestrians decreases with increasing density. At a density of approximately 0.6 person per m^2 walking starts feeling more obstructed, whereas at a density of 1 person per m^2 the motion of the pedestrians is highly impeded. When, finally, density reaches a level of 1.5 people per m^2, moving independently becomes almost elusive and the behavior of the pedestrians is dependent on the rest occupants of the bridge [43]. Therefore, synchronization between the pedestrians is more likely to occur at bigger crowd densities.

An interesting experiment on the effects that sensory stimuli have on the dynamic load induced by people bouncing showed that audio, visual and tactile stimuli have a positive impact on the synchronization between two people bouncing. Moreover, in the case of audio stimuli, the synchronization improves when the distance between the people decreases and therefore there is a greater possibility to have eye-contact and touch each other. For the set of the experiments conducted by Vitomir et al., the best synchronization was achieved for bouncing at 2 Hz, probably because of the smaller energy consumption needed for bouncing on this rate in comparison with bouncing slower or faster [50].

Synchronization between pedestrians and bridge

Synchronization between pedestrians and bridge can occur either in the lateral direction, or in the vertical direction. Most of the cases reported concern synchronization in the lateral direction. Usually the synchronization between the pedestrians and the structure happens simultaneously with the synchronization among the pedestrians and this leads to an increase in the response of the structure, also known as lock-in effect. Factors that influence the synchronization between the crowd and the structure are: the density and the velocity of the crowd, the walking frequency, the effective force per person in a crowd as a function of the frequency and of the amplitude of the vibrations of the bridge [55].

- **Lateral synchronization** After the Millennium bridge incident, many studies were performed to define the causes of the lock-in effect. A description of the loading effect noted that " chance footfall correlation, combined with the synchronization that occurs naturally within a crowd, may cause the bridge to start to sway horizontally". If the horizontal swaying is noticeable by the pedestrians, they start to adjust their walking pace and synchronize with the swaying of the bridge, since this makes easier the prediction of the movement of the bridge and the maintenance of their lateral balance. However, this behavior ensures that the walking loads are applied at a resonant frequency of the bridge and with such a phase that has as a consequence the increase of the amplitude of the motion and the increase of the imposed lateral force of the pedestrians [14]. The pedestrian-induced force is therefore modeled as the

Table 2.2 : Comparison of the enhancement factors proposed by different authors (taken by [Caprani and Fanning])

Author	Enhancement factor m	Structural frequency f Hz	Crowd density people/m^2
Matsumoto et al.	$m = \sqrt{N}$ $m_{min} = 2.0$	$1.8 - 2.2$ $1.6 - 1.8\&2.2 - 2.4$	
Bachmann&Ammann [6]	$m = \sqrt{N}$	2	0.55
Grundmann et al.	$m = 0.135N$	$1.5 - 2.5$	0.44
Fujino et al.	$m = 0.2N$	2	2.11
EC5 [17]	$m = 0.23N$	$1.5 - 2.5$	0.6

source of negative damping to the lateral motion of the bridge and a critical number of pedestrians may be found, above which the cumulative negative damping force of the pedestrians exceeds the inherent damping of the bridge [21]. The critical number of pedestrians is given by the following equation:

$$N_{cr} = \frac{8\pi\zeta\omega_1 m_1}{k} \tag{2.8}$$

Where ζ is the damping ratio, ω_1 is the first transverse natural frequency, m_1 is the modal mass and k is the lateral walking force proportionality factor.

- **Vertical synchronization** Most of the existing literature proposes the use of enhancement factors in order to model the crowd loads of pedestrians that synchronize and can cause excessive vertical vibrations. However, the factors proposed from the available literature are given for specific synchronization proportions, crowd densities and bridge frequencies.

2.3 Codes and Guidelines

2.3.1 Eurocodes

In Eurocode reference for the design of footbridges is made in EN 1990, EN 1991 and EN 1995 for timber structures.

Eurocode 0 (EN 1990)

Verifications regarding vibrations for footbridges due to pedestrian traffic are given in the National Annex A2 part A2.4.3 of Eurocode 0. It is mentioned that:

- The design situations should be selected according to pedestrian traffic to be admitted on the individual footbridge during its design lifetime.
- The presence of a group of approximately 8 to 15 people walking normally should be considered for design situations considered as persistent. The number of the group members depends on the area of the deck.
- Other traffic categories should be specified when needed, depending on the deck area that can be either permanent, transient or accidental. These loads include:
  - The presence of streams of pedestrians (considerably more than 15 persons).
  - Choreographic or festive events, happening occasional.

When it comes to the serviceability, EN1990 suggests that "the comfort criteria should be defined in terms of maximum acceptable acceleration of any part of the deck [1]." The maximum recommended values given, are:

- $0.7 m/s^2$ for vertical vibrations.
- $0.2 m/s^2$ for horizontal vibrations due to normal use.
- $0.4 m/s^2$ in case of exceptional crowd conditions.

Moreover, it is proposed that "a verification of the comfort criteria should be performed if the fundamental frequency of the deck is less than:

- 5 Hz for vertical vibrations
- 2.5 Hz for lateral and torsional vibrations."

Eurocode 1 (EN 1991)

In Chapter 5.7 of EN 1991 more information is given regarding the dynamic models of pedestrian loads [16].
More specifically it is asked to:

- Determine the relevant natural frequencies (corresponding to vertical, lateral, torsional vibrations) of the main structure of the bridge deck through an appropriate structural model and taking into account the dynamic characteristics of the structure (mass, stiffness).

- Take into account in the limit state of verifications the forces induced by pedestrians with a frequency equal to the natural frequency of the bridge that may cause resonance. It is proposed by the code, that a pedestrian normally walking exerts on the bridge periodic forces, with:
  - Frequency range between 1-3 Hz, in the vertical direction
  - Frequency range between 0.5-1.5 Hz, in the horizontal direction
  - Frequency equal to 3 Hz in case of groups of joggers
- Define appropriate dynamic models of the pedestrian loads and comfort criteria.

However specific dynamic loads are not proposed but are left to be determined by the National Annexes of each country.

Eurocode 5 (EN 1995)

Information about vibrations caused by pedestrians is given on Annex B of EN 1005. The rules given, apply to timber bridges with simply supported beams or truss systems excited by pedestrians. Regarding the vertical vibrations, the comfort criteria of Eurocode 0 should be satisfied and formulas are proposed for the calculation of the maximum accelerations for 3 different load cases [17]:

- For a single person crossing the bridge:

$$a_{vert,1} = \begin{cases} \dfrac{200}{M\zeta} & \text{for } f_{vert} \leq 2.5Hz \\ \dfrac{100}{M\zeta} & \text{for } 2.5Hz < f_{vert} \leq 5Hz \end{cases} \tag{2.9}$$

  where M is the total mass of the bridge in kg, equal to the mass per unit length times the span of the bridge, ζ is the damping ratio and f_{vert} is the fundamental natural frequency of the bridge for vertical vibrations.

- For several people crossing the bridge:

$$a_{vert,n} = 0.23 a_{vert,1} n k_{vert} \tag{2.10}$$

  where n is the number of pedestrians, taken as $n = 13$ for a distinct group of pedestrians, or $n = 0.6A$ for a continuous stream of pedestrians (A being the area of the bridge deck). And k_{vert} is a coefficient according to the figure 2.6:

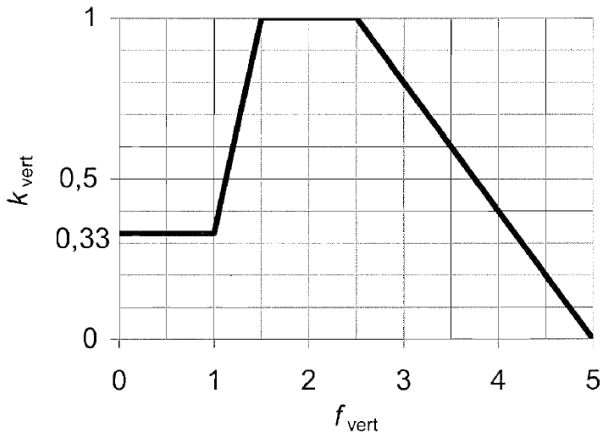

Figure 2.6 Relationship between the vertical fundamental frequency f_{vert} and the coefficient k_{vert} [17]

.

- For a single person running over the bridge:

$$a_{vert,1} = \frac{600}{M\zeta} \quad for \quad 2.5Hz < f_{vert} \leq 3.5Hz \tag{2.11}$$

  Even though these regulations are for timber structures, since the material characteristics that influence the dynamic behavior are not inserted in the equations, the above equations could be used also for other materials, with slight modifications.

British National Annex for EN 1991

In the British national annex, a more specific dynamic model for pedestrian actions on footbridges is given, when it comes to the comfort criteria. According to the paragraph NA.2.44.1 two distinct analysis are required [18].

- The determination of the maximum vertical acceleration of the deck and its comparison with the comfort criteria.
- The determination of the likelihood of large synchronized lateral responses.

The dynamic models proposed by the British National Annex do not include forces induced by: mass gathering, like marathons and demonstrations, deliberate pedestrian synchronization and vandal loading.
The British Annex advices to categorize bridges into 4 classes according to their usage, in order to determine the appropriate actions of the pedestrians.

Table 2.3 Recommended crowd densities for design [18]

Bridge Class	Bridge usage	Group size (walking)	Group size (jogging)	Crowd density ρ people/m^2 (walking)
A	Rural locations seldom used and in sparsely populated areas	N = 2	N = 0	0
B	Suburban location likely to experience slight variations in pedestrian loading intensity on an occasional basis	N = 4	N = 1	0.4
C	Urban routes subject to significant variation in daily usage (i.e. structures serving access to offices or schools)	N = 8	N = 2	0.8
D	Primary access to major public assembly facilities such as sports stadium or major public transportation facilities	N = 16	N = 4	1.5

Regarding the vertical response calculations, it should be satisfied that the peak vertical accelerations of the deck due to the human-induced actions are less than the predefined limits of the British Code. In addition to this, in order to calculate the maximum vertical accelerations, the load models should be applied on the most unfavorable location of the bridge deck and the effect of torsional or other motions should be included, while it might be needed to take into account more modes and not just the fundamental.

- For a single pedestrian or a group of pedestrians, the human-induced load is represented as a vertical pulsating force $F[N]$, moving across the span of the bridge at a constant speed v_t :

$$F = F_0 k(f_v)\sqrt{1+\gamma(N-1)}\sin(2\pi f_v t) \tag{2.12}$$

  where N is the number of pedestrians determined by the table, F_0 is the reference amplitude of the applied force given in Table 2.4, $k(f_v)$ is a combined factor to take into account the effects of a more realistic pedestrian population, harmonic responses and the relative weighting of sensitivity of the pedestrian to response -given in Figure 2.7, γ is a reduction factor due to the unsynchronized combination of pedestrian actions when in group, taken from Figure 2.8.

Table 2.4 Parameters to be used in the calculation of pedestrian response

Load Parameters	Walking	Jogging
Reference load, $F_0[N]$	280	910
Pedestrian crossing speed v_t $[m/s]$	1.7	3

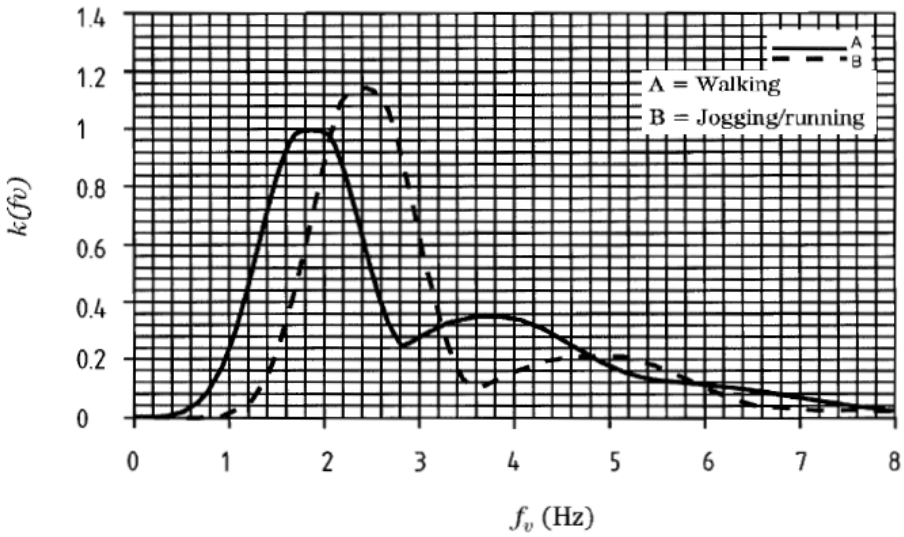

Figure 2.7 Relationship between $k(f_v)$ and mode frequency f_v for walking and jogging loads [18].

- In the case of crowded conditions, the pedestrian load is represented by a vertical pulsating distributed load $w[N/m^2]$, applied to the deck for a sufficiently long time, so that the following steady state conditions are achieved:

$$w = 1.8\left(\frac{F_0}{A}\right)k(f_v)\sqrt{\frac{\gamma N}{\lambda}}\sin(2\pi f_v t) \tag{2.13}$$

  where, $N = \rho A = \rho Sb$ is the total number of pedestrians distributed over the span S of the bridge, ρ is the required crowd density with a maximum value of 1 person/m^2, γ is a reduction factor taken from Figure 2.8, $\lambda = 0.634(S_{eff}/S)$ is a factor for reducing the effective number of pedestrian when only a part of the span contributes to the mode into consideration.

Finally, the maximum recommended serviceability limit for the vertical acceleration should be less than:

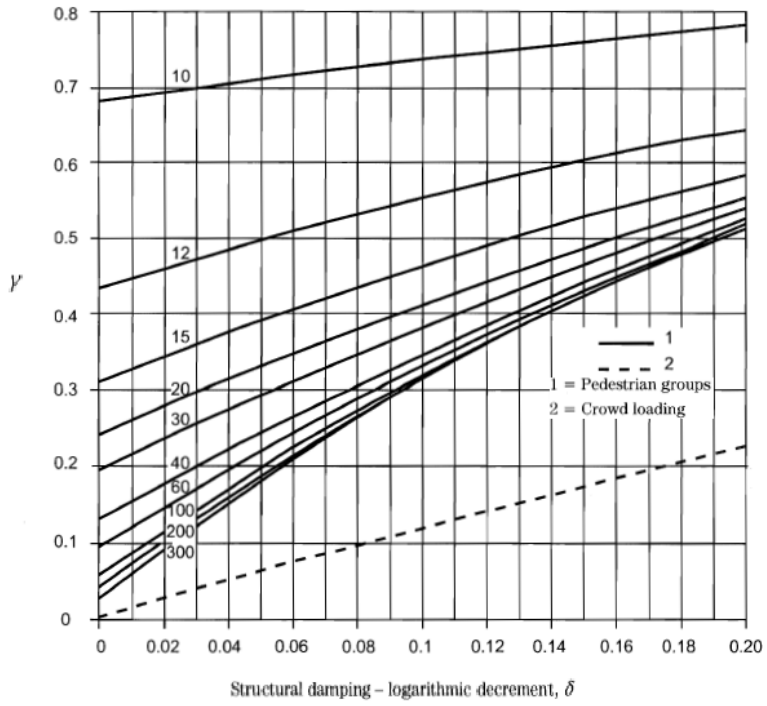

Figure 2.8 Reduction factor γ [18]

$$a_{limit} = 1.0k_1k_2k_3k_4[m/s^2] \qquad and \quad 0.5m/s^2 \leq a_{limit} \leq 2.0m/s^2 \tag{2.14}$$

where, k_1, k_2 and k_3 are given by tables 2.5 to 2.7 and k_4 is an exposure factor taken equal to 1.0 unless determined otherwise.

Table 2.5 Recommended value of site usage factor k_1 [18]

Bridge function	k_1
Primary route for hospitals or other high sensitive routes	0.6
Primary route for school	0.8
Primary routes for sports stadia or other high usage routes	0.8
Major urban centers	1.0
Suburban crossings	1.3
Rural environments	1.6

Table 2.6 Recommended value of site usage factor k_2 [18]

Route redundancy	k_2
Sole means of access	0.7
Primary route	1.0
Alternative routes readily available	1.3

Table 2.7 Recommended value of site usage factor k_3 [18]

Bridge height	k_3
Greater than 8 m	0.7
4 m to 8 m	1.0
Less than 4 m	1.1

2.3.2 British Standards (BS 5400)

The requirements for serviceability of bridges under human-induced vibrations can be found in Appendix C of BS 5400. According to the British Standards, if the fundamental natural frequency of vibration of the unloaded bridge f_0 is higher than 5 Hz, the vibration serviceability requirement is satisfied. However, if f_0 is smaller than 5 Hz, the peak vertical acceleration at any part of the structure, should be limited to:

$$a_{limit} = 0.5\sqrt{f_0}[m/s^2] \tag{2.15}$$

The determination of the maximum vertical acceleration can be simplified in the case of single, or two-or three-span continuous, symmetric structures, of constant cross sectional area that are supported on bearing that may be idealized as simple supports. The expression of the acceleration is then found to be:

$$a = 4\pi 2 f_0^2 y_s K \Psi \tag{2.16}$$

where, y_s is the static deflection (calculated in [m] by applying a vertical concentrated load of 0.7 kN at the midpoint of the main span), K is the configuration factor, given in Table 2.8 and Ψ is the dynamic response factor, taken from Figure 2.9. If f_0 is larger than 4 Hz, the maximum calculated acceleration can be reduced linearly, by zero reduction for 4 Hz to 70% reduction for 5 Hz.

Table 2.8 Configuration factor K [8].

Bridge configuration		K
	—	1.0
	—	0.7
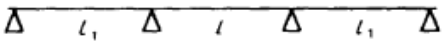	**Ratio l_1/l**	
	1.0	0.6
	0.8	0.8
	0.6 or less	0.9

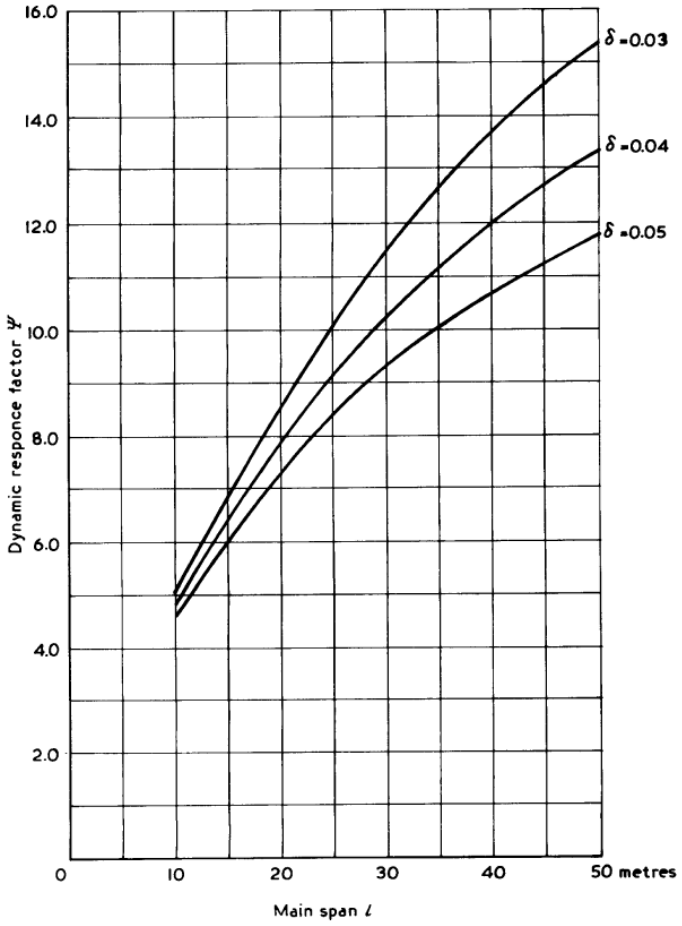

Figure 2.9 Dynamic response factor Ψ [8]

For the structures that don't imply in the above described case, a vertical pulsating point load $F[N]$, moving across the main span at a constant speed $v_t = 0.9 f_0$ [in m/s], is applied in order to find the maximum vertical acceleration and it is given by the expression 2.17:

$$F = 180\sin(2\pi f_0 t) \tag{2.17}$$

The peak acceleration can be reduced in the same way as before in the case that $f_0 > 4Hz$s. The only mention of vandal loading in the British Standards, advices to place bearing of robust construction with adequate provision to resist upward and/or lateral movement. In addition to this, it is recommended to provide prestressed concrete constructions with sufficient unstressed reinforcement, in order to prevent gross cracking due to the reversal of the static live load bending moment when resonant might happen [8].

2.3.3 EUR 23984 EN

EUR 23984 is a joint report about the "Design of lightweight footbridges for human induced vibrations" that acts as a background document in support to the implementation, harmonization and further development of the Eurocodes. In the report the guideline for the design steps that should be followed in order to ensure that the footbridge will meet the comfort criteria when vibrating. This guideline is presented in the flowchart 2.10:

1. **Evaluation of the natural frequencies**
   One of the breakthroughs of this code considering the calculation of the natural frequencies, in comparison with the Codes presented before, is that it recommends to take into consideration the mass of the humans, if the modal mass of the pedestrians is larger than 5% of the modal mass of the deck. In this way the human-structure interaction is somehow included in the design. For the estimation of the new modal mass, including the additional static pedestrian mass, formula 2.18 is proposed:

   $$m^{**} = \rho \int_{L_D} \mu_D(\Phi(x))^2 dx = \rho m^* \tag{2.18}$$

   where ρ_D [kg/m] is the mass per unit length of the bridge deck, $\rho = \frac{\rho_D + \rho_p}{\rho_D}$ is the influence factor for the additional pedestrian mass, ρ_p [kg/m] is the mass per unit length of the pedestrians and $\Phi(x)$ is the mode shape.

2. **Check of critical range of natural frequencies**
   In this step the calculated frequencies are compared with the proposed critical ranges of the natural frequencies for footbridges. These ranges are:

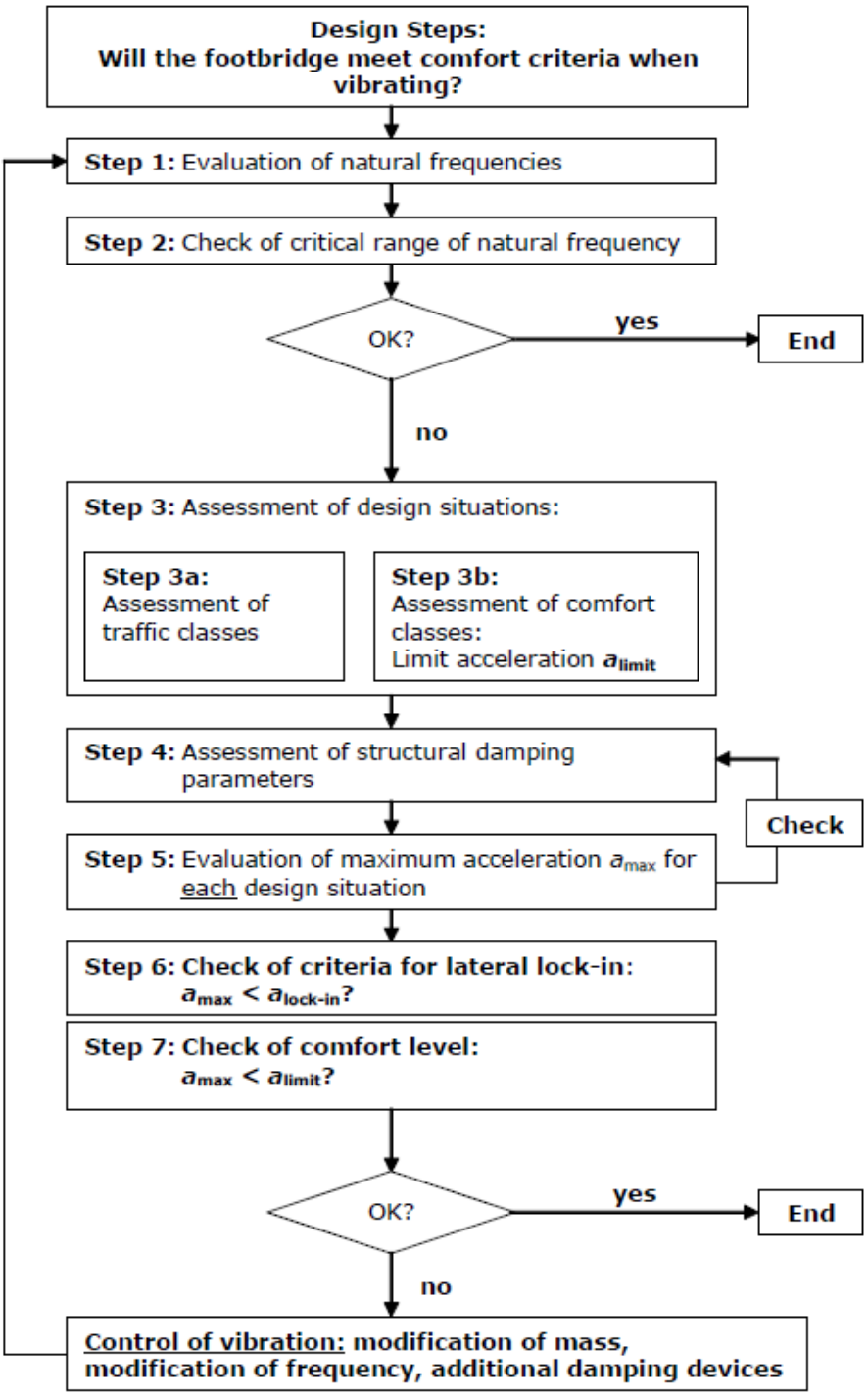

Figure 2.10 Flowchart for the use of the guidelines of EUR 23984 [15]

$$\begin{aligned} &\text{for vertical and longitudinal vibrations: } 1.25Hz \leq f_i \leq 4.6 \\ &\text{for vertical and longitudinal vibrations: } 0.5Hz \leq f_i \leq 1.2 \end{aligned} \tag{2.19}$$

If the natural frequencies of the pedestrian bridge are out of that range, then the comfort criteria are met and there is no need for further investigation. If on the other hand, one or more frequencies of the structure are in this range, further calculations are needed.

3. **Assessment of design situation**
   In order to define the different loads applied on the footbridge and the appropriate combinations of loads, the expected traffic density and the comfort requirements should be determined. EUR 23984 divides the traffic in 5 different classes with recommended densities (Table 2.10) and proposes four different comfort classes and their acceleration limits (Table 2.9). In that way, the owner of the bridge decides the desirable comfort class for each different design situation (i.e. for inauguration or special events, for commuter traffic, etc) and the designer by applying the expected crowd densities can evaluate the response of the bridge.

Table 2.9 Comfort classes and their acceleration ranges [18]

Comfort Class	Degree of comfort	Vertical a_{limit}	Lateral $a_{lat,limit}$
CL 1	Maximum	$< 0.50\ m/s^2$	$< 0.10\ m/s^2$
CL 2	Medium	$0.50 - 1.00\ m/s^2$	$0.10 - 0.30\ m/s^2$
CL 3	Minimum	$1.00 - 2.50\ m/s^2$	$0.30 - 0.80\ m/s^2$
CL 4	Unacceptable discomfort	$> 2.50\ m/s^2$	$> 0.80\ m/s^2$

4. **Assessment of structural damping**
   The determination of the structural damping, as already mentioned, is a complex procedure with many uncertainties. It is recommended to use the linear viscous damping model, where the damping force is proportional to the velocity and leads to linear dynamic equilibrium equations. However, it is only a good approximation for low levels of vibrations.

5. **Determination of maximum acceleration**
   There are three different possible ways to calculate the maximum acceleration of a footbridge, the Single Degree of Freedom method (SDOF), the Finite Element Method (FEM) and the use of Response Spectra. In the case of SDOF or FEM, a harmonic load model is applied on the structure, for the different load cases. This is done by modifying the traffic stream of n pedestrians walking randomly (which is a stochastic load) into an idealized stream of $n_\prime$ synchronized pedestrians among themselves (which can be modelled as a deterministic load). There are two different load models for

Table 2.10 Pedestrian traffic classes and densities [15].

Traffic Class	Density d (P = pedestrian)	Description	Characteristics
TC 1*)	group of 15 P; d=15 P / (B L)	Very weak traffic	(B=width of deck; L=length of deck)
TC 2	d = 0,2 P/m²	Weak traffic 	Comfortable and free walking Overtaking is possible Single pedestrians can freely choose pace
TC 3	d = 0,5 P/m²	Dense traffic 	Still unrestricted walking Overtaking can intermittently be inhibited
TC 4	d = 1,0 P/m²	Very dense traffic 	Freedom of movement is restricted Obstructed walking Overtaking is no longer possible
TC 5	d = 1,5 P/m²	Exceptionally dense traffic	Unpleasant walking Crowding begins One can no longer freely choose pace

the determination of the footbridge response, depending on the traffic density. The uniformly distributed harmonic load $p(t)[N/m^2]$ is common for both load models and is simulated as:

$$p(t) = P\cos(2\pi f_s t)n'\phi \tag{2.20}$$

where $P\cos(2\pi f_s t)$ is the harmonic load induced by a single pedestrian, f_s is the step frequency and is assumed equal to the natural frequency of the footbridge under consideration, n' is the equivalent number of pedestrians on the loaded surface S and ϕ is a reduction factor that takes into account the probability of a footfall frequency approaching the critical range of the natural frequencies considered.

Table 2.11 Parameters P , n' and ϕ for the load models of TC1 to TC5 [15].

P [N]		
Vertical	Longitudinal	Lateral
280	140	35
Reduction coefficient ψ		
Vertical and longitudinal		Lateral
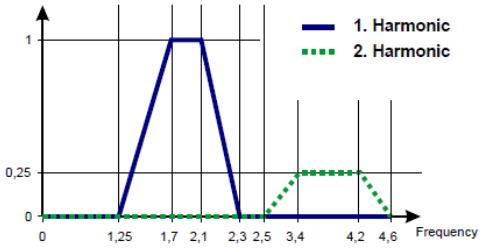		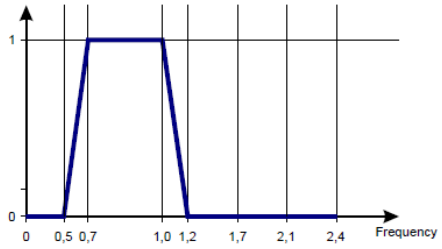
Equivalent number n' of pedestrians on the loaded surface S for load model of:		
TC1 to TC3 (density d < 1,0 P/m²): $n' = \frac{10{,}8\sqrt{\xi \times n}}{S}$ [m⁻²]		
TC4 and TC5 (density d ≥ 1,0 P/m²): $n' = \frac{1{,}85\sqrt{n}}{S}$ [m⁻²]		

For dense crowds the velocity of the stream diminishes and the synchronization of the pedestrians increases. However, beyond the upper limit 1.5 person/m^2 walking becomes really hard, so the dynamic effects reduce remarkably.

For the SDOF method, the structure is transformed into several different harmonic SDOF systems, each one of which has as a natural frequency one of the natural frequencies of the system and as a mass the corresponding modal mass of the structure. By considering every equivalent SDOF system separately, the natural frequencies of the footbridge that are in the critical range, can be checked and the maximum accelerations at resonance of each one of the SDOF systems can be calculated by:

$$a_{max} = \frac{p^*}{m^*}\frac{\pi}{\delta} = \frac{p^*}{m^*}\frac{1}{2\varepsilon} \tag{2.21}$$

where $p^* = \int_{L_D} p(x)\Phi(x)dx$ is the generalized load, $m^* = \int_{L_D} \mu_D(\Phi(x))^2 dx$ is the generalized modal mass and ε is the structural damping ratio. In case the response spectra method is used, the maximum acceleration is defined as:

$$a_{max,d} = k_{a,d}\Sigma_a \tag{2.22}$$

where $k_{a,d}$ is a peak factor and Σ_a is the standard deviation of the acceleration. This method provides design values with a specific confidence level, while the factors are derived from numerical time step simulations of a variety of pedestrian streams on diverse bridge geometries of the Monte Carlo simulations. More information can be found in the bibliography.

6. **Check of criteria for lateral lock-in**
   The critical number of pedestrians that could cause lateral lock-in is defined as:

$$N_L = \frac{8\pi\varepsilon m^* f}{k} \tag{2.23}$$

   Where ε, m^*, f are the structural damping ratio, modal mass and natural frequency, as defined before and k is a constant, equal to 300Ns/m for a range of 0.5-1.0 Hz.

7. **Check of comfort level**
   Since the accelerations are determined for every loading case, it is now possible to check if they are within the limits of the comfort class chosen by the owner of the bridge. If they don't comply to these limits, the dynamic behavior of the bridge should be ameliorated through a series of measures like modifying the mass, or the frequency or the structural damping of the structure or adding damping through special devices. In the appendix two additional load models are described, one for a single pedestrian walking, and one for joggers. The walking load is modelled by a Fourier series:

$$F_{p,vert}(t) = P\left[1 + \sum_{i=1}^{n} a_{i,vert}\sin(2\pi i f_s t - \phi_t)\right] \tag{2.24}$$

   Where the body weight is usually given as 700 or 800 N and the Fourier coefficients are found by SYNPEX as presented on table 2.13.

   For the representation of the jogging load, it is proposed to use a single load which is moving along the footbridge with a constant velocity . The load is expressed through the expression 2.25:

Table 2.12 Fourier coefficients and phase angles for vertical excitation due to walking of a single pedestrian [15]

Author	**Fourier coefficients phase for vertical excitation**	**Comment**	**Activity**
SYNPEX	$a_1 = 0.0115 f_s^2 + 0.2803 f_s - 0.2902$ $\phi_1 = 0$ $a_2 = 0.0669 f_s^2 + 0.1067 f_s - 0.0417$ $\phi_2 = -99.76 f_s^2 + 478.92 f_s - 387.8$ $a_3 = 0.0247 f_s^2 + 0.1149 f_s - 0.1518$ If $f_s < 2.0Hz$: $\phi_3 = -150.88 f_s^3 + 819.65 f_s^2 - 1431.35 f_s + 811.93$ If $f_s \geq 2.0Hz$: $\phi_3 = 813.12 f_s^3 - 5357.6 f_s^2 - 11726 f_s - 8505.9$ $a_4 = -0.0039 f_s^2 + 0.0285 f_s - 0.0082$ $\phi_4 = 34.19 f_s - 65.14$	Derived from step-by-step load model which represents mean human ground reaction forces	Walking

$$P(t,v) = P\cos(2\pi f t)n'\phi \tag{2.25}$$

where P, n' and ϕ are presented in Table 2.13.

Table 2.13 Maximum force P , reduction coefficient ϕ and equivalent number of pedestrians n' for jogging load. [15].

P [N]			$n' = n$ [ ]
Vertical	**Longitudinal**	**Lateral**	
1250	—	—	
Vertical reduction coefficient ψ			
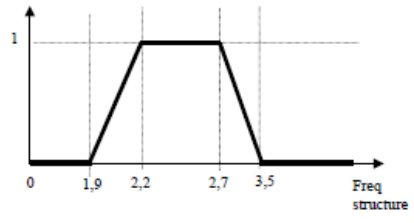			

It is assumed that the synchronization between the joggers and the bridge is perfect, therefore $n' = n$ and f the natural frequency of the bridge. The velocity of the joggers is usually assumed to be: $v = 3m/s$.

2.3.4 Sétra

What is referred to as Sétra, is the technical guide about the assessment of vibrational behavior of footbridges under pedestrian loading that was published by the French association of civil engineering. The guideline for the evaluation of the comfort level of a pedestrian bridge is quite similar to the one of EUR23984. The first step is to determine the class of the footbridge. There are four different classes (table 2.14), each of them able to carry a certain level of traffic. Taking into account the use of the bridge and the possible changes in the traffic levels over time, the owner of the bridge is asked to determine the footbridge class.

Table 2.14 Footbridge classes according to Sétra [49]

Class	Description of class
Class I	Urban footbridge linking high pedestrian density areas or frequently used by dense crowds (demonstrations, tourists) subjected to very heavy traffic.
Class II	Urban footbridge linking populated areas, subjected to heavy traffic and maybe occasionally loaded throughout its bearing area.
Class III	Standard use footbridge, maybe occasionally crossed by large groups of people but never loaded throughout its bearing area.
Class IV	Seldom used footbridge, linking sparsely populated areas or ensuring continuity of pedestrian footpath in motorway or express lane areas.

If a footbridge belongs to Class IV then no further calculations are needed to check its dynamic behavior.

Subsequently, the owner needs to decide on the comfort level of the footbridge by considering the population that will use it (for example students, patients, elder people, etc) and the importance of the bridge. There are three identified comfort levels, assessed through reference to the accelerations of the structure. It is noted, that the comfort levels are subjective and perceived differently from different users, therefore these criteria are not absolute. The three comfort levels are as follow:

- *Maximum comfort*: Accelerations developed by the structure are practically unperceivable by the users.
- *Average comfort*: Accelerations developed by the structure are merely perceivable by the users.

- *Minimum comfort*: Under certain loading that rarely occurs, the developed accelerations are conceivable by the users, but they are tolerable.

The ranges of the accelerations according to the comfort level are presented in Table 2.15 for the case of vertical vibrations.

Table 2.15 Acceleration ranges for vertical vibrations according to Sétra [49]

Acceleration ranges $[m/s^2]$	0	0.5	1	2.5
Range 1	Maximum			
Range 2		Average		
Range 3			Minimum	
Range 4				Unacceptable

The next step is to calculate the frequency of the structure and to classify it. There are four frequency ranges with regard to the risk of resonance occurring in the structure (2.16).

Table 2.16 Frequency ranges for vertical vibrations according to Sétra [49]

Frequency $[Hz]$	0	1	1.7	2.1	2.6	5
Range 1: Maximum risk of resonance						
Range 2: Medium risk of resonance						
Range 3:Low risk of resonance						
Range 4:Negligible risk of resonance						

After determining the natural frequency and frequency range of the structure, as well as the footbridge class, a dynamic analysis is carried out for all or part of a set of 3 load cases, defined as presented in Table 2.17.

Table 2.17 Load cases to be checked according to Sétra [49]

Traffic Type	Class	Natural Frequency Range		
		Range 1	Range 2	Range 3
Sparse	III		No calculations	
Dense	II	Case 1		Case 3
Very dense	I	Case 2		

In the case that calculations are required, the accelerations that are found from the dynamic analysis are compared with the acceleration ranges given in table 2.15 to verify if

the comfort level chosen is satisfied. If it is not satisfied, then appropriate measures should be taken, like modification of the natural frequencies, structural reduction of accelerations-for example by increasing the mass of the structure or use of highly damping materials as structural members-, installation of dampers. The dynamic load cases that need to be applied to the structure for the corresponding footbridge class and traffic type, have been formed for each natural mode of vibration, the frequency of which has been identified within a range of risk of resonance.

- **Case 1: Sparse and dense crowds**

  The density of the pedestrian crowd is chosen accordingly to the footbridge class, as presented in Table 2.18.

  Table 2.18 Crowd densities for load case 1 for traffic classes II and III [49]

Traffic class	Density d of the crowd
III	$0.5 persons/m^2$
II	$0.8 persons/m^2$

  The crowd is assumed to be uniformly distributed over the total area of the footbridge and the total number of pedestrians is: $n = d \cdot S$. The equivalent number of pedestrians, i.e. the number of pedestrians who are fully synchronized is: $n' = 10.8\sqrt{\xi n}$. The vertical load per unit area that is applied on the structure is given by equation 2.26.

  $$F(t) = d \cdot 280\cos(2\pi f_v t) \cdot 10.8\sqrt{\frac{\xi}{n}} \cdot \psi \left[N/m^2\right] \tag{2.26}$$

  where d is the crowd density, f_n is the natural frequency of the mode considered, ξ is the damping ratio and ψ is a reduction factor that takes into consideration the decreased probability of resonance happening outside of the critical frequency range (Figure 2.11).

  This load doesn't take into account the static part of the action of the pedestrian, because it doesn't influence the acceleration. However, it is mentioned that the mass of the pedestrians should be incorporated within the mass of the footbridge.

- **Case 2: Very dense crowd**

  Case 2 loading is only considered for footbridge class I and the pedestrians are assumed to be walking with the same frequency but having random phases. The crowd density

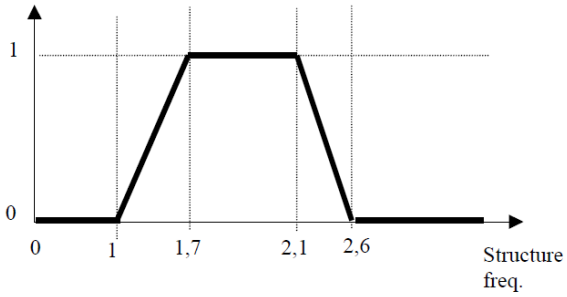

Figure 2.11 Reduction factor ψ of vertical load in the case of walking

is $d = 1 person/m^2$ and the equivalent number of pedestrians fully synchronized is: $n' = 1.85\sqrt{n}$. The vertical dynamic load due to the pedestrians is given by equation 2.27 and ψ is taken by figure 2.11.

$$F(t) = 1 \cdot 280\cos(2\pi f_v t) \cdot 1.85\sqrt{\frac{1}{n}} \cdot \psi \left[N/m^2\right] \tag{2.27}$$

- **Case 3: Effect of the second harmonic of the crowd**

  This loading case is only considered for footbridge classes I and II and regards the second harmonic of the stresses caused by people walking, with a natural frequency approximately equal to 2 times the first natural frequency. The crowd densities for each class are presented in Table 2.19.

Table 2.19 Crowd densities for load case 3 for traffic classes I and II [49]

Traffic class	Density d of the crowd
I	$1.0 person/m^2$
II	$0.8 persons/m^2$

The load applied to the footbridge according to its class is given in Equation 2.28, where ψ is given in Figure 2.12.

$$\begin{aligned} \text{Class I} &: F(t) = 1 \cdot 70\cos(2\pi f_v t) \cdot 1.85\sqrt{\frac{1}{n}} \cdot \psi \left[N/m^2\right] \\ \text{Class II} &: F(t) = 0.8 \cdot 70\cos(2\pi f_v t) \cdot 10.8\sqrt{\frac{\xi}{n}} \cdot \psi \left[N/m^2\right] \end{aligned} \tag{2.28}$$

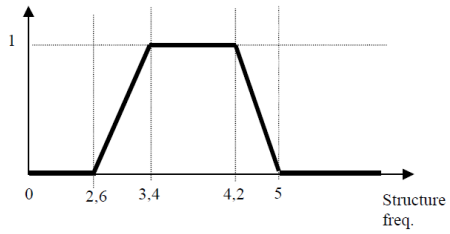

Figure 2.12 Reduction factor ψ of vertical load in the case of walking for load case 3

2.3.5 ISO2631-1

ISO 2631-1 deals with the evaluation of human exposure to whole-body vibration. According to ISO 2631-1, the primary quantity of the magnitude of vibrations should be the acceleration but in the case of very low frequencies or low vibration magnitudes, the velocity could be measured instead and translated to acceleration values later. For the assessment of the vibrations weighted root-mean-square (r.m.s.) accelerations are always used, calculated according to equation 2.29:

$$a_w = \left[\frac{1}{T}\int_0^T a_w^2(t)dt\right]^{\frac{1}{2}} \tag{2.29}$$

where $a_w(t)$ is the weighted acceleration as a function of time (time history) in m/s^2 and T is the duration of the measurement in seconds. Frequency-weighting curves are recommended, and their numerical values can be seen in Tables 2.20 and 2.21. For the application of the basic evaluation method, the crest factor is defined:

$$f_{crest} = \frac{\text{maximum instantaneous peak acceleration}}{\text{root mean square value of acceleration}} \tag{2.30}$$

For vibrations with crest factors equal or smaller than 9, the basic evaluation method is usually sufficient. In the case where the crest factor is larger than 9 alternative measures are proposed (the running r.m.s. and the fourth power vibration dose value).

- The running r.m.s method

  The magnitude of the vibration is defined as a maximum transient vibration value (MTVV), expressed as the maximum of $a_w(t_0)$ in time, given by:

$$a_w(t_0) = \left[\frac{1}{\tau}\int_{t_0-\tau}^{t_0} (a_w(t))^2\, dt\right]^{\frac{1}{2}} \tag{2.31}$$

where $a_w(t)$ is the instantaneous frequency-weighted acceleration, τ is the integration time for running averaging and t_0 is the time of observation. Therefore:

$$MTVV = max\left[a_w(t_0)\right] \tag{2.32}$$

- The fourth power vibration dose method

  This method is more sensitive to peaks than the basic evaluation method, because - as its name mentions - uses the fourth power of the acceleration instead of the second. The fourth power vibration dose value (VDV) is given by equation 2.33:

$$VDV = \left[\int_0^T \left(a_w(t)\right)^4 dt\right]^{\frac{1}{4}} \tag{2.33}$$

  For the frequency weighting of the acceleration spectra, the overall weighted acceleration should be determined according to equation 2.34.

$$a_w = \left[\sum_i \left(W_i a_i\right)^2\right]^{\frac{1}{2}} \tag{2.34}$$

  where a_w is the frequency-weighted acceleration and W_i is the weighting factor for the i^{th} one-third octave band and a_i is the r.m.s acceleration for the same band. The third-octave band spectrum is determined by filtering and cutting off frequencies outside a band, where the maximum frequency in every band is equal to $2^{\frac{1}{3}}$ times the minimum frequency. The weighting factors can be found in Tables 3.18 and 3.19.

In ISO 2631-1 no limit of acceleration is proposed in general for the assessment of vibrations. However, some comfort levels are mentioned in Annex C. These are presented in Table 2.22.

2.3.6 ISO10137

ISO 10137 deals with the serviceability of buildings and walkways against vibrations. It is remarked that there should be specified serviceability limits for the receivers, chosen by the designer with a small variability. In general, a certain probability of exceedance of the serviceability criteria has to be accepted. Nevertheless, for cases that this would result in irreversible results (like cracking or settlements) a lower probability of exceedance should be chosen, according to ISO2394.

Table 2.20 Principal frequency weightings in one-third octaves [27]

Frequency band number[1] x	Frequency f Hz	W_k factor ×1 000	W_k dB	W_d factor ×1 000	W_d dB	W_f factor ×1 000	W_f dB
−17	0,02					24,2	−32,33
−16	0,025					37,7	−28,48
−15	0,031 5					59,7	−24,47
−14	0,04					97,1	−20,25
−13	0,05					157	−16,10
−12	0,063					267	−11,49
−11	0,08					461	−6,73
−10	0,1	31,2	−30,11	62,4	−24,09	695	−3,16
−9	0,125	48,6	−26,26	97,3	−20,24	895	−0,96
−8	0,16	79,0	−22,05	158	−16,01	1 006	0,05
−7	0,2	121	−18,33	243	−12,28	992	−0,07
−6	0,25	182	−14,81	365	−8,75	854	−1,37
−5	0,315	263	−11,60	530	−5,52	619	−4,17
−4	0,4	352	−9,07	713	−2,94	384	−8,31
−3	0,5	418	−7,57	853	−1,38	224	−13,00
−2	0,63	459	−6,77	944	−0,50	116	−18,69
−1	0,8	477	−6,43	992	−0,07	53,0	−25,51
0	1	482	−6,33	1 011	0,10	23,5	−32,57
1	1,25	484	−6,29	1 008	0,07	9,98	−40,02
2	1,6	494	−6,12	968	−0,28	3,77	−48,47
3	2	531	−5,49	890	−1,01	1,55	−56,19
4	2,5	631	−4,01	776	−2,20	0,64	−63,93
5	3,15	804	−1,90	642	−3,85	0,25	−71,96
6	4	967	−0,29	512	−5,82	0,097	−80,26
7	5	1 039	0,33	409	−7,76		
8	6,3	1 054	0,46	323	−9,81		
9	8	1 036	0,31	253	−11,93		
10	10	988	−0,10	212	−13,91		
11	12,5	902	−0,89	161	−15,87		
12	16	768	−2,28	125	−18,03		
13	20	636	−3,93	100	−19,99		
14	25	513	−5,80	80,0	−21,94		
15	31,5	405	−7,86	63,2	−23,98		
16	40	314	−10,05	49,4	−26,13		
17	50	246	−12,19	38,8	−28,22		
18	63	186	−14,61	29,5	−30,60		
19	80	132	−17,56	21,1	−33,53		
20	100	88,7	−21,04	14,1	−36,99		
21	125	54,0	−25,35	8,63	−41,28		
22	160	28,5	−30,91	4,55	−46,84		
23	200	15,2	−36,38	2,43	−52,30		
24	250	7,90	−42,04	1,26	−57,97		
25	315	3,98	−48,00	0,64	−63,92		
26	400	1,95	−54,20	0,31	−70,12		

1) Index x is the frequency band number according to IEC 1260.

NOTES

1 For tolerances of the frequency weightings, see 6.4.1.2.

2 If it has been established that the frequency range below 1 Hz is unimportant to the weighted acceleration value, a frequency range 1 Hz to 80 Hz is recommended.

3 The values have been calculated including frequency band limitation.

Table 2.21 Additional frequency weighting in one-third octaves [27]

Frequency band number[1] x	Frequency f Hz	W_c		W_e		W_j	
		factor ×1 000	dB	factor ×1 000	dB	factor ×1 000	dB
−10	0,1	62,4	−24,11	62,5	−24,08	31,0	−30,18
−9	0,125	97,2	−20,25	97,5	−20,22	48,3	−26,32
−8	0,16	158	−16,03	159	−15,98	78,5	−22,11
−7	0,2	243	−12,30	245	−12,23	120	−18,38
−6	0,25	364	−8,78	368	−8,67	181	−14,86
−5	0,315	527	−5,56	536	−5,41	262	−11,65
−4	0,4	708	−3,01	723	−2,81	351	−9,10
−3	0,5	843	−1,48	862	−1,29	417	−7,60
−2	0,63	929	−0,64	939	−0,55	458	−6,78
−1	0,8	972	−0,24	941	−0,53	478	−6,42
0	1	991	−0,08	880	−1,11	484	−6,30
1	1,25	1 000	0,00	772	−2,25	485	−6,28
2	1,6	1 007	0,06	632	−3,99	483	−6,32
3	2	1 012	0,10	512	−5,82	482	−6,34
4	2,5	1 017	0,15	409	−7,77	489	−6,22
5	3,15	1 022	0,19	323	−9,81	524	−5,62
6	4	1 024	0,20	253	−11,93	628	−4,04
7	5	1 013	0,11	202	−13,91	793	−2,01
8	6,3	974	−0,23	160	−15,94	946	−0,48
9	8	891	−1,00	125	−18,03	1 017	0,15
10	10	776	−2,20	100	−19,98	1 030	0,26
11	12,5	647	−3,79	80,1	−21,93	1 026	0,22
12	16	512	−5,82	62,5	−24,08	1 018	0,16
13	20	409	−7,77	50,0	−26,02	1 012	0,10
14	25	325	−9,76	39,9	−27,97	1 007	0,06
15	31,5	256	−11,84	31,6	−30,01	1 001	0,00
16	40	199	−14,02	24,7	−32,15	991	−0,08
17	50	156	−16,13	19,4	−34,24	972	−0,24
18	63	118	−18,53	14,8	−36,62	931	−0,62
19	80	84,4	−21,47	10,5	−39,55	843	−1,48
20	100	56,7	−24,94	7,07	−43,01	708	−3,01
21	125	34,5	−29,24	4,31	−47,31	539	−5,36
22	160	18,2	−34,80	2,27	−52,86	364	−8,78
23	200	9,71	−40,26	1,21	−58,33	243	−12,30
24	250	5,06	−45,92	0,63	−63,99	158	−16,03
25	315	2,55	−51,88	0,32	−69,94	100	−19,98
26	400	1,25	−58,08	0,16	−76,14	62,4	−24,10

1) Index x is the frequency band number according to IEC 1260.

NOTES

1 For tolerances of the frequency weightings, see 6.4.1.2.

2 If it has been established that the frequency range below 1 Hz is unimportant to the weighted acceleration value, a frequency range 1 Hz to 80 Hz is recommended.

3 The values have been calculated including frequency band limitation.

Table 2.22 Acceleration ranges with respect to confort levels according to Annex C of ISO2631

Comfort level	Acceleration ranges $[m/s^2]$
Not uncomfortable	< 0.315
A little uncomfortable	$0.315 - 0.63$
A little uncomfortable	$0.315 - 0.63$
Fairly uncomfortable	$0.50 - 1.00$
Uncomfortable	$0.80 - 1.60$
Very uncomfortable	$1.25 - 2.50$
Extremely uncomfortable	> 2

The vertical action of the pedestrians can be expressed in the frequency domain as a Fourier series (equation 2.35:

$$F_v(t) = Q\left(1 + \sum_{n=1}^{k} a_{n,v} \sin(2\pi n f t + \phi_{n,v})\right) \tag{2.35}$$

where $a_{n,v}$ is a numerical coefficient corresponding to the n^{th} harmonic for the vertical direction, Q is the static load of the participating person, f is the frequency component of repetitive loading and $\phi_{n,v}$ is the phase angle of the n^{th} harmonic for the vertical direction. For walking or running the numerical coefficients proposed for the vertical directions are presented in Table 2.23. In the case of groups of pedestrians, the dynamic action induced by them depends mainly on the weight of the pedestrians, the maximum density $person/m^2]$ and on the degree of coordination. The force applied by the group of pedestrians is defined as:

$$F(t)_N = F(t) \cdot C(N) \tag{2.36}$$

where $C(N)$ is the coordination factor that is equal to $C(t) = \sqrt{N}/N$ where N is the number of the pedestrians.

It is recommended to consider four different load cases:

- One person crossing the bridge while the other is standing at mid-span
- An average pedestrian flow based on the expected daily occurrence, for example group of 8 to 15 people
- The presence of streams of pedestrians (significantly more than 15 persons)

- Occasional festive or choreographic events.

Like in the case of ISO 2631 in order to check the serviceability, the r.m.s. values of the acceleration are checked, with a recommended averaging time of 1s. If no other definitive data are available, the level of vertical vibrations should be limited to the values of the relevant base curve, given in Figure 2.14, multiplied by a factor 60. In the case of one or more people standing still on the footbridge the multiplying factor should be limited to 30. When considering the critical frequency range of slender bridges ($f < 5Hz$) these values correspond to a maximum acceleration of $0.6m/s^2$ and a minimum acceleration of $0.3m/s^2$ (if there are standing people on the footbridge these limits are even smaller). These values are more conservative than the ones proposed in the Eurocodes and British Standards. However, in ISO the root mean square values of the accelerations are checked and not the peak acceleration.

Table 2.23 Design parameters for moving forces due to one person [26]

Activity	Harmonic number n	Common range of forcing frequency $f\ [Hz]$	Numerical coefficient for verticla direction $a_{n,v}$
Walking	1	$1.2-2.4$	$0.37(f-1.0)$
	2	$2.4-4.8$	0.1
	3	$3.6-7.2$	0.06
	4	$4.8-9.6$	0.06
	5	$6.0-12.0$	0.06
Running	1	$2.0-4.0$	1.4
	2	$4.0-8.0$	0.4
	3	$6.0-12.0$	0.1

2.3.7 Comparison of the guidelines of the different codes

From a look on the guidelines described in the preceding paragraphs it can be concluded that in general a dynamic analysis is obligatory in the cases that the natural frequencies of the footbridge are smaller than 5 Hz. In the case of the EUR 23984 this limit is $4.6Hz$. What is of great interest is the limits of maximum accelerations proposed from the different codes and guidelines. It is obvious that they vary a lot, from the conservative $0.6m/s^2$ and $0.7m/s^2$ proposed in ISO 10137 and Eurocode 0 respectively, to the maximum of $2.5m/s^2$ proposed in EUR23984 and Setra for a minimum comfort level. However, the British

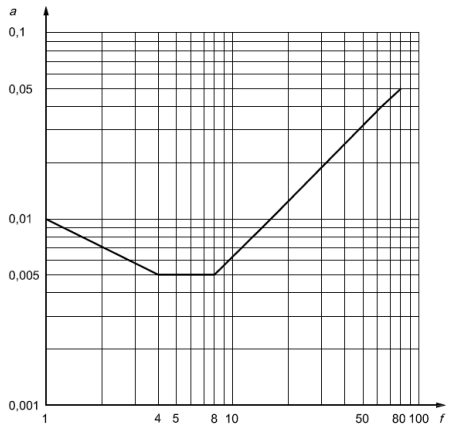

Figure 2.13 Base curve for vertical accelerations [26]

Standards do not set a fixed value for the acceleration limit, instead they give a formula that takes into account the natural frequency of the bridge. The British Annex also proposes a formula for the identification of the acceleration limit, derived from factors dependent on the site usage, redundancy, height of structure and the exposure. Nevertheless, this acceleration limit should be smaller than $2m/s^2$. For the determination of the maximum developed accelerations most of the codes propose the modeling of the pedestrian load as a periodic force, either concentrated or uniformly distributed. In some cases (Eurocode 5, British Standards), simplified formulas of the acceleration are given if certain assumptions are met. The British National Annex to EC 1, EUR 23984, Setra and ISO 10137, include in their load models the number of pedestrians using the bridge and the influence of the synchronization among them. Notwithstanding, the British codes (both the British standards and the national annex) recommend to model the pedestrian force as a moving load with a constant speed, while Sétra and EUR 23984 assume uniformly distributed loads. (EUR 23984 in its appendix mentions that a single pedestrian load for walking and jogging can be modeled as a moving load). From these guidelines, only EUR 23984 proposes a way to calculate the influence of the human participation in the dynamic characteristics of the structure, whereas Setra mentions that the mass of the pedestrians should be considered in the mass of the combined structure, but does not give more information about it. Finally, one of the most interesting observations is that ISO 2631 and ISO 10137 use the root mean squared value of the accelerations in order to check the serviceability, unlike the rest of the codes and guidelines that propose to take into account the peak acceleration, something more conservative.

2.4 Perception of vertical vibrations on bridges

The perception of vertical vibrations by humans is a complicated term and not easy to measure. That is because there are many "sensitive" parameters influencing it, like:

- Number of people using the bridge
- Position of the human body (standing-with bend or straight knees, walking, sitting)
- Age of users
- Height of the bridge above ground or water
- Exposure time to vibrations
- Dynamic characteristics of the bridge
- Appearance of the bridge
- Frequency of use
- Knowledge of the source of vibration
- Familiarity with vibration

It is found that people are more sensitive to vibrations when they are standing rather than when they are walking. An experiment conducted by Kasperski measured the vibration response of a bridge and the behavior of the pedestrians using it. A limiting value for the acceleration was used and it was noticed that the number of annoyed and alarmed people increases when the exceeding time of this limit is increased. [29]. Another set of experiments conducted by Mackenzie et al. studied the different influencing factors of the comfort the pedestrians perceive. By interviewing pedestrians crossing four different footbridges, it was realized that not only the vibration level influences the pedestrian's comfort feeling but also factors like the height of the structure, the height of the parapet, the existence of an alternative route and the site of the bridge. [32] Users of bridges located near hospitals or schools might be more sensitive to vibrations than hikers or joggers that are crossing the footbridge while exercising. Even the appearance of the bridge can have a great impact on the perception of the pedestrians. It was found that users crossing two different looking bridges but with very similar dynamic characteristics had quite different experiences of the vibrations they felt. [15] As can be seen, there are many different factors that influence the total assessment of a footbridge as comfortable or not. It is proposed by Živanović to evaluate the serviceability of bridges by defining limits that correspond to different probabilities of unsatisfied users, rather than using a pass/fail criterion of accelerations as given by the guidelines [53].

2.5 Measures against excessive vibrations

There are different types of measures that can be used to predict, prevent or solve the problems introduced by the dynamic behavior of footbridges. There are three categories of measures that can be taken.

2.5.1 Frequency tuning

Frequency tuning is a measure taken to prevent the problems, by avoiding the critical frequency ranges of the modes. These frequency ranges for vertical vibrations are $1.6-2.4Hz$ for the first walking harmonic and $3.5-4.5Hz$ for the second harmonic [55]. A way to do this is by increasing the stiffness of the structure while trying to avoid a simultaneous increase of the mass or limit it as much as possible. An alternative way is to reduce the mass of the structure, for example by using lightweight concrete instead of normal, with only a small reduction in stiffness. [49]

2.5.2 Detailed vibration response evaluation

This is the bases of the code and guidelines described in section 3. However, there are many uncertainties that enter the analysis, for example many assumptions for the loading models are made and the acceleration limits that need to be checked are somewhat arbitrary.

2.5.3 Reduction of the vibration response

A reduction of the vibration response is succeeded by increasing the damping of the structure. A reduction of the acceleration amplitudes can be achieved by adding a "heavy" deck from concrete or asphalt that will increase the mass of the construction while adding damping to the structure. Another way is to use materials that are naturally damping, however in order for them to get activated they should be part of the overall rigidity. Finally, the damping can be increased by adding extra damping devices, like viscous dampers or Tuned Mass Dampers (TMD) [49].

Tuned Mass Dampers (TMD)

A tuned mass damper (TMD) consists of a mass, a spring and a damper connected to a structure in order to reduce the dynamic response of the structure. The damper is tuned to a particular frequency, so that when the bridge is excited in that frequency, the TMD will be out of phase with the response of the bridge [13]. The TMDs are usually attached to the

main girder, either beneath the deck or above it in the plane of the handrails. Although their maintenance is easy and low-cost, over time their effectiveness can be reduced due to the loss of viscous oil or due to the change in the dynamic properties of the structure over time. In such cases de-tuning occurs, that can be however treated by replacing the passive damper of the TMD with a semi-active one[55]. The optimum frequency and damping factor that minimize the steady-state displacement of the structure, in the case that the construction doesn't have its own damping, are given by equations 2.37 and 2.38.

$$f_{opt} = \frac{1}{1+\mu} f_s \tag{2.37}$$

$$\xi_{opt} = \sqrt{\frac{3}{8}\frac{\mu}{(1+\mu)^3}} \tag{2.38}$$

Where, f_s is the natural frequency of the structure and $\mu = m/M$ with m being the mass of the TMD and M being the mass of the structure.

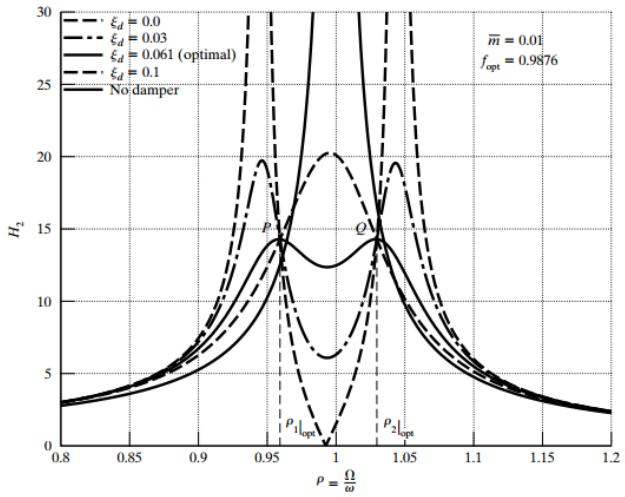

Figure 2.14 Response curve for amplitude of systems with optimally tuned TMD [13]

Chapter 3

Ultra High Performance Concrete

Ultra-High Performance Concrete (UHPC) is a relatively new type of concrete, with improved mechanical properties compared to normal strength concrete and high strength concrete and a remarkable increase in durability. In essense, UHPC refers to materials with a cement matrix and a characteristic compressive strength above 150 MPa that can even reach 250 MPa. Its "ultra" high performance is achieved through the use of:

- A very low water-cement ratio of about 0.20 to 0.25 that results in the creation of notably denser and stronger hydration products and the minimization of capillary pores.
- Fine aggregates (maximum aggregate size should be less than $7mm$) in order to decrease the mechanical effects of heterogeneity [47].
- Pozzolans (silica fume and/or silica flour) in the binder matrix that act both as fillers and pozzolanic material and lead to reduction of the water demand and of the porosity and at the same time to an increase of the compressive strength (Figure 3.1) .
- Admixtures like superplasticizers, that increase the workability of the mixture (otherwise the workability levels are low due to the low w/c ratio).
- Steel or synthetic fibers that increase the energy absorption capacity, the tension, bending tension and shear strength and lead in a more ductile final product [45].

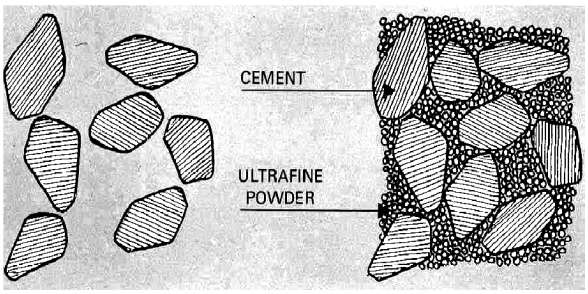

Figure 3.1 Silica fume acting as a "micro-filler" of the space between the cement grains

Table 3.1 Compressive strength and modulus of elasticity of different types of concrete

Concrete Type	Range of Compressive Strength f_c $[MPa]$	Modulus of Elasticity E_c GPa
Normal Strength Concrete	$20-60$	$20-35$
High Strength Concrete	$60-110$	$35-40$
Ultra-High Strength Concrete	$150-250$	$50-70$

3.1 Material Properties

3.1.1 Mechanical Properties

Compressive strength

As mentioned, the compressive strength of the UHPFRC varies between 150 MPa and 250 MPa. The main influencing factors for the high compressive strength are the low water/cement ratio and the fine aggregates and silica fume used, that lead to a dense mixture. Indicative, the range of compressive strength of the different types of concrete are presented on Table 6.1.

Tensile strength

The tensile strength of the matrix of UHPC is in the range of 10 MPa, significantly higher than the usual tensile strength of concretes, and therefore the tensile strength is taken into consideration during the design process [Hussein and Amleh]. Due to the high density and the low water/cement ratio the fiber-free matrix is very brittle, however when fibers are added in the mixture the material gains more ductility and the tensile strength behavior consists of three parts:

- Linear-elastic behavior up to the level of the tensile strength of the matrix

- Pseudo-strain hardening behavior resulting from multi-microcracking
- Strain softening with localization of deformation

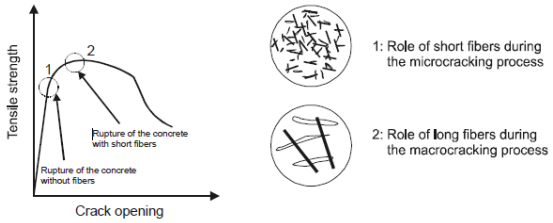

Figure 3.2 The role of fibers in different stages of concrete tensile cracking [36]

The maximum strength reached during the linear elastic behavior coincides with the tensile strength of the matrix $f_{ct,m}$, and at that point the first crack is created; this is barely influenced by the presence or not of fibers. The modulus of elasticity in this phase is the initial modulus of elasticity in compression E_c. During the pseudo-strain hardening, the tensile stress increases with increasing deformation but in a much slower rate than in the linear-elastic part. In this stage microcracking occurs, namely a great number of tiny, closely spaced and well distributed cracks are formed. The maximum strain than can be reached before strain softening begins, is ε_u and is typically around $0.2-0.2\%$ at a stress level of f_{ct}. When the material enters the strain softening phase, the transfer of the same or higher level of stress can't be pursued anymore for increasing deformation. The microcrack of the weakest section of the element develops into a macrocrack and the stress starts decreasing. [47]

- Multi-microcracking mechanism

  What makes UHPFRC stand out from the rest types of concretes, is its pseudo-hardening behavior. This mechanism is activated when the first microcrack is formed in the matrix. The presence of fibers (assuming their resistance is sufficient) restricts the further opening of the cracks and as the crack's width increases slightly so does the stress which is transferred by the fibers crossing the crack faces (Figure 3.2). This crack-bridging mechanism is a combination of a number of different actions:

  - Fiber deformation
  - Fiber pullout: cracking of the interface between the matrix and the fiber and frictional slip
  - Deformation of the pulled-out fiber

- Fiber rupture

  The most desirable energy dissipation mechanism that will ensure the pseudo-hardening behavior is the fiber pullout. In order to achieve this, a sufficiently strong matrix and fiber-matrix interface should be provided in order to develop adequate bond and further frictional resistance during pullout. [47]

Bending tensile strength

The bending strength of a UHPFRC depends mainly on the type and amount of fibers used, but the orientation and distribution of them as well as the shape of the element might have a significant influence as well. The bending strength for UHPFRC is up to 36 MPa, while in the case that no fibers are added in the mixture, the material is quite brittle with a bending strength around 22 MPa and a modulus of elasticity of more than about 45 GPa. [45](in the range of 50 to 70 GPa [47])

3.1.2 Other Material Properties

Durability

The low porosity and the absence of capillary pores lead to a high durability and improved resistance to all kinds of harmful gases and liquids, as well as to frost and freezing and thawing attacks. [45]

Creep and Shrinkage

UHPFRC has a high autogenous shrinkage (around $550\mu m/m$) that develops rapidly and could indicate a high risk of microcracking at early stages, if the element is constrained. [31] Nevertheless, due to the low water/cement ratio the water amount of the concrete is really small and therefore it has barely no drying shrinkage. Consequently, most of the shrinkage of UHPFRC is caused due to the autogenous shrinkage that appears in the early stages of concrete, whereas most of the shrinkage of regular concrete comes from the drying shrinkage. All in all, even though UHPFRC has a high autogenous shrinkage, the final shrinkage is lower than in the case of regular concrete. [Paškvalin]. According to Lafarge, the producer of Ductal®, if heat treatment is applied on the concrete, the shrinkage development is completed at the end of the treatment and no residual shrinkage occurs after that [2]. Normal concrete has a creep coefficient which is up to $3-4$. The creep coefficient of the UHPC however is much reduced (less than 0.8 for Ductal® and if it's thermal treated as low as 0.2), but the delayed strain is already higher than the elastic one. The low creep coefficient can have

Table 3.2 Advantages and disadvantages of UHPFRC in comparison with regular concrete [51]

Advantages	Disadvantages
High Strength	Hard homogeneous distribution of fibers
High durability	Higher material cost per m^3 than for conventional concrete
Lower transportation costs	Not many guidelines available
Longer service life	concrete (add polypropylene fibres)
Low maintenance cost	
Ductile behavior	

significant effects in case prestressing is used, since the prestress losses due to creep will diminish.

The application of UHPFRC on footbridges, would lead to smaller cross sections and longer spans and consequently less material used, making the structure more attractive. However, this results to a high slenderness that might have negative effects in the dynamic behavior of the structure, which needs to be taken into consideration during the design.

3.2 Design Methods

UHPC is a relatively new material and therefore there are still no national codes and standards to use during the design procedure. There are however available some Recommendations provided by the AFGC/SETRA group, and they will be used as a guideline for further calculations. In the case that fiber-reinforced concrete under tension is used, a partial safety factor γ_{bf} should be used in the ULS in order to take into consideration any manufacturing defects.

3.2.1 Normal force verification for serviceability limit states

For the analysis to be carried out, two fundamental assumptions need to be made: 1) plane sections remain plane and 2) the stresses in the uncracked part of the concrete are proportional to the strains. The term of the characteristic length l_c is introduced in order to transform a constitutive law of stress-crack width to a stress-strain law. For rectangular or tee cross sections with a depth of h the characteristic length can be taken as $l_c = \frac{2}{3}h$ and $\varepsilon = \frac{f_{tj}}{E_{ij}} + \frac{w}{l_c}$.

Pre-tensioned or post-tensioned prestress

In the case of prestressing additional assumptions need to be made. These are for:

1. Calculation for uncracked section (for pre-tensioned prestressing)
    - The concrete withstands tensile stress
    - No relative slippage occurs between the constituent materials
2. Calculation for cracked section (for both pre- or post- tension)
    - No relative slippage occurs between the constituent materials
    - When the strain of a concrete is zero at a reinforcement, then the tension in the reinforcement is
        - 0 if it's passive reinforcement
        - $\sigma_{pd} + n_i \sigma_{bpd}$ (with $n_i = 4$) if it is prestressing reinforcement, where σ_{bpd} represents the concrete stress at the considered reinforcement under permanent actions and prestressing P_d

The stress-strain law of the concrete is described by the diagram in figure 3.3 for the case of strain hardening and in figure 3.4 for the case of strain softening.

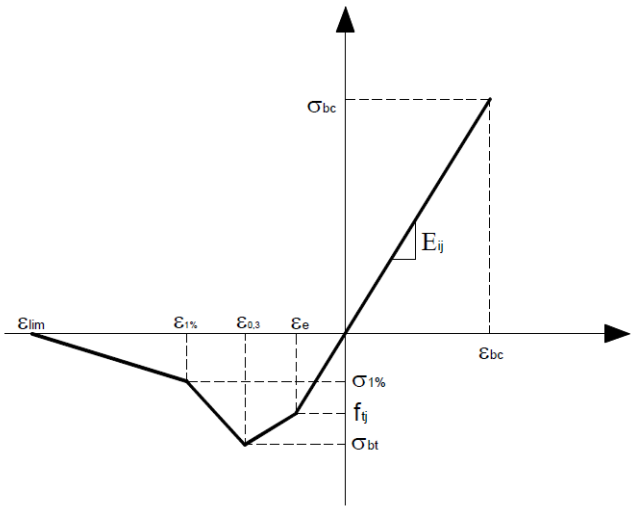

Figure 3.3 Strain hardening law for SLS according to the recommendations of AFGC SETRA [5]

Where

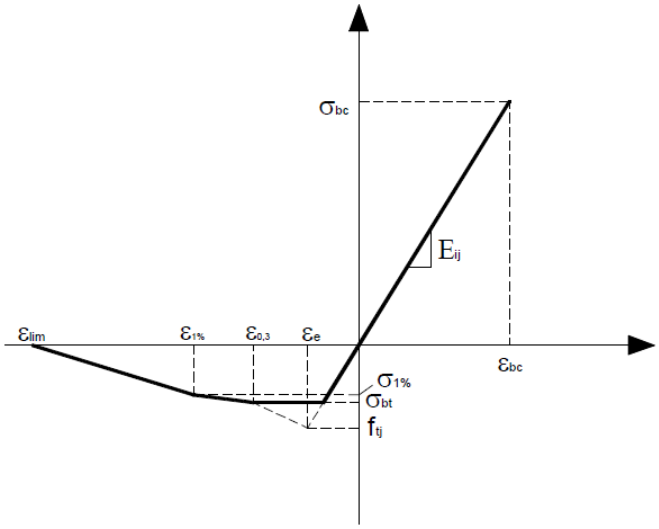

Figure 3.4 Strain softening law for SLS according to the recommendations of AFGC SETRA [5]

Table 3.3 Design properties of UHPFRC for SLS according to the recommendations of AFGC SETRA [5]

Elastic tensile strain	$\varepsilon_e = \frac{f_{ct,m}}{E_c}$
Strain at a crack width of $w = 0.3mm$	$\varepsilon_{0.3} = \frac{w_{0.3}}{l_c} + \frac{f_{ct,m}}{E_c}$
Strain at a crack width of $w_{1\%} = 0.01H$ (H is the height of the test specimen)	$\varepsilon_{1\%} = \frac{w_{1\%}}{l_c} + \frac{f_{ct,m}}{E_c}$
Maximum possible strain (l_f being the fibre length)	$\varepsilon_{lim} = \frac{l_f}{4l_c}$
Maximum compressive stress	$\sigma_{bc} = 0.6 f_{ck}$
Maximum tensile stress	$\sigma_{bt} = \frac{\sigma(w_{0.3})}{K}$
Stress at a crack width of $w_{1\%} = 0.01H$	$\sigma_{1\%} = \frac{\sigma(w_{1\%})}{K}$
Correction coefficient to take into account the influence of unfavorable fiber orientation	$K = 1.25$ for general loading $K = 1.75$ for local effects
Characteristic length	$l_c = \frac{2}{3}h$

3.2.2 Normal force verification for ultimate limit states

Just like in the case of the serviceability limit state, here also some assumptions are made. These are: 1) plane sections remain plane, 2) no relative slippage occurs in the concrete and the passive reinforcements or pre-tensioned prestressing reinforcement, 3) for the reinforcements the stress has to be divided by $\gamma_s = 1.15$ or $\gamma_p = 1.15$ (these values are equal to 1 in the case of accidental combinations). For the strength calculation of the section, a simplified method can be used, however this method is somewhat pessimistic because it doesn't take into account the full potential of the fibers. In this method, there are 3 ultimate strains *A*, *B* and *C*.

Point A: This point corresponds to an increase of elongation by 1% for the furthest from the center reinforcement. If $\frac{l_f}{4l_c} + \frac{f_{ct,m}}{E_c} < 1\%$, the participation of the FRC is neglected (i.e. case of very deep beams). *Point B*: This point corresponds to a 0.3% shortening of the most severely compressed outermost point of the section. *Point C*: It corresponds to a shortening of the concrete by $\frac{\sigma_{bc}}{E_c}$ at a distance $\left(1 - \frac{1000\sigma_{bc}}{3E_c}\right)h$ from the most severely compressed outermost point.

The stress-strain diagram of the concrete is given by figures 3.5 and 3.6, and it comes from the transformation of the SLS diagram.

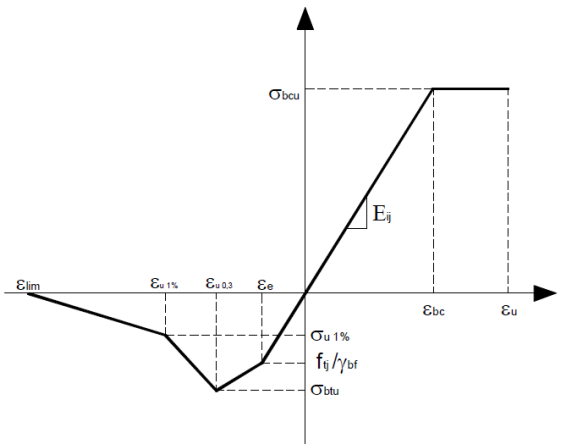

Figure 3.5 Strain hardening law for ULS according to the recommendations of AFGC SETRA [5]

Where

The influence of the correction factor *K* that acts like a safety factor γ_f is depicted in figure 3.7.

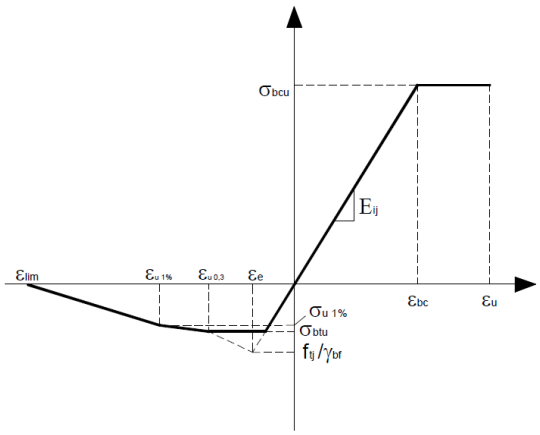

Figure 3.6 Strain softening law for ULS according to the recommendations of AFGC SETRA [5]

Table 3.4 Design properties of UHPFRC for ULS according to the recommendations of AFGC SETRA [5]

Ultimate compressive strain	$\varepsilon_u = 0.3\%$
Strain at a crack width of $w = 0.3mm$	$\varepsilon_{u,0.3} = \frac{w_{0.3}}{l_c} + \frac{f_{ct,m}}{\gamma_{bf} E_c}$
Strain at a crack width of $w_{1\%} = 0.01H$ (H is the height of the test specimen)	$\varepsilon_{u,1\%} = \frac{w_{1\%}}{l_c} + \frac{f_{ct,m}}{\gamma_{bf} E_c}$
Maximum possible tensile strain (l_f being the fibre length)	$\varepsilon_{lim} = \frac{l_f}{4l_c}$
Maximum compressive stress	$\sigma_{bc,u} = \frac{0.85}{\theta \gamma_b} f_{ck}$
Maximum tensile stress	$\sigma_{bt,u} = \frac{\sigma(w_{0.3})}{K\gamma_{bf}}$
Stress at a crack width of $w_{1\%} = 0.01H$	$\sigma_{1\%} = \frac{\sigma(w_{1\%})}{K\gamma_{bf}}$
Correction coefficient to take into account the influence of unfavorable fiber orientation	$K = 1.25$ for general loading $K = 1.75$ for local effects
Characteristic length	$l_c = \frac{2}{3}h$

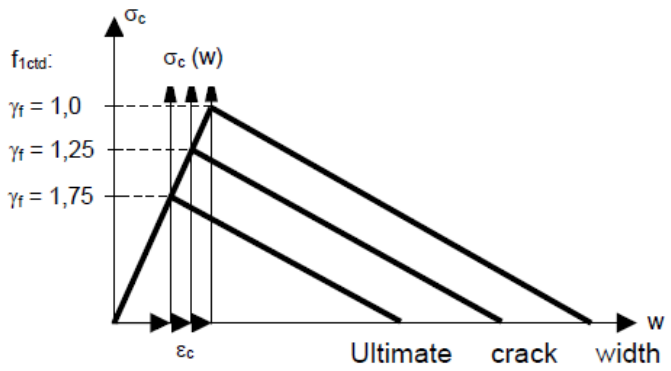

Figure 3.7 Influence of the fiber orientation on the tensile strength according to the recommendations of AFGC SETRA [5]

Chapter 4

Derivation of Comfort Limits

4.1 Test description

The initial goal of this project is to evaluate the stringiness of the available codes and to define for which limits of accelerations the pedestrians feel comfortable and safe and what is the connection between the deformations and the accelerations when it comes to the perception of vibrations and the comfort of humans. To do that, a number of experiments were performed on some slender footbridges in the wider area of Rotterdam, namely: Poortugaal brug, De Heerlijkheid brug and Brug D of Bonairepark in Rotterdam.

The scope of the experiments was to analyze the response of the footbridges and to derive characteristics of its dynamic behavior, like the eigenfrequencies and the damping ratios, the amplitude of the displacements and the maximum accelerations developed. For each one of the bridges, five different load types were applied. The first one was the heel test, where one person was standing on the midspan of the bridge and by hitting his foot on the deck, caused vibrations of the bridge. This test is mainly used to identify the eigenfrequency of the pedestrian bridge, as well as its damping ratio. The 4 remaining load types consist of loads induced due to walking, running, jumping freely and jumping at a prescribed frequency, close to the eigenfrequency of the footbridge, with the help of a metronome (vandal loading).

It is of great importance not only to evaluate the way the structure responds under the applied loads, but also to assess the behavior of the pedestrians and their sense of safety and comfort while using the bridge. For this reason, the pedestrians that participated in the experiments were asked to fill in a questionnaire about the way they perceived the vibrations and the level of comfort and safety that they felt during each test. It has already been mentioned that the perception of vibrations is a complicated term which is not easy to be measured, since many sensitive parameters are influencing it. Two of those parameters that are easy to be measured are: the number of people using the bridge and their posture

(standing straight, walking, running, jumping). Since it is important to understand how these parameters in combination with the different accelerations and displacements influence firstly, the level of vibrations the pedestrians perceive and secondly, the pedestrians' sense of comfort and safety, it was decided to perform a number of tests for each loading type, where both standing and moving people would participate and give feedback of their experience. The sequence of the experiments is as follows:

Firstly, a number of heel tests were performed, where only one person was standing on the bridge. For the heel tests only the accelerations were measured, using a smartphone application named VXacc, and a Fourier forward transform was applied on site to derive the natural frequency of the footbridge when it performs a free vibration after an impact loading. The calculated first eigenfrequency of the bridge is written down and is used later on to excite the footbridge under vandal loading, when the metronome is used.

Next the experiments of the walking pedestrians took place. For a n number of participants, n different tests were performed for each load type. The first test consisted of 1 person crossing the bridge and $(n-1)$ people standing at the midspan. The second test consisted of 2 people crossing the bridge and $(n-2)$ people standing, etc. The last test comprised of n people crossing the bridge. For each individual crossing of the bridge, the time history of the accelerations was recorded with the smartphone application VXacc, whereas for recording the time history of the displacements, a sticker was placed on the middle of the span and a camera was videotaping its movement while the bridge was vibrating.

Simultaneously with the completion of each crossing, each participant was asked to fill in the questionnaire, grading the vibration level he sensed from 1 (for unperceivable vibrations) to 10 (for intolerable vibrations). Moreover, they evaluated the level of comfort they felt (comfortable, medium comfort, uncomfortable) and the level of safety (safe, unsafe), according to their action (standing or walking).

Once the experiments for the walking load were completed, the experiments for running, jumping freely and jumping with a metronome were carried on, all performed as described above. Note that, for the cases of jumping, both the standing and the jumping group were located at the midspan and the group of jumping people was jumping on the spot, and not moving across the bridge. Subsequently, the analysis of the measurements started. For each test, the time-history of the accelerations was used as input to perform a Forward Fourier Transform (FFT) and determine the frequencies of this vibration. The damping ratio of this specific oscillation was also calculated, as well as the maximum acceleration developed. The video-clips of the displacements were analyzed with "ClipAnalyzer" to get the time-history of the vertical displacements at the mid-span of the footbridge and to find the amplitude of the displacements.

Successively, the questionnaires of the participants were analyzed. The main concern of this part of the project is not to find the percentage of the people who felt uncomfortable or sensed a certain level of vibration for the occurring acceleration and/or displacement, but to identify from a variety of different accelerations, different load types and different perceptions, the limits of the accelerations where the average person stops feeling comfortable and/or starts feeling uncomfortable or unsafe. Therefore, during the processing of the data, the following assumptions were made:

1. The replies that corresponded to standing people and the replies that corresponded to people that were moving (either running, walking or jumping), were analyzed separately. In this way, the limits for the active and passive users of the bridge could be calculated and compared.

2. The representative level of vibration of each test is defined as the average of the replies of the pedestrians. The scale counts from 1 to 10, with 1 representing the case that vibrations are not perceivable by users, 3 representing light vibrations, 6 corresponding to medium vibrations and 10 standing for intolerable levels of vibration.

3. The representative level of comfort of each test is defined as the average of the replies of the pedestrians. The terms: "good comfort", "medium comfort" and "bad comfort" were used to describe the level of comfort the users sense.

4. Finally, the feeling of safety of each test is defined as the average feeling of the corresponding replies of the pedestrians. The terms: "safe" and "unsafe" were used to define the threshold limit above which the pedestrians felt unsafe.

5. For each test, there are determined 2 scales for the level of vibration perceived, 2 scales for the level of comfort and 2 scales for the feeling of safety, one for the active and one for the passive pedestrians.

More information about the set-up of the experiments is provided in Appendix A, whereas a detailed description of the bridges tested and the accelerations, frequencies and damping ratios measured on site for the different tests is presented in Appendix B.

4.2 Perception of vibrations, limits of comfort and limits of safety

4.2.1 With respect to the maximum accelerations

In Figures 4.1 and 4.2 the level of vibrations and the level of comfort that the active people perceive are presented (either when walking, running or jumping) with regard to the maximum accelerations developed in the footbridge.

It can be observed by the acceleration-comfortability diagram that up to accelerations of 3.15 m/s^2 people responded that they feel completely comfortable, since 100% of the pedestrians agreed that the level of comfort is good. By comparing the results of the comfortability with the results of the level of vibrations they felt, it can be seen that for the same acceleration (3.15 m/s^2) the level of vibrations is either unperceivable or low (light vibrations). For accelerations between 3.15 m/s^2 and 5.8 m/s^2 the level of vibrations felt by the pedestrians increases at a level 4-5 (light-to-medium vibrations) and the level of comfort decreases, and is now considered good-to-medium and medium comfort. For accelerations above $5.8-6$ m/s^2 the level of vibrations perceived increases to medium and large vibrations whereas people start feeling more uncomfortable. However, accelerations larger than 5.8 m/s^2 do not necessarily mean that the comfort level will be bad, since the perceived comfort varies from relatively good to bad for similar acceleration values. It is apparent that only the vibrations caused by intentional jumping are thought to be uncomfortable to the people that induce them. The vibrations due to walking and running are hardly noticeably to the pedestrians crossing the bridge.

Nevertheless, the responses of the standing crowd for the level of vibrations and the comfort they experience are quite different than those of the moving crowd, as can be seen in Figures 4.1 and 4.2. It is apparent that passive pedestrians feel uncomfortable at much lower accelerations. It can be confirmed what was already known from the literature study: that standing people are more sensitive to vibrations than moving people. In the case of vibrations due to walking, the maximum acceleration produced was 0.6 m/s^2 and the people standing felt comfortable. For accelerations higher than 1 m/s^2 the people standing started experiencing stronger vibrations (above 6 in the scale used) and feeling medium comfort and/or high discomfort.

In general, the passive crowds feel less comfortable when the active crowds are running than when they are walking. Nevertheless, with the exception of a single observation of one pedestrian, the comfort level felt by the standing people due to running is considered medium comfort for values of acceleration up to 2.2 m/s^2. For jumping and jumping with a

metronome the discomfort increases. It can be correlated by the two graphs that for standing groups medium level of comfort is exceeded for accelerations above 1.36 m/s^2, whereas for the same comfort level of a moving group the acceleration was 5.8 m/s^2 (3.5 times higher). In addition, it is apparent from the rate that the level of vibrations increases for the two crowds (moving and standing) that the standing people are much more sensitive.

When it comes to the feeling of safety of the bridge, it is apparent that people start feeling unsafe for accelerations higher than 5.9 m/s^2 when they are moving (jumping), whereas in the case they are standing the limit of acceleration that makes them feel less safe drops to 1.5 m/s^2 (figure 4.3). In addition to this, it can be observed that the people feel unsafe only in some cases of jumping, either freely or with metronome, whereas in the cases of walking and running they feel safe even for accelerations higher than the observed limit (2.2 m/s^2 instead of 1.5 m/s^2).

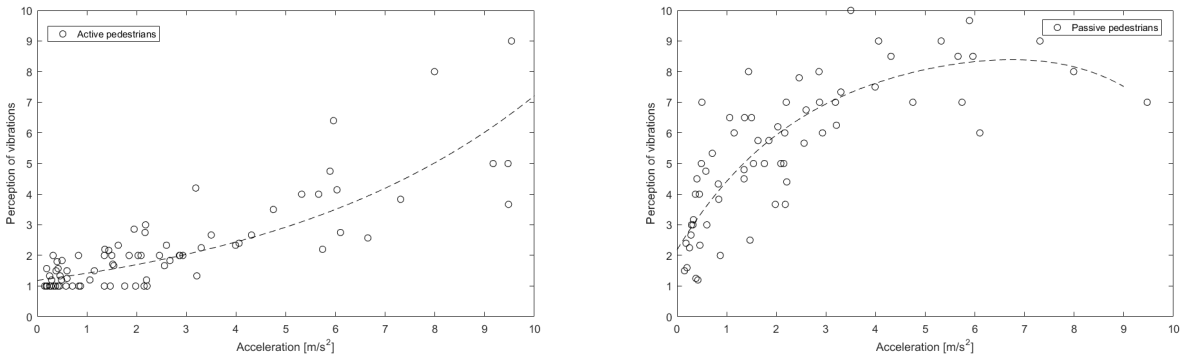

(a) Active pedestrians

(b) Passive pedestrians

Figure 4.1 Level of vibrations with respect to the maximum accelerations developed, as it was perceived by active and passive pedestrians

4.2.2 With respect to the root mean square accelerations

While analyzing the data and finding the limits of the maximum accelerations for which people feel safe or unsafe and comfortable or uncomfortable, it was observed that for higher accelerations, there was a wide range of different comfort levels experienced for similar acceleration values. To eliminate this phenomenon that might be caused due to extreme local peaks at the acceleration time history, the limits for the comfortability of people will be considered not for the maximum acceleration value, but for the root mean square of the acceleration.

ISO 2631-1 and ISO 10137 recommend to use the root mean square acceleration when evaluating the serviceability of a footbridge and propose to calculate the r.m.s. acceleration

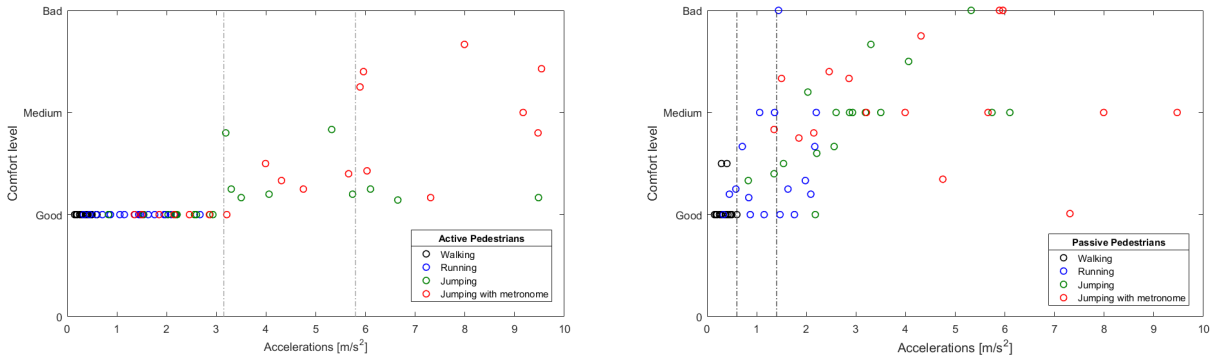

(a) Active pedestrians (b) Passive pedestrians

Figure 4.2 Level of comfort with respect to the maximum accelerations developed, as perceived by active and passive pedestrians

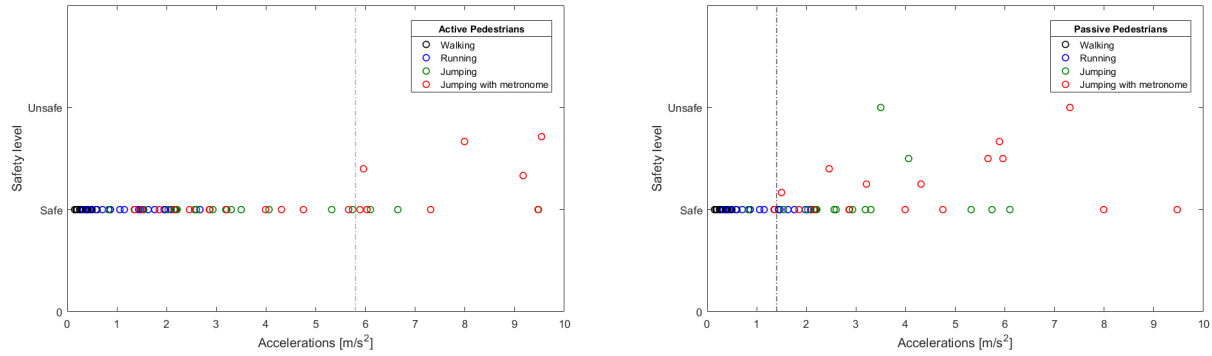

(a) Active pedestrians (b) Passive pedestrians

Figure 4.3 Level of Safety with respect to the maximum accelerations developed, as perceived by active and passive pedestrians

according to the formula 4.1.

$$a_w = \left[\frac{1}{T}\int_0^T a_w^2(t)dt\right]^{\frac{1}{2}} \tag{4.1}$$

where T is the duration of the measurement and a_w is the weighted acceleration as a function of time. Since the data from the measurements were not in the form of an equation but in the form of pair of values (acceleration and time), the r.m.s acceleration was calculated according to the formula 4.2.

$$a_{rms} = \sqrt{\frac{\sum_{i=1}^{N} x_i^2}{N}} \tag{4.2}$$

where N is the number of pairs corresponding to the time duration chosen. After some trials where different time periods and time steps were used, it was chosen to calculate the r.m.s. of acceleration a_{rms} over a time period of $T = 0.50\ s$ with a time step of calculation equal to $\Delta t = 0.15\ s$. Once the graph of the r.m.s. accelerations with respect to time was plotted and compared to the time history of the accelerations, the maximum value of the a_{rms} was selected. Once the representative value of the a_{rms} for each one of the tests was known, the same procedure as for a_{max} was followed to find the comfort limits. A plot of the a_{rms} with respect to time and its maximum value can be seen in Figure 4.4.

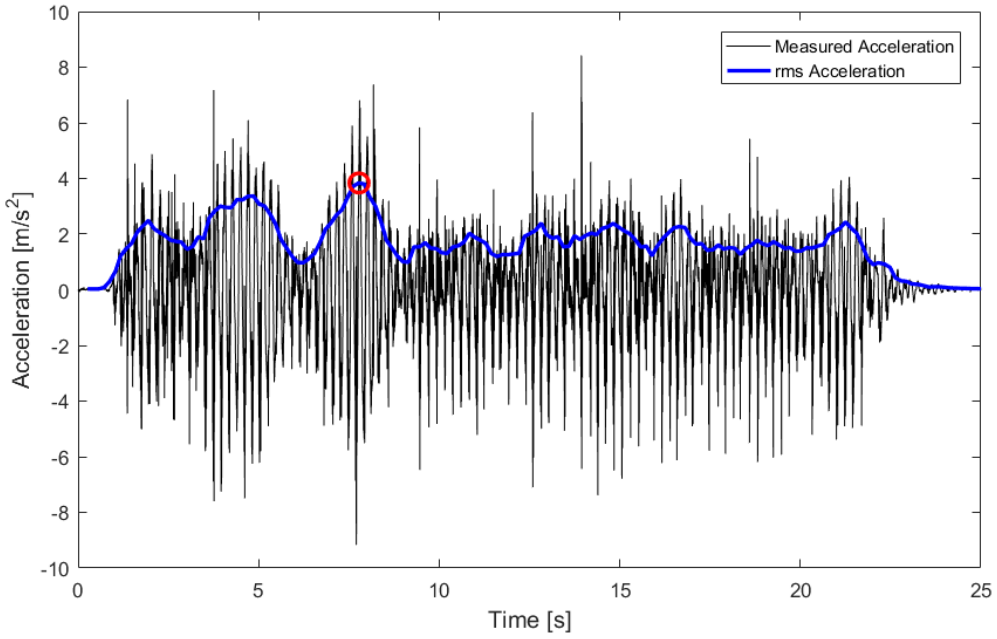

Figure 4.4 Time history of acceleration and r.m.s accelerations caused by 6 people jumping with metronome on Brug D

By the Figures 4.5 to 4.6 ,the first observation that can be made is that the acceleration limits are reduced in the case that the root mean square of the acceleration is used, something that was expected. Both in the case of moving and walking crowds, it can be seen that the data are closer to the fitted regression line. It is apparent that for moving crowds, the phenomenon of different comfort levels corresponding to the same acceleration has vanished. However, for standing crowds the comfort - r.m.s. acceleration diagram is still unclear for higher accelerations.

The limits that can be recognized by the graphs are much lower than in the case that the maximum accelerations are considered. For moving crowds, the acceleration range in between which a medium comfort level is achieved falls from $3.15 - 5.8\ m/s^2$ to $1.8 - 3.6$

m/s^2, with values above $3.6m/s^2$ corresponding to feelings of discomfort. For standing crowds, the limit above which people experience discomfort is even lower, at $1m/s^2$.

When it comes to safety, the a_{rms} limit above which people in motion have expressed feelings of unsafety is $3.6m/s^2$, whereas the same limit for people standing still is 1 m/s^2. It is reminded that the equivalent limits in the case they are expressed as maximum accelerations are: $6m/s^2$ for moving crowds and 1.5 m/s^2 for people standing.

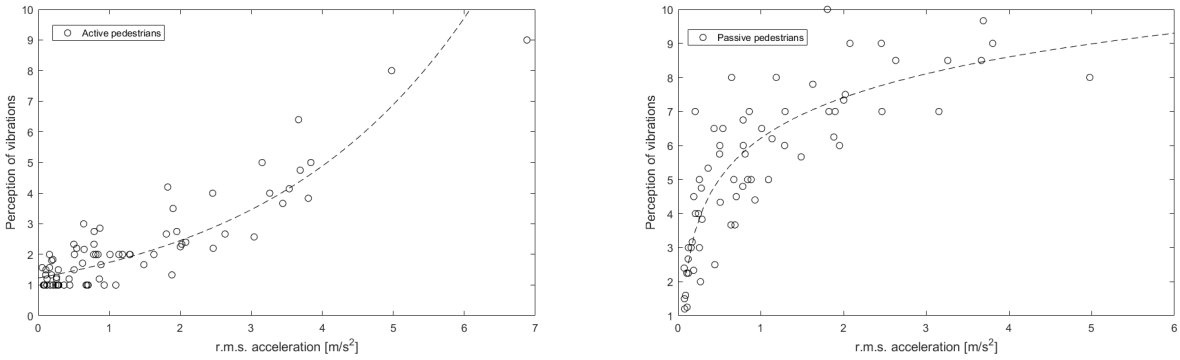

(a) Active pedestrians (b) Passive pedestrians

Figure 4.5 Level of vibrations with respect to the root mean square accelerations developed, as it was perceived by active and passive pedestrians

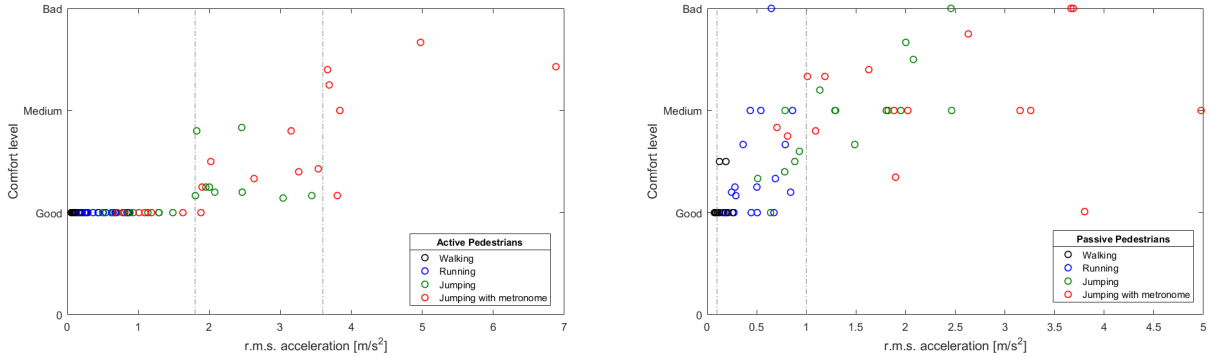

(a) Active pedestrians (b) Passive pedestrians

Figure 4.6 Level of comfort with respect to the root mean square accelerations developed, as perceived by active and passive pedestrians

4.2.3 With respect to the deflections

When the displacement is chosen as a method of measurement of the vibration levels and the comfortability, it can be observed that for vibrations with amplitudes around 2 *mm* the

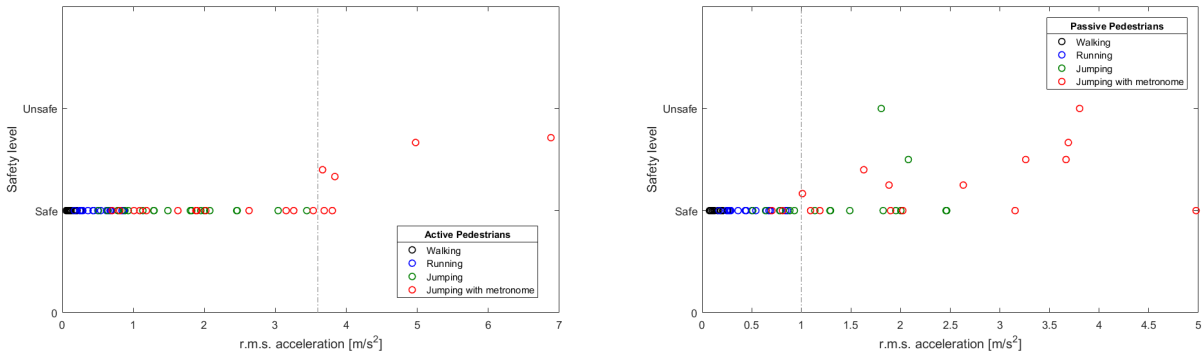

(a) Active pedestrians

(b) Passive pedestrians

Figure 4.7 Level of Safety with respect to the root mean square accelerations developed, as perceived by active and passive pedestrians

comfort level is excellent, since all the test subjects replied that they felt very comfortable and the vibrations were either light or not noticeably at all. Even for amplitudes of vibrations between $2-6.5$ *mm* the comfort level is still good to medium and the level of vibrations that the moving crowds perceive is light to medium, reaching values up to 5 in the scale used. For responses with amplitudes above 7 *mm*, people feel more uncomfortable (at a vibration level above 5.5-6 - medium). By comparing the comfort felt with regard to the accelerations (Figure 4.2) and with regard to the deflections (Figure 4.9) it can be seen that in the case of the deflections the comfort limits are more clear, since especially for the bigger deformations (>6 *mm*) an increase in the deflections signifies an increase in the discomfort. Unlike the case of accelerations, where with an increased acceleration (particularly for more than 6 m/s^2) high levels of discomfort are reached but simultaneously also good and medium comfort levels exist. For displacements among 2 and 6 *mm* there is a small overlapping, where up to 4.5 *mm* the comfort level is considered good to medium comfort and from 4.5 *mm* to 6 *mm* the comfort felt approaches "medium" levels of comfort. (Figure 4.9).

When it comes to standing crowds, it can be seen once more that people standing are more sensitive than people walking, running or jumping. Oscillations due to walking are causing people to feel comfortable and in a few cases good-to-medium comfort. Whereas running loads lead to comfort levels that vary between good and medium comfort. For amplitudes greater than 1.4 *mm* people start feeling discomfort. Nevertheless, for vibrations with amplitudes up to 4 *mm* it is not very apparent the level of discomfort people sense for each different amplitude of vibrations, since for the same amplitude of displacement the comfort level varies from comfortable to uncomfortable, according to the replies of the standing group. This leads us to believe that there are more factors influencing the perception of the vibrations, like the type of load applied, the characteristics of the people standing (in

general women seem to be more sensitive than men), the time of exposure to the vibrations etc. Finally, for amplitudes larger than 5 *mm* the level of discomfort becomes maximum and the perception of the comfort and of the level of vibrations is clear, since no overlapping is noticed.

Regarding the limits of displacements above which people start feeling unsafe, it can be seen that for people jumping this limit is above 6.5 *mm*, whereas for people standing this limit is much lower and equal to 2 *mm*.

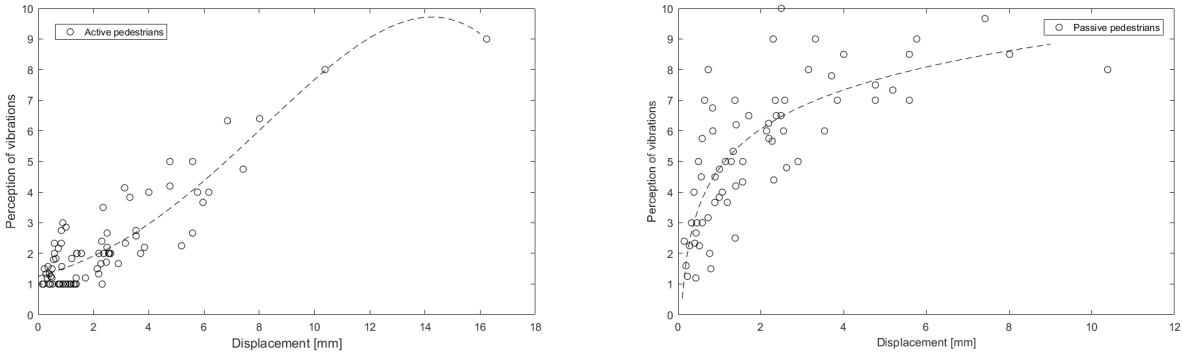

(a) Active pedestrians (b) Passive pedestrians

Figure 4.8 Level of vibrations with respect to the displacements developed, as it was perceived by active and passive pedestrians

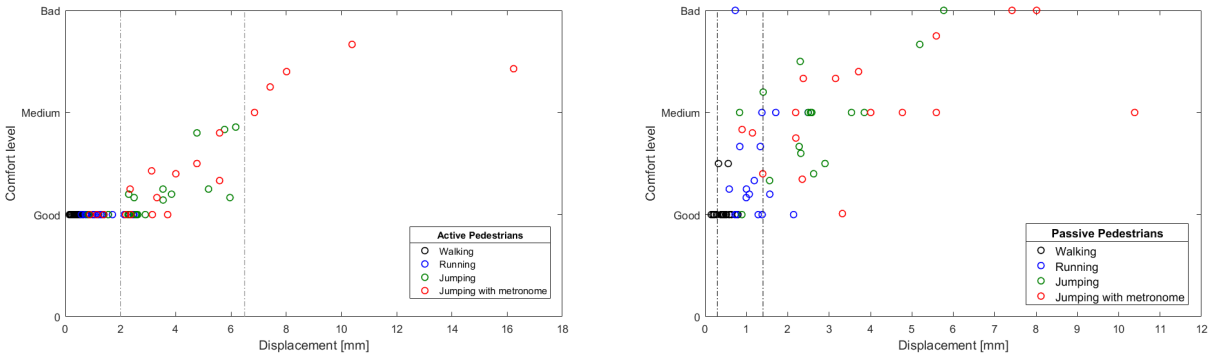

(a) Active pedestrians (b) Passive pedestrians

Figure 4.9 Level of comfort with respect to the displacements developed, as perceived by active and passive pedestrians

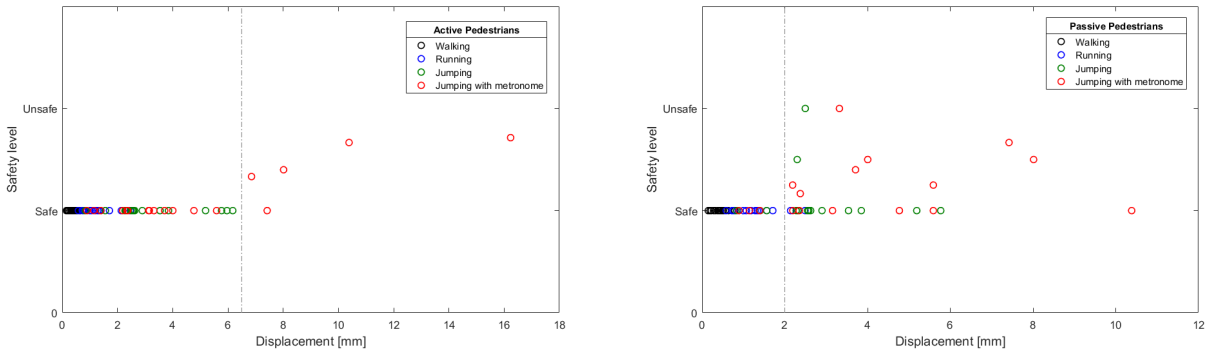

(a) Active pedestrians

(b) Passive pedestrians

Figure 4.10 Level of Safety with respect to the displacements developed, as perceived by active and passive pedestrians

4.2.4 With respect to the ratio acceleration/displacement

It is well-known that the acceleration is the second derivative of the displacement. When the response of the displacement of the structure is described as a function of time:

$$u(t) = (A\cos(\omega_D t) + B\sin(\omega_D t))\, e^{-i\omega_n t} + C\sin(\omega t) + D\cos(\omega t)$$

the acceleration will be described as:

$$\begin{aligned} a(t) = &-\omega_D^2 (A\cos(\omega_D t) + B\sin(\omega_D t))\, e^{-i\omega_n t} \\ &- 2i\omega_n\omega_D (-A\sin(\omega_D t) + B\cos(\omega_D t))\, e^{-i\omega_n t} \\ &- \omega^2 (C\cos(\omega t) - D\sin(\omega t)) \end{aligned}$$

This would mean that the amplitude of the acceleration is connected to the amplitude of the displacements through the natural frequency of the structure and the frequency of the applied force. Therefore, by dividing the amplitudes of the acceleration and the displacement, the influence of the frequencies in the amplification of the acceleration could be found. For example, if a structure A has the same amplitude of displacements with a structure B, but the frequency of A is lower than the frequency of B, the acceleration measured for structure B will be higher for the same applied load. Additionally, if the same accelerations are developed in structures A and B, but their natural frequencies are different, the amplitude of their displacements will also be different. That could explain why people experiencing the same accelerations in different structures felt different levels of discomfort.

By comparing the graphs in Figures 4.11 and 4.12 that present the level of vibrations and the comfort level perceived by the active people with respect to the $\left|\frac{a(t)}{u(t)}\right|$ ratio, it can be observed that there are 4 discreet zones. The first zone is observed for values of $\left|\frac{a(t)}{u(t)}\right|$ up to 550 s^{-2} where the vibrations are hardly noticeable and the comfort level is excellent. For values between $550-1000$ s^{-2} the vibrations are much stronger and easier to notice and the people experience great discomfort. In this range of acceleration/displacement ratio, there is a variety of different responses about the level of vibrations and comfort perceived. In the case of running and walking the experience of the users is better, since they feel lighter vibrations and they are not feeling discomfort. However for jumping with and without metronome the vibrations are more noticeable for the people causing them, reaching a maximum level of 9 out of 10, with 10 representing intolerable level of vibrations as already explained. The third zone consists of values of $|a/u|$ which are between $1000-2000$ s^{-2} that represent cases where users were feeling good to medium comfort and the vibrations were noticeable to medium, but not strong. The last zone, for $|a/u| > 2200$ s^{-2} includes cases where the comfortability level of the users is excellent while users feel light vibrations occurring.

In the case of standing groups, the same pattern is noticed. For values of $|a/u| < 500$ s^{-2} the level of vibrations is low (Figure 4.11), hence people feel only light vibrations and this makes them feel comfortable. For frequencies that are higher, the vibrations are more intense and the disturbance that the standing people feel increases. More specifically, for values of acceleration over displacement between 500 and 2200 s^{-2} the vibration level can reach up to really strong, intolerable vibrations. A similar array of values, where 500 $s^{-2} < |a/u| < 2000$ s^{-2} , describes the area where great discomfort can be observed.

However, it should be noted that a ratio $|a/u|$ between 500 and 2200 s^{-2} does not necessarily make the response of the structure uncomfortable, since for the same range of ratios all three different levels of comfort were observed. It is however an indication that among those limits, the pedestrians are more sensitive to the vibrations and the chances of experiencing discomfort are higher. However, the ranges below 500 s^{-2} and above 2200 s^{-2} do indicate that in these ranges people will feel comfortable.

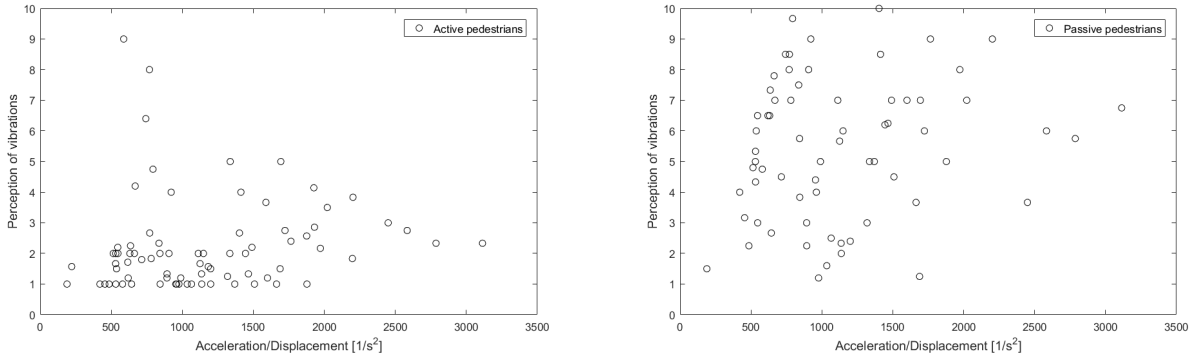

(a) Active pedestrians (b) Passive pedestrians

Figure 4.11 Level of vibrations with respect to the ratio acceleration/displacement, as it was perceived by active and passive pedestrians

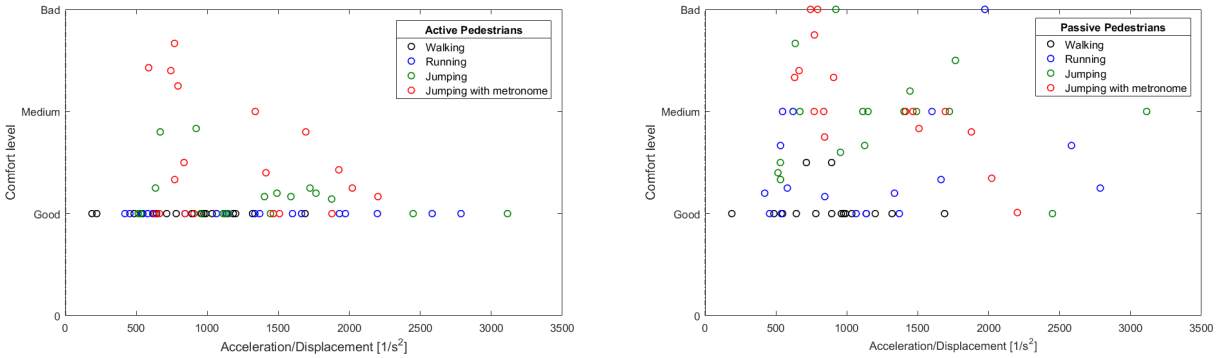

(a) Active pedestrians (b) Passive pedestrians

Figure 4.12 Level of comfort with respect to the ratio acceleration/displacement, as perceived by active and passive pedestrians

4.3 Conclusions and remarks

The limits of accelerations and displacements derived for active and passive pedestrians for different levels of comfort and safety are presented in tables 4.1 to 4.4. In table 4.5 are presented the acceleration limits proposed by Sétra and EUR23984 for different comfort classes. It is apparent that the limits of a_{max} derived by the experiments for passive pedestrians resemble the limits proposed by the guidelines. For the maximum level of comfort those are 0.5 m/s^2 and 0.6 m/s^2 for the guidelines and from the tests respectively. Whereas for minimum comfort the acceleration should be above 1 m/s^2 for the case of the guidelines and above 1.36 m/s^2 for the limits derived by the tests.

It is evident that the limits proposed by the codes satisfy the comfortability of the pedestrians that are standing on the bridge and not of those that are crossing it. Those limits

Table 4.1 Limits of accelerations and displacements for comfortability of active people

Active Pedestrians			
Comfort	a_{max} $[m/s^2]$	a_{rms} $[m/s^2]$	u $[mm]$
Good	$0.00-3.15$	$0.00-1.80$	$0.00-2.00$
Medium	$3.15-5.80$	$1.80-3.60$	$2.00-6.50$
Bad	>5.80	>3.60	>7.00

can indeed be used in the case that the bridge will be placed in a picturesque or very busy area, where people will often stop and stand on it and it will be important for the client to ensure maximum comfort for the standing pedestrians. Nevertheless, it is conservative to design for the comfort of standing pedestrians since they can walk off the bridge anytime they experience discomfort.

When it comes to the use of the comfort limits with respect to the maximum accelerations or with respect to the root mean square accelerations, the following two things were noticed:

- The phenomenon where the same high acceleration value could correspond to different comfort levels disappears when root mean square accelerations are considered instead of maximum accelerations.
- The comfort limits expressed with regard to the root mean square acceleration are lower than in the case they are expressed as maximum accelerations, reduced almost by half for the case of active pedestrians.

Therefore in the case of testing the serviceability of existing structures, where some high peaks are observed locally only a few times, checking the root mean square acceleration with the corresponding limits is less conservative. For example, if the maximum peak is much higher than the rest peaks but it is only observed once or twice throughout the test, it could be caused because of a local disturbance or an error and it wouldn't be necessarily perceived by the pedestrians, since they would be only exposed to this acceleration for a very short period of time. Using the root mean square accelerations, helps to prevent cases like that. However, for the design of new structures, when performing a dynamic analysis of the bridge, those local peaks are not present and if the load model is sufficiently accurate, the maximum accelerations and displacements calculated will simulate the real accelerations that will develop in the footbridge. In that case, the limits for the maximum accelerations can be used.

Table 4.2 Limits of accelerations and displacements for comfortability of passive people

Passive Pedestrians			
Comfort	a_{max} $[m/s^2]$	a_{rms} $[m/s^2]$	u $[mm]$
Good	$0.00-0.60$	$0.00-0.15$	$0.00-0.30$
Medium	$0.60-1.36$	$0.15-1.00$	$0.50-1.40$
Bad	>1.36	>1.00	>1.40

Table 4.3 Limits of accelerations and displacements for feeling of safety of active people

Active Pedestrians			
Safety	a_{max} $[m/s^2]$	a_{rms} $[m/s^2]$	u $[mm]$
Safe	$0.00-5.90$	$0.00-3.60$	$0.00-6.50$
Unsafe	>5.90	>3.60	>6.50

Table 4.4 Limits of accelerations and displacements for feeling of safety of passive people

Passive Pedestrians			
Safety	a_{max} $[m/s^2]$	a_{rms} $[m/s^2]$	u $[mm]$
Safe	$0.00-1.50$	$0.00-1.00$	$0.00-2.00$
Unsafe	>1.50	>1.00	>2.00

Table 4.5 Limits of accelerations for comfortability according to Setra and EUR23984 [49]

Comfort Class	Degree of comfort	Vertical a_{limit} $[m/s^2]$
CL 1	Maximum	< 0.50
CL 2	Medium	$0.50 - 1.00$
CL 3	Minimum	$1.00 - 2.50$
CL 4	Unacceptable discomfort	> 2.50

4.3.1 Remarks

The limits proposed in this chapter are the outcome of a number of tests that were performed on 3 footbridges, above small canals at a rural area. The natural frequencies of the bridges varied between $4 - 6.5\ Hz$, the number of people that participated in the experiments were 7 and their age varied from 23-29 years old. The source of the vibrations (pedestrian loads) was known. Finally, no relation was observed between the mass of the pedestrians and the dynamic characteristics of the footbridges (natural frequency and/or damping ratio), so no conclusion for the human-structure interaction could be made. However, the mass of the pedestrians was low compared to the mass of the bridge. More specifically the total mass of the seven pedestrians was approximately 4% of the total mass of the bridge. It is possible that a higher percentage would cause noticeably changes in the dynamic characteristics of the vibrations.

It is recommended for further studies to perform more tests in a greater number of bridges, with more pedestrians participating. Moreover, it would be ideal to perform these experiments on footbridges with even lower natural frequencies. Finally, using more accurate ways to measure the displacements and the accelerations could also lead to improved, more clear results.

Chapter 5

Application of Theoretical Pedestrian Loads on the Model of Excercitsiebrug

As mentioned in Chapter 2, the different codes and guidelines suggest to follow certain models to predict the dynamic behavior of the footbridges under pedestrian loading and to verify if the serviceability criteria are met. However, these models are in most cases simplified sinusoidal loads of one term, consisting either of one concentrated moving force across the bridge, or of a distributed sinusoidal load over the length of the bridge. Even though the modern codes present a variety of ways to calculate the maximum acceleration induced by walking or running loads, when it comes to vandal loading the modern codes lack information concerning designing against vandal loading.

The purpose of this chapter is to simulate the pedestrian loads for walking, running and jumping proposed by the different researchers and compare them with the real loads applied on the bridges tested. Since it was not possible to measure the force that was applied by the pedestrians while they were walking on the bridge, the validity of the proposed loads will be checked by comparing the response (accelerations and displacements) measured during the tests performed on one of the tested bridges and the response that resulted from the FEM analysis of this bridge.

The chosen bridge is called Excercitiebrug and it is a bridge that was constructed by the municipality of Rotterdam a few months before the test took place. The deck of the footbridge was fabricated at the factory with an initial length of 20.04 m and later on, when the parapets were added, it was transferred to the site, where it got clamped at both sides with a final length of 17.04m. Consequently, the material and cross-sectional properties used in the design were known and since only little time had passed since its construction, the bridge hadn't undergone degradation. By knowing the weight of the people participating in

the test and their walking/running/jumping frequency, as well as the damping ratio in each one of the tests performed it was possible to perform a quite realistic simulation.

5.1 Modeling of Excercitiebrug

The bridge was simulated by use of the software VericalX, a FEM program (Figure 5.1) developed by dr.ir C.B.M. Blom. The properties of the cross-section and of the material are presented in table 5.1, whereas more information about how a dynamic analysis is performed in a FEM program is provided in Appendix C.

Table 5.1 Cross-sectional and material properties of Excercitiebrug

Modulus of Elasticity	E	$[MPa]$	18365
Poisson ratio	ν	$[-]$	0.2
Shear Modulus	G	$[MPa]$	7652
Density	ρ	$[ton/m^3]$	0.619
Cross-sectional area	A	$[m^2]$	0.438
Moment of inertia	I_y	$[m^4]$	$22.65 \cdot 10^{-4}$
Length	L	$[m]$	17.04

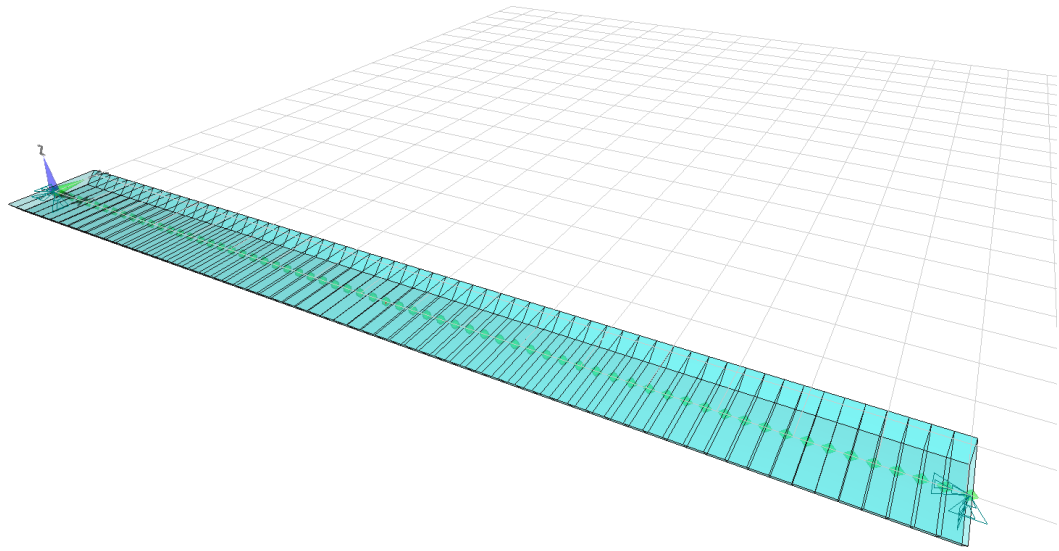

Figure 5.1 Finite Element Model of Excercitiebrug in VericalX

5.2 Overview of the theoretical load models applied

According to the bibliography, the vertical pedestrian loads can be expressed in the frequency domain as the Fourier series presented in equation 5.1.

$$F_v(t) = G_0 \left(1 + \sum_{n=1}^{k} a_{n,v} \sin(2\pi n f t - \phi_{n,v}) \right) \tag{5.1}$$

The DL factors $a_{n,v}$ and the phase angles $\phi_{n,v}$ proposed by the different authors are presented in table 5.2. Note that the loads according to Young, Schulze and SYNPEX for running included 4 or 5 terms, however since the FEM program used had a limitation of up to 3 terms and since the last terms had a very small influence to the load, it was decided not to take them into account.

Table 5.2 Dynamic load factors and phase angles for different types of loading according to different authors

Walking	Bachmann	$a_1 = 0.4$ $\phi_1 = 0$	$a_2 = 0.1$ $\phi_2 = \frac{\pi}{2}$	$a_3 = 0.1$ $\phi_3 = \frac{\pi}{2}$
	Young	$a_1 = 0.37(f_s - 0.95)$ $\phi_1 = 0$	$a_2 = 0.054 + 0.0088 f_s$ $\phi_2 = 0$	$a_3 = 0.026 + 0.015 f_s$ $\phi_3 = 0$
	Schulze	$a_1 = 0.37$ $\phi_1 = 0$	$a_2 = 0.1$ $\phi_2 = 0$	$a_3 = 0.12$ $\phi_3 = 0$
	Kerr	$a_1 = 0.4$ $\phi_1 = 0$	$a_2 = 0.07$ $\phi_2 = 0$	$a_3 = 0.06$ $\phi_3 = 0$
	SYNPEX	$a_1 = 0.0115 f_s^2 + 0.2803 f_s - 0.2902$ $\phi_1 = 0$	$a_2 = 0.0669 f_s^2 + 0.1067 f_s - 0.0417$ $\phi_2 = -99.76 f_s^2 + 478.92 f_s - 387.8 [^o]$	$a_3 = 0.0247 f_s^2 + 0.1149 f_s - 0.1518$ $\phi_3 = -150.88 f_s^3 + 819.65 f_s^2 - 1431.35 f_s + 811.93 [^o]$ if $f_s < 2Hz$ $\phi_3 = 813.12 f_s^3 - 5357.6 f_s^2 + 11726 f_s - 8505.9 [^o]$ if $f_s \geq 2Hz$
Running	Bachmann	$a_1 = 1.6$ $\phi_1 = 0$	$a_2 = 0.7$ $\phi_2 = 0$	$a_3 = 0.2$ $\phi_3 = 0$
	ISO10137	$a_1 = 1.4$ $\phi_1 = 0$	$a_2 = 0.4$ $\phi_2 = 0$	$a_3 = 0.1$ $\phi_3 = 0$
Jumping	Bachmann	$a_1 = 1.7$ $\phi_1 = 0$	$a_2 = 1.1$ $\phi_2 = 0$	$a_3 = 0.5$ $\phi_3 = 0$

5.2.1 Walking

The first test consisted of a pedestrian with self-weight $G_0 = 920N$ crossing the bridge with a step frequency of $f_s = 2.8Hz$ and an approximate velocity of $v = 1.4m/s$. The damping of the bridge in that particular crossing was found to be 5%.

The response of accelerations and the displacements of the bridge for a single pedestrian crossing are presented through figures 5.2 to 5.6 for the different authors.

From the presented graphs that are associated with the response of the bridge due to walking loads, the following observations can be made: the load model proposed by SYNPEX overestimates both the accelerations and the displacements induced when the real weight of the pedestrian is used. The models proposed by Kerr, Young and ISO10137 conclude into

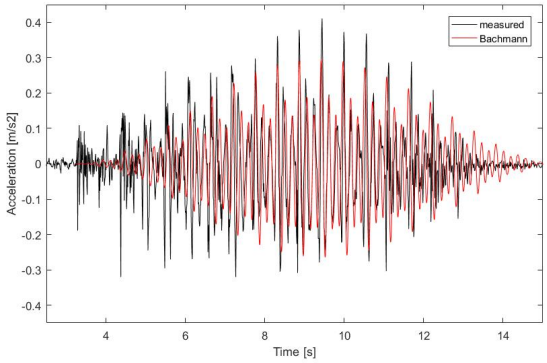

(a) Accelerations

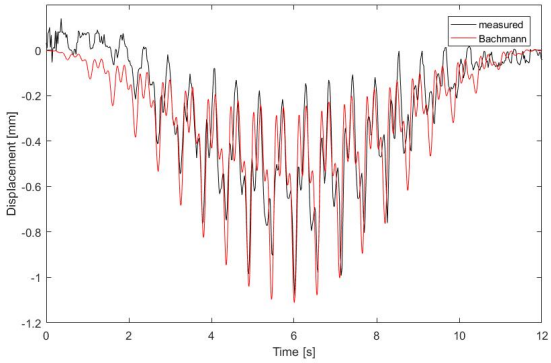

(b) Displacements

Figure 5.2 Accelerations and displacements determined according to the Bachmann model for 1 pedestrian walking

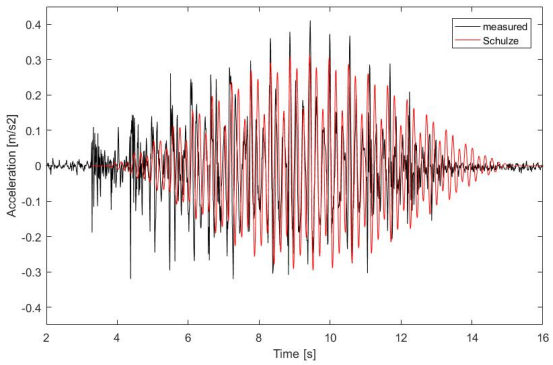

(a) Accelerations

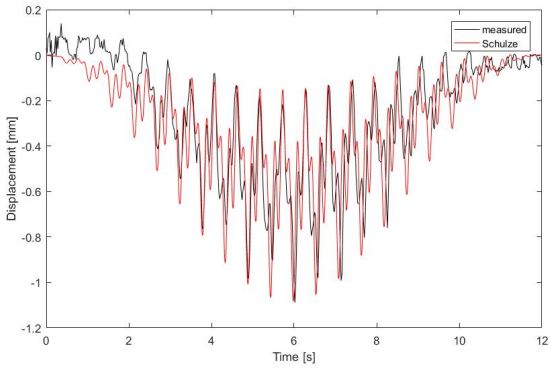

(b) Displacements

Figure 5.3 Accelerations and displacements determined according to the Schulze model for 1 pedestrian walking

very similar results for the accelerations and the displacements, however they underestimate the response of the structure, giving lower expected values than the ones measured. The load models that best match the behavior of the bridge are the ones proposed by Bachmann and Schulze. More specifically, the Bachmann model gives a better representation of the acceleration, predicting in a more accurate way the highest and lowest peaks of the accelerations whereas the model of Schulze enters two high peaks next to each other. On the other hand, the displacement is best described by the model of Schulze. Nevertheless, both models predict a maximum acceleration of 0.3 m/s^2 and fail to predict the actual maximum acceleration reached, which is 0.4 m/s^2.

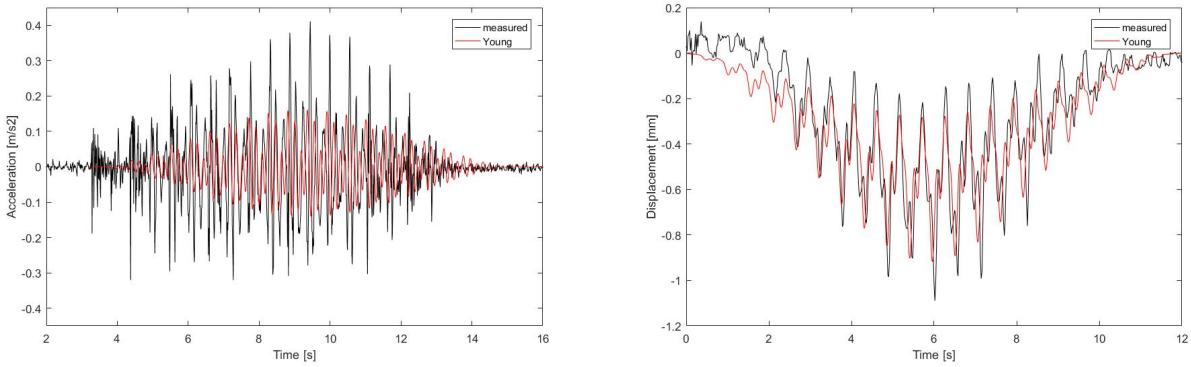

(a) Accelerations (b) Displacements

Figure 5.4 Accelerations and displacements determined according to the Young model for 1 pedestrian walking

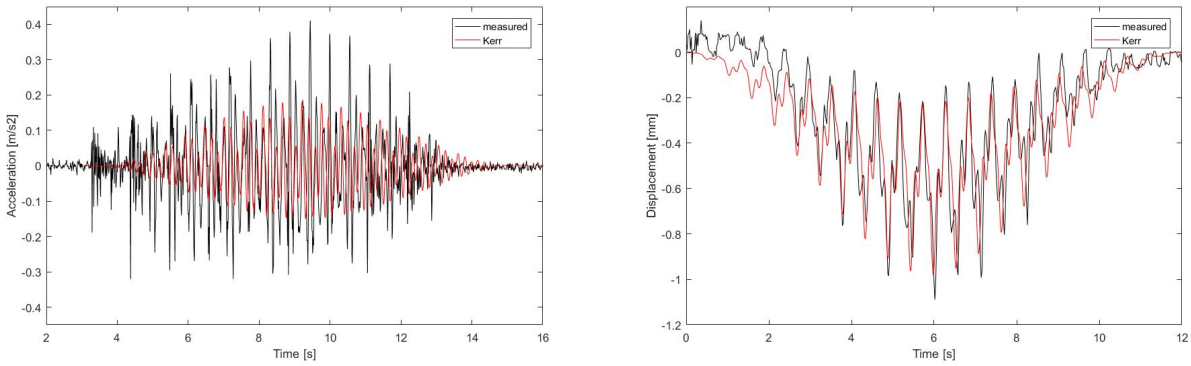

(a) Accelerations (b) Displacements

Figure 5.5 Accelerations and displacements determined according to the Kerr model for 1 pedestrian walking

5.2.2 Running

In the case of running, the subject running was weighting $G_0 = 920\ N$ and the step frequency and velocity measured were approximately: $f_s = 2.87\ Hz$ and $v = 2.84\ m/s$ respectively. The damping of the bridge was still measured equal to $\xi = 5\%$. The number of proposed models for running loads are less than for walking, with only 2 available suggestions, a model proposed by Bachmann and a model proposed proposed by ISO. Generally, the DLF for the running loads are more than 3 times higher than the DLF proposed for walking, resulting in final running loads that can easily change sign over time.

Unlike the case of walking, during running the jogger's feet are not constantly in contact with the deck, but a period of time is spent on air. Moreover, it is impossible for a pedestrian

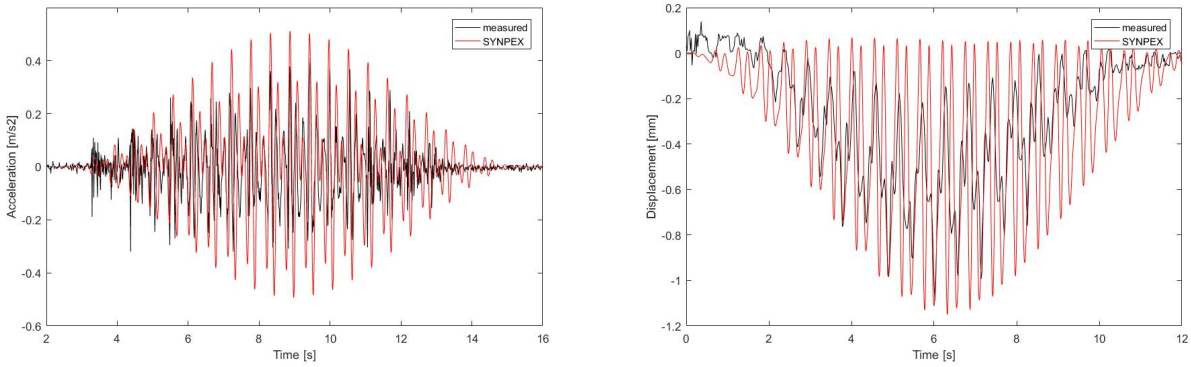

(a) Accelerations (b) Displacements

Figure 5.6 Accelerations and displacements determined according to the SYNPEX model for 1 pedestrian walking

to apply direct tension on the deck of the bridge while moving on it. In consideration of these two facts, some researchers propose to modify the load applied by the joggers by setting its value to zero when there is no contact between the jogger and the deck. In this thesis both cases were tested, first the case where the running load could change sign and secondly the case where there was a time period of no contact, when the force applied would turn to zero, like presented in equation A.2.

$$F(t) = \begin{cases} G_0 \cdot \left(1 + \sum_{n=1}^{k} a_{n,v} \sin(2\pi n f t - \phi_{n,v})\right), & \text{if } F(t) < 0 \\ 0, & \text{otherwise.} \end{cases} \tag{5.2}$$

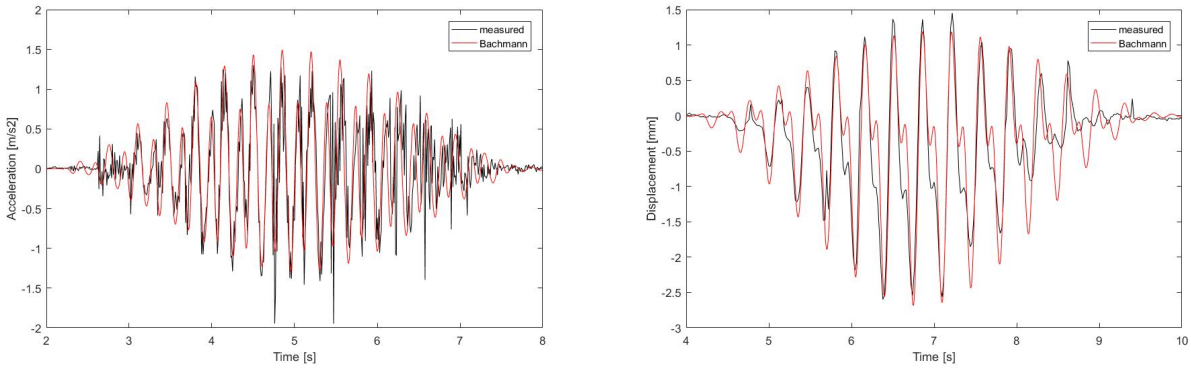

(a) Accelerations (b) Displacements

Figure 5.7 Accelerations and displacements determined according to the Bachmann model for 1 pedestrian running

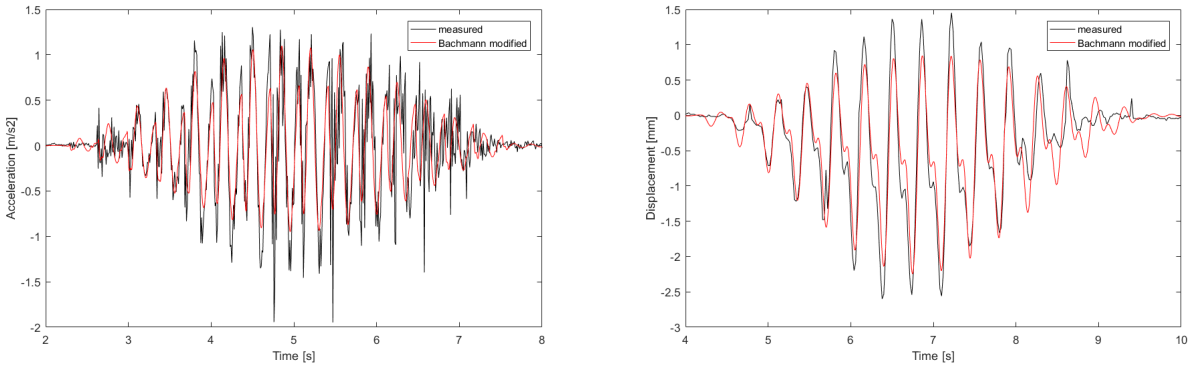

(a) Accelerations (b) Displacements

Figure 5.8 Accelerations and displacements determined according to the modified Bachmann model for 1 pedestrian running

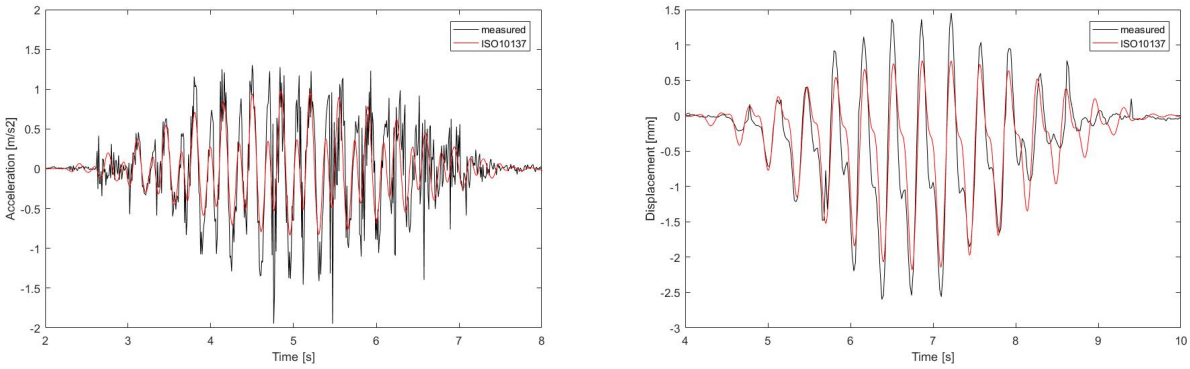

(a) Accelerations (b) Displacements

Figure 5.9 Accelerations and displacements determined according to the ISO10137 model for 1 pedestrian running

Unlike what might have been expected, the more realistic load consideration, where a time of no contact is taken into account during which no force is applied (figures 5.8 and 5.10) gives less accurate results than the case where the load is applied continuously and is allowed to change direction. The prediction resulting from the application of the original Bachmann model is approximating very satisfyingly the real response of the structure (figure 5.7). The calculated displacements match almost perfectly the measured ones, whereas the accelerations have a good fit as well, with the maximum calculated acceleration being exceeded locally only two times.

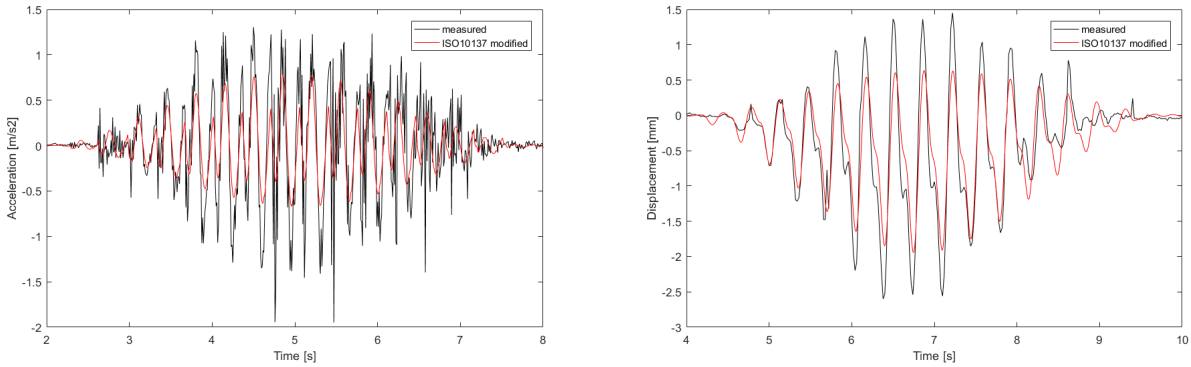

(a) Accelerations (b) Displacements

Figure 5.10 Accelerations and displacements determined according to the modified ISO10137 model for 1 pedestrian running

5.2.3 Jumping

When it comes to jumping, the test subject had a weight of $G_0 = 920\,N$ and was jumping with a frequency equal to the natural frequency of the bridge $f_s = 4.67\,Hz$, keeping it constant with the help of a metronome. Just like in the case of running, during one jump circle, the vandal spends an amount of time in contact with the deck and the rest of the jump circle on air. Therefore, the same two considerations will be taken into account for the vandal loading. Firstly, a continuous load that can change direction of application will be considered according to Bachmann, and secondly, the same load will be applied but the change in direction will be restricted, resulting consequently in a fraction of time where the applied force is zero (no contact).

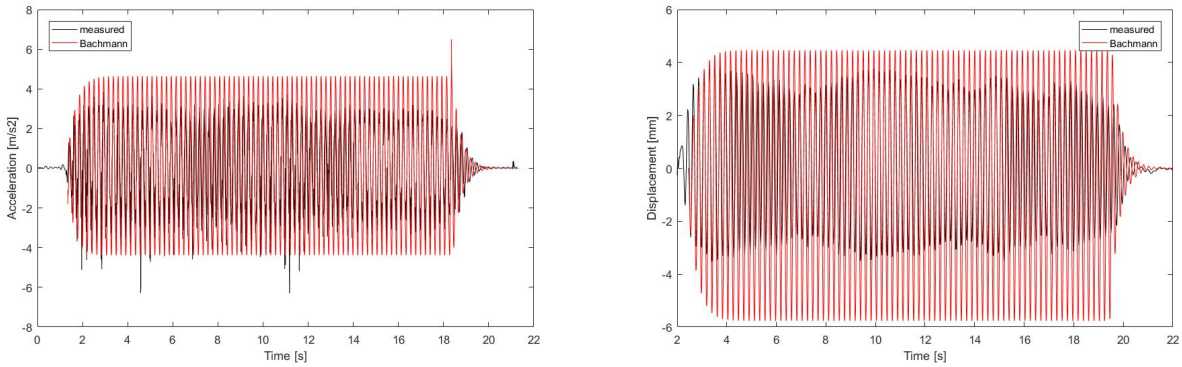

(a) Accelerations (b) Displacements

Figure 5.11 Accelerations and displacements determined according to the Bachmann model for 1 pedestrian jumping

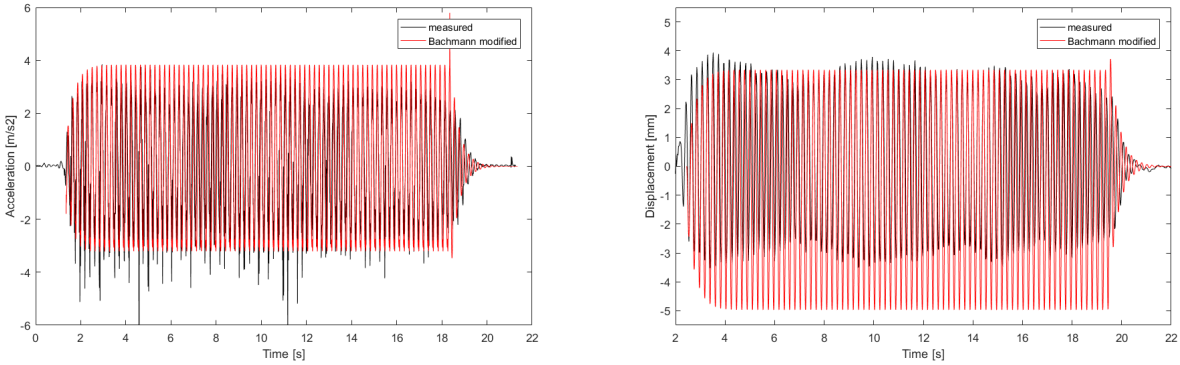

(a) Accelerations (b) Displacements

Figure 5.12 Accelerations and displacements determined according to the modified Bachmann model for 1 pedestrian jumping

By comparing the two different cases of the vandal loading one can see that in the case that the vandal loading is considered a continuous function of time that can also change sign, the accelerations and displacements are higher than in the other case. When comparing the results of the FEM analysis with the measured time-histories of the accelerations and displacements it is apparent that the less conservative and closer to the reality load case is the one that takes into account the time interval when the vandal is on air (figure 5.12). In both cases, the accelerations measured on site exceed locally the numerically calculated accelerations. However, the analyses were performed assuming a very high damping ($\xi = 9\%$) in order to simulate the real behavior of the bridge as much as possible. Usually when a dynamic analysis is performed, a lower structural damping is assumed. A lower structural damping will lead to increased accelerations and displacements, and therefore taking into account a more stringent model to counterpart the local peaks of the accelerations of this test, is considered conservative.

After investigating which load models best simulate the real force applied by a single pedestrian, it is interesting to observe what happens when more than one pedestrians are on the bridge. The cases when two and four people were walking, running and jumping on the bridge perfectly synchronized were considered and the results of the analyses were plotted against the results from the test measurements. The graphs can be seen in figures 5.13 to 5.18.

From the graphs it can be seen that the response of the bridge in reality is lower than the one predicted by the FEM analyses, for full synchronization of the pedestrians; and the difference between the predicted value and the measured one increases with increasing

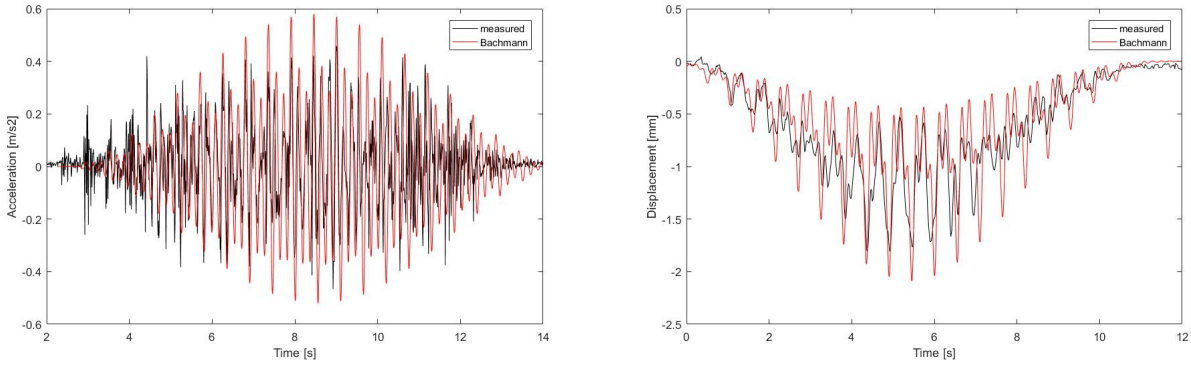

(a) Accelerations (b) Displacements

Figure 5.13 Accelerations and displacements determined according to the Bachmann model for 2 pedestrians walking synchronized

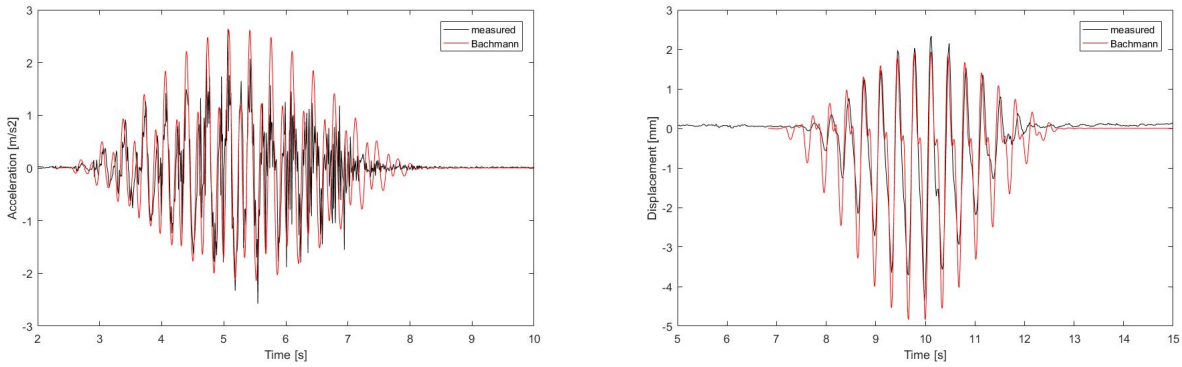

(a) Accelerations (b) Displacements

Figure 5.14 Accelerations and displacements determined according to the Bachmann model for 2 pedestrians running synchronized

number of people. That could be another way to correlate the load applied on the bridge with the number of users and the synchronization among themselves.

All in all, after investigating which pedestrian load models resemble better the real behavior of the bridge tested, it can be concluded that for walking the load models proposed by Bachmann and Schulze work best, however without predicting the maximum accelerations developed. A solution to that could be to use either higher load factors or to check instead of the maximum accelerations, the maximum displacement amplitude that was predicted with a better approximation. Concerning running it can be concluded that the model proposed by Bachmann is a very accurate approximation and can be used when a more realistic load than the ones proposed in the codes needs to be used. Finally, the modified model of Bachmann

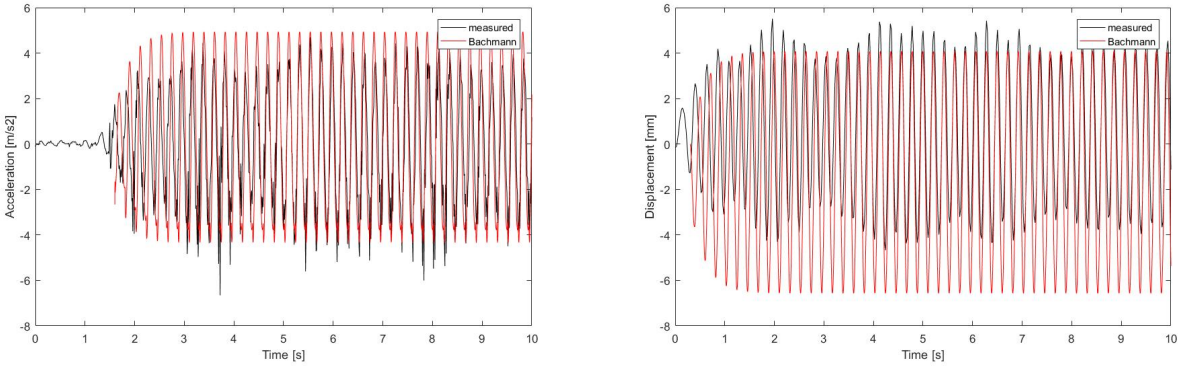

(a) Accelerations (b) Displacements

Figure 5.15 Accelerations and displacements determined according to the modified Bachmann model for 2 pedestrians jumping synchronized

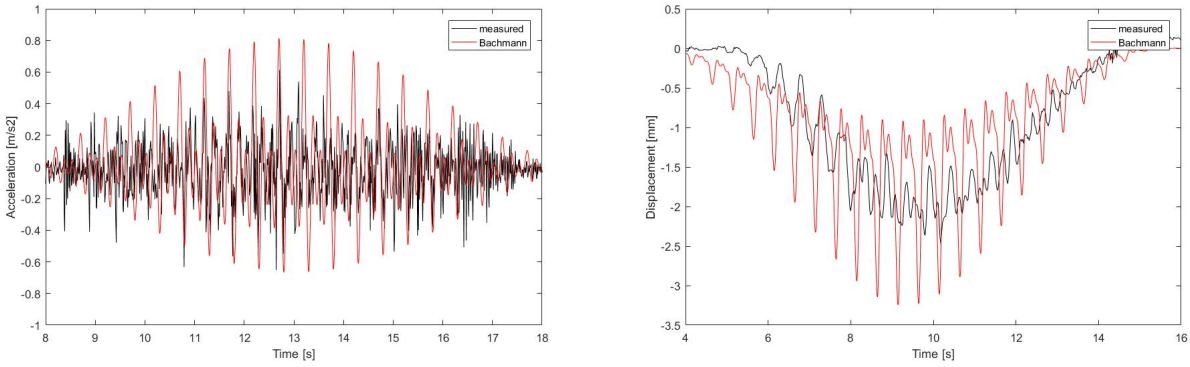

(a) Accelerations (b) Displacements

Figure 5.16 Accelerations and displacements determined according to the Bachmann model for 4 pedestrians walking synchronized

for jumping loads seems to be a good approximation and due to the absence of other proposed models for vandal loading in the codes, it will be used from now on for further verifications.

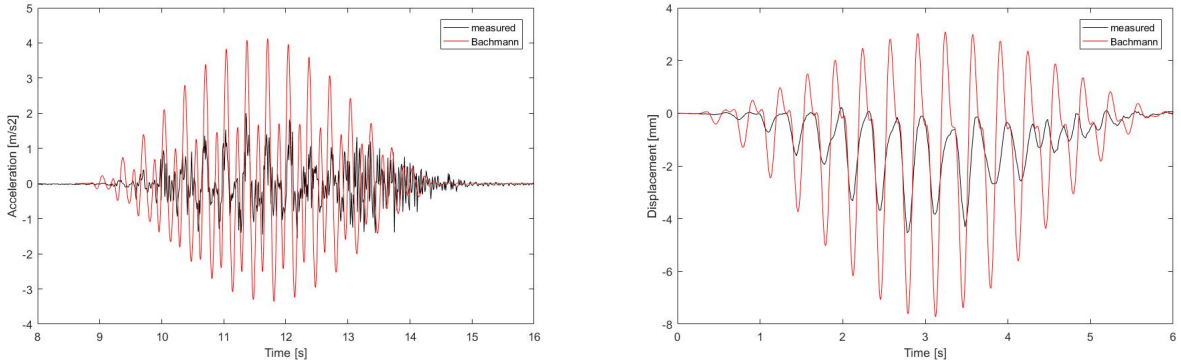

(a) Accelerations (b) Displacements

Figure 5.17 Accelerations and displacements determined according to the Bachmann model for 4 pedestrians running synchronized

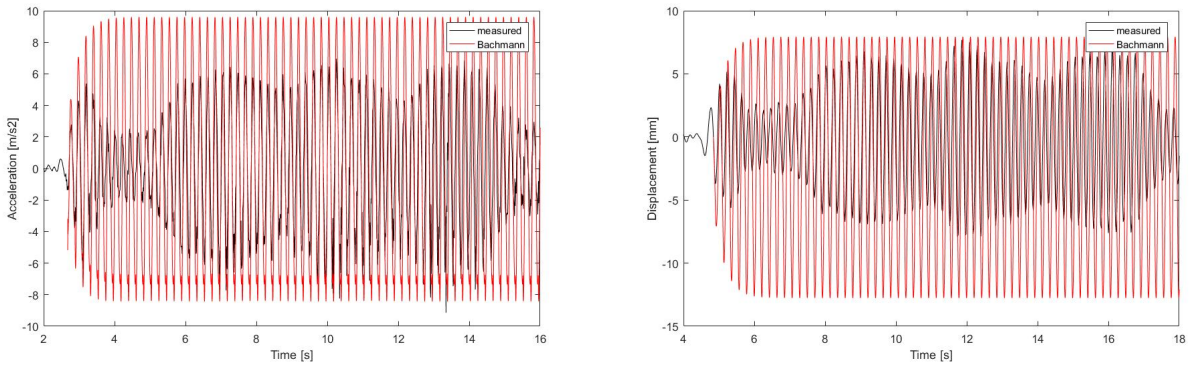

(a) Accelerations (b) Displacements

Figure 5.18 Accelerations and displacements determined according to the modified Bachmann model for 4 pedestrians jumping synchronized

Chapter 6

Dynamic Analysis and serviceability of pedestrian bridge from UHPFRC

The main purpose of this chapter is to analyze the dynamic behavior of a pedestrian bridge built from UHPFRC, due to human-induced vibrations. Initially, the analyses will be performed according to the load models proposed by the different codes and guidelines. The identified accelerations will be compared with the acceleration limits proposed by each code, to check whether the design satisfies the required comfort criteria. Moreover, the more realistic load models described in the previous chapter will be applied, and their effect on the bridge will be compared with the acceleration and deflection limits derived from the tests on site (described in chapter 4). Finally, since no model is proposed by the codes for checking bridges against vandal loading, the dynamic behavior of the bridge due to vandal loading will be tested for different number of vandals, different structural damping ratios and different frequencies of jumping.

6.1 Design of pedestrian bridge from UHPFRC

The footbridge used in the analysis is a post-tensioned single-span bridge, clamped at both ends, with a length of $L = 18.54m$ and a rectangular cross-section of dimensions $h \times b = 0.25m \times 1.9m$ (figures 6.1 and 6.2). Consequently, the bridge has a big slenderness of $\lambda = 1/74.16$. The prestressing tendons have a parabolic profile, with eccentricities $e_{sup} = 40mm$ at the supports and $e_{mid} = 53mm$ at midspan. The material chosen for the design is the concrete of B170/200 of Ductal. The design procedure, from the determination of the tendon profile to the calculation of the prestressing losses and the check of the bending moment and shear capacity of the cross sections are presented in Appendix D.

Table 6.1 Geometrical properties of bridge

Length $[m]$	L	18.54
Height $[m]$	h	0.25
Width $[m]$	b	1.90
Area $[m^2]$	$A_c = b \cdot h$	0.475
Moment of Inertia $[m^4]$	$I_c = \frac{1}{12} b \cdot h^3$	$24.74 \cdot 10^{-4}$

Table 6.2 Material properties of B170/200

Characteristic compressive strength	f_{ck}	$170MPa$
Characteristic tensile strength	$f_{ctk_{0.05}}$	$9MPa$
Modulus of elasticity	E_c	$58GPa$
Density	ρ	$2500kg/m^3$

Table 6.3 Prestressing properties

Maximum Prestressing force	P_{max}	$[kN]$	6534.00
Prestressing force at $t = 0$	P_{m0}	$[kN]$	6277.50
Prestressing force at $t = \infty$	$P_{m\infty}$	$[kN]$	5289.13
Eccentricity at support	e_{sup}	$[mm]$	-40
Eccentricity at mid-span	e_{mid}	$[mm]$	53
Area of prestressing	A_p	$[mm^2]$	4500

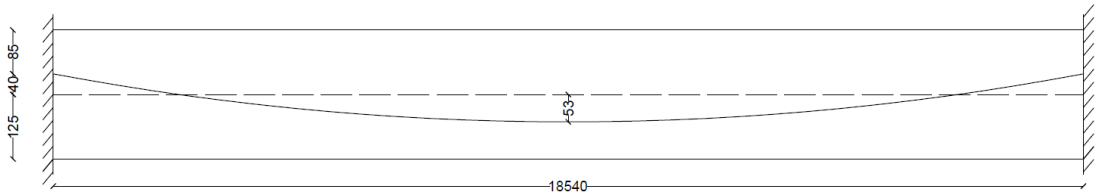

Figure 6.1 Tendon profile of footbridge (length measured in mm)

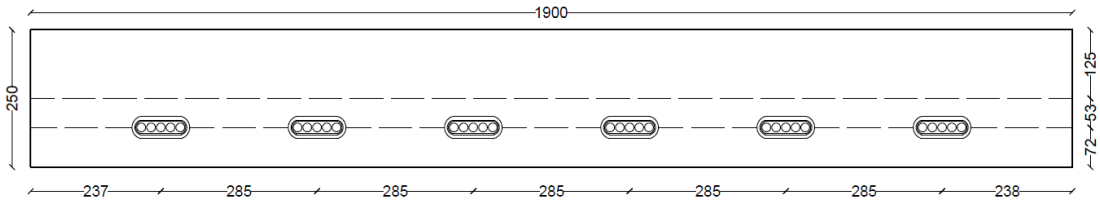

Figure 6.2 Cross-section of mid-span (length measured in mm)

6.2 Dynamic behavior of footbridge according to the codes

Once the geometrical and material properties of the bridge are defined, the dynamic properties of the bridge can also be determined. The stiffness, the mass and the boundary conditions are the parameters that define the natural frequency of the footbridge. The first natural frequency of a single-span bridge with clamped supports, is given by formula 6.1.

$$f_0 = \frac{22.4}{2\pi}\sqrt{\frac{EI}{\rho AL^4}} = 3.60Hz \tag{6.1}$$

A critical parameter that influences the dynamic behavior of the structure is the damping ratio of the structure ξ. In the verification of the comfort criteria, the damping ratio proposed by the corresponding code will be used. However, it should be kept in mind that the damping properties of a structure are difficult to be characterized.

In the following subsections is presented the verification of the comfort of the footbridge, according to the different codes. It is reminded that a verification is necessary if the natural frequency of the footbridge is smaller than 5 Hz. The applied loads vary from code to code, for the British Standards and British National Annex a concentrated pulsating force is applied that moves across the footbridge, whereas in Setra and EUR 23984 a distributed sinusoidal load is applied on the deck of the footbridge. The maximum accelerations obtained by the load model proposed by each code are compared with the corresponding acceleration limits to verify that a good comfort level is assured.

6.2.1 British Standards

According to the British Standards, for the determination of the maximum acceleration, a vertical pulsating load $F = 180\sin(2\pi f_0 t) = 180\sin(22.62t)$ (in N), is applied on the structure, that moves across the span with a constant speed of $v_t = 0.9 f_0 = 3.24\ m/s$. The British Standards propose a logarithmic decrement of $\delta = 0.05$ for prestressed concrete, therefore in this case the structural damping ratio used is $\xi = \delta/(2\pi) = 0.8\%$. The response of the acceleration is presented in 6.3. The maximum acceleration developed according to this model is equal to $a_{max} = 0.48\ m/s^2$ (figure 6.3), whereas the acceleration limit that ensures the comfortability of the pedestrians is given by $a_{lim} = 0.5\sqrt{f_0} = 0.95\ m/s^2$. Consequently, the comfort criteria are satisfied.

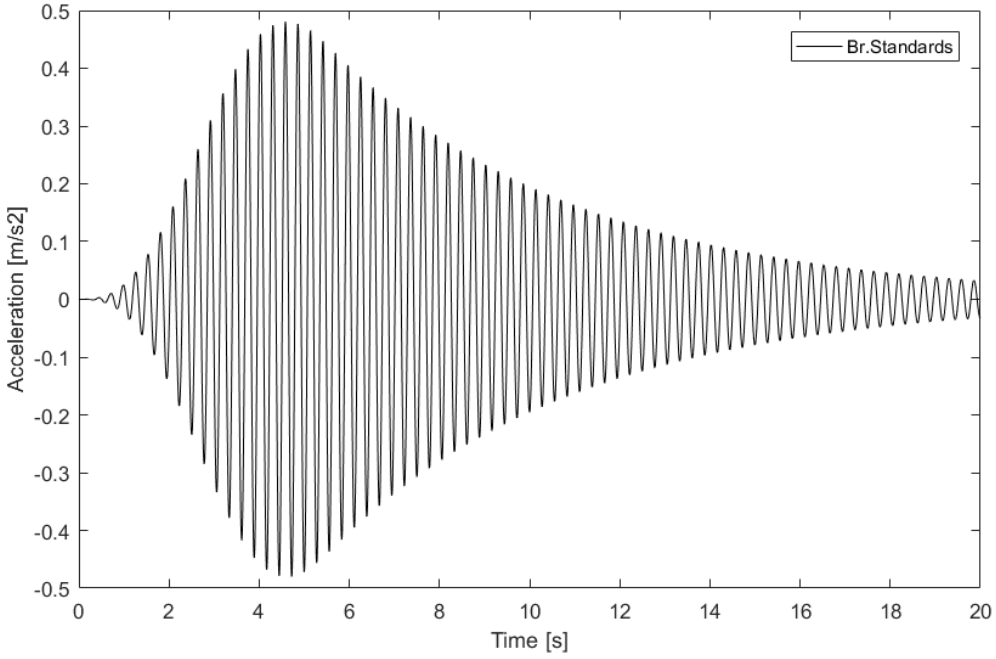

Figure 6.3 Acceleration response according to British Standards

6.2.2 British National Annex of EN1

As mentioned already in Chapter 2, the British National Annex categorizes the bridge into four different classes, according to the bridge usage. By choosing a bridge of class D, that is used as "primary access to major public assembly facilities like sports stadia or major transportation facilities" the recommended group sizes for walking and running, as well as the crowd density for walking are found. The damping ratio, according to EN1 for prestressed

concrete is given by: $\xi = 1 + 0.07 \cdot (20 - L) = 1.1\%$. The vertical pulsating force for groups is given by the equation 6.2, whereas the vertical pulsating distributed crowd load by equation 6.3. The factors for the different load cases applied are presented in Table 6.4.

$$F = F_0 k(f_v) \sqrt{1 + \gamma(N-1)} \sin(2\pi f_v t) \tag{6.2}$$

$$w = 1.8 \frac{F_0}{A} k(f_v) \sqrt{\gamma N/\lambda} \sin(2\pi f_v t) \tag{6.3}$$

Table 6.4 Dynamic actions representing pedestrian groups according to Br. National Annex of EN1

	Groups		Crowd
	Walking	Running	Walking
Number N /density of pedestrians $\rho\ [p/m^2]$	16	4	1.5
Load amplitude $F_0\ [N]$	280	910	280
Combined factor $k(f_v)$	0.36	0.12	0.36
Reduction factor γ	0.42	0.42	0.09
Reduction factor λ	–	–	0.634
Velocity $v\ [m/s^2]$	1.7	3	–
Applied load	$272\sin(22.63t)$	$164\sin(22.63t)$	$15\sin(22.63t)$
Maximum derived accelerations $a_{max}\ [m/s^2]$	0.92	0.41	1.22

The maximum allowed acceleration according to the British Annex should be limited to: $a_{lim} = k_1 k_2 k_3 k_4$. The factors chosen should agree with the bridge class. In this case, it is considered that the bridge functions as primary route for sports stadia or other high usage routes $k_1 = 0.8$, the route redundancy factor is taken as $k_2 = 1$ and the bridge height will be less than $4m$, so $k_3 = 1.1$. The exposure factor k_4 is usually taken as 1. Consequently, the acceleration limit for comfort is: $a_{lim} = 0.88 m/s^2$ and the comfort limit is not satisfied in the case of walking crowds or groups.

6.2.3 Sétra

The guidelines of Sétra require a dynamic analysis for the evaluationg of the comfort criteria if the natural frequency of the bridge is smaller than 5 Hz. The natural frequency of the bridge is $f_0 = 3.6Hz$ that classifies the bridge into Range 3, which corresponds to low risk of resonance. The most severe traffic type, named as Traffic class I, corresponds to urban footbridges subjected to very heavy traffic and dense crowds (like demonstrations and

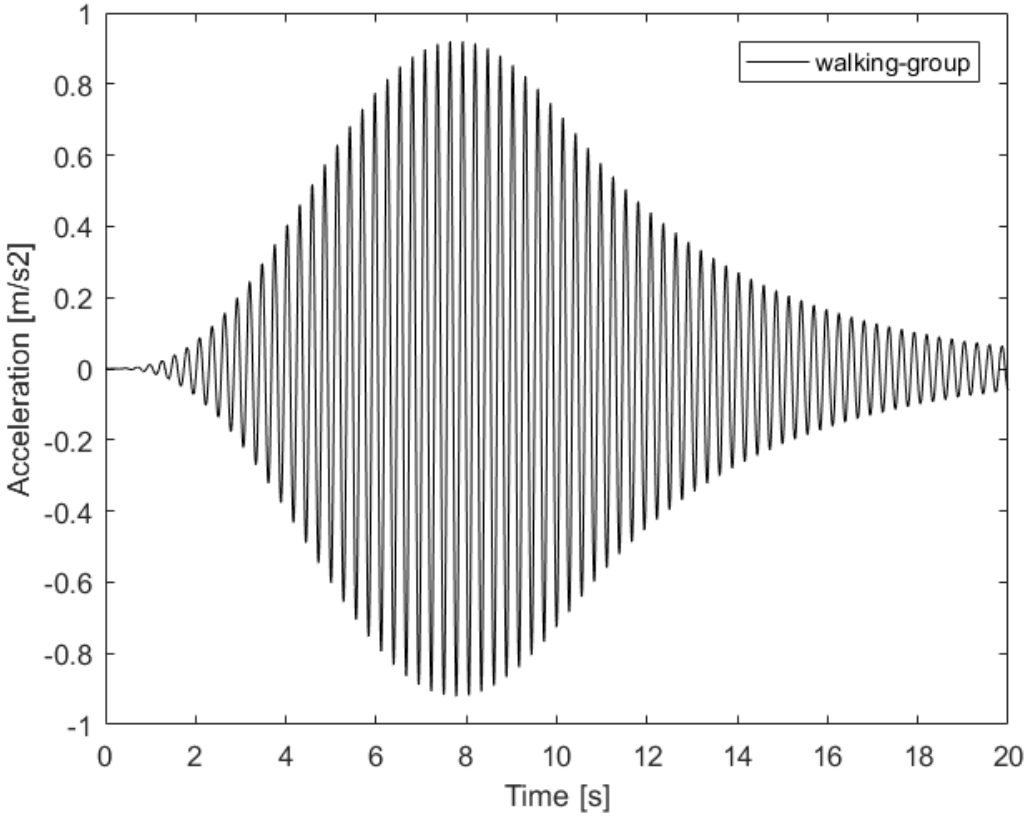

Figure 6.4 Acceleration response for groups walking according to British Annex of EN1

tourists). The combination of the traffic class and the frequency range results in a distributed load over the bridge span given by equation 6.4,

$$w = dF_0 \cos(2\pi f_v t) 1.85 \sqrt{\frac{1}{n}} \psi \tag{6.4}$$

where the crowd density is $d = 1$ person per m^2, the individual force $F_0 = 70\ N$, the equivalent number of pedestrians is $n = d \cdot S = 1 \cdot 1.6 \cdot 18.54 = 29.66$ and $\psi = 1$, whereas the recommended damping ratio for prestressed concrete is $\xi = 1\%$. Therefore the distributed crowd load is equal to:

$$w = 23.78 \cos(22.63t) \left[N/m^2\right]$$

The maximum acceleration calculated is equal to $a_{max} = 2.06\ m/s^2$ which classifies the bridge in a minimum, yet acceptable comfort level of the pedestrians. However, if the traffic class is reduced to class II, "urban footbridge linking populated areas, subjected to heavy traffic that may occasionally be loaded throughout its bearing area", the applied load is

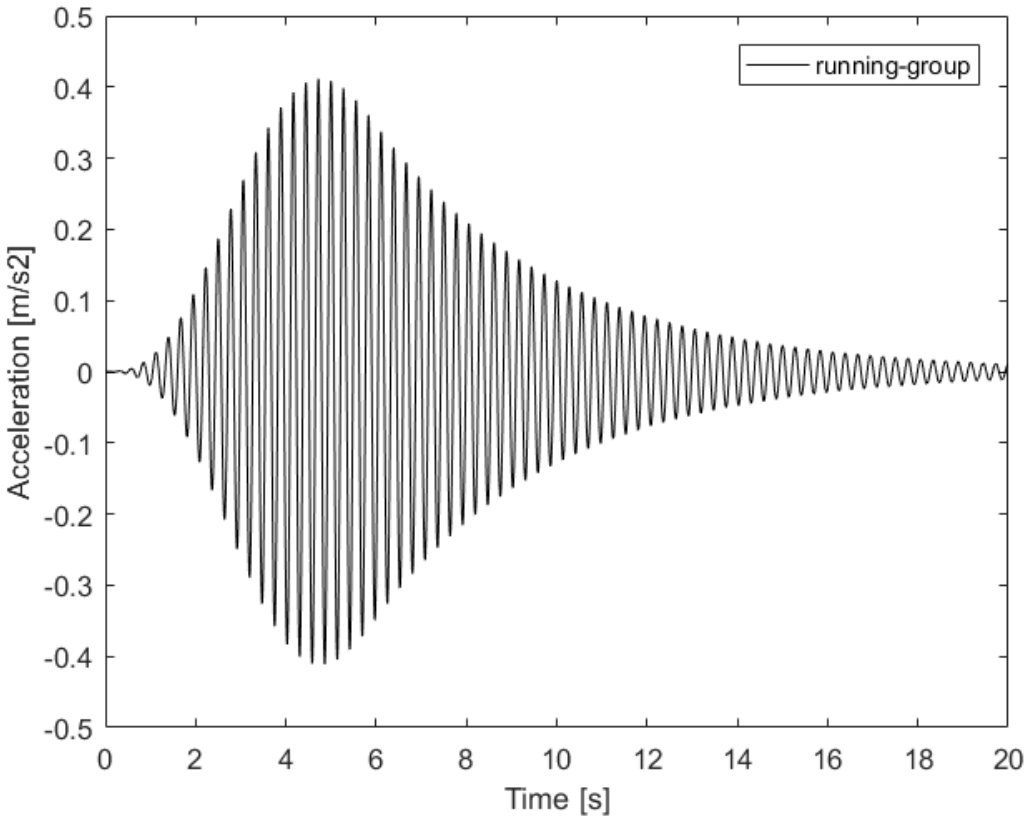

Figure 6.5 Acceleration response for groups running according to British Annex of EN1

reduced to:

$$w = 0.8 \cdot 70\cos(22.63t)10.8\sqrt{\frac{0.01}{0.8 \cdot 1.6 \cdot 18.54}} \qquad = 12.42\cos(22.63t)\left[N/m^2\right]$$

This traffic class gives a maximum acceleration of 1 m/s^2 that classifies the comfort of the pedestrians on the limit between mean and minimum comfort.

6.2.4 EUR23984

Finally, the guidelines of the EUR23984 that are very similar to the ones of Sétra, for a traffic class TC4 with $d = 1P/m^2$, $P = 280N$, $n' = 1.85\sqrt{n}/S$, $n = d \cdot S$, $S = b_{eff}L$, $\psi = 0.25$ and a recommended mean value of damping equal to $\xi = 1\%$, the load distributed on the bridge deck is equal to:

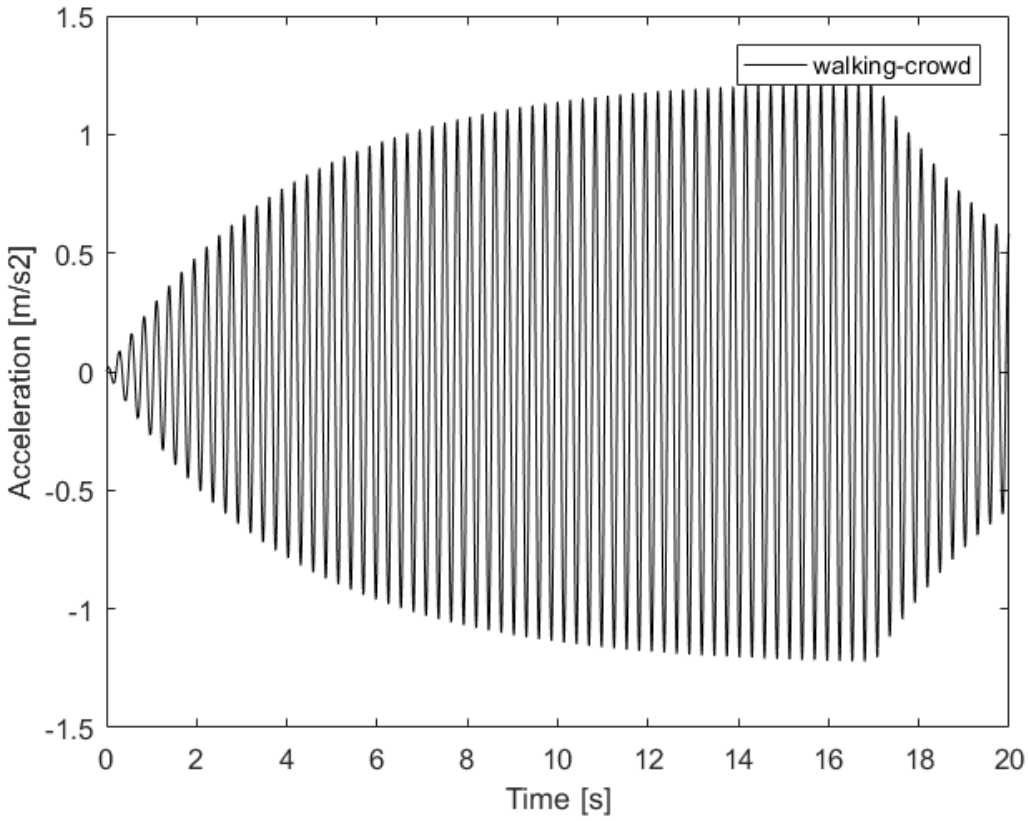

Figure 6.6 Acceleration response for crowds walking according to British Annex of EN1

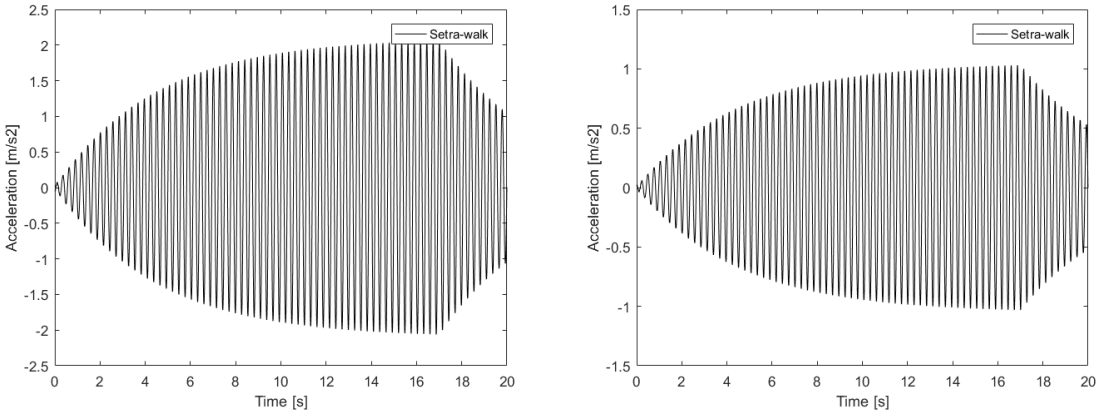

(a) Traffic class I

(b) Traffic class II

Figure 6.7 Response of acceleration for walking crowds according to Setra guidelines for traffic classes I and II

$$p(t) = P\cos(2\pi f_0 t)n'\psi = 280 \cdot \cos(22.63t) \cdot 0.34 \cdot 1 = 23.78\cos(22.63t)\left[N/m^2\right] \quad (6.5)$$

It is apparent that the load distribution according to EUR23984 and to Setra are the same, and consequently so are the maximum accelerations and the comfortability limits.

EUR23984 also proposes a model for the determination of the accelerations when the bridge is excited by joggers. The load consists of a concentrated force moving across the bridge with a velocity $v = 3m/s$, given by the expression 6.6. However, the reduction coefficient ψ is zero for natural frequencies of the structure outside of the range 1.9-3.5 Hz. Therefore in this case, there is no requirement for the application of a jogging load.

$$P(t,v) = 1250\cos(2\pi ft)n\psi \tag{6.6}$$

6.3 Dynamic behavior of the bridge according to more realistic loads

In chapter 5 a comparison was made between the expressions of the pedestrian loads proposed by different researchers. The more realistic loads were found to be the ones proposed by Bachmann. These walking loads will be applied on the bridge for different numbers of people walking.

6.3.1 Walking loads according to Bachmann

Since the exact weight of the pedestrians is not known, a weight of $G = 800\ N$ is chosen. The walking frequency of a pedestrian is between 1.6-2.4 Hz. Two different walking frequencies will be examined, a walking frequency of $f_s = f_0/2 = 1.8\ Hz$ (equal to half the natural frequency), and a walking frequency of $f_s = 2Hz$. The walking load applied on the bridge due to a single pedestrian crossing it with a constant velocity of $v = 1.7m/s$ is given by expression 6.7.

$$F(t) = 0.8 + 0.32\sin(2\pi f_s t) + 0.08\sin\left(4\pi f_s t - \frac{\pi}{2}\right) + 0.08\sin\left(6\pi f_s t - \frac{\pi}{2}\right) \tag{6.7}$$

By the figures 6.8 and 6.9 it is apparent the influence of the step frequency of the pedestrians and its relation to the natural frequency of the footbridge. The maximum acceleration in the case of a frequency of 1.8 Hz is 0.30 m/s^2, whereas the amplitude of the displacements is approximately 0.62 mm. Both the acceleration and displacement satisfy the limits of comfort. Their ratio $a/u = 477\ s^{-2}$ also agrees with the case that good comfort is achieved. In the case of a step frequency of $2Hz$ the maximum acceleration, amplitude of

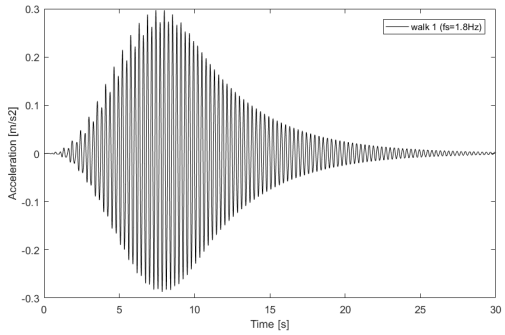

(a) Step frequency $f_s = 1.8Hz$

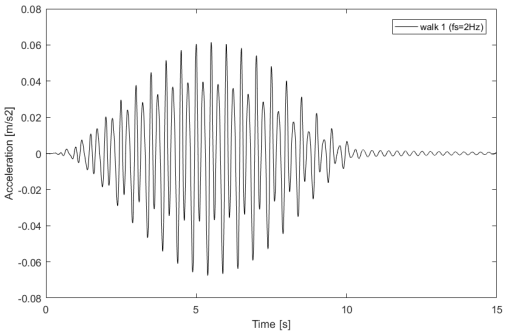

(b) Step frequency $f_s = 2Hz$

Figure 6.8 Response of acceleration for single pedestrian for different step frequencies

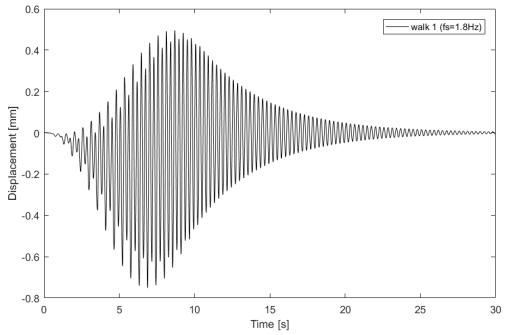

(a) Step frequency $f_s = 1.8Hz$

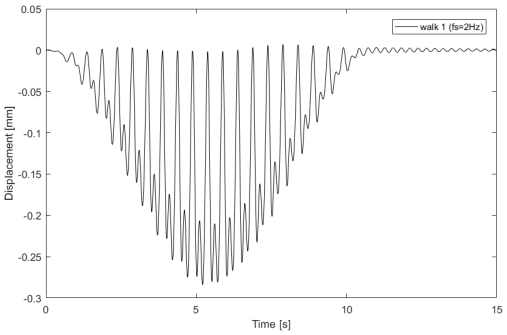

(b) Step frequency $f_s = 2Hz$

Figure 6.9 Response of displacement for single pedestrian for different step frequencies

displacements and ratio a/u are 0.06 m/s^2, 0.15 mm and 422 s^{-2} respectively and therefore the comfort level is very good.

With an increased number of people, the degree of synchronization between themselves and the bridge is reduced. To examine the effect of the synchronization between pedestrians, a group of 8 people walking in line was simulated. In the first case, all 8 pedestrians were walking with the same step frequency $f_s = \frac{f_0}{2} = 1.8Hz$, completely synchronized with each other. In the second case, the 8 pedestrians were walking with step frequencies that were ranging between $[1.7Hz, 1.9Hz]$, so $f_{s_i} = \frac{f_0}{2} \pm 5.5\% \frac{f_0}{2}$. The response of te accelerations and the displacements for the described cases are presented in figures 6.10 and 6.11.

A group of 8 people walking in complete synchronization produces accelerations that can reach a maximum value of $a_{max} = 2.38\ m/s^2$, however when the 8 pedestrians are not fully synchronized but their step frequencies slightly vary, it can be seen that the maximum acceleration falls to a value of $a_{max} = 0.68\ m/s^2$, 3.5 times less than if the pedestrians were completely synchronized. The average amplitude of the displacements when the maximum

acceleration is reached is around 4.7 *mm* (medium comfort according to displacement limits) for the synchronized group and 1.15 *mm* (good comfort) for the unsynchronized one. For the case of the synchronized crowd, the ratio $a/u = 505\ s^{-2}$ is just on the limit between the range of good comfort and the range where bad comfort could appear. For the unsynchronized crowd, both the maximum acceleration and the displacement amplitude are considered to be of good comfort, however the ratio a/u is equal to $590s^{-2}$, which puts the bridge in the critical range where bad comfort can also be noticed. It is apparent, that the ratio a/u cannot stand individually for the characterization of a footbridge as sufficiently comfortable or not.

Even if the pedestrians are completely synchronized, but in a frequency not close to the natural frequency or its dividers, the effect of the synchronization on the response of the bridge is reduced. As an example, the responses of the bridge when the same group of 8 people is walking synchronized with a step frequency equal to $f_s = 2Hz$ or with varying step frequencies between $[1.6, 2.4\ Hz]$ are presented in figures 6.12 and 6.13. The maximum displacements and acceleration are much less than they were for the same synchronized group of people at $f_s = 1.8Hz$.

This can only mean two things. Firstly, that pedestrian loads that represent groups walking with step frequency equal to the natural frequency of the bridge, even if this frequency is out of the bounds of what is considered natural walking (e.g. $f_s > 2.4Hz$), give higher accelerations than the ones expected in reality. Secondly, that the synchronization between the pedestrians has also a big effect on the response of the structure. These two parameters are taken into account in the British Annex through factors $k(f_v)$ and γ and in Sétra and EUR23984 through n' and ψ.

To represent a more realistic case of the traffic flow on a bridge, the following randomly chosen scenario was simulated. A group of 8 people crossing the bridge with direction from the left to the right and random step frequencies varying between 1.6-2.4 Hz. A group of 6 people completely synchronized with $f_s = 1.8Hz$ with direction from the right to the left. And 14 individual pedestrians with frequencies in between 1.6 and 2.4 Hz, 3 of them crossing from the right to the left and the rest crossing from the left to the right. The velocity of the pedestrians varies from 1.5 to 1.8 m/s. In total, 29 people walk simultaneously on the bridge deck, which is equivalent to a crowd density of $d = 29/(1.6 \cdot 18.54) \approx 1P/m^2$. The results can be seen in figure 6.14 . The maximum acceleration reached ($3.2\ m/s^2$) is higher than the one calculated from the Sétra and EUR23984 model for the same density. However, this acceleration occurs the moment that the last two pedestrians cross from the midspan. The maximum acceleration is therefore felt by 2 pedestrians only, whereas the rest of the pedestrians receive/feel a reduced acceleration, depending on their location on the bridge (figure 6.15). The maximum accelerations of the different points of the bridge are developed

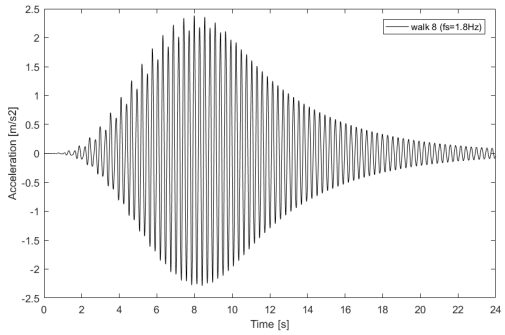

(a) Complete synchronization at $f_s = 1.8Hz$

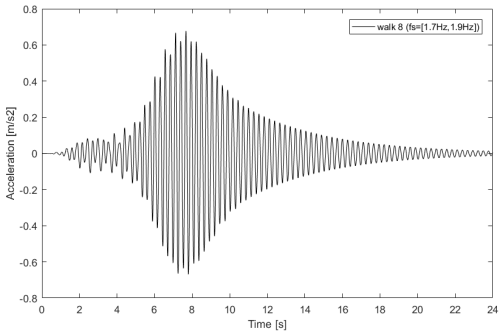

(b) Partial synchronization $f_s = 1.7 - 1.9Hz$

Figure 6.10 Response of acceleration for a group of pedestrians with different degrees of synchronization, for step frequencies around $f_s = 1.8Hz$

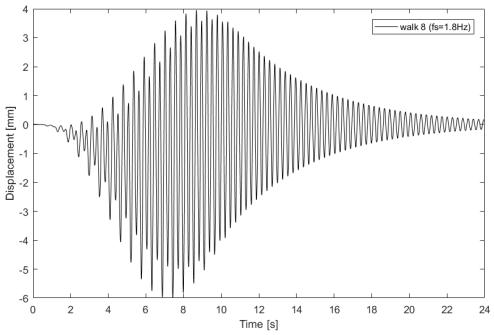

(a) Complete synchronization at $f_s = 1.8Hz$

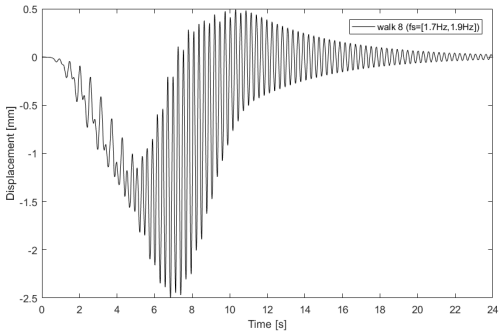

(b) Partial synchronization $f_s = 1.7 - 1.9Hz$

Figure 6.11 Response of displacement for a group of pedestrians with different degrees of synchronization, for step frequencies around $f_s = 1.8Hz$

almost simultaneously (in between the time interval 8.2-8.47 s). According to the acceleration limits of the codes, the comfort level in this case would be unacceptable. However if the acceleration limits derived from the site tests are used the resulting comfort of the active pedestrians is considered medium (the limit between good and medium comfort is $3.15m/s^2$ and the measured acceleration is $3.2m/s^2$). As for the displacements, the bridge would be characterized as a bridge with medium comfort. However, the ratio a/u is approximately 520 s^{-2}, which classifies the bridge to good comfort.

Naturally, the step frequencies of the pedestrians cannot be predicted neither can be predicted the synchronization between themselves. However, the absolute synchronization between the pedestrians and simultaneously between the pedestrians and the bridge is extremely hard to be achieved.

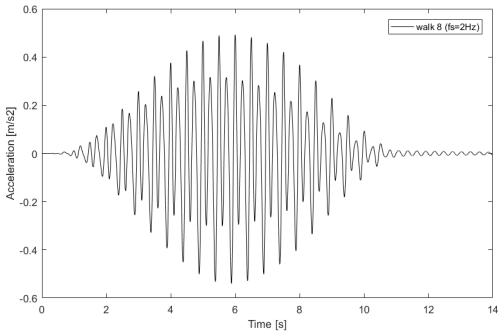

(a) Complete synchronization at $f_s = 1.8Hz$

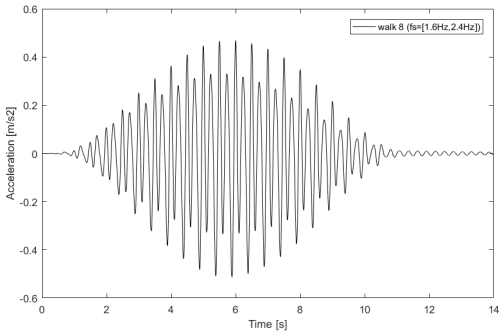

(b) Partial synchronization $f_s = 1.6 - 2.4Hz$

Figure 6.12 Response of acceleration for a group of pedestrians with different degrees of synchronization, for step frequencies around $f_s = 2Hz$

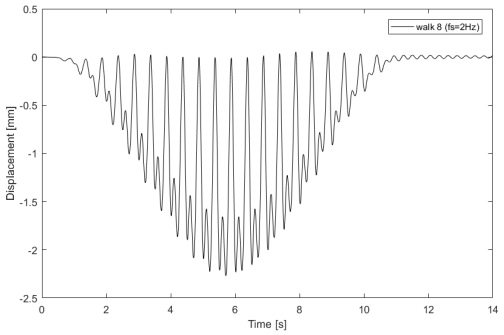

(a) Complete synchronization at $f_s = 2Hz$

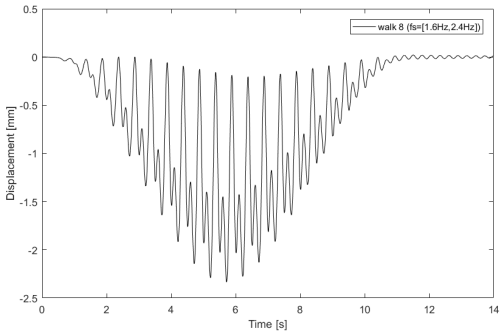

(b) Partial synchronization $f_s = 1.6 - 2.4Hz$

Figure 6.13 Response of displacement for a group of pedestrians with different degrees of synchronization, for step frequencies around $f_s = 2Hz$

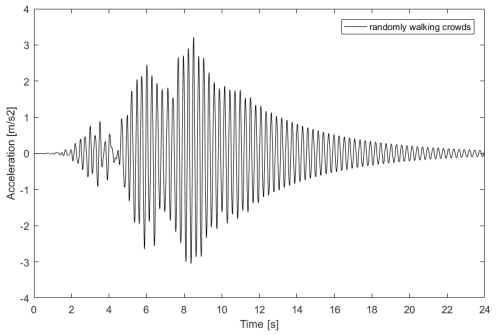

(a) Acceleration

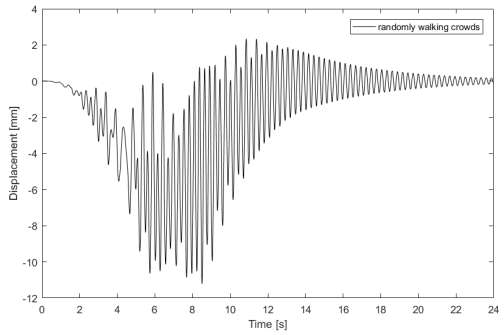

(b) Displacement

Figure 6.14 Response of acceleration and displacement for randomly walking crowds

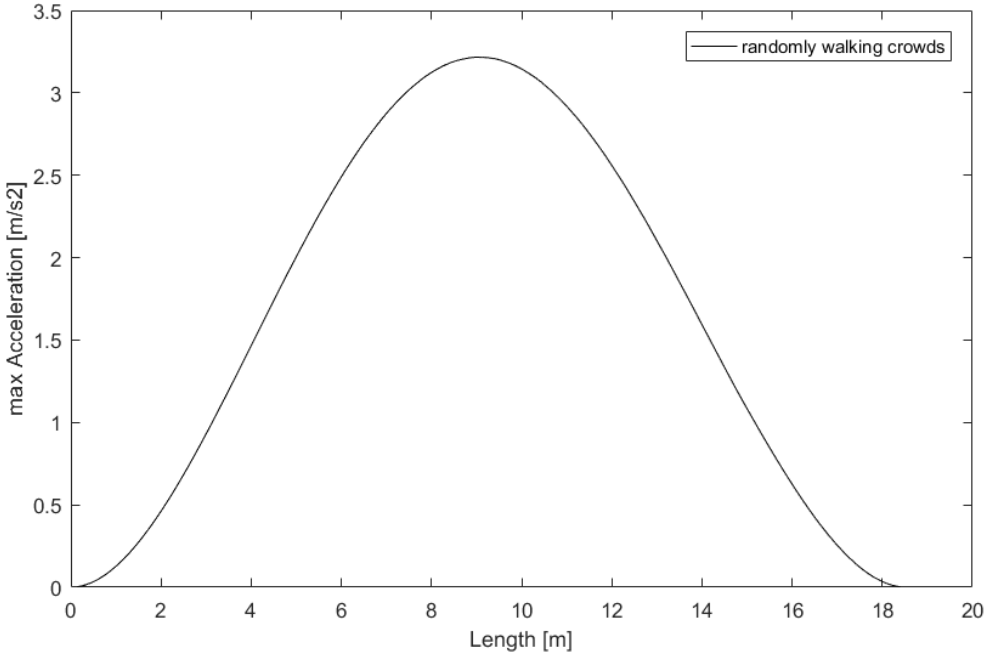

Figure 6.15 Maximum accelerations developed across the bridge for randomly walking crowds

6.4 Comparison between realistic load cases and codes

Between the available representations for the pedestrian loading, the ones closer to the reality are the models proposed by Sétra and EUR23984. Not only the value of the maximum acceleration is closer to the value obtained by the randomly walking realistic crowd, but also the acceleration limits for comfort are wider and less absolute than they are in the rest codes.

The randomly chosen walking crowd resulted in a higher acceleration than Setra. Should that worry the designer that the load model of Setra/EUR23984 is not accurate enough? The load model proposed by Setra and EUR23984 does not represent the realistic behavior of pedestrians walking, which is more complicated and hard to predict. However, it seems to be a good approximation since it is taking into account parameters like the synchronization of the pedestrians and the influence of the frequency. Moreover, the comfort limits proposed are lower than the comfort limits that were deduced from the tests for active pedestrians, which means that even if more complicated, exceptional pedestrian load combinations cause higher accelerations than the one derived, the comfort limit for which the active pedestrians start feeling heavy discomfort ($a > 5.8 m/s^2$) will still not be easily reached.

Chapter 7

Dynamic Analysis of a UHPFRC Footbridge Under Vandal Loading

As vandal loading is considered the intentional, well-coordinated action of one or more persons on the bridge with the intention to excite the bridge to its maximum response. For very slender structures, constructed from new materials, vandal actions could prove critical in the ULS design. The modern design codes and guidelines do not provide load models to describe the actions due to vandals. In this chapter, the modified load model for jumping proposed by Bachmann will be applied on the bridge's midspan to examine its behavior with respect to the number of people jumping, the degree of synchronization between the vandals, the synchronization between the vandals and the bridge and finally the damping ratio of the bridge.

7.1 Description of the load model

The main load used is the modified jumping expression proposed by Bachmann:

$$F(t) = \begin{cases} G_0 \cdot (1 + 1.7\sin(2\pi f_s t) + 1.1\sin(4\pi f_s t) + 0.5\sin(6\pi f_s t)), & \text{if } F(t) > 0 \\ 0, & \text{otherwise.} \end{cases} \tag{7.1}$$

The pedestrian is assumed to have a weight of $G_0 = 800\ N$ and the load is applied on the midspan of the bridge for a time period that is long enough to cause the maximum displacement and acceleration under this load to be reached. (steady state).

Since the main concern of the vandal loading is not the comfortability level of the users, but that the strength of the bridge should be high enough to withstand the vandal loading,

the maximum bending moment and shear force will be derived instead of the maximum acceleration. In that way, it can be checked if the capacity of the bridge is sufficient or if it is needed to be increased.

7.2 Effect of the number of vandals and of the structural damping on the response of the structure

As mentioned in Chapter 2, it is very hard to model mathematically the damping mechanisms of a structure. The estimation of the actual damping of a structure can only be achieved through measurements once the structure is completed. It is therefore of great importance to see how different damping ratios affect the maximum forces developed in a structure.

By knowing the resistance of the structure (M_{Rd} and V_{Rd}) and the estimated structural damping ξ, the critical number of vandals that can cause failure (if $M_{Ed} > M_{Rd}$ or $V_{Ed} > V_{Rd}$) can be found. The cross-sections that are more severely loaded are the supports and the mid-span. The load combination applied consists of the self-weight of the bridge, the weight of the handrails, the prestressing load and the vandal loading: $G_0 + G_p + P_\infty + F(t)$. Since the vandal loading is a dynamic load, the critical cross-sections should be checked in both directions, so that the alternation of the bending moments caused by the dynamic character of the external load is taken into account. In figures 7.1 to 7.5 are presented the resulting bending moments and shear force caused by this combination of loads, with their algebraic signs. For clarification, maximum bending moments are considered the bending moments that result when the vandal loading causes tension on the same fiber as the self-weight and minimum bending moments are considered those that result when the vandal loading and the self-weight cause tension on the opposite fibers.

As expected an increase in the number of people jumping synchronized leads to an increase in the forces that the cross-sections are asked to undergo. However, the most interesting observation is the influence of the damping ratio. As it can be seen, a really small damping ratio $\xi = 0.1\%$ or $\xi = 0.2\%$ results in big bending moments and the capacity of the bridge is exceeded even if only 1 person (for $\xi = 0.1\%$), or two persons (for $\xi = 0.2\%$) are jumping. Nevertheless, as damping increases the number of people that can act on the bridge increases as well. A damping of 1% already increases the number of synchronized people that the bridge can withstand to 5. Moreover, from the slope of each line it is apparent that with increasing damping, the influence of the number of people decreases. Indicatively, the maximum bending moments produced by 10 people jumping synchronized, for the damping ratios $\xi = 0.2\%$, $\xi = 1\%$ and $\xi = 5\%$ are respectively 6.5, 3.5 and 1.7 times larger

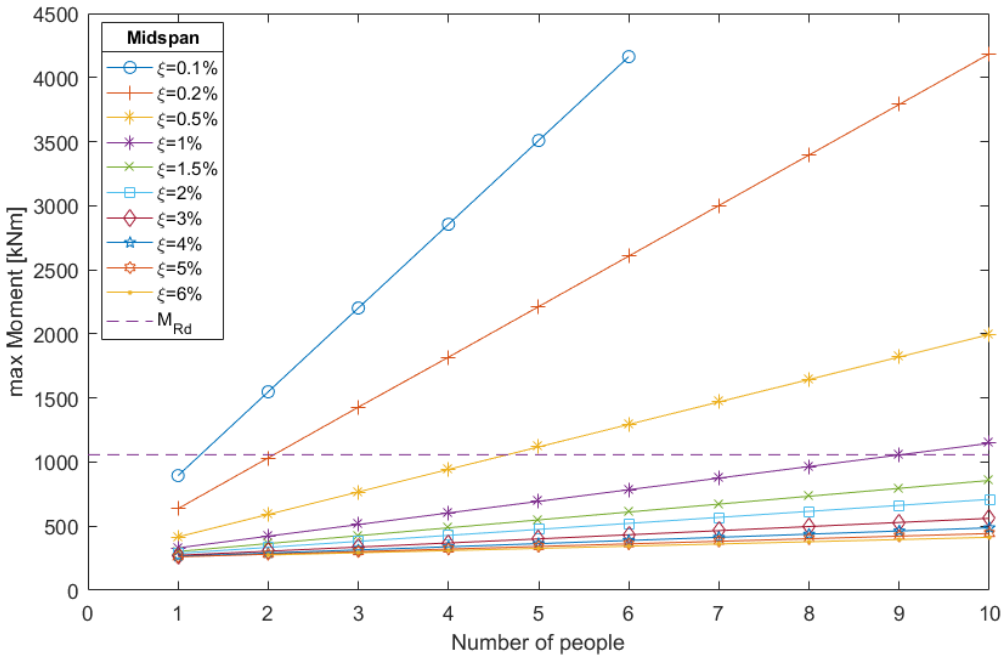

Figure 7.1 Maximum bending moment developed at mid-span for different number of vandals and different damping ratios

than the bending moment produced by only a single person jumping. What is also worth mentioning is that vibrations with big amplitudes, usually have increased damping as well. As an indication the Sétra regulations for prestressed concrete propose a damping ratio of 2% for high amplitude vibrations, instead of the 1% proposed in other cases. This phenomenon, of the increase of the damping with the increase of the amplitude, was also observed in the tests performed on site, where in some cases damping ratios as high as 8% was observed (Appendix B)

7.3 Effect of the degree of synchronization between the vandals and the structure

The next parameter that is of interest is the significance of the degree of synchronization between the pedestrians and the bridge. It has been observed that the pedestrians can identify the frequency of the structure better when the amplitude of the displacement is higher.

To investigate the effect of the degree of synchronization between the pedestrians and the bridge, the bending moments that result from five pedestrians jumping synchronized between themselves were plotted for different frequencies of jumping, while the damping ratio of the

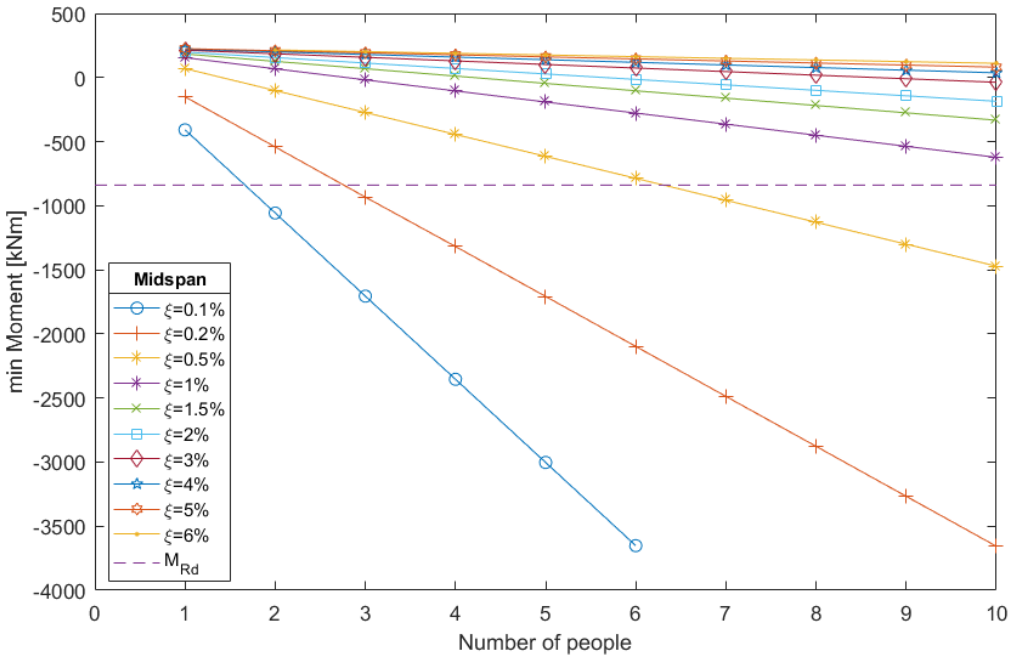

Figure 7.2 Mimimum bending moment developed at mid-span for different number of vandals and different damping ratios

bridge was taken as $\xi = 1\%$. The jumping frequencies used were chosen as a percentage of the natural frequency of the footbridge, that means that tests were run with frequencies in the range of $0.4f_n - 1.1f_n$. The resulting bending moments and shear forces (including the participation of the self-weight and the prestressing load) are presented in Figures 7.6 to 7.10. The bending moments are referred to as min and max in the same way as for section 7.2.

In each one of the figures 7.6 to 7.10 two peaks are detected. The highest peak (in absolute value) takes place for a ratio $\omega_s/\omega_n = 1$, while the second peak is observed at a ratio of $\omega_s/\omega_n = 0.5$. It is really interesting that although the vandals in these tests are completely synchronized between themselves, even a small divergence of 1% from the natural frequency, leads to a reduction of the bending moments/shear due to the vandal loading approximately equal to 22%. Moreover, the bending moments and shear forces that are developed due to a load applied with half frequency are approximately $45\% - 50\%$ reduced in comparison with the bending moments when the synchronization is perfect, and that level of drop occurs also for divergence of 3% around the natural frequency.

Two things can be concluded from these graphs: Firstly, the influence of the synchronization between the vandals and the bridge is substantial, since even a small change in the step frequency can result to diminished results. Secondly, bridges with natural frequencies that are out of the range of frequencies than can be humanly achieved, should be tested for

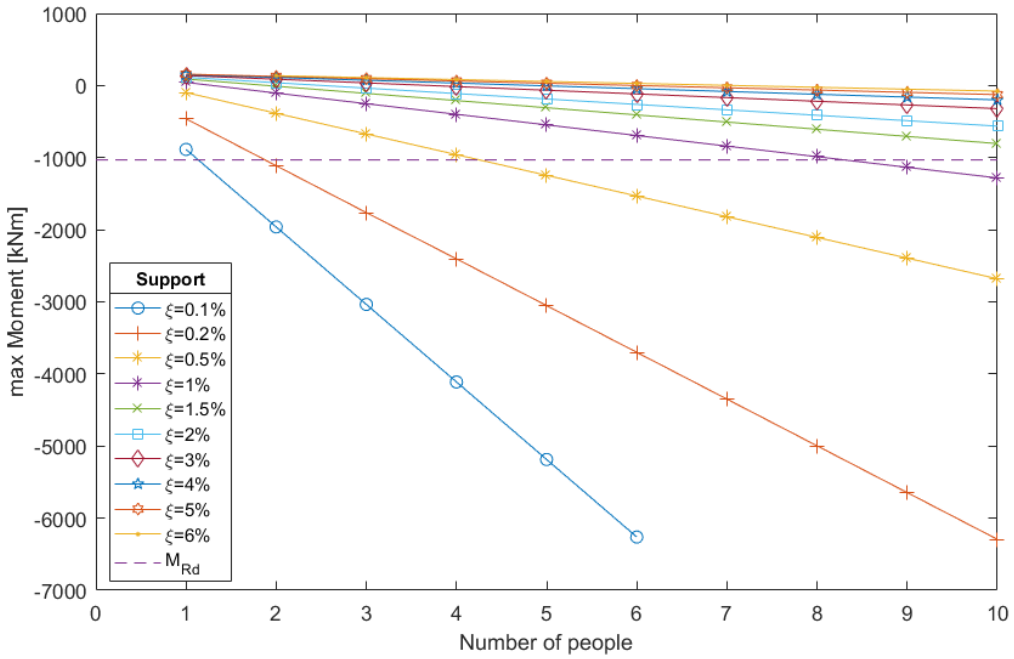

Figure 7.3 Maximum bending moment developed at supports for different number of vandals and different damping ratios

jumping frequencies equal to $0.5 f_n$, if this value falls in the range of jumping frequencies that can be achieved by humans.

In reality, perfect synchronization is hard to be achieved. The first obstacle that the vandals need to surpass is to recognize the natural frequency of the bridge which is not always an easy thing to do. The second one is to manage to keep their jumping frequency constant throughout time, without losing their step. The third, finally, is to manage to maintain the synchronization between themselves constant, a phenomenon that is harder to achieve the larger the number of the people acting.

7.4 Effect of synchronization between the pedestrians

One of the parameters that the modern codes try to incorporate in the pedestrian load models is the influence of the degree of synchronization between the pedestrians on the response of the structure. In order to examine how the response of the bridge is influenced by the degree of synchronization between pedestrians the group of 5 vandals used in section 7.3 is used again in this section. To investigate what happens when the pedestrians are not completely synchronized two jumping frequencies were used, the first one was equal to the

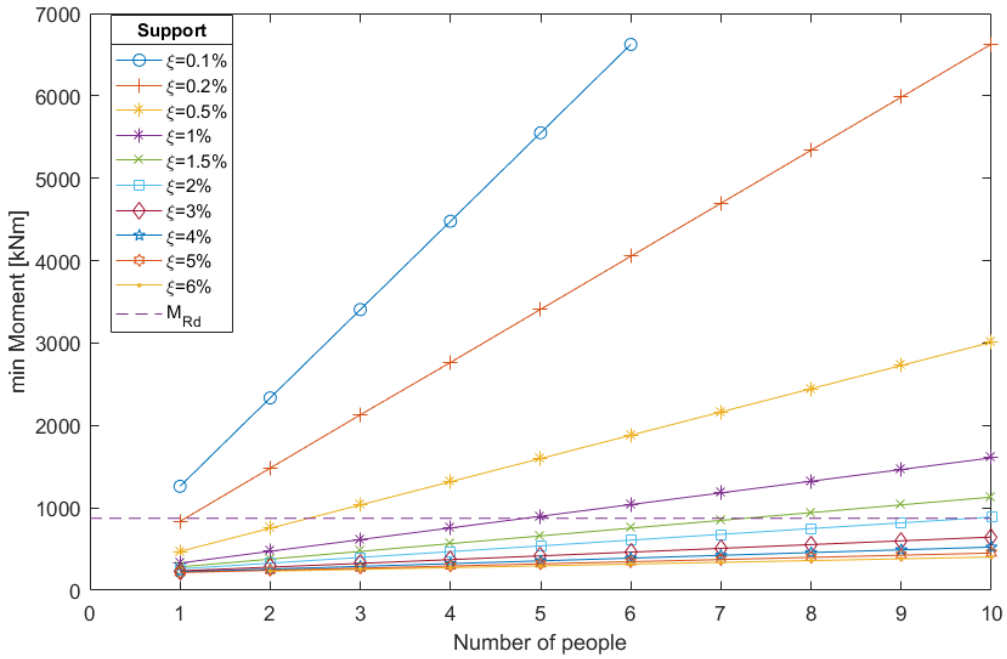

Figure 7.4 Mimimum bending moment developed at support for different number of vandals and different damping ratios

natural frequency of the bridge which excites the bridge to its maximum response ($f_s = f_n$) and a slightly reduced jumping frequency by 1%, equal to $f_s = 0.99 f_n$. Subsequently, the following combinations of synchronization were applied.

- 5 persons fully synchronized at $f_s = f_n$
- 4 persons fully synchronized at $f_s = f_n$ & 1 person at $f_s = 0.99 f_n$
- 3 persons fully synchronized at $f_s = f_n$ & 2 person synchronized at $f_s = 0.99 f_n$
- 2 persons fully synchronized at $f_s = f_n$ & 3 person synchronized at $f_s = 0.99 f_n$
- 1 persons fully synchronized at $f_s = f_n$ & 4 person synchronized at $f_s = 0.99 f_n$
- 5 persons fully synchronized at $f_s = 0.99 f_n$

The results of the response for the different cases are presented in figures 7.11 to 7.13. The values of the bending moments and the shear forces presented are solely due to the vandal loading, the participation of the self-weight and the prestressing are not presented in these graphs. The maximum response and forces are produced when all the vandals jump with a frequency equal to the natural frequency of the bridge, as expected. Nonetheless, if

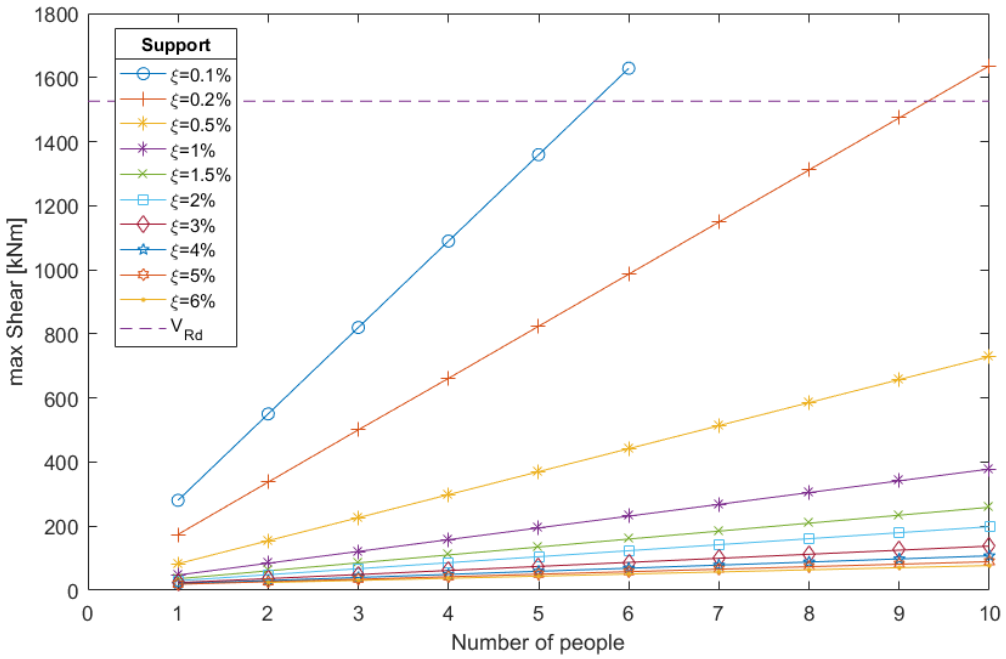

Figure 7.5 Mimimum bending moment developed at support for different number of vandals and different damping ratios

one of the participants is 1% out of synchronization from the rest, the max response decreases by approximately 20%, almost as much as it reduced for a synchronized group of 5 jumping in a frequency $0.99 f_s$. The smaller the number of synchronized people, the lower the bending moments/shear force produced. If there is such a big reduction in the produced forces when there is only such a small difference in the frequency and when only one person out of five is not synchronized with the rest, one can only imagine how less severe the response will be when more people are unsynchronized and when their jumping frequencies vary more.

As for the ability of vandals to synchronize between themselves an easy way to calculate the degree of synchronization is to measure the maximum accelerations that develop on site when a number of people walk on the bridge and compare them with the accelerations that are derived from the application of the same load on the finite element model, assuming perfect synchronization between the people. The ratio between the measured maximum acceleration and the calculated maximum acceleration for full synchronization is thought to be the degree of synchronization. The level of synchronization was derived in that way by using the vandal tests performed in Excercitsiebrug and is presented in Table 7.1.

As can be seen in figure 7.14, the degree of synchronization drops to 85% when two people are jumping simultaneously, while for four people jumping the synchronization is even more reduced leading to a reduction of the maximum potential acceleration by

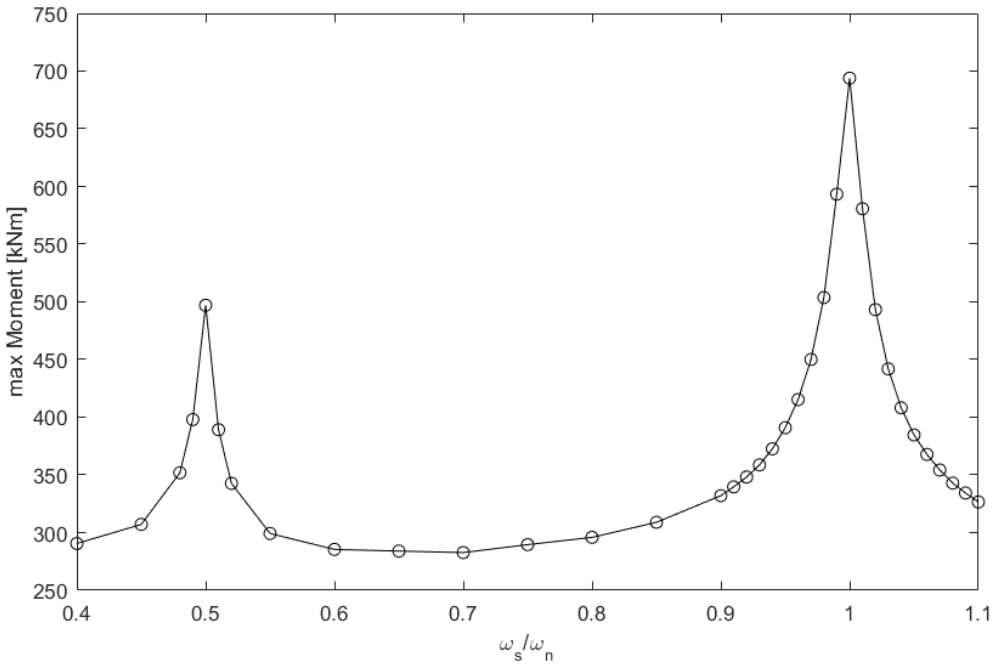

Figure 7.6 Maximum bending moments developed at mid-span for different jumping frequencies

40%. From this graph, it can be concluded that the degree of synchronization between the pedestrians drops for an increasing number of people. This is very important in the case that a dynamic analysis of a footbridge under pedestrian loading is performed, since not taking into account this considerate drop in the degree of synchronization with increasing number of people, overestimates by far the applied load on the footbridge and leads to the calculation of responses with much higher amplitudes than they are expected in reality.

Unfortunately, since the number of pedestrians/vandals used in the tests is small and since the number of tests performed on the Excercitsiebrug and then simulated in the FEM program is restricted, it was not feasible to define an analytical relation between the number

Table 7.1 Accelerations and degree of synchronization for Excercitsiebrug

Number of people $n\ [-]$	Weight $[kg]$	Measured acceleration $a_m\ [m/s^2]$	Calculated acceleration $a_c\ [m/s^2]$	Synchronization a_m/a_c
1	92	6.31	6.29	1.00
2	142	6.65	7.85	0.85
4	276	9.14	15.26	0.60

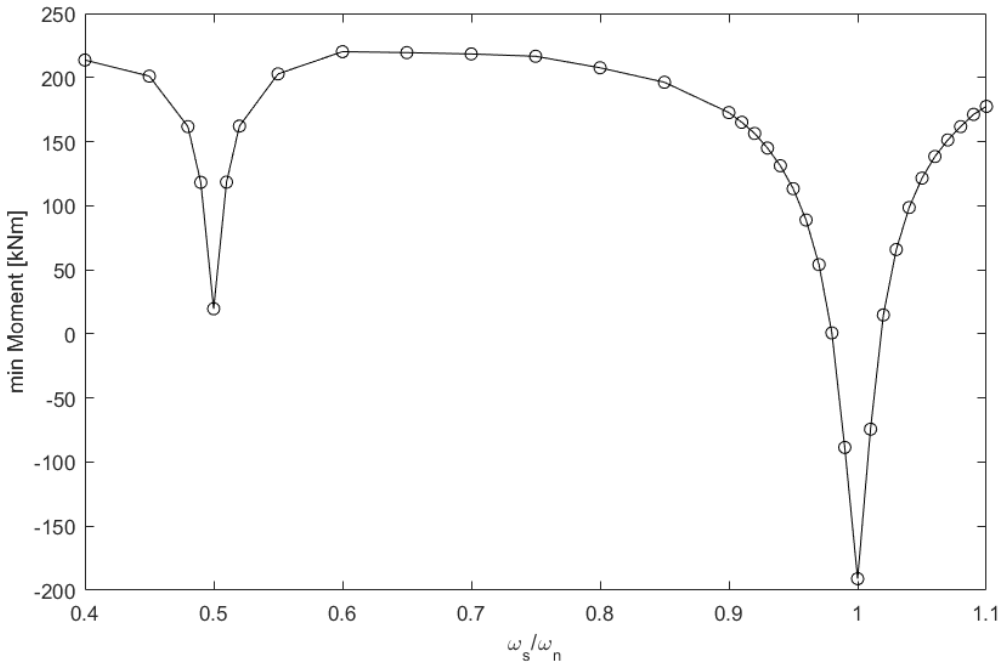

Figure 7.7 Mimimum bending moment developed at mid-span for different jumping frequencies

of pedestrians and their synchronization. However, further research on that subject is recommended.

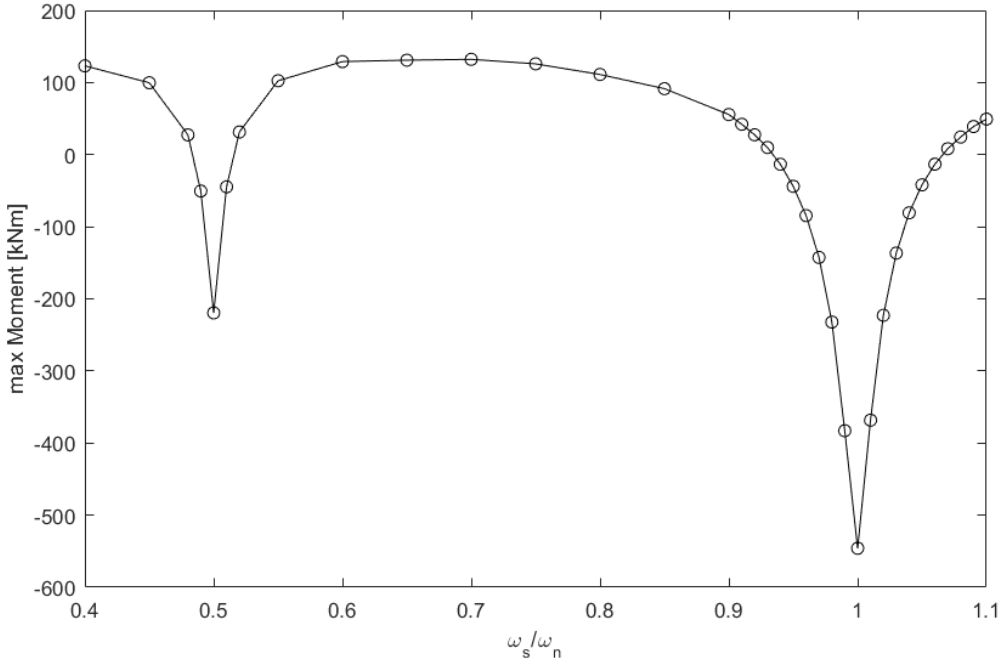

Figure 7.8 Maximum bending moments developed at the supports for different jumping frequencies

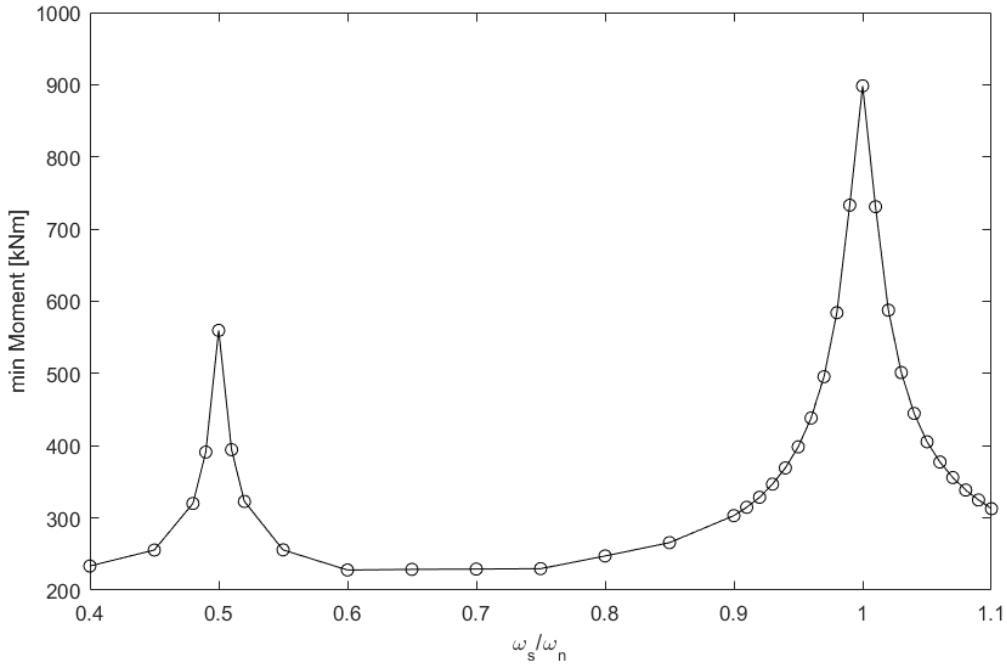

Figure 7.9 Mimimum bending moment developed at the supports for different jumping frequencies

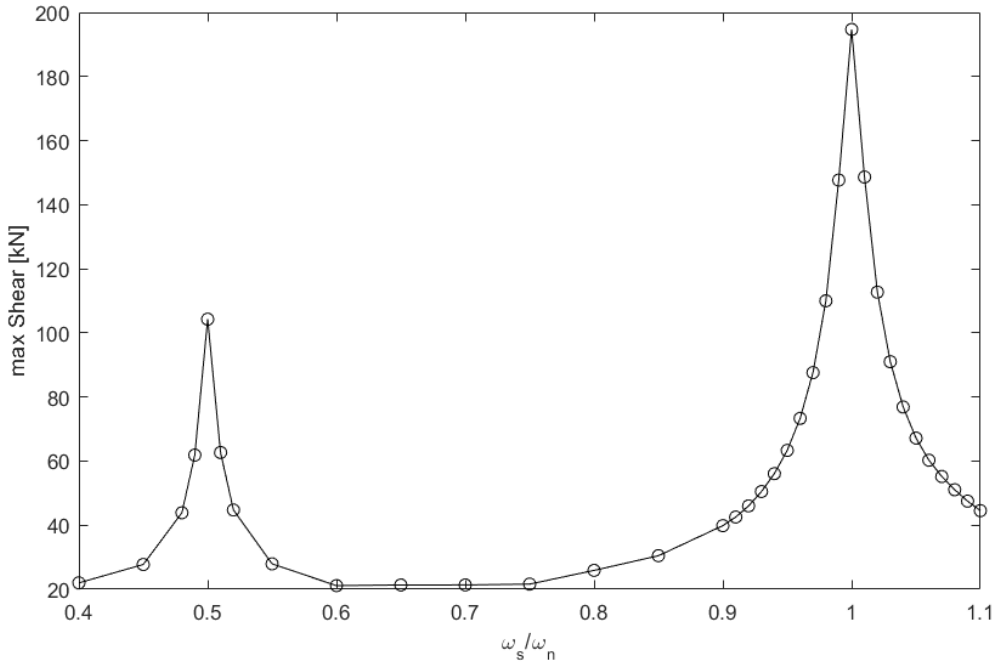

Figure 7.10 Maximum shear force developed at the supports for different jumping frequencies

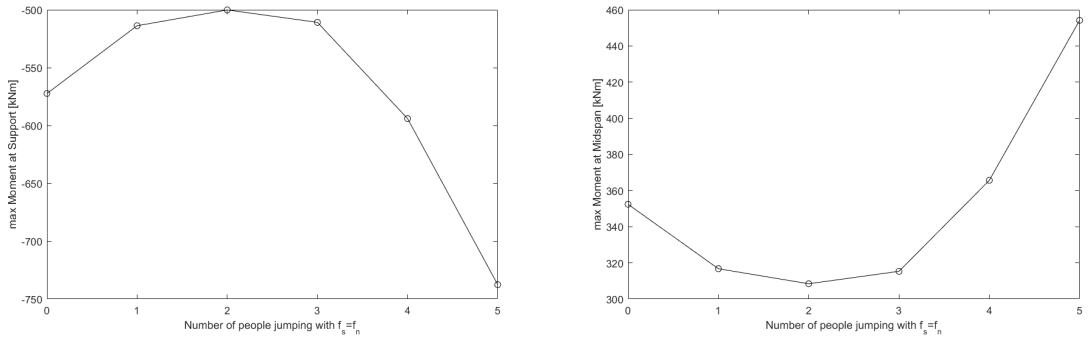

(a) Support (b) Mid-span

Figure 7.11 Maximum bending moments at the support and at the midspan for different number of synchronized people

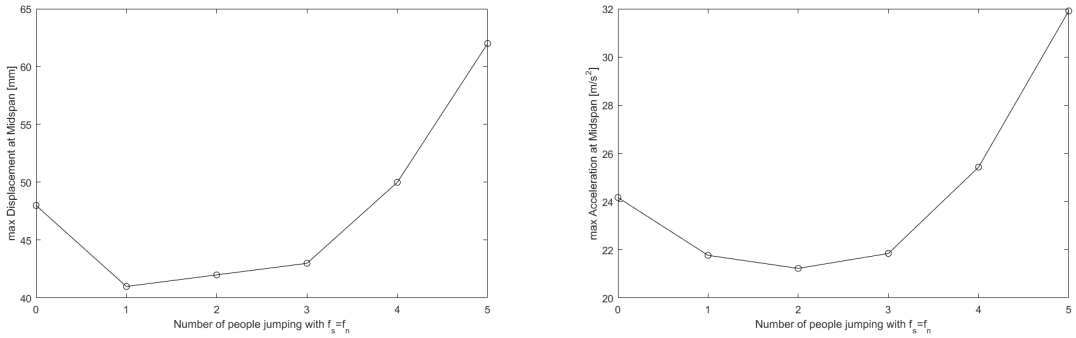

(a) Displacement (b) Acceleration

Figure 7.12 Maximum displacements and accelerations at the midspan for different number of synchronized people

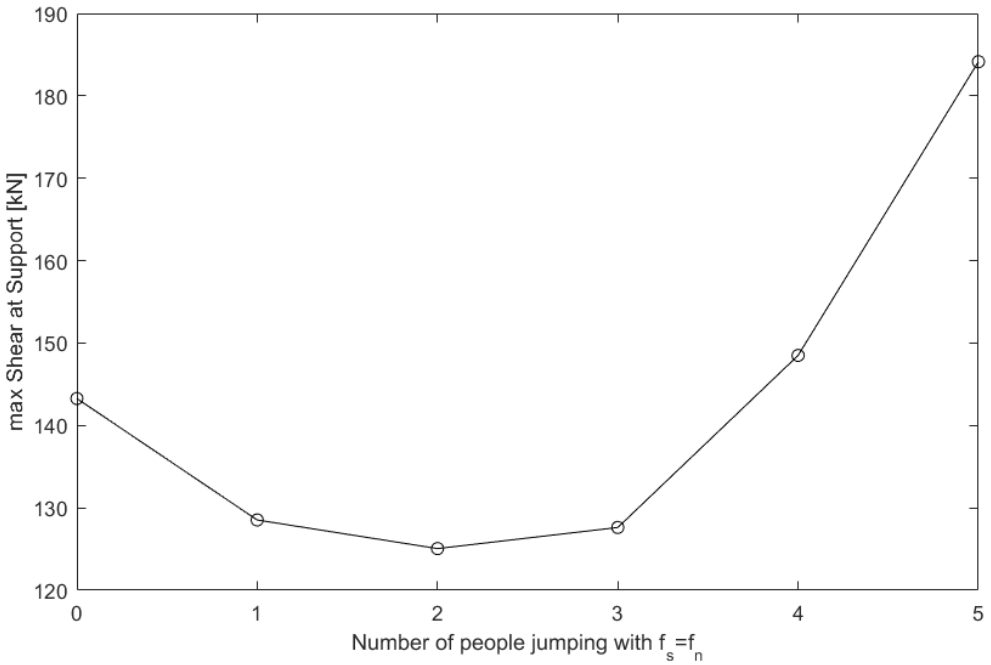

Figure 7.13 Maximum shear at the support for different number of synchronized people

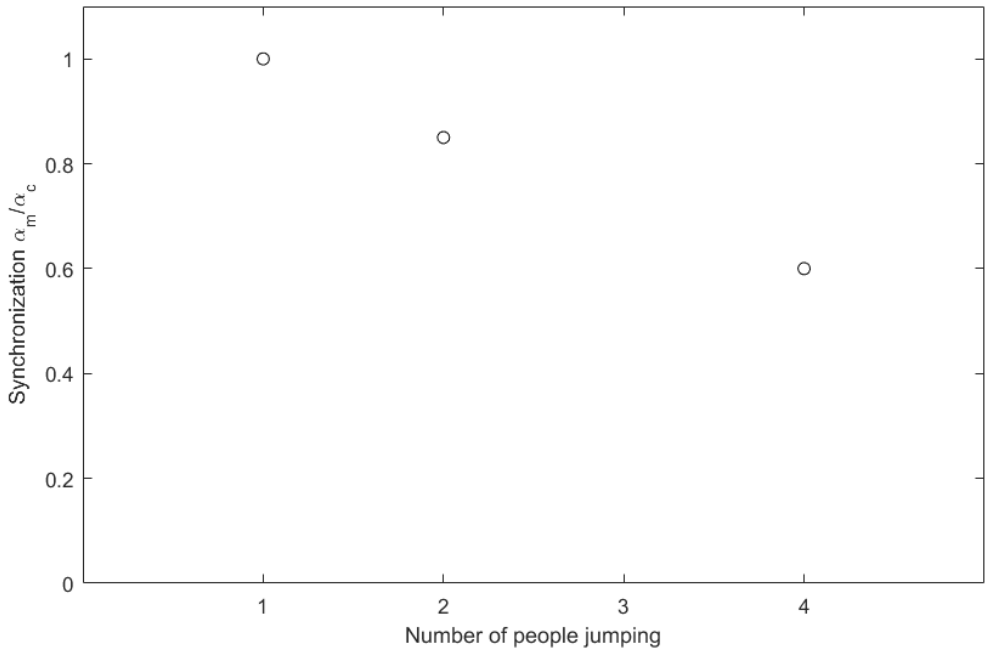

Figure 7.14 Degree of synchronization of jumping people for test on Excercitsiebrug

Chapter 8

Conclusion

8.1 Conclusions

The purpose of this master thesis was firstly, to investigate the sufficiency and stringiness of the available codes and guidelines concerning the pedestrian load models and the acceleration limits proposed in order to guarantee the comfort of the pedestrians. Secondly, the establishment of a load model that represents accurately the vandal loading applied on a slender footbridge and the dynamic response of the structure.

1. In order to investigate the limits of accelerations and displacements that if exceeded cause discomfort to the pedestrians, several tests were performed on three footbridges. The analyses of the measurements showed that:

    - Standing people are more sensitive to vibrations than moving people.
    - It is less conservative to define a range of limits between which the pedestrians feel a certain level of comfort than to have a fixed value that needs to be satisfied. In that way the comfort level required for each bridge will also define the limits for the accelerations or displacements that can be developed. Moreover, since the perception of vibrations and the comfort felt by the pedestrians is a complex phenomenon based a lot on the personal experience of each individual pedestrian, it is more realistic to consider a range of accelerations that correspond to a certain comfort level, than a single threshold value.
    - The comfort levels with respect to the maximum accelerations derived from the tests for moving crowds are much higher than the equivalent limits of acceleration proposed by the codes.

- The acceleration limits derived from the tests for the standing crowds are close to the acceleration limits proposed by the available codes and guidelines.
- The limits derived with respect to the displacements seem to describe the comfort limits more clear, since for increasing amplitude of displacements, the discomfort clearly increases, whereas for increasing amplitude of accelerations the level of comfortability covers a wider range of comfort.
- There are ranges "acceleration/displacement", that could be translated in ranges of frequencies, where the pedestrians are more affected by the vibrations.

2. The pedestrian loads are described best when they are simulated as a Fourier series of the form: $F(t) = G_0\left(1 + \sum_{n=1}^{k} a_n \cdot \sin(2n\pi ft)\right)$. By simulating one of the tested footbridges and applying on it the different load models proposed in literature, it was concluded that the load model proposed by Bachmann leads to a more realistic dynamic response of the structure. The following factors have a great influence on the response of the structure:

   - The synchronization between the pedestrians - When the synchronization between the pedestrians is not perfect and even a small percentage is walking/running/jumping out of phase with the rest, the amplitude of the accelerations, displacements and forces produced is decreased significantly.
   - The synchronization between the pedestrians and the footbridge - More specifically, if the step frequency of the pedestrians is equal to the natural frequency of the footbridge, resonance could occur and the amplitude of accelerations and displacements is maximum. However, even a small divergence of the step frequency leads to a significant drop in the response of the structure.
   - Damping of the structure - It is well-known that higher structural damping leads to lower amplitudes of displacements and acceleration. However, it was also observed that vandal loading causes higher damping ratios than walking or running loads. Hence, the bigger the amplitude of vibration is, the higher is the damping.

3. Vandal loading could be the critical load combination in ULS during the design of slender, lightweight short footbridges. The analyses performed applying the modified Bachmann load for jumping, demonstrated that a small increase in the damping increases the number of "vandals" which can act on the bridge synchronized without causing damage, whereas even a small degree of unsynchronism between the pedestrians and/or the bridge leads to a significant reduction of the reaction forces and bending

moments produced. Therefore, by taking into account the increased damping in the case of jumping, the difficulty of synchronizing an increasing number pedestrians, the human inability to recognize the natural frequency of a bridge and to maintain it for an extended amount of time while jumping, it is very improbable that vandal loading would cause the collapse of the structure.

All in all, by analyzing the slender footbridge from UHPFRC according to the British National Annex to EN1, it is concluded that the acceleration limit is exceeded and therefore measures should be taken to decrease the maximum acceleration of the footbridge. The dynamic analysis performed according to the Setra and EUR23984 recommendations classified the footbridge as a mimimum comfort level (for high crowd densities) or medium comfort (for medium crowd density). Nevertheless, when the more realistic load models of Bachmann are applied and the maximum derived acceleration is compared to the acceleration limits for the active pedestrians, then the resulting comfort level of the footbridge is good.

This is an important observation, since according to the codes the designer should change the design of the bridge in order to satisfy the acceleration limits in the serviceability limit state. In the examined case, following the regulations of the codes makes the SLS design more critical than the ULS, requiring a change in the design to reduce the amplitude of the response of the structure. So, if the design is made according to the codes and guidelines, one way to encounter the problem is to increase the structural height of the footbridge, increasing in that way the natural frequency of the footbridge. If the natural frequency is above 5Hz, no further check is required. Another way is to increase the damping of the structure by adding a "heavy" deck of concrete or asphalt that will add extra damping, but also extra mass, or install damping devices, like tuned mass dampers. All these solutions however cost more and make the use of materials like UHPFRC less attractive. On the other hand, the use of more realistic load models and the adoption of wider acceleration limits that describe the comfortability of the moving pedestrians do not require to change the design of the bridge or to take additional measures for the reduction of the response.

8.1.1 Summary of proposed dynamic analysis

- Simulation of the footbridge on a FEM program and calculation of the natural frequency.
- Choose a damping ratio between 1 and 3% for walking, depending on the material of the structure.
- Choose the required comfort level of the bridge.

- Application of the Bachmann load model for walking with a step frequency equal to the natural frequency of the footbridge if the natural frequency is between 1.6-2.4 Hz. Otherwise if the natural frequency is higher, apply the load with a step frequency equal to half the natural frequency of the bridge (most critical cases).
- If there is available a relation between the number of pedestrians and the degree of synchronization apply it on model by reducing the force applied accordingly. If no relationship is known, decrease the maximum response accordingly, like presented in figure 7.14.
- Perform the dynamic analysis.
- Check maximum acceleration produced and compare it with the acceleration limits of the comfort level you chose. If not ok, check also amplitude of displacement and ratio a/u. At least the acceleration or the displacement should be satisfied. The ratio a/u by itself is not sufficient to classify the comfort level of the footbridge, except if it is smaller than $500s^{-2}$ that the comfort level is considered always good. If both the max acceleration and the displacements are satisfied the design is sufficient.
- For the case of vandal loading instead of accelerations and displacements, check the bending moments and shear forces developed.

8.2 Recommedations for further investigation

1. Derive acceleration and displacement limits for comfort and safety based on a greater number of people of different characteristics, like age and gender and on bridges with a bigger variety of site usage and length.
2. Investigate in greater depth the relation between the accelerations and the displacements and how it affects the feeling of comfort of the people.
3. Investigate the behavior of longspan bridges.
4. Derive a relationship that describes the degree of synchronization between pedestrians with respect to their number and their activity.
5. Finally, it would be interesting to perform a probabilistic analysis on walking and running crowds of existing bridges. That would shed light on characteristics like the walking and running frequencies but also the velocities of people, that could be used in the more realistic load models.

Bibliography

[1] 1990:2002+A1:2005, E. (2002). *Eurocode: Basis of structural design*. European Committee of Standardization.

[2] Acker, P. and Behloul, M. (2004). Ductal Technology: A Large Spectrum of Properties, a Wide Range of Applications. In *International Symposium on Ultra High Performance Concrete*.

[3] Alipour, a. and Zareian, F. (2008). Study Rayleigh Damping in Structures; Unceratinties and Treatments. *14 th World Conference on Earthquake Engineering: Innovation Practice Safety*.

[4] Andriacchi, T Ogle, . J. A. and Galante, J. (1977). Walking speed as a basis for normal and abnormal gait measurements. *Journal of Biomechanics*, 10:261–268.

[5] Association Française de Génie Civil (2002). Ultra High Performance Fibre-Reinforced Concretes. *LCP-Con*, page 98.

[6] Bachmann, H. and Ammann, W. (1987). *Vibrations in Structures: Induced by Man and Machines*.

[7] Bachmann, H. e. a. (1995). *Vibration Problems in Structures: Practical Guidelines*.

[8] BRITISH STANDARDS INSTITUTION (2000). BS 5400: Steel, concrete and composite bridge - Part 2: Specification for loads.

[9] Caetano, E. Cunha, A. and Moutinho, C. (2011). Vandal Loads and Induced Vibrations on a Footbridge. *Bridge Engineering*, 10:375–382.

[10] Cappellini, A. Manzoni, S. and Vanali, M. (2012). Experimental and Numerical Studies of the People Effects on a Structure Modal Parameters. In *Topics on Dynamics of Civil Structures, 30th IMAC, A Conference on Structural Dynamics*.

[Caprani and Fanning] Caprani, C.C Keogh, J. A. P. and Fanning, P. *Computers and Structures*, (102-103):87–96.

[12] Chopra, A. K. (1995). *Dynamics of Structures, Theory and Applications to Earthquake Engineering*.

[13] Connor, J. (2002). *Introduction to Structural Motion Control*.

[14] Dallard, P. Fitzpatrick, T. F. A. L. A. S. R. W. M. and Roche, M. (2001). London Millenium Bridge: Pedestrian- Induced Lateral Vibration. *Bridge Engineering*, 6:412–417.

[15] EN, E. . (2009). *Design of Lightweight Footbridged for Human Induced Vibrations*.

[16] EN 1991-1-1:2002 (2002). Eurocode 1: Actions on structures - Part 1-1: General actions - Densities, self-weight, imposed loads for buildings. *European Committee for Standardization*, 2(2005).

[17] EN1995-2 (2004). *Eurocode 5: Design of Timber Structures- Part 2 Bridges*. European Committee of Standardization.

[18] European Committee for Standardisation (2010). BS EN 1991-1-4; UK National Annex to Eurocode 1 – Actions on structures actions; Part 1-4: General actions- Wind actions. (1):1–46.

[19] Fehling, E Leutbecher, T. and Bunje, K. (2004). Design Relevant Properties of Hardened Ultra High Performance Concrete. In *Proceedings of the International Symposium on Ultra High Performance Concrete*.

[20] for Technical Approvals, E. O. (2013). *European Technical Approval ETA- 13/0815*.

[21] Fujino, Y. and Siringoringo, D. M. (2015). A Conceptual Review of Pedestrian-Induced Lateral Vibration and Crowd Synchronization Problem on Footbridges. *Journal of Bridge Engineering*, (2005):C4015001.

[22] Galbraith, F. and Barton, M. (1970). Ground Loading from Footsteps. *Journal of the Acoustic Society of America*, 48:1288–1292.

[23] Georgakis, C. T. and Jørgensen, N. G. (2013). Change in Mass and Damping on Vertically Vibrating Footbridges Due to Pedestrians. In *Topics in Dynamics of Bridges, A Conference on Structural Dynamics, 31st IMAC*.

[24] Graybeal, B. A. and Hartmann, J. L. (2003). Stregth ad Durability of Ultra-High Performance Concrete. In *2003 Concrete Bridge Conference*.

[Hussein and Amleh] Hussein, L. and Amleh, L. *Construction and Building Materials*, 93:1105–1116.

[26] International Organization for Standardization (ISO) (2007). ISO 10137:2007. Bases for design of structures - Serviceability of buildings and walkways against vibrations. 10137:44.

[27] ISO 2631-1, . (1997). Mechanical vibration and shock- Evaluation of human exposure to whole-body vibration-Part 1:General requirements.

[28] Kareem, A. and Gurley, K. (1996). Damping in structures: its evaluation and treatment of uncertainty. *Journal of Wind Engineering and Industrial Aerodynamics*, 59:131–157.

[29] Kasperski, M. (2006). Vibration Serviceability for Pedestrian Bridges. *Structures & Buildings*, 159.

[30] Leonard, D. (1966). *Human Tolerance Levels for Bridge Vibrations*.

[31] Ma, J. Dehn, F. T. N. V. O. M. and D. Schmidt, D. (2004). Comparative Investigations on Ultra-High Performance Concrete with and without Coarse Aggregates. In *International Symposium on Ultra High Performance Concrete*.

[32] Mackenzie, D. Barker, C. M. N. and Allison, B. (2005). Footbridge Pedestrian Vibration Limits- Part 2. In *Proceedings of the Second International Conference on Footbridges*.

[33] Martinez, M. (2006). Analysis of Structural Damping.

[34] Matsumoto, Y. Nishioka, T. S. H. and Matsuzaki, K. (1978). Dynamic design of footbridges. In *IABSE Proceedings*.

[35] Occhiuzzi, A. Spizzuoco, M. and Ricciardelli, F. (2008). Loading models and response control of footbridges excited by running pedestrians. *Structural Control and Health Monitoring*, 15:349–368.

[36] Orgass, M. and Klug, Y. (2004). Fibre Reinforced Ultra-High Strength Concretes. In *International Symposium on Ultra High Performance Concrete*.

[Paškvalin] Paškvalin, A. Application of Ultra High Performance Concrete in the new Leiden Bridge. Master's thesis, TU Delft.

[38] Pedersen, L. (2012). Damping Effect of Humans. In *Topics on Dynamics of Civil Structures, 30th IMAC, A Conference on Structural Dynamics*.

[39] Pedersen, L. (2013). Some Implications of Human-Structure Interaction. In *Topics in Dynamics of Civil Structures, 31st IMAC, A Conference on Structural Dynamics*.

[40] Puthanpurayil, A. M., Dhakal, R. P., and Carr, A. J. (2011). Modelling of In-Structure Damping : A Review of the State-of-the-art. (091).

[41] Qin, J. W., Law, S. S., Yang, Q. S., and Yang, N. (2013). Pedestrian-bridge dynamic interaction, including human participation. *Journal of Sound and Vibration*, 332(4):1107–1124.

[42] Reimert, Z. (2014). Human-Induced Vibrations on Footbridges, A probability-based approach of the vibration serviceability of footbridges uder vertical pedestrian loading.

[43] Roos, I. (2009). Human Induced Vibrations.

[44] Salyards, K. A. and Firman III, R. J. (2011). Human-Structure Interaction: Effects of Crowd Characteristics. In *Civil Engineering Topics, 29th IMAC, A Conference on Structural Dynamics*.

[45] Schmidt, M. and Fehling, E. (2004). Ultra-High-Performance Concrete : Research , Development and Application in Europe. *7th International Symposium on the Utilization of High-Strength/High-Performance Concrete*, SP-228.

[46] Schwartz, C. Alexis, B. B. O. F. B. C. J.-L. and Denoël, V. (2014). Experimental Study of the Human Ability to Deliberately Excite a Flexible Floor. In *5th International Conference on Structural Engineering, Mechanics and Computation*.

[47] Spasojević, A. (2008). Structural Implications of Ultra-High Performance Fibre-Reinforced Concrete in Bridge Design. 4051:203.

[48] Spijkers, J. Vrouwenvelder, A. and Klaver, E. (2006). *Dynamics of Structures Part 1: Vibration of Structures*. TU Delft.

[49] Sétra/AFGC (2006). *Footbridges: Assessment of vibrational behavior of footbridges under pedestrian loading*.

[50] Vitomir, R. Brownjohn, J. W. S. E. M. T. and Wing, A. (2013). Effect of Sensory Stimuli on Dynamic Loading Induced by People Bouncing. In *Topics in Dynamics of Civil Structures, 31st IMAC, A Conference on Structural Dynamics*.

[51] Walraven, J. (2004). Designing with Ultra High Strength Concrete: Basics, Potential and Perspectives. In *Proceedings of the International Symposium on Ultra High Performance Concrete*.

[52] Wheeler, J. (1982). Prediction and control of pedestrian induced vibration in footbridges. *Journal of the Structural Division*, 108:2045–2065.

[53] Zivanovic, S. and Pavia, A. (2009). Probabilistic Assessment of Human Response to Footbridge Vibration. *Journal of Low Frequency Noise, Vibration and Active Control*, 28:255–268.

[54] Zivanovic, S., Pavic, A., and Reynolds, P. (2005). Human – structure dynamic interaction in footbridges. *ICE, Bridge Engineering*, 158:165–177.

[55] Živanović, S., Pavic, A., and Reynolds, P. (2005). *Vibration serviceability of footbridges under human-induced excitation: A literature review*, volume 279.

[56] Zuo, D., Hua, J., and Van Landuyt, D. (2012). A model of pedestrian-induced bridge vibration based on full-scale measurement. *Engineering Structures*, 45:117–126.

Appendix A

Set-up of the experiments and description of the analysis procedure

A.1 Test set-up

The tests performed on the bridges for the different load types, included the recording of the response of the acceleration and the displacement. The means that were used to record these responses were inexpensive devices. A smartphone application (VXacc) was used for the recording of the accelerations and a videocamera for the recording of the displacements. More information can be found below.

A.1.1 Measuring the displacements

The first step for measuring the displacements was to place a sticker at the side of the mid-span, where the maximum accelerations and displacements are expected, in a way that the sticker would be visible from the position of the camera. The sticker was round and was consisting of two colors, black and yellow, so that there would be a clear distinction between the sticker and the bridge. The person using the camera would then focus on the area of the footbridge around the sticker. For each one of the tests, the cameraman would record the response of displacements of the mid-span, by videotaping the motion of the sticker. At the beginning of each video the cameraman would mention the name of the test, for example "Walk 5", for the case that 5 people were walking across the footbridge and 2 remaining people were standing at the mid-span. This made easier the analyses of the recordings later on. In figure A.1 the placing of the sticker in Brug D is presented.

Figure A.1 Sticker used for the recording of the displacements

A.1.2 Measuring the accelerations

For the measurement of the accelerations the smartphone used was placed on top of the footbridge's deck, at the same location as the sticker. For each one of the tests a file of the accelerations produced during the test was recorded and saved in a .txt format under a specific number. When saving each one of the recordings, the conductor of the experiment would also write down the number of the file next to the name of each test performed. An example of how the application looks is presented in figure A.2.

A.1.3 Describing the perception of vibrations and the comfort level

For every different footbridge tested a questionnaire was handed to the test subjects and they were asked to describe the level of vibrations they perceived and the level of discomfort and safety they experienced. The level of vibrations was described with a scale ranging from 1 to 10, with 1 representing unperceivable vibrations, 3 representing light vibrations, 6 corresponding to medium vibrations and 10 describing intolerably strong vibrations. Furthermore, the pedestrians were asked to correlate the level of comfort they felt to a different color. Green color was used to describe the feeling of being comfortable, yellow for medium comfort and red to describe discomfort. Simultaneously, to express the feeling of safety the letter S (for safe) was filled in the appropriate color of comfort (and the letter U for unsafety).

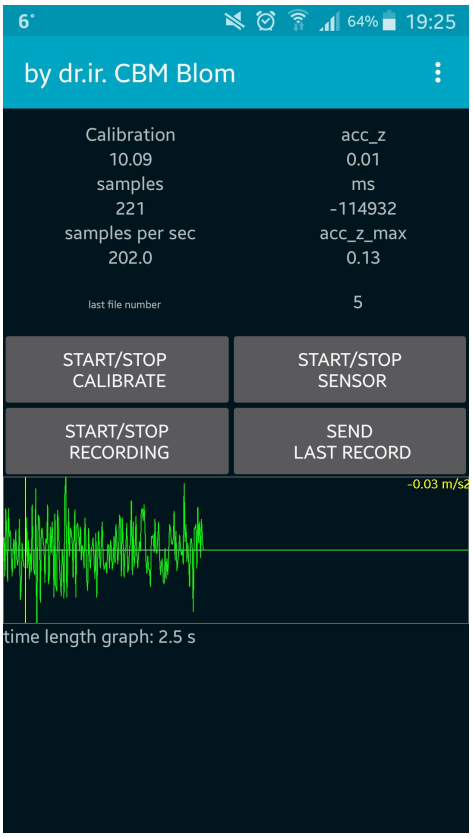

Figure A.2 Application VXacc used for the recording of vertical accelerations

Finally, the activity of the test subjects was described. The questionnaire had the form that appears in figure A.3.

A.2 Analyzing the recorded data

A.2.1 Analyzing the displacements

The extraction of the displacements from the movie clip is achieved by using ClipAnalyser. The steps followed are quite simple, first the number of frames per second used by the videocamera are input, then the sticker is inscribed in a circle, the diameter of which is set equal to the real diameter of the sticker (95mm in this case). In that way, the program transforms the pixels in millimeters. Consequently, a certain color is defined, in our case that color is the yellow color of the sticker. Furthermore, the center of the circle is defined as well as the center of the selected color. It's ideal that the two centers coincide. In addition, an area around the circle is defined, in which the program will search for pixels with the same color tone as the one defined (yellow). When the user selects "scan all files", the program

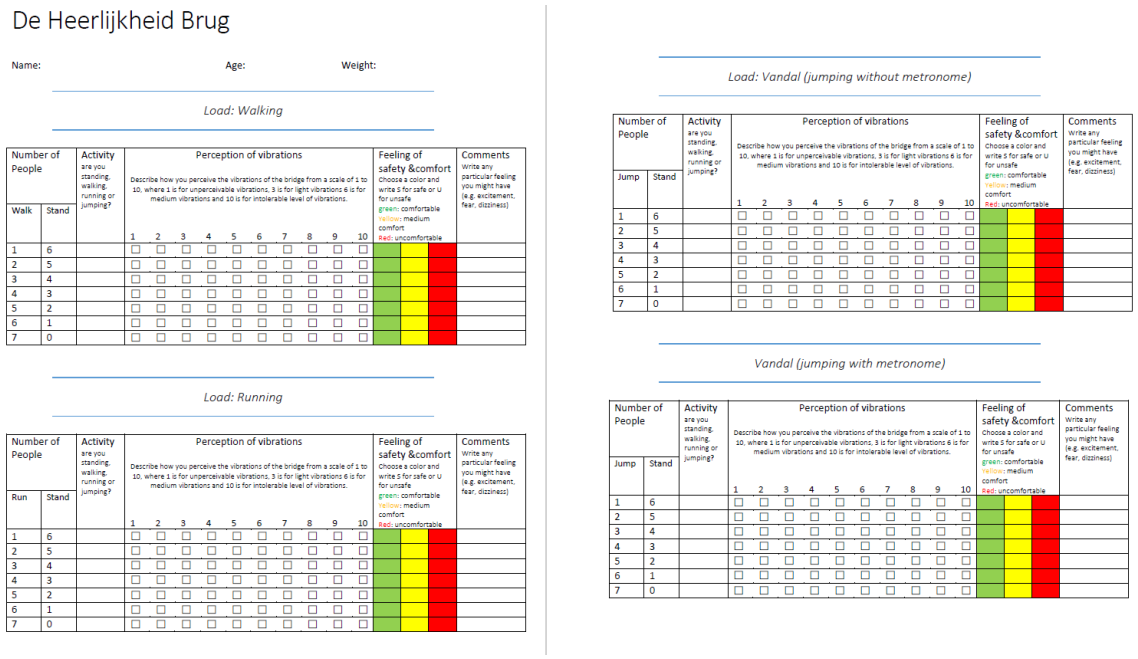

De Heerlijkheid Brug

Name: Age: Weight:

Load: Walking

Number of People		Activity	Perception of vibrations										Feeling of safety &comfort	Comments
Walk	Stand		1	2	3	4	5	6	7	8	9	10		
1	6													
2	5													
3	4													
4	3													
5	2													
6	1													
7	0													

Load: Running

Number of People		Activity	Perception of vibrations										Feeling of safety &comfort	Comments
Run	Stand		1	2	3	4	5	6	7	8	9	10		
1	6													
2	5													
3	4													
4	3													
5	2													
6	1													
7	0													

Load: Vandal (jumping without metronome)

Number of People		Activity	Perception of vibrations										Feeling of safety &comfort	Comments
Jump	Stand		1	2	3	4	5	6	7	8	9	10		
1	6													
2	5													
3	4													
4	3													
5	2													
6	1													
7	0													

Vandal (jumping with metronome)

Number of People		Activity	Perception of vibrations										Feeling of safety &comfort	Comments
Jump	Stand		1	2	3	4	5	6	7	8	9	10		
1	6													
2	5													
3	4													
4	3													
5	2													
6	1													
7	0													

Figure A.3 Questionnaire used to describe the perception of vibrations, safety and comfort

scans every each one of the frames and calculates for each frame the relative position of the center of the defined color with respect to its initial position in frame 1, then in translated this distance from pixels to millimeters. By exporting the relative displacements in excel the response of the displacements can be plotted. The program used is presented in figure A.4.

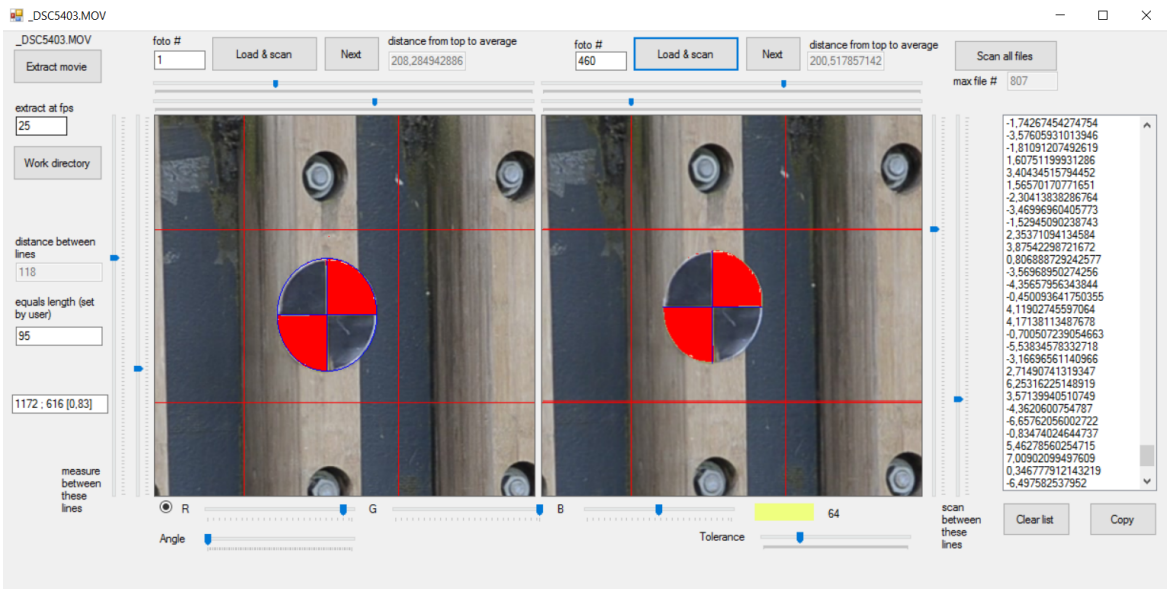

Figure A.4 ClipAnalyser

The next step is to plot the response of the displacements with respect to time and find the maximum and minimum displacements as well as the average amplitude of the biggest displacements. This procedure is presented in figure A.5.

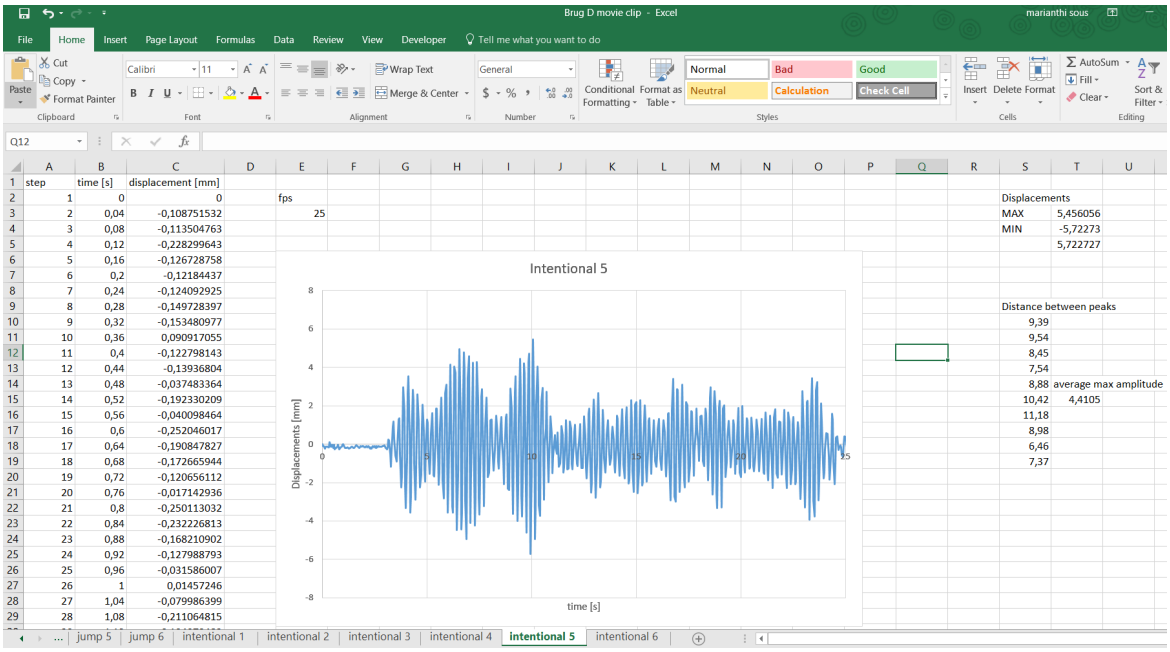

Figure A.5 Analyzing the response of the displacements

A.2.2 Analyzing the accelerations

For the analysis of the accelerations, the recorded files are input in Excel. By use of the Fourier transform, the eigen-frequencies of the response are calculated. In the case of walking and running, often the step frequency of the pedestrians was also visible along with the main frequency of vibration that in most cases was double the step frequency. Moreover, the time history of the acceleration is plotted and the damping ratio is calculated by fitting to the real response, the response that comes from the expression A.1, where A is the amplitude of the response, ζ is the damping ratio found with trial and error until the two curves match, and $\omega_D = \sqrt{1-\zeta^2} \cdot \omega$ with omega being the main frequency of vibration of the bridge. Two examples of the analysis are presented in figures A.6 and A.7. In figure A.6 the case of a group of 5 people running is presented, where the step frequency of the pedestrians is visible, and in figure A.7 the case of the vandal loading applied by the same group of 5 people, in this case the step frequency is equal to the natural frequency of the footbridge.

$$a(t) = A \cdot e^{-\zeta \omega t} \sin(\omega_D t) \tag{A.1}$$

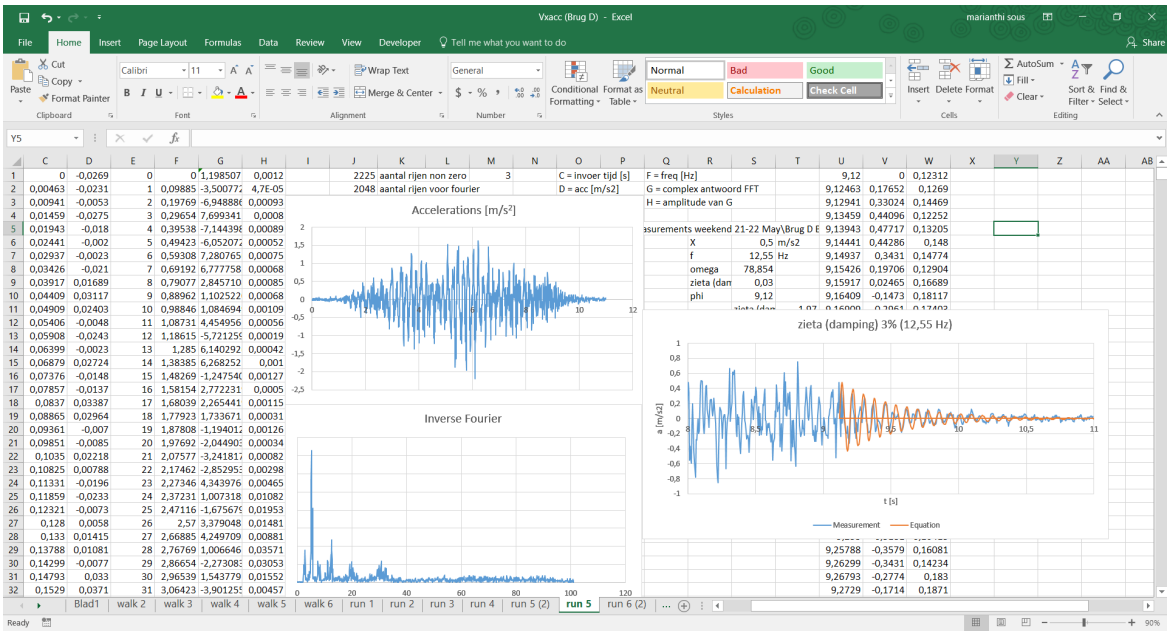

Figure A.6 Analyzing the response of the accelerations for running loads

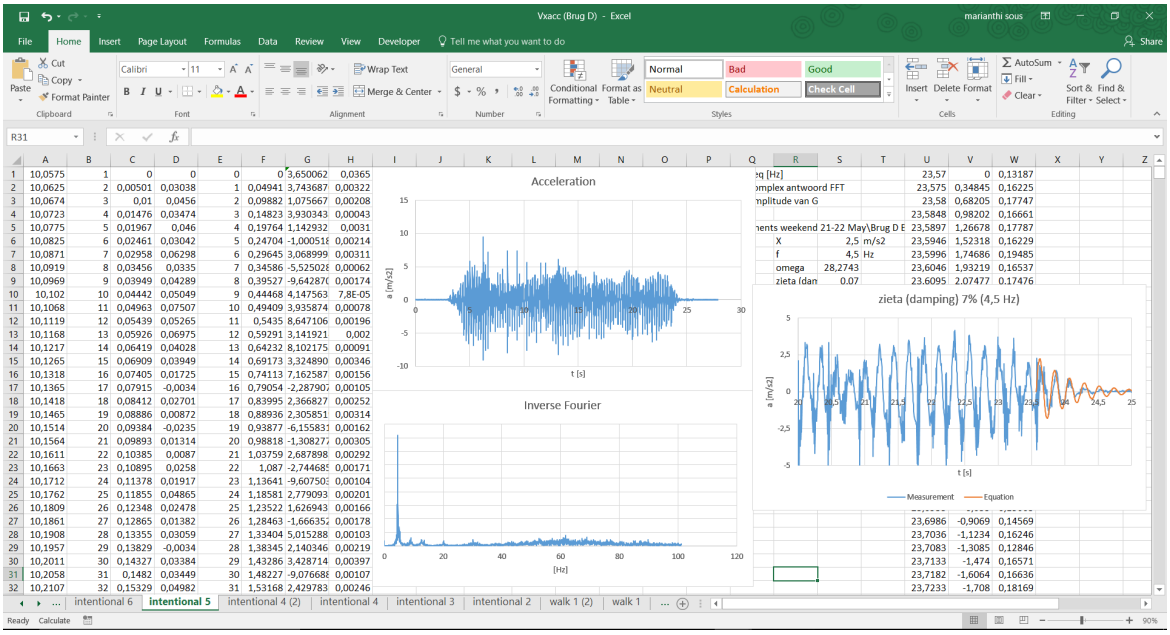

Figure A.7 Analyzing the response of the accelerations for vandal loading

A.2.3 Evaluating the questionnaires

For the evaluation of the comfort level, first, the terms "Comfortable", "Medium comfort" and "Uncomfortable" were substituted by the numbers "1", "2" and "3" respectively. Consequently, the responses of the pedestrians were separated in two, with respect to the action

of the pedestrians (standing or moving). Following that, the weighted arithmetic mean is calculated for the two cases. For example, in the case that four people were jumping intentionally on de Poortugaal Brug and three people were standing, the maximum acceleration measured was $4.75 m/s^2$. For this acceleration, two of the standing people replied that they felt uncomfortable ("3") and one answered that he experienced medium comfort ("2"). In the case of the jumping people, one of them replied that the level of comfort was medium ("2") and the rest three that the level of comfort was good ("1"). Consequently, the weighted arithmetic mean that describes the comfort level of the jumping pedestrians is given by expression A.2 and the one that describes the comfort level of the standing pedestrians is given by expression A.3. Translating the numbers "1", "2" and "3" back to comfort limits it is observed that for the jumping people the average comfort was good to medium (closer to good), and for the people standing it was very close to bad comfort.

$$\frac{3 \cdot \mathbf{1} + 1 \cdot \mathbf{2}}{4} = \mathbf{1.25} \tag{A.2}$$

$$\frac{2 \cdot \mathbf{3} + 1 \cdot \mathbf{2}}{3} = \mathbf{2.67} \tag{A.3}$$

Appendix B

Dynamic characteristics and dynamic behavior of bridges tested

B.1 Bridges tested

B.1.1 Poortugaal bridge

The Poortugaal bridge is a three span footbridge that is located in the area Poortugaal of Rotterdam. From the heel tests it was found that it has an eigenfrequency of 6.13 Hz. According to the modern design codes and guidelines this bridge satisfies the comfort criteria since its natural frequency is above 5 Hz.

Figure B.1 Poortugaal brug

B.1.2 Heerlijkheid brug

Heerlijkheid brug is a one-span bridge close to the park Bonairepark in Rotterdam. It has a natural frequency of 4.35 Hz, as found after performing a number of heel tests, and therefore according to the codes its comfort criteria need to be confirmed.

Table B.1 Properties of Poortugaal brug

Length	L	$[m]$	26.2
Width	b	$[m]$	3.77
Height	h	$[m]$	0.30
Mass per length	m	$[kg/m]$	< 463
Stiffness	EI	$[kNm^2]$	$7.7 \cdot 10^4$
Eigenfrequency	f_0	$[Hz]$	6.13

Figure B.2 Heerlijkheid brug

Table B.2 Properties of Heerlijkheid brug

Length	L	$[m]$	20.00
Width	b	$[m]$	1.50
Eigenfrequency	f_0	$[Hz]$	4.35

B.1.3 Brug D in Bonairepark

Brug D is a bridge in Bonairepark, a quiet park at the outskirts of Rotterdam. Its natural frequency as found by performing heel tests is 5.34 Hz and just like Poortugaal, it would be considered to satisfy the serviceability criteria and no further verification would be necessary.

Figure B.3 Brug D (Bonairepark)

Table B.3 Properties of brug D

Length	L	$[m]$	16.70
Width	b	$[m]$	1.50
Height	h	$[m]$	0.625
Mass per length	m	$[kg/m]$	< 299
Stiffness	EI	$[kNm^2]$	$9.5 \cdot 10^4$
Eigenfrequency	f_0	$[Hz]$	5.34

B.2 Dynamic behavior of the bridges tested

B.2.1 Poortugaal bridge

As already mentioned, Poortugaal bridge has an eigenfrequency larger than 5 Hz and according to the modern codes (EC1, British Standards, EUR23984 and Setra) the comfort criteria are met, and therefore, no extra verification is needed. However, after conducting the series of tests described in chapter 4 and Appendix A and measuring the maximum accelerations that developed in the bridge per test (Figure B.5), it was observed that the acceleration limits introduced by the codes were exceeded in many of the tests. More specifically, the accelerations developed due to people walking are small (maximum value is $0.5m/s^2$) and remain below the limits that the codes set. However, running loads produce accelerations that are higher than the $0.7m/s^2$ limit of EC0 and EC1, with maximum produced acceleration for running being $2.17m/s^2$. The limit of the British Annex $1.76m/s^2$ is exceeded when 4 and 7 people are jogging simultaneously, whereas the limit of the British Standards is satisfied only in the case that one person is running. As for the comfort classes introduced by EUR23984 and Setra and their corresponding acceleration ranges, it can be seen that the bridge design ensures maximum comfortability when pedestrians are walking, whereas for joggers the comfort is minimum. In the extreme occasion that people are jumping on

the deck, minimum comfort is attained when up to 2 people are jumping (with or without metronome), but for a bigger number of people jumping the comfort level is unacceptable. The maximum acceleration that is noted is $7.1 m/s^2$ for the case of 6 people jumping with the help of a metronome.

The root mean square (r.m.s) accelerations of each test, for a period of integration of $t = 0.5s$ and a step of $\Delta t = 0.15s$, are also presented in Figure B.6. By comparing them with the maximum values of the accelerations it is noticed that although in most cases the r.m.s acceleration increases or decreases in the same way as observed in the maximum accelerations graph, the values of the r.m.s. are in most cases more than 2 times smaller than the corresponding maximum values.

It can be observed that in general an increasing number of pedestrians leads to higher accelerations. Naturally, there are a few cases that for the same load type a lower acceleration is observed for a larger number of pedestrians, but this is attributed to the synchronization of the pedestrians in those particular tests and to some local peaks, that might not be very representative of the acceleration time history.

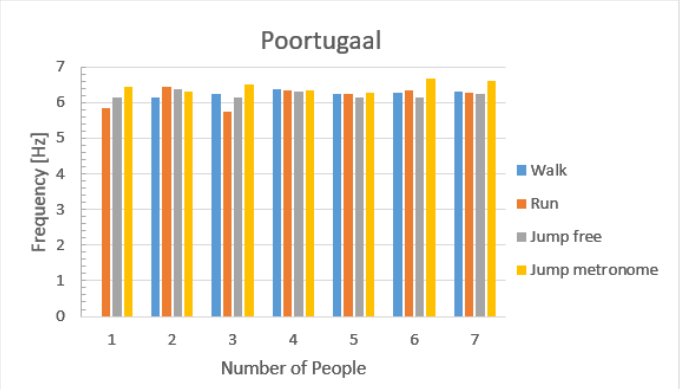

Figure B.4 Frequencies of vibration of Poortugaal bridge for different number of active people and different types of loading

In figure B.7 the amplitude of displacements can be seen for the four different load types and for a varying number of people. For walking loads, the amplitude of displacements is less than 1 mm, whereas in the case of walking this value of 1mm is exceeded in two cases, with the amplitude reaching values of 1.6 and 2.5 mm when 2 and 5 people are running on deck respectively. For the cases of jumping the displacements are bigger, reaching values up to 4mm. However, the maximum amplitudes of displacement for each load type are not always observed at the tests where the maximum accelerations occur.

The frequency of vibration of each test performed varies slightly around the value of the fundamental frequency 6.13 Hz. Another interesting observation is that the damping

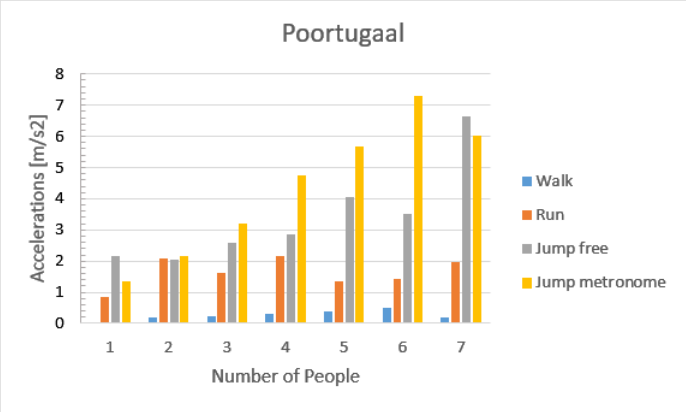

Figure B.5 Maximum accelerations of Poortugaal bridge for different number of active people and different types of loading

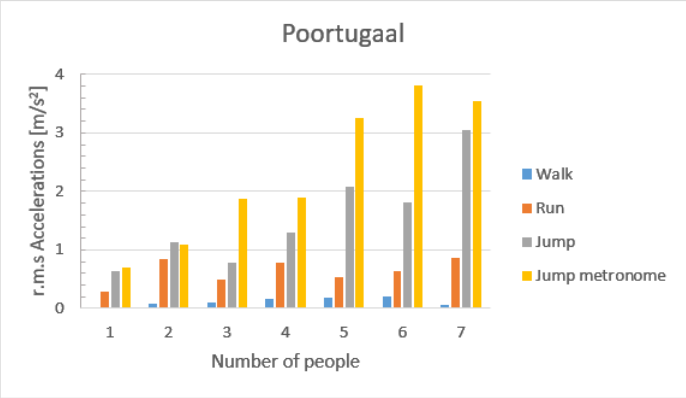

Figure B.6 Root mean square accelerations of Poortugaal bridge for different number of active people and different types of loading

ratio is higher for the cases of jumping with or without metronome. Comparing the damping ratio with the accelerations produced, it can be concluded that the tests in which higher accelerations and displacement amplitudes were developed, also developed higher damping ratio. However, although a relation can be identified between the high amplitudes due to different load types and the damping ratios, a precise relation between amplitudes and damping cannot be given. A higher acceleration or displacement doesn't necessarily mean higher damping, as can be seen by comparing the graphs of Figures B.5 and B.7 and B.8.

Unfortunately, no clear pattern can be discerned about the way the mass of the passive people influences the frequency and the damping of the vibrations. However, the total mass of the pedestrians participating at the test is 493 kg, which is only 4% of the total mass of the footbridge. Possibly a larger percentage of mass would influence the vibrations in a more clear way.

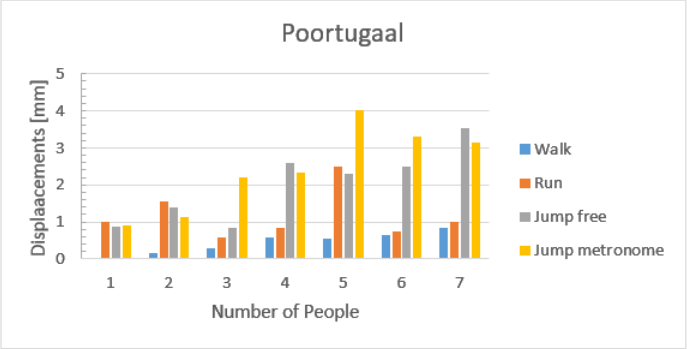

Figure B.7 Amplitude of displacements of Poortugaal for different number of active people and different load types

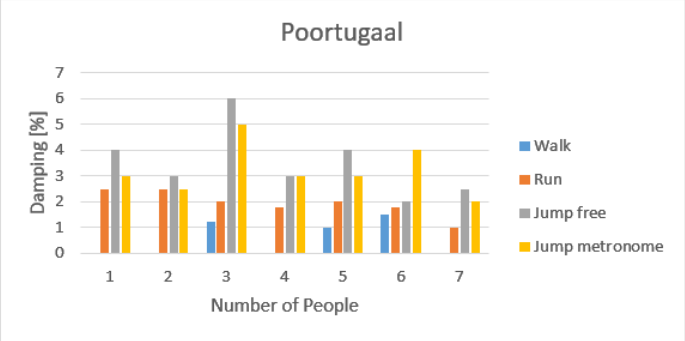

Figure B.8 Damping of Poortugaal for a different number of active people and different types of loading

B.2.2 Heerlijkheid bridge

As it can be seen from Figure B.9, the frequency of vibrations in the case of Heerlijkheid bridge varies more than it did in the case of the Poortugaal bridge. What is of great interest is that the main frequency of vibrations in the case of running loads is lower than in the cases of the other 3 types of loading, however a number of higher eigenfrequencies is also participating. The step frequency of the joggers according to Bachmann et al is 2-3.5 Hz, therefore in the case of running the main vibrating frequency of the bridge is indeed the step frequency of the joggers, whereas in the case of walking the main frequencies participating are multiples of the walking frequency of the pedestrians, which is around 1.6-2.4 Hz. Therefore, for the cases that 1 to 4 people are crossing the bridge, the main frequency of vibration is equal to the 2nd multiple of the walking frequency of the pedestrians, while for 5 to 7 people crossing the bridge the main participating frequency is the 3rd multiple of the walking frequency.

When it comes to the maximum accelerations developed, it can be seen that for walking loads the acceleration limits are satisfied and maximum comfortability is achieved, since the maximum acceleration developed is $0.42m/s^2$. For running loads the limits of EC0 and EC1 are exceeded when more than 4 people are running on the deck of the footbridge, however the limits of the British Annex are satisfied. Even when 2 people are running, maximum comfortability is still achieved according to EUR 23984 and Setra, but for a group of 3 or 4 joggers the comfortability becomes medium, while for more than 5 joggers the footbridge is considered to have minimum comfort. Moreover, the accelerations induced in Heerlijkheid bridge due to running are smaller than the accelerations that developed in Poortugaal bridge (the maximum acceleration observed for running is $1.52m/s^2$ for 7 people running), even though the natural frequency of the bridge is lower than 5 Hz and certainly lower than Poortugaal's. Why is that? The fact that the bridge is not vibrating with a frequency equal or close to its natural frequency but with a smaller frequency (1.5-1.7 times smaller), results in a decreased magnitude of accelerations.

Accelerations due to jumping freely or with a metronome are to some extent higher than in the previous bridge. Even though the natural frequency of Heerlijkheid is considered more critical than the one of Poortugaal bridge, the accelerations for walking and running are smaller than they were in Poortugaal, whereas for jumping freely it seems that the accelerations developed are in some cases higher for Poortugaal and in some others higher for Heerlijkheid. Finally, jumping with a metronome produced high accelerations (up to $9m/s^2$), bigger than for Poortugaal bridge. An attributing factor to that is the lower frequency of Heerlijkheid that made easier and less tiring the maintenance of the jumping frequency of the users and lead to an improved synchronization between the users, unlike in the case of Poortugaal bridge.

The amplitudes of the displacements, just like the accelerations are smaller in the case of walking and in some tests including running. However, for groups of 4 and more than 5 joggers and for all the tests that were concerning jumping loading, the amplitudes of displacements were higher than they were in Poortugaal bridge, even if the corresponding accelerations were smaller. Especially for the case of intentional excitation with metronome, the displacements were from 2-5 times larger, reaching a maximum amplitude of 15mm (Figure B.12).

Finally, the damping of the Heerlijkheid brug is in general higher than it is for Poortugaal. It can be seen that in most cases the damping of the structure in case of vandal loading (jumping) is higher, this enhances the observation that the damping is higher when vibrations with higher amplitudes occur. The lower damping occurs in the case of walking load. For running the damping varies from 3 to 10% (with 10% being the highest damping observed).

Jumping also produces higher damping, with values exceeding 5% and even reaching 9% in one case.

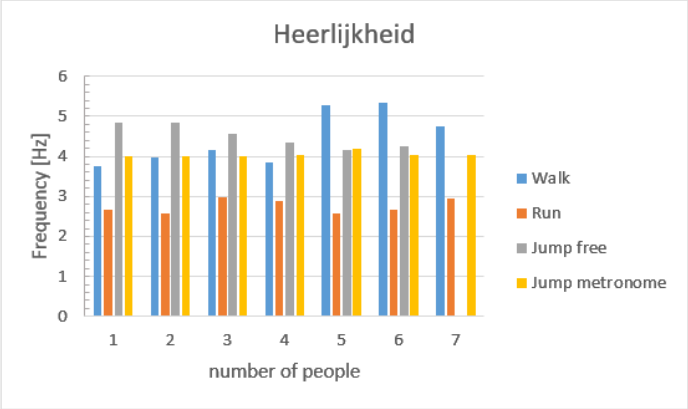

Figure B.9 Frequency of vibrations for a different number of active people and for different types of loads

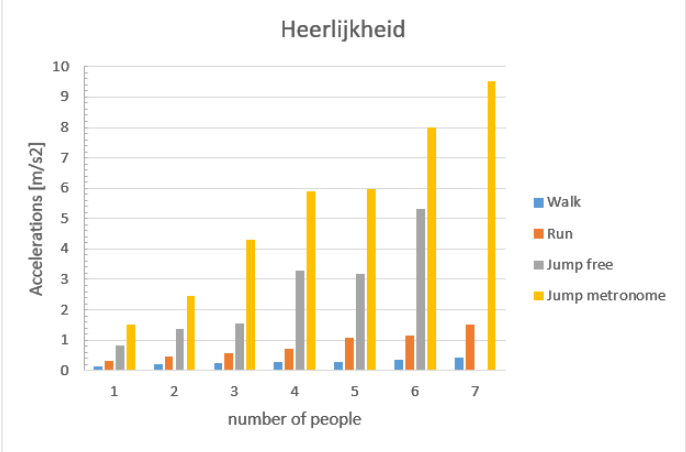

Figure B.10 Maximum accelerations of Poortugaal bridge for different number of active people and different types of loading

B.2.3 Brug D

The natural frequency of this bridge is found to be 5.34 Hz and according to the codes it would be considered to satisfy the serviceability criteria and no further verification would be necessary, just like Poortugaal.

The main frequencies of vibrations in the cases of walking seem to be equal or a bit higher than the natural frequency of the footbridge, which is approximately equal to the 3rd

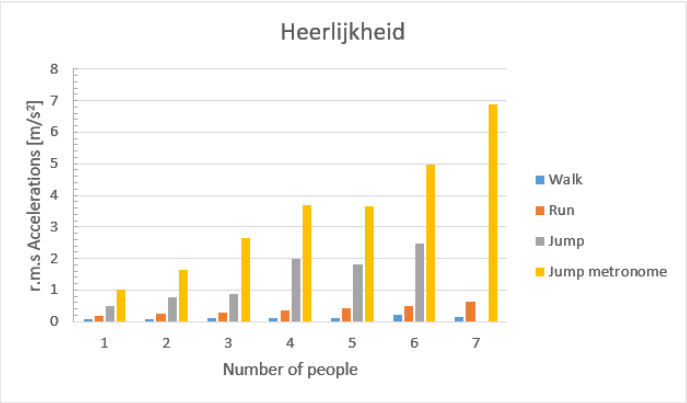

Figure B.11 Root mean square of accelerations of Heerlijkheid bridge for different number of active people and different loading types

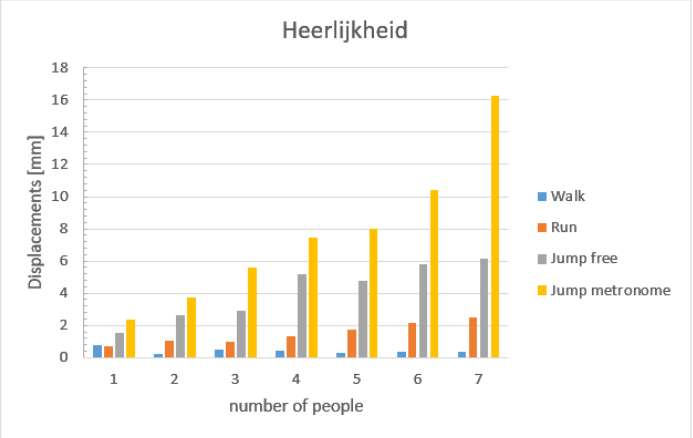

Figure B.12 Amplitude of displacements of Heerlijkeid bridge for different number of active people and different load types

multiple of the walking frequency of the pedestrians. As for running, in most of the tests more than one eigenfrequencies participate. The participating frequencies are multiples of the running frequency of the pedestrians, around $2.7 - 2.8Hz$.

By taking a look at the accelerations developed one can see that the accelerations due to walking do not exceed the limits set by the codes for comfortability, however the accelerations that are produced due to running loads exceed the limits of the eurocodes EC0 and EC1. The limit of the British Annex ($1.76m/s^2$) is exceeded for the cases that more than 5 people are running, whereas the British Standards' limit is only satisfied in the case of one person running. Even for the more flexible limits of Setra and EUR 23984 the comfortability is considered minimum and even unacceptable when 6 or more people are running. When vandal loading (jumping) is applied, the limits are over-exceeded and the comfort is in the

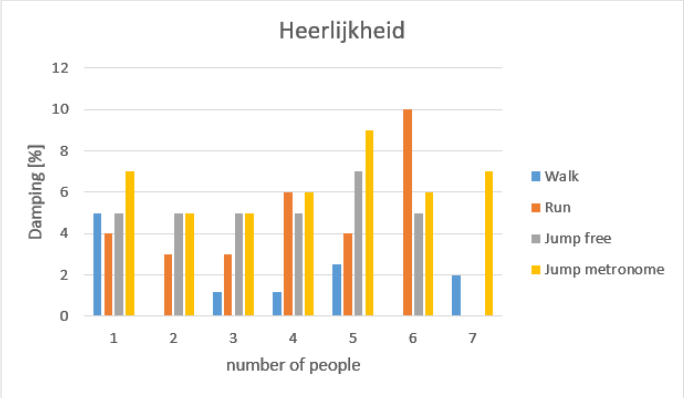

Figure B.13 Damping of vibrations of Heerlijkheid bridge for different number of active users and different types of load

majority of the cases unacceptable. The accelerations developed due to jumping, with or without metronome, easily reach maximum values up to $9m/s^2$. The r.m.s. accelerations have values that are approximately 2 times smaller than the maximum accelerations developed at the equivalent tests.

The displacements developed at Brug D are in general larger than those of Poortugaal bridge, with the exception of a few tests of running and walking. The deformations that occur in the Heerlijkheid bridge are larger for the case of jumping loads and running of groups consisting of more than 4 joggers. The rate of increase on the displacements is closer to the rate of increase of the r.m.s. accelerations, and not the maximum accelerations.
When it comes to the damping ratio, it is obvious that the damping of the footbridge while people are walking is much lower than in the other cases and it has a value of around 2%. Damping is higher in the cases of jumping with metronome, varying from 4 to 11%, whereas damping in the case of running and of jumping freely is quite similar in most cases, with an approximate value of 5%.

B.3 Verification of requirements of codes for comfort

It is interesting to compare the measured accelerations with the acceleration limits that are proposed by the codes. The three bridges that were used for the measurements were in a rural area at the outskirts of Rotterdam. In order to calculate the acceleration limit according to the British Annex, coefficients k_1,k_2,k_3 and k_4 need to be identified. For a bridge built in a rural environment and used as primary route $k_1 = 1.6$ and $k_2 = 1$ and since the bridges were less than 4m above the ground level $k_3 = 1.1$ and k_4 is usually taken as 1. Regarding the calculation of the acceleration limit according to the British Standards the natural frequency

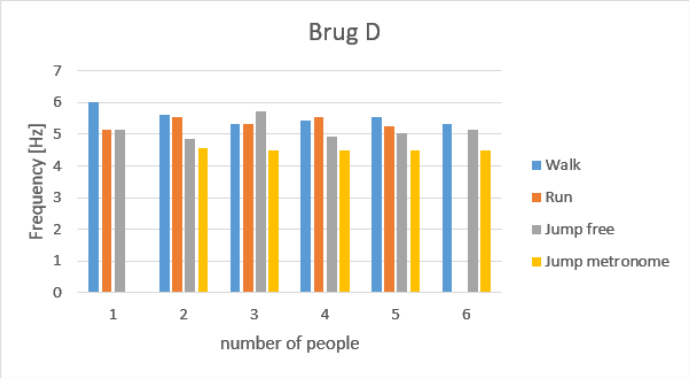

Figure B.14 Frequencies of vibrations of Brug D for a different number of active people and for different types of loads

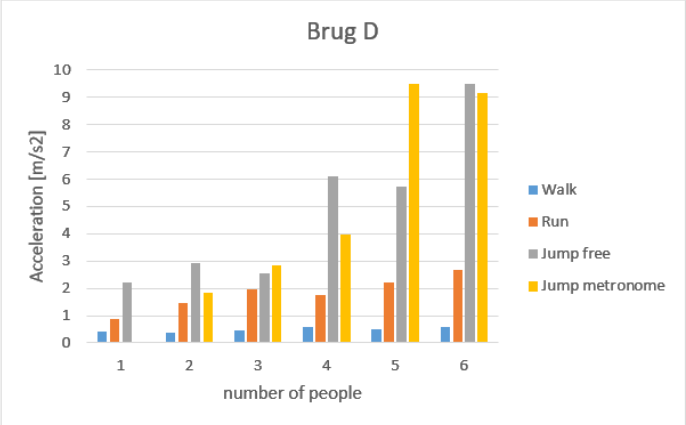

Figure B.15 Maximum accelerations of Brug D for different types of loading and different number of active people

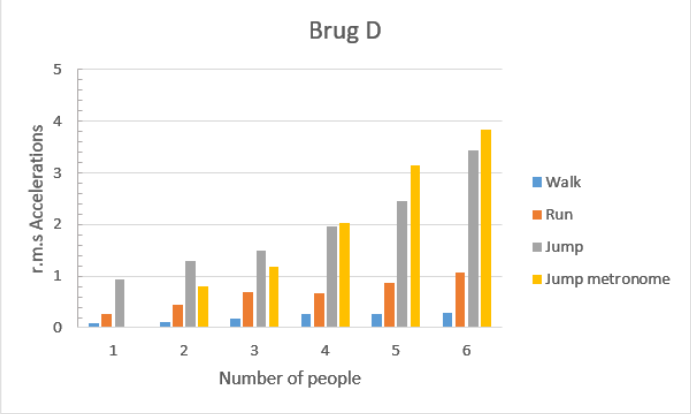

Figure B.16 Root mean square of accelerations of Brug D for different load cases and different numbers of active people

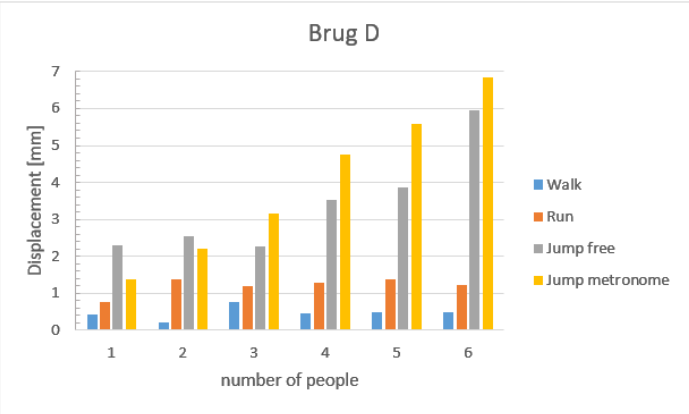

Figure B.17 Amplitude of displacement of Brug D for different load types and different numbers of active people

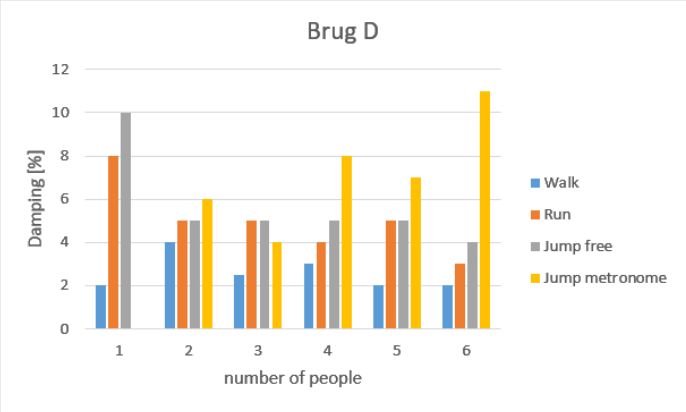

Figure B.18 Damping of vibrations of Brug D for different number of actve people and different load types

of the footbridge is needed. This is calculated by performing a series of heel tests on the bridge while recording the acceleration history and performing a Fourier transform to find the eigen-frequencies. The acceleration limits proposed by the different codes are presented in table B.4.

For Poortugaal brug, no verification is required from the codes since the natural frequency is higher than $5Hz$. The acceleration limits of all the codes are satisfied in the case of walking groups. However, for running the limit proposed by the British Standards is exceeded when more than 2 people are running across the footbridge. The comfort limit proposed by the British Annex is also exceeded in the tests where 2, 4 and 7 people were jogging. Finally, according to Setra the comfort limit for running is considered minimum.

For Heerlijkheid brug, comfortability is satisfied according to all the proposed limits when the pedestrians are walking. However, if more than 5 joggers run across the bridge,

Table B.4 Acceleration limits according to the different codes

Code	Acceleration limit $[m/s^2]$
EN0 and EN1	0.7
British Annex to EN1	1.76
British Standards	1.24 for Poortugaal 1.16 for Brug D 1.04 for Heerlijkheid
Setra and EUR23984	$< 0.50 - 1.00$ max comfort $0.50 - 1.00$ medium comfort $1.00 - 2.50$ min comfort > 2.50 unacceptable

the comfort level of the bridge is unsatisfactory according to the British Standards, whereas according to Setra when 3 or 4 joggers are running the comfort level is medium and when the number increases to more than 5 joggers minimum comfort is achieved.

In the case of Brug D, no verification is required since its natural frequency exceeds $5Hz$. Just like for Poortugaal and Heerlijkheid, the comfort level during walking is always satisfied. However, for running loads the accelerations developed are higher than the other two bridges. According to the British Annex for more than 3 joggers running across the bridge, the footbridge doesn't satisfy the comfort criteria. For the British Standards, even a group of 2 joggers is enough to characterize the comfort of the bridge insufficient, whereas for Setra and EUR 23984 for a group of 6 people the comfort level is characterized unacceptable and the design shouldn't suffice.

Naturally, the maximum accelerations due to jumping and jumping synchronized are even higher, reaching values as high as $7 - 9m/s^2$. However, since jumping is considered an exceptional load case that causes issues in the ULS and not in the SLS, no comparison will be done between the maximum accelerations for jumping and the acceleration limits of the codes.

Finally, it is also interesting to make a comparison between the damping measured on site, and the damping proposed by the codes. Setra proposes values of critical damping ranging between 0.1% and 2.0% and advises to not overestimate structural damping in order to avoid under-dimensioning. A look at the damping ratios calculated according to the British Standards and the British National Annex in Chapter 6.2 (0.8% and 1.1% respectively) shows that the damping ratios used in analyses are usually quite low. From the analyses of the responses of the three bridges, it was observed that the damping ratios taking place are in

most cases higher than that. More specifically, the lowest damping ratios were observed in Poortugaal bridge, where the damping ratios for walking and running vary between 1 and 2%. In Heerlijkheid brug for walking, the damping varies mostly between 1% and 2% but is exceeded two times reaching values up to 4% for walking, whereas for Brug D damping for walking varies between 2-4%. When it comes to running, both for Brug D ad Heerlijkheid the damping is larger than 3%, reaching values even as high as 6, 8 or 10%. As for the case of jumping, a minimum damping of 5% is observed in Heerlijkheid and Brug D. However, for Poortugal, the minimum damping for jumping starts at 2% and a maximum damping ratio of 6% is reached.

What can be concluded is that the assumption of a damping ratio between 1 and 2% for the case of walking agrees with the findings from the experiments performed. However, in the case that vandal loading is applied, a damping ratio of at least 2% should be considered so that the design will not be considered conservative.

Appendix C

Dynamic analysis of a footbridge in Finite Element Programs

When modeling a structure in a finite element program, there are certain things that have a big influence on the final results. The boundary conditions of the structure, the interface between the elements, the correct material and cross-sectional properties, the selection of a sufficiently dense mesh and many more. However, when a dynamic analysis is performed things get even more complicated. Some of the parameters that influence the most the final outcome and should be treated with care are presented below.

C.1 Important parameters in a dynamic analysis

- Stiffness m
- Mass m
- Damping c
- Natural frequency $\omega_n = \sqrt{k/m}$

From these terms, the stiffness and sometimes the mass are also used during the static analysis of a system. However the damping is a property that is not encountered in other cases. The damping represents the energy dissipation of the structure and it usually consists of material-internal damping, structural damping or fluid-viscous damping. The most commonly used damping model is the viscous damping model because of its simplicity [55]. When analyzing multiple degree of freedom systems with similar damping mechanisms distributed throughout the structure, classical damping is considered an appropriate idealization. Usually, the Rayleigh damping is used, as presented in equation C.1. [12]

$$\mathbf{c} = a_0\mathbf{m} + a_1\mathbf{k} \tag{C.1}$$

The damping ratio of the n^{th} mode of such a system is:

$$\zeta_n = \frac{a_0}{1}\frac{1}{\omega_n} + \frac{a_1}{2}\omega_n \tag{C.2}$$

If it is assumed that both modes have the same damping ratio ζ, then the coefficients a_0 and a_1 are defined as:

$$a_0 = \zeta\frac{2\omega_i\omega_j}{\omega_i + \omega_j} \quad a_1 = \zeta\frac{2}{\omega_i + \omega_j} \tag{C.3}$$

C.2 Dynamic analysis with Finite Element Method

In order to formulate the equations of motion for a structure using the finite element method, the following steps are followed:

1. Simulate the structure as the aggregation of finite elements interconnected only at the nodes and define the degrees of freedom at these nodes.

2. Form for every finite element the element matrices of stiffness $\mathbf{K_e}$ and mass $mathbfM_e$ and the element vector of the applied force $\mathbf{P_e}(t)$.

3. Form the global stiffness matrix of the structure $\mathbf{K}$, the global mass matrix $\mathbf{M}$ and the applied force vector $\mathbf{P}(\mathbf{t})$. In addition, form the global damping matrix C as described in equation C.1. ($\mathbf{C} = a_0\mathbf{M} + a_1\mathbf{K}$). The natural frequencies needed for the calculation of the coefficients a_0 and a_1 are found by solving the eigenvalue problem: $\mathbf{K}\phi = \omega^2\mathbf{M}\phi$.

4. Formulate the equations of motion:

$$\mathbf{Ma} + \mathbf{Cv} + \mathbf{K}u = \mathbf{P}(t) \tag{C.4}$$

   where $a = \ddot{u}$ is the acceleration and $v = \dot{u}$ is the velocity.

5. Solve the system of equations C.4. The numerical method used in the finite element program that was used in this thesis, is the Newmark method.

C.2.1 Newmark method

The Newmark method is a time-step method developed in 1959 by N.M. Newmark, based on the following equations [12] :

$$\dot{u}_{i+1} = \dot{u}_i + [(1-\gamma)\Delta t]\,\ddot{u} + (\gamma\Delta t)\ddot{u}_{i+1} \tag{C.5}$$

$$u_{i+1} = u_i + (\Delta t)\dot{u}_i + \left[(0.5-\beta)(\Delta t)^2\right]\ddot{u} + \left[\beta(\Delta t)^2\right]\dddot{u}_{i+1} \tag{C.6}$$

Typical choices for the parameters γ and β are $\gamma = \frac{1}{2}$ and $\frac{1}{6} \leq \beta \leq \frac{1}{4}$. In the software used it is chosen: $\beta = 0.25$ and $\gamma = 0.5$. The procedure followed ca be described with the following steps:

1. Initial calculations
   (a) Select Δt
   (b) Solve: $\mathbf{M a_0} = \mathbf{P_0} - \mathbf{C v_0} - \mathbf{K u} \leftrightarrow \mathbf{a_0} = [\mathbf{M}]^{-1}(\mathbf{P_0} - \mathbf{C v_0} - \mathbf{K u})$
   (c) $\hat{\mathbf{K}} = \mathbf{K} + \frac{1}{\beta(\Delta t)^2}\mathbf{M} + \frac{\gamma}{\beta\Delta t}\mathbf{C}$
   (d) $\mathbf{A} = \frac{1}{\beta\Delta t}\mathbf{M} + \frac{\gamma}{\beta}\mathbf{C}$ and $\mathbf{B} = \frac{1}{2\beta}\mathbf{M} + \Delta t\left(\frac{\gamma}{2\beta} - 1\right)\mathbf{C}$
2. Calculations for each time step i
   (a) $\mathbf{P_i}$ is known
   (b) $\Delta\mathbf{P_i} = \mathbf{P_{i+1}} - \mathbf{P_i}$
   (c) $\Delta\hat{\mathbf{P}}_\mathbf{i} = \Delta\mathbf{P_i} + \mathbf{A v_i} + \mathbf{B a_i}$
   (d) Solve: $\hat{\mathbf{K}}\Delta\mathbf{u_i} = \Delta\mathbf{P_i} \leftrightarrow \Delta\mathbf{u_i} = \hat{\mathbf{K}}^{-1}\Delta\mathbf{P_i}$
   (e) $\Delta\mathbf{v_i} = \frac{\gamma}{\beta\Delta t}\Delta\mathbf{u_i} - \frac{\gamma}{\beta}\mathbf{v_i} + \Delta t\left(1 - \frac{\gamma}{2\beta}\right)\mathbf{a_i}$
   (f) $\Delta\mathbf{a_i} = \frac{1}{\beta(\Delta t)^2}\Delta\mathbf{u_i} - \frac{1}{\beta\Delta t}\mathbf{v_i} - \frac{1}{2\beta}\mathbf{a_i}$
   (g) $\mathbf{u_{i+1}} = \mathbf{u_i} + \Delta\mathbf{u_i}$, $\mathbf{v_{i+1}} = \mathbf{v_i} + \Delta\mathbf{v_i}$ and $\mathbf{a_{i+1}} = \mathbf{a_i} + \Delta\mathbf{a_i}$
3. Repetition for the next time step. Replace i with i_1 and repeat steps to of the previous step.

C.2.2 Dynamic analysis in VericalX

For the simulation and the dynamic analysis of the footbridge VericalX, a finite element program was used. For the simulation of the footbridge, first the properties of the materials used are defined (modulus of elasticity, poisson ratio, mass density (figure C.1)). Then the properties of the cross-section are defined and the footbridge is simulated as a beam, that is divided (meshed) in smaller elements (figure C.3). Once an appropriately fine mesh is chosen, the boundary conditions and the loads are applied (figure C.4). Finally, to perform the dynamic analysis, first a modal analysis needs to be run in order to obtain the natural frequencies of the structure, and then a transient analysis is performed by defining a sufficiently small time step Δt and a damping ratio ξ (figure C.5). Once the analysis is over, we can export the desirable results of the nodes of interest (figure C.6).

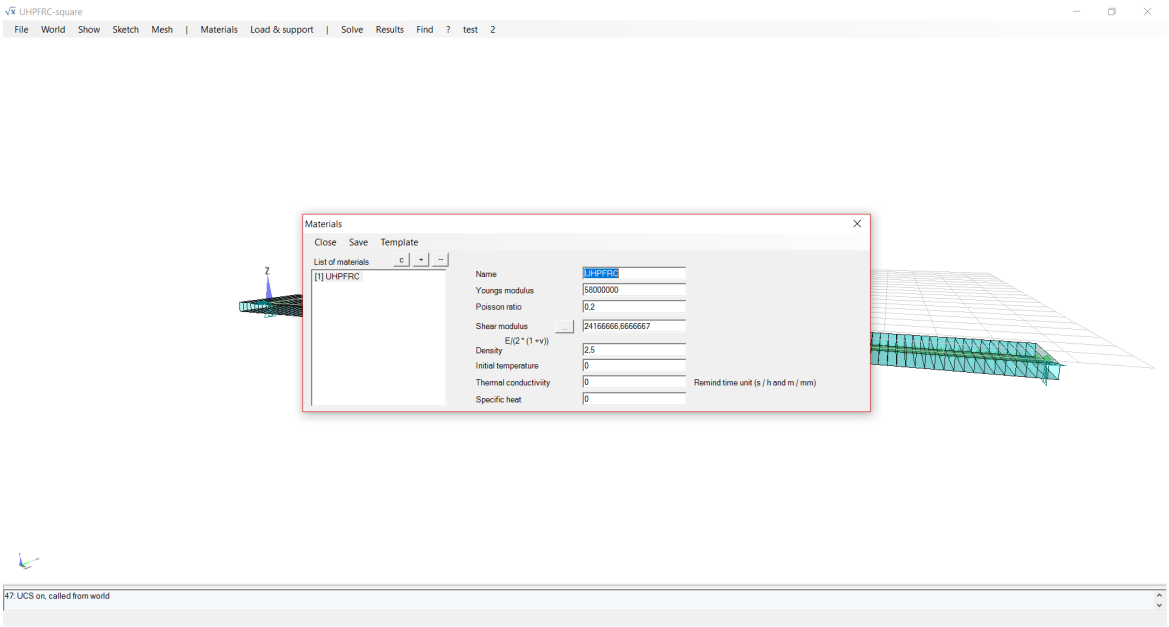

Figure C.1 Defining the material properties of the footbridge in VericalX

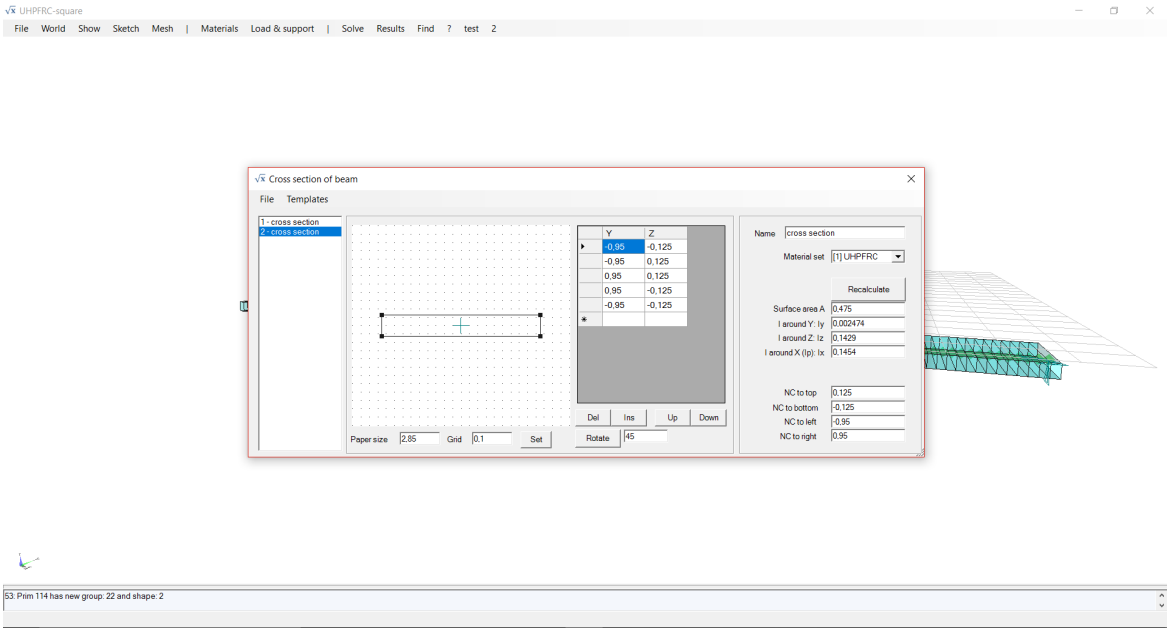

Figure C.2 Defining the cross-sectional properties of the footbridge in VericalX

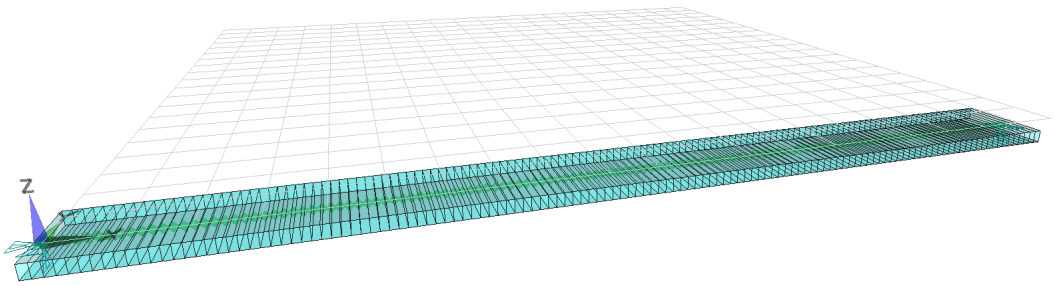

Figure C.3 Designing and meshing the footbridge in VericalX

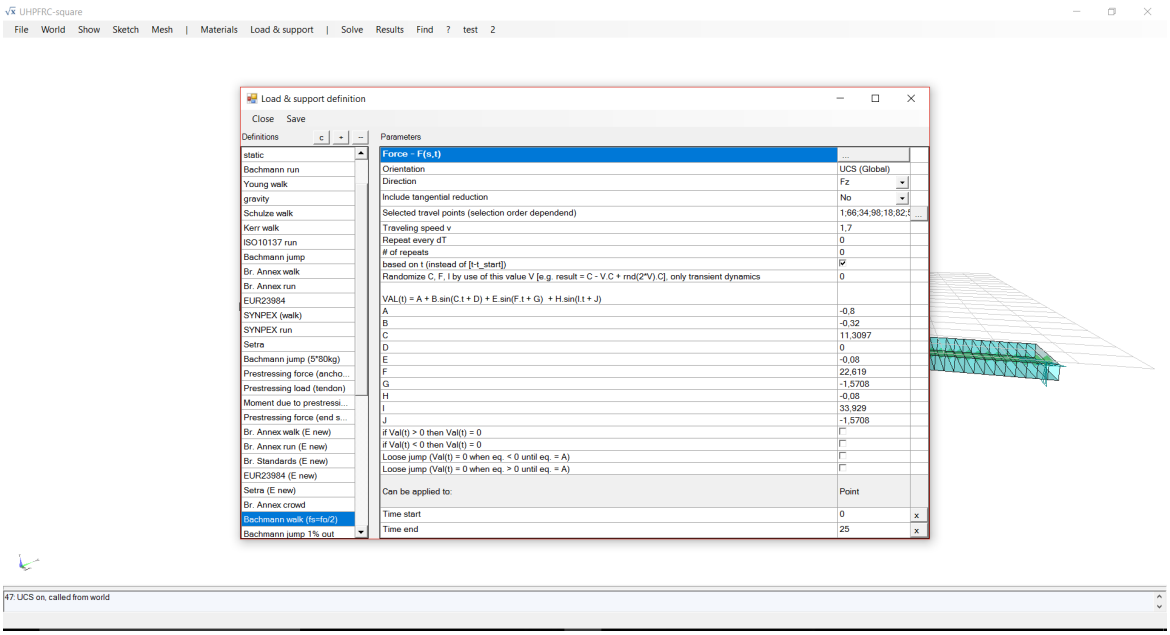

Figure C.4 Applying the load on the footbridge in VericalX

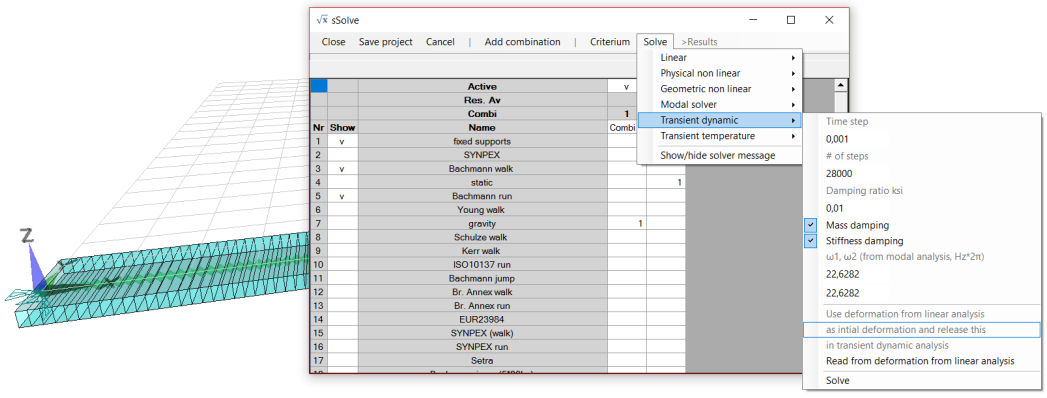

Figure C.5 Performing a dynamic analysis in VericalX

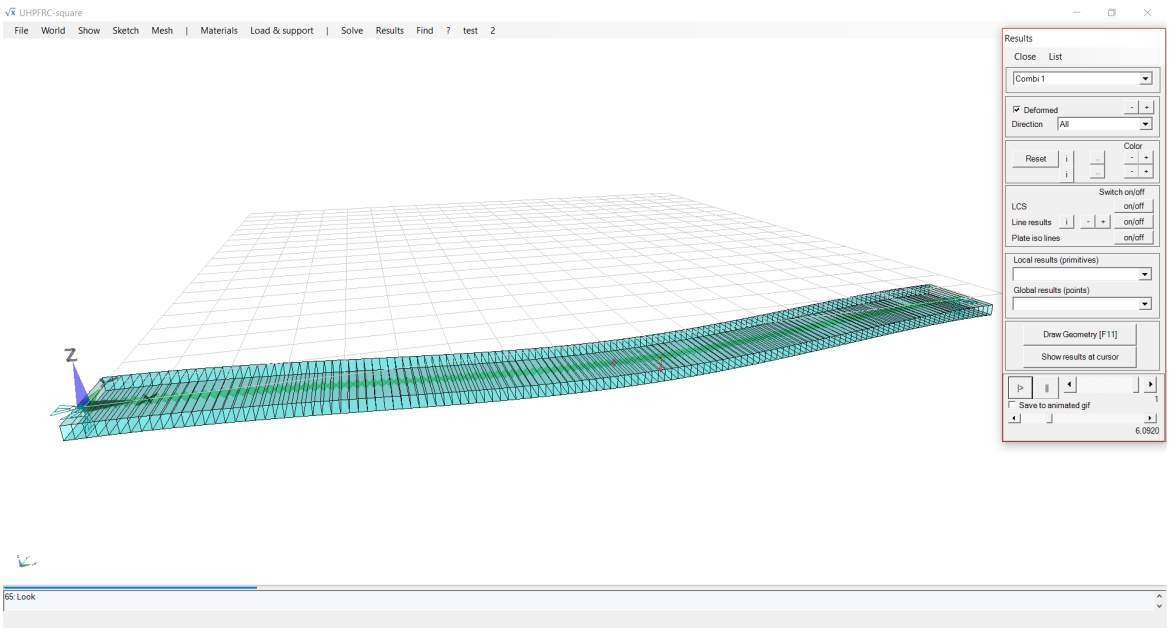

Figure C.6 Exporting the desirable results of the footbridge in VericalX

Appendix D

Design of the UHPFRC bridge

D.1 Defining the applied loads

The loads that should be applied on the structure according to EN2 (enter citation) are the following:

Table D.1 External loading according to EN2

self-weight:	$G_0 = \gamma \cdot A_c = 11.875 kN/m$
self-weight of handrail:	$G_p = 38.5 kg/m \cdot 2 \cdot g/1000 = 0.77 kN/m$
uniformly distributed crowd load:	$Q_{fk} = \left(2 + \frac{120}{(L+30)}\right) \cdot b_{eff} = 7.155 kN/m$
action on parapets:	$Q_p = 3 kN/m$

D.2 Calculation of bending moment and shear diagrams

The bridge chosen is an one-span bridge with fixed supports, that is prestressed with post-tensioning. The bending moments at the support and at mid-span for the different loads are presented in Table D.2.

Table D.2 Bending moment of supports and mid-span due to self-weight and external loading

Type of load	Support	Mid-span
self-weight:	0	$\frac{1}{8} \cdot G_0 \cdot L^2 = 510.23 kNm$
self-weight of handrail:	$-\frac{1}{12} \cdot G_p \cdot L^2 = -22.06 kNm$	$\frac{1}{24} \cdot G_p \cdot L^2 = -11.03 kNm$
uniformly distr. crowd load:	$-\frac{1}{12} \cdot Q_{fk} \cdot L^2 = -204.96 kNm$	$\frac{1}{24} \cdot Q_{fk} \cdot L^2 = 102.48 kNm$
action on parapets:	$-\frac{1}{12} \cdot Q_p \cdot L^2 = -85.93 kNm$	$\frac{1}{24} \cdot Q_p \cdot L^2 = 42.97 kNm$

The shear force due to the external loads and the self weight is equal to:

$$V = \frac{1}{2} \cdot (G_0 + G_p + Q_{kf} + G_p) \cdot L = 211.36kN$$

D.3 Defining the tendon profile

Since the bridge chosen has fixed supports, the optimum tendon profile that would counterbalance the external loads (self weight and variable load) is the one that the shape of its layout is the opposite shape of the bending moment diagram, therefore an eccentricity at the supports that produces positive bending moment at the support, and an eccentricity at the mid-span that produces negative bending moment. The best way to define the optimum combination of prestressing force and eccentricity in each section is by checking the stress limits for the tensile and compressive stress in transfer and in service. By plotting the governing equations, the Magnel diagram can be created.

D.3.1 Magnel diagram

Transfer phase

$$-\frac{P_0}{A_c} + \frac{P_0 \cdot e}{w_2} - \frac{M_{G_0}}{w_2} \leqslant f_{ct_I} \Leftrightarrow \frac{1}{P_0} \geqslant \frac{-1 + \frac{e}{k_1}}{\left(f_{ct_I} + \frac{M_{G_0}}{w_2}\right) \cdot A_c} \tag{D.1}$$

$$-\frac{P_0}{A_c} - \frac{P_0 \cdot e}{w_1} + \frac{M_{G_0}}{w_1} \geqslant f_{cc_I} \Leftrightarrow \frac{1}{P_0} \geqslant \frac{-1 + \frac{e}{k_2}}{\left(-f_{cc_I} + \frac{M_{G_0}}{w_1}\right) \cdot A_c} \tag{D.2}$$

Service phase

$$-\frac{P_\infty}{A_c} + \frac{P_\infty \cdot e}{w_2} - \frac{M_{total}}{w_2} \geqslant f_{cc_{II}} \Leftrightarrow \frac{1}{P_0} \leqslant R \cdot \frac{-1 + \frac{e}{k_1}}{\left(f_{cc_{II}} + \frac{M_{total}}{w_2}\right) \cdot A_c} \tag{D.3}$$

$$-\frac{P_\infty}{A_c} - \frac{P_\infty \cdot e}{w_1} + \frac{M_{total}}{w_1} \leqslant f_{ct_{II}} \Leftrightarrow \frac{1}{P_0} \leqslant R \cdot \frac{1 + \frac{e}{k_2}}{\left(-f_{ct_{II}} + \frac{M_{total}}{w_1}\right) \cdot A_c} \tag{D.4}$$

Where it is assumed that the prestressing losses are 15%, so $R = 0.85$ and $f_{ct_I} = f_{ct_{II}} = f_{ctk_{0.05}} = 9MPa$,$f_{cc_I} = f_{cc_{II}} = 0.6f_{ck} = -102MPa$, $k_1 = \frac{w_2}{A_c}$, $k_2 = \frac{w_1}{A_c}$. w_1 is in the case of the mid-span the ratio $\frac{I_c}{y_{bot}}$ and in the case of the supports $\frac{I_c}{y_{top}}$ and w_2 is in the case of the mid-span the ratio $\frac{I_c}{y_{top}}$ and in the case of the supports $\frac{I_c}{y_{bot}}$. Note that the bending moments are substituted by their absolute values.

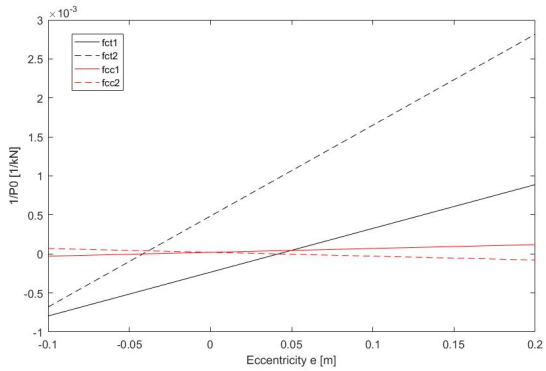

(a) Support

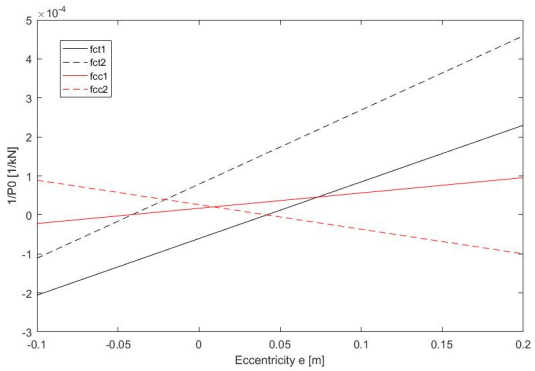

(b) Mid-span

Figure D.1 Magnel diagram for the cross-section of the support and the midspan

Solving the equations results in the following Magnel diagrams for the support and the mid-span.

It was decided to use flat GDP plastic ducts $91x22$ with 5 strands (figure D.2). The maximum available eccentricity is calculated to be:

$$e_{max} = \frac{h}{2} - c_{nom} - \frac{\frac{\Phi_{ext}+\Phi_{in}}{2}}{2} = 0.053m \tag{D.5}$$

For the midspan it was chosen to place the maximum available eccentricity, whereas at the support a slightly reduced one was selected to make anchoring easier. Therefore, for the parabolic tendon profile chosen stands:

$$e_{mid} = 0.053m$$

$$e_{sup} = 0.040m$$

$$f = e_{mid} + e_{sup} = 0.093m$$

$$R = \frac{L^2}{8f} = 462.00m$$

The required prestressing force arises from the Magnel diagram for the midspan and the resulting number of required strands is $n = 6$. The tendons have a parabolic profile, as presented in figure D.3.

D.3.2 Losses due to prestressing

Having defined the tendon profile and the number of tendons, the next step is to calculate the losses. The losses are divided into to categories, immediate losses due to friction and

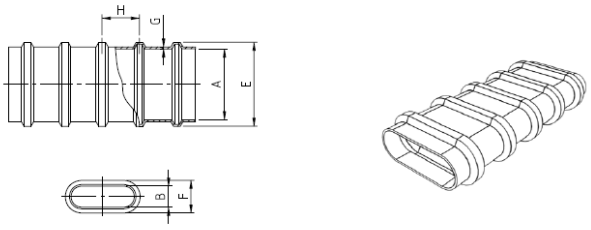

Flat GDP plastic duct			38 × 22	72 × 21	76 × 25	91 × 22
Number of strands ∅ 15.7 mm			2	3	4	5
Dimensions of cross section						
inside	A	mm	37.5	71.0	75.5	91.0
	B	mm	21.5	21.0	25.0	22.0
ribbs	E	mm	52.5	85.5	90.0	105.0
	F	mm	36.5	36.0	40.0	40.0
Wall thickness	G	mm	2.0	2.0	2.0	2.0
Rib distance	H	mm	40.0	40.0	40.0	40.0
Distance of supports		m	0.5			
Wobble coefficient	k	rad/m	0.008			
Friction coefficient						
weak axis	μ	rad^{-1}	0.12			
strong axis	μ	rad^{-1}	0.14	0.15	0.20	0.25

NOTE Dimensions rounded to the closest 0.5 mm.

Figure D.2 Flat GDP plastic duct

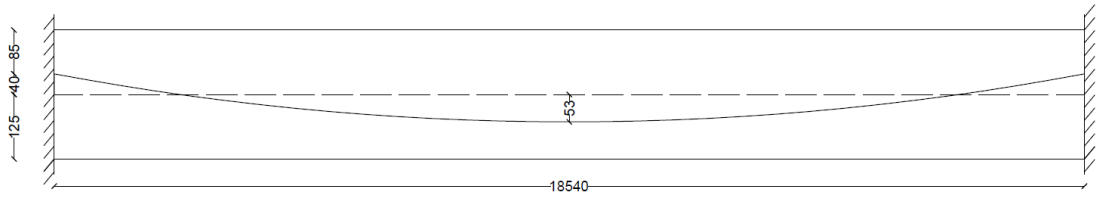

Figure D.3 Profile of prestressing tendons

wobble effect, wedge draw-in and elastic shortening (for post-tensioned prestressing) and to long-term losses due to creep, shrinkage and relaxation.

Losses due to friction and Wobble-effect

The losses due to friction and wobble effect are calculated by the relation:

$$\Delta P(x) = P_{max}\left(1 - e^{-\mu(kx+\theta)}\right) \tag{D.6}$$

where P_{max} is the maximum force at the jack during the tensioning, k is the angular rotation per unit length caused by the Wobble-effect, μ is the friction coefficient for the interface between the tendon and the duct, x is the distance of the cross-section considered from the location of the jack and θ is the total angular rotation of the tendon (in radians) between the considered cross-section and the jack.(insert citation) For the selected ducts the friction coefficient and the angular rotation of the Wobble-effect are:

$$k = 0.008 rad/m$$

$$\mu = 0.12 rad^{-1}$$

Table D.3 Prestressing losses due to friction and Wobble-effect

x $[m]$	$\theta = \frac{x}{R}$ $[rad]$	$\frac{\Delta P_\mu}{P_{max}}$ $[-]$	$\frac{\sigma_p(x)}{\sigma_{P_{max}}}$ $[-]$	$\sigma_{p\mu}(x)$ $[MPa]$
0	0	0	1	1488
9.27	0.02006	0.0112	0.9888	1471.27
18.54	0.04013	0.0224	0.9776	1454.73

Losses due to wedge draw-in

When wedges are used, during the release of the jack some wedge slip occurs. The wedges slip until the force at the anchorage is fully developed, consequently some prestress losses take place. The length over which the wedge set influences the prestressing force is given by the expression:

$$l_w = \frac{w \cdot E_p}{\Delta\sigma_{p\mu m}} \tag{D.7}$$

where $\Delta\sigma_{p\mu,m}$ is the mean stress reduction in the tendon caused by friction over the length l_w, since there are no kinks the mean stress reduction can be found easily as:

$$\Delta\sigma_{p\mu,m} = \frac{\sigma\left(\frac{L}{2}\right) - \sigma(0)}{\frac{L}{2}} = 1.805 MPa/m$$

Therefore, the length l_w and the stress at the anchor can be calculated as:

$$l_w = \sqrt{\frac{wE_p}{\Delta\sigma_{p\mu,m}}} = 18.004m$$

$$\sigma_{p\mu}(0) = \sigma_{P_{max}} - 2l_w\Delta\sigma_{p\mu,m} = 1423.015 MPa$$

Losses due to elastic shortening

Elastic shortening occurs in the case of post-tensioning with more than one tendon. When the first tendon is stressed, the operator applies prestress until the required prestressing force is reached. During this process the beam shortens but this is compensated by the fact that the tendon is stressed until the required force is achieved. However, when the second tendon is tensioned, the beam shortens again, causing strains at the level of the first tendon that result in prestressing losses. Consequently, every new tendon stressed causes losses to the tendons that were stressed before it. The losses of each tendon i due to the stressing of the tendons stressed after it are given by expression:

$$\Delta\sigma_i = \frac{E_p}{E_c}\frac{(n-i)}{n^2}\sigma_{c,s}(x) \tag{D.8}$$

with $\sigma_{c,s}(x)$ being the stress of the concrete at the level of tendon i due to the maximum prestressing force P_{max} applied at the level of tendon j, expressed by the formula:

$$\sigma_{c,s}(x) = \frac{P_{max}}{A_c} + \frac{P_{max}e_j}{I_c}e_i \tag{D.9}$$

In the considered case all the tendons are at the same height, consequently the stresses of the concrete at the level of the tendons for the supports and the mid-span are:

$$\sigma_{c,s}(0) = \frac{A_p\sigma_{P_{max}}}{A_c} + \frac{A_p\sigma_{P_{max}}e_{sup}^2}{I_c} = 18427.39 kPa$$

$$\sigma_{c,s}\left(\frac{L}{2}\right) = \frac{A_p\sigma_{P_{max}}}{A_c} + \frac{A_p\sigma_{P_{max}}e_{mid}^2}{I_c} = 21699.66 kPa$$

The losses of each one of the tendons at the location of the support and at the location of the mid-span are presented in the next table:

Table D.4 Prestressing losses due to elastic shortening

tendon i	ΔP_i [kN]	
	Mid-span	Support
1	45.597	38.721
2	36.478	30.977
3	27.358	23.233
4	18.239	15.489
5	9.119	7.744
6	0.000	0.000
Sum	136.792	116.164

The mean stress losses due to the elastic shortening are:

$$\Delta\sigma_{el,sh} = \frac{\Delta P_{sup} + \Delta P_{mid}}{2A_p} = 28.106MPa$$

By adding all the initial losses, the remaining stress in each cross-section of the bridge can be calculated. The maximum remaining stress should be smaller than $\sigma_{pm_0} = 1395MPa$. As it can be seen in Table ..., this is not the case, since the stress is exceeded. Therefore a smaller initial prestressing force should be selected to satisfy the condition. The maximum applied stress is found to be equal to:

$$\sigma_{pmax} = 1452MPa$$

Table D.5 Remaining stress in tendon after initial losses for applied stress $\sigma_{P_{max}} = 0.8f_{pk}$

x $[m]$	$\sigma_{P_{max}}$ $[MPa]$	$\Delta\sigma_{friction}$ $[MPa]$	$\Delta\sigma_{el.short}$ $[MPa]$	$\Delta\sigma_{wedge}$ $[MPa]$	$\sigma_{P_0}(x)$ $[MPa]$
0.00	1488	0.000	28.106	64.985	1394.91
9.27	1488	16.730	28.106	31.437	1411.73
18.00	1488	32.321	28.106	0.000	1427.57
18.54	1488	33.272	28.106	0.000	1426.62

(add graph of losses)

Table D.6 Remaining stress in tendon after initial losses for applied stress $\sigma_{p_{max}} = 1452MPa$

x $[m]$	$\sigma_{p_{max}}$ $[MPa]$	$\Delta\sigma_{friction}$ $[MPa]$	$\Delta\sigma_{el.short}$ $[MPa]$	$\Delta\sigma_{wedge}$ $[MPa]$	$\sigma_{P_0}(x)$ $[MPa]$
0	1452	0.000	25.189	63.846	1362.96
9.27	1452	16.325	25.189	31.284	1379.20
18.23	1452	31.923	25.189	0.000	1394.89
18.54	1452	32.467	25.189	0.000	1394.34

Long-term losses

Additionally to the immediate losses, the time dependent losses of the prestress due to the creep and the shrinkage of the concrete, as well as the long term relaxation of the prestressing steel at time $t = \infty$ should be determined, resulting in a prestressing force equal to:

$$P_{m\infty}(x) = P_{m0}(x) - \Delta P_{c+s+r}(x) \tag{D.10}$$

A simplified method to calculate the time dependent losses at a location x at $t = \infty$ is given by EN2 by applying the following formula:

$$\Delta P_{c+s+r} = A_p \cdot \Delta\sigma_{p,c+s+r} = A_p \frac{\varepsilon_{cs}E_p + 0.8\Delta\sigma_{pr} + \frac{E_p}{E_{cm}}\varphi(\infty,t_0)\sigma_{c,QP}}{1 + \frac{E_p}{E_{cm}}\frac{A_p}{A_c}\left(1 + \frac{A_c}{I_c}z_{cp}^2\right)[1 + 0.8\varphi(\infty,t_0)]} \tag{D.11}$$

where: E_p is the modulus of elasticity of the prestressing steel E_{cm} is the modulus of elasticity of the concrete

$\Delta\sigma_{p,c+s+r}$ is the absolute value of the variation of stress in the tendons due to creep, shrinkage and relaxation

e_{cs} is the estimated shrinkage strain in absolute value calculated according to the chapter 3.1.4 of EN2. The strain due to shrinkage can be expressed as a sum of the drying shrinkage and the autogenous shrinkage:

$$\varepsilon_{cs} = \varepsilon_{cd} + \varepsilon_{ca} \tag{D.12}$$

where ε_{cd} is the drying shrinkage, expressed as:

$$\varepsilon_{cd}(t) = \beta_{ds}(t,t_s)k_h\varepsilon_{cd,0} \tag{D.13}$$

with

$$\beta_{ds}(t,t_s) = \frac{(t-t_s)}{(t-t_s)+0.04\sqrt{h_0^3}} \tag{D.14}$$

, where $t_s = 28$ days is the age of the concrete at the beginning of the drying shrinkage and $h_0 = 2A_c/u$ is the notional size of the cross-section. The coefficient k_h depends on the notional size and in this case is equal to $k_h = 0.806$. The unrestrained drying shrinkage is equal to $\varepsilon_{cd,0} = 0.00021$. Therefore, the drying shrinkage at time $t = \infty$ is equal to: $\varepsilon_{cd}(\infty) = 0.000169$ The autogenous shrinkage at $t = \infty$ or approximated by $t = 57 years$ is given by the expression

$$\varepsilon_{ca}(\infty) = 2.5(f_{ck} - 10)10^{-6} = 0.0004 \tag{D.15}$$

Therefore the total strain due to shrinkage is equal to:

$$\varepsilon_{cs} = 0.00057$$

$\varpi(\infty,t_0) = 0.8$ is the creep coefficient at time $t = \infty$ and a load application at time $t_0 = 100$ for concrete C90 and relative humidity $RH = 80\%$.

$\Delta\sigma_{pr}$ is the absolute value of the variation of stress in the tendons at position x and time t due to the relaxation of the prestressing steel for an initial stress due to the prestressing and quasi-permanent actions. For Class 2 of prestressing steel the relaxation loss is given by the expression:

$$\Delta\sigma_{pr} = 0.66\rho_{1000}e^{6.7\mu}\left(\frac{t}{1000}\right)^{0.75(1-\mu)}10^{-5} \tag{D.16}$$

where $\sigma_{pi} = \sigma_{pm0} = 1395 MPa$, $\mu = \sigma_{pi}/f_{pk} = 0.75$, $\rho_{1000} = 2.5\%$ is the value of relaxation loss (in %), at 1000 hours after tensioning. For the calculation of the final long term relaxation losses the time can be taken as $t = 500000h$. This results in relaxation losses equal to:

$$\Delta\sigma_{pr} = 67.948 MPa$$

$\sigma_{c,QP}$ is the stress in the concrete adjacent to the tendons, due to self-weight and initial prestress and other quasi-permanent actions, given by:

$$\sigma_{c,QP,sup} = \frac{P_{m0}}{A_c} + \frac{P_{m0}e_{sup}^2}{I_c} - \frac{M_{tot,sup}e_{sup}}{I_c} = 13.033 MPa$$

$$\sigma_{c,QP,sup} = \frac{P_{m0}}{A_c} + \frac{P_{m0}e_{mid}^2}{I_c} - \frac{M_{tot,mid}e_{mid}}{I_c} = 19.587 MPa$$

$A_p = n \cdot 5 \cdot 150 = 4500mm^2$ is the area of the prestressing at the considered location x

$A_c = 0.475m^2$ is the cross-sectional area of the concrete

$z_{cp,sup} = e_{sup}$ and $z_{cp,mid} = e_{mid}$ are the distances between the center of gravity of the cross-section of the concrete and the tendons for each checked cross-section.

Now the long-term losses due to creep, relaxation ad shrinkage can be found for the supports and the mid-span by substituting the calculated values in equation B... This gives for the two supports:

$$\Delta\sigma_{p,c+s+r,sup} = 844.207kN \longrightarrow R = \frac{P_{m0} - \Delta\sigma_{p,c+s+r,sup}}{P_{m0}} = 86\%$$

$$\Delta\sigma_{p,c+s+r,mid} = 908.154kN \longrightarrow R = \frac{P_{m0} - \Delta\sigma_{p,c+s+r,mid}}{P_{m0}} = 85\%$$

The real long-term losses are almost identical with the assumed losses, so we can go on with the design.

$$P_{m\infty} = 5289.13kN$$

Table D.7 Remaining stress in tendon after initial losses for applied stress $\sigma_{P_{max}} = 0.8f_{pk}$

t $[m]$	σ $[MPa]$	$\Delta\sigma_{friction}$ $[MPa]$	$\Delta\sigma_{el.short}$ $[MPa]$	$\Delta\sigma_{wedge}$ $[MPa]$	$\sigma_{P_0}(x)$ $[MPa]$
0.00	1488	0.000	28.106	64.985	1394.91
9.27	1488	16.730	28.106	31.437	1411.73
18.00	1488	32.321	28.106	0.000	1427.57
18.54	1488	33.272	28.106	0.000	1426.62

D.3.3 Non-prestress reinforcement

According to chapter 7.3.2 of the EN2 no minimum reinforcement is required in sections of prestressed members if under the characteristic combination of loads and characteristic value of prestress the concrete section is in compression or if the tensile stress is lower than $\sigma_{ct,p}$, which in this case is equal to $f_{ctk,0.05}$. The characteristic combination of loads is the critical one for the serviceability limit state. Now that the exact value of the prestressing force and the exact tendon profile are known, the bending moment diagram for the characteristic load combination can be found and through this the stresses in the critical cross-sections. The bending moment due to the characteristic load combination and the characteristic prestressing force for the supports and the mid-span is given by:

$$M_{sup} = M_{tot,sup} + P_{m\infty} \cdot e_{sup} = -252.80 + 5289.13 \cdot 0.04 = -41.23kNm$$

$$M_{mid} = M_{tot,mid} - P_{m\infty} \cdot e_{mid} = 636.63 - 5289.13 \cdot 0.053 = 353.31kNm$$

And the stresses at the top and bottom fiber during SLS for the two cross-sections are given by:

$$\sigma_{c,sup,top} = -\frac{P_{m\infty}}{A_c} - \frac{M_{sup} \cdot \frac{h}{2}}{I_c} = -9.051MPa$$

$$\sigma_{c,sup,bot} = -\frac{P_{m\infty}}{A_c} + \frac{M_{sup} \cdot \frac{h}{2}}{I_c} = -13,218MPa$$

$$\sigma_{c,mid,top} = -\frac{P_{m\infty}}{A_c} - \frac{M_{,id} \cdot \frac{h}{2}}{I_c} = -29.138MPa$$

$$\sigma_{c,mid,bot} = -\frac{P_{m\infty}}{A_c} + \frac{M_{sup} \cdot \frac{h}{2}}{I_c} = 6.868MPa$$

It is apparent that since the stress in the SLS are less than $f_{ctk,0.05} = 9MPa$, no longitudinal regular reinforcement is required.

D.4 Ultimate Limit State Calculation

D.4.1 Bending moment Resistance

Supports

The combination of loads for the ULS according to EN0 is:

$$\gamma_G (G_0 + G_p) + \gamma_P q P_{\text{inf}} + \gamma_{Q1} Q_{fk} + \gamma_{Q2} \psi_0 Q_p \tag{D.17}$$

where $\gamma_G = 1.2$, $\gamma_{Q1} = \gamma_{Q2} = 1.5$ and $\psi_0 = 0.4$.

Therefore the design bending moment for the support and the mid-span are calculated as follows:

$$M_{Ed,sup} = -\frac{1}{12} \cdot \left(\gamma_G G_p + \gamma_{Q1} Q_{fk} + \gamma_{Q2} \psi_0 Q_p\right) L^2 + \gamma_P P_{\text{inf}} e_{sup} = -173.91kNm$$

$$M_{Ed,mid} = \frac{1}{8}\gamma_G G_0 L^2 + \frac{1}{24}\left(\gamma_G G_p + \gamma_{Q1} Q_{fk} + \gamma_{Q2}\psi_0 Q_p\right) L^2 - \gamma_P P_\infty e_{mid} = 525.24 kNm$$

As mentioned in chapter 3, one of the advantages of UHPFRC over regular concrete is that its tensile strength contributes in the final strength capacity of the member. The distribution of stresses over the cross-section are presented in the following figure (put figure of how strains and stresses are in cross-section). The first step into defining the bending moment resistance of the cross-section is to calculate the height of the compressive zone, through equilibrium of horizontal forces. The cross-section is divided in regions according to the distribution of concrete stresses, as see in Figure. The following relations stand:

$$\frac{\varepsilon_{cu}}{x_u} = \frac{\varepsilon_{bc}}{x_2} \Leftrightarrow x_2 = \frac{\varepsilon_{bc}}{\varepsilon_{cu}} x_u \tag{D.18}$$

$$x_1 + x_2 = x_u \Leftrightarrow x_1 = \left(1 - \frac{\varepsilon_{bc}}{\varepsilon_{cu}}\right) x_u \tag{D.19}$$

$$\frac{\varepsilon_{ctd}}{x_3} = \frac{\varepsilon_{cu}}{x_u} \Leftrightarrow x_3 = \frac{\varepsilon_{ctd}}{\varepsilon_{cu}} x_u \tag{D.20}$$

$$\frac{\varepsilon_{0.3}}{x_3 + x_4} = \frac{\varepsilon_{cu}}{x_u} \Leftrightarrow x_4 = \left(\frac{\varepsilon_{0.3} - \varepsilon_{ctd}}{\varepsilon_{cu}}\right) x_u \tag{D.21}$$

$$\frac{\varepsilon_{lim}}{x_3 + x_4 + x_5} = \frac{\varepsilon_{cu}}{x_u} \Leftrightarrow x_5 = \left(\frac{\varepsilon_{lim} - \varepsilon_{0.3}}{\varepsilon_{cu}}\right) x_u \tag{D.22}$$

$$\frac{\varepsilon_{cu}}{x_u} = \frac{\varepsilon_{cu} + \Delta\varepsilon_p}{d_p} \Leftrightarrow \Delta\varepsilon_p = \left(\frac{d_p}{x_u} - 1\right) \varepsilon_{cu} \tag{D.23}$$

In the case that: $x_1 + x_2 + x_3 + x_4 + x_5 > h > x_1 + x_2 + x_3 + x_4$ the forces of the concrete are:

$$N_1 = f_{cd} x_1 b \tag{D.24}$$

$$N_2 = \frac{1}{2} f_{cd} x_2 b \tag{D.25}$$

$$N_3 = \frac{1}{2} f_{ctd} x_3 b \tag{D.26}$$

$$N_4 = f_{ctd} x_4 b \tag{D.27}$$

$$N_{5a} = \frac{1}{2}\left(f_{ctd} - f_{top}\right) y b \tag{D.28}$$

$$N_{5b} = f_{top} y b \tag{D.29}$$

Where $y = h - (x_1 + x_2 + x_3 + x_4)$ and $f_{top} = \dfrac{f_{ctd}}{x_5}(x_1 + x_2 + x_3 + x_4 + x_5 - h)$.

The equilibrium of forces gives:

$$\Sigma H = 0 \Leftrightarrow N_1 + N_2 = N_3 + N_4 + N_{5a} + N_{5b} + P_\infty + \Delta N_p \tag{D.30}$$

Where

$$\Delta N_p = A_p(\sigma_{pu} - \sigma_{p\infty}) \tag{D.31}$$

where

$$\sigma_{pu} = \begin{cases} f_{pd} + \frac{f_{pu} - f_{pd}}{\varepsilon_{pu} - \varepsilon_{pd}}(\varepsilon_p - \varepsilon_{pd}), & \text{if } \varepsilon_p > \varepsilon_{pd} \\ E_p \varepsilon_p, & \text{otherwise.} \end{cases}$$

where $\varepsilon_p = \varepsilon_\infty + \Delta\varepsilon_p$

By giving different values to x_u the one that satisfies the equation of equilibrium can be found. In this case, it is equal to: $x_u = 62.595mm$. Therefore the rest of the unknowns can now be find:

$x_1 = 22.608mm$ $y = 148.948mm$ $N_3 = 5.916kN$
$x_2 = 39.987mm$ $\Delta N_p = 1646.659kN$ $N_4 = 494.019kN$
$x_3 = 0.899mm$ $N_1 = 4774.712kN$ $N_{5a} = 397.779kN$
$x_4 = 37.557mm$ $N_2 = 4222.435kN$ $N_{5b} = 1163.687kN$

The bending moment capacity of the cross section is:

$$\begin{aligned} M_{Rd} = &-N_1\frac{x_1}{2} - N_2\left(x_1 + \frac{x_2}{3}\right) + N_3\left(x_1 + x_2 + \frac{2x_3}{3}\right) + N_4\left(x_1 + x_2 + x_3 + \frac{x_4}{2}\right) \\ &+ N_{5a}\left(h - \frac{2y}{3}\right) + N_{5b}\left(h - \frac{y}{2}\right) + \Delta N_p\left(\frac{h}{2} + e_{sup}\right) + P_{m\infty}\frac{h}{2} \\ &= 1032.35kNm \end{aligned}$$

The bending moment resistance in the other direction can be found by following the same steps. The results are presented below:

$x_1 = 21.345mm$ $y = 154.594mm$ $N_3 = 5.586kN$
$x_2 = 37.753mm$ $\Delta N_p = 1125.786kN$ $N_4 = 466.420kN$
$x_3 = 0.849mm$ $N_1 = 4507.963kN$ $N_{5a} = 453.860kN$
$x_4 = 35.459mm$ $N_2 = 3986.540kN$ $N_{5b} = 1125.786kN$

The bending moment resistance in this directions is equal to:

$$M_{Rd} = -N_1\frac{x_1}{2} - N_2\left(x_1+\frac{x_2}{3}\right) + N_3\left(x_1+x_2+\frac{2x_3}{3}\right) + N_4\left(x_1+x_2+x_3+\frac{x_4}{2}\right)$$
$$+ N_{5a}\left(h-\frac{2y}{3}\right) + N_{5b}\left(h-\frac{y}{2}\right) + \Delta N_p\left(\frac{h}{2}-e_{sup}\right) + P_{m\infty}\frac{h}{2}$$
$$= 873.52kNm$$

Mid-span

For the mid-span the same procedure is followed with the only difference being the eccentricity of the tendon. The bending moment capacity of the cross-section in the direction that resists the external loads is equal to:

$x_1 = 22.677mm$ $y = 148.642mm$ $N_3 = 5.934kN$
$x_2 = 40.108mm$ $\Delta N_p = 1673.550kN$ $N_4 = 495.519kN$
$x_3 = 0.902mm$ $N_1 = 4789.205kN$ $N_{5a} = 394.944kN$
$x_4 = 37.671mm$ $N_2 = 4235.252kN$ $N_{5b} = 1165.323kN$

$$M_{Rd} = -N_1\frac{x_1}{2} - N_2\left(x_1+\frac{x_2}{3}\right) + N_3\left(x_1+x_2+\frac{2x_3}{3}\right) + N_4\left(x_1+x_2+x_3+\frac{x_4}{2}\right)$$
$$+ N_{5a}\left(h-\frac{2y}{3}\right) + N_{5b}\left(h-\frac{y}{2}\right) + \Delta N_p\left(\frac{h}{2}+e_{mid}\right) + P_{m\infty}\frac{h}{2}$$
$$= 1057.66kNm$$

whereas in the opposite direction:

$x_1 = 20.277mm$ $y = 159.366mm$ $N_3 = 5.306kN$
$x_2 = 35.864mm$ $\Delta N_p = 743.582kN$ $N_4 = 443.090kN$
$x_3 = 0.807mm$ $N_1 = 4282.481kN$ $N_{5a} = 507.707kN$
$x_4 = 33.685mm$ $N_2 = 3787.139kN$ $N_{5b} = 1080.862kN$

$$M_{Rd} = -N_1\frac{x_1}{2} - N_2\left(x_1+\frac{x_2}{3}\right) + N_3\left(x_1+x_2+\frac{2x_3}{3}\right) + N_4\left(x_1+x_2+x_3+\frac{x_4}{2}\right)$$
$$+ N_{5a}\left(h-\frac{2y}{3}\right) + N_{5b}\left(h-\frac{y}{2}\right) + \Delta N_p\left(\frac{h}{2}+e_{sup}\right) + P_{m\infty}\frac{h}{2}$$
$$= 839.26kNm$$

D.4.2 Shear Resistance

The shear force acting at the support of the bridge is equal to:

$$V_{Ed} = \frac{1}{2}\left(\gamma_G G_p + \gamma_{Q1} Q_{fk} + \gamma_{Q2}\psi_0 Q_p - \gamma_P q_{P_{inf}}\right) L = 233.65kN \tag{D.32}$$

According to the Setra recommendations about designing with UHSFRC, the ultimate shear strength V_u is described as the summation of three terms, one that describes the participation of the concrete (V_{Rb}), one for the participation of the fibres $\left(V_f\right)$ and one for the participation of the shear reinforcement (V_a), if needed. So,

$$V_{Rd} = V_{Rb} + V_f + V_a \tag{D.33}$$

with

$$V_{Rb} = \frac{1}{\gamma_E}\frac{0.24}{\gamma_b}\sqrt{f_{cj}} b_0 z \tag{D.34}$$

$$V_f = \frac{S\sigma_p}{\gamma_{bf}\tan\beta_u} \tag{D.35}$$

where: γ_E is a safety coefficient such that $\gamma_E \cdot \gamma\gamma_b = 1.5$, $\beta_u = 45^o$ is the angle of the compression struts, $S = b_0 z = 0.9 b_0 d_p = 282150mm^2$ is the area of the fibre effect, and

$$\sigma_p = \frac{1}{K}\frac{1}{w_{lim}}\int_0^{w_{lim}} \sigma(w)dw$$

is the residual tensile strength, with $w_{lim} = max\,(w_u; 0.3mm)$ and $w_u = l_c\varepsilon_u = 2/3h \cdot 3\%_{,} = 0.5mm$ and $K = 1.25$ is the orientation coefficient for general effects. To calculate the residual tensile strength the area under the post-cracking stress for crack width is measured.

Table D.8 Calculation of residual tensile strength

ε_i $[-]$	w_i $[mm]$	σ_i $[MPa]$	A_i $[MPa]$
0.000	0.000	0.000	0.000
ε_{ctd}	$\varepsilon_{ctd} \cdot l_c = 0.0199$	$f_{ctd} = 6.923$	0.0689
$\varepsilon_{u0.3}$	$w_{0.3} = 0.3000$	$f_{ctd} = 6.923$	1.9392
$\varepsilon\varepsilon_{lim}$	$w_l im = 0.5000$	0.000	0.6923
$\sigma_p = \frac{1}{K}\frac{1}{w_{lim}}\sum_i A_i = 4.321$ MPa			

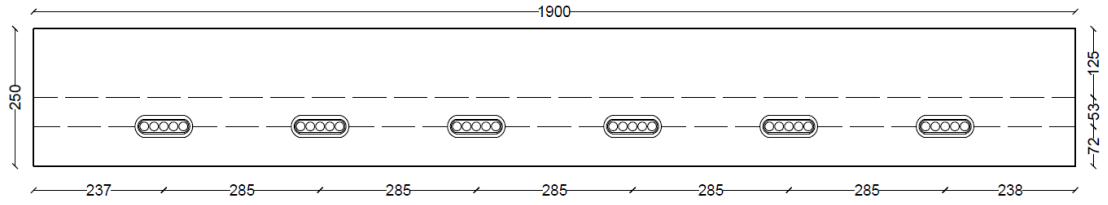

Figure D.4 Cross-section of midspan

Consequently, the shear resistance due to the concrete is equal to $V_{Rb} = 588.606kN$ and the shear resistance due to the fibres is equal to $V_f = 937.734kN$. In total the shear capacity due to the concrete and fibres participation is equal to:

$$V_{Rd} = 1526.34kN$$

The shear capacity of the cross-section in the ULS is greater than the maximum shear acting on the beam, therefore no shear reinforcement is required.

The cross-section of the midspan of the footbridge is presented in figure D.4.

D.5 Anchorage

In the case of post-tensioning, the tensile stresses in the tendons are introduced to the structure, through the prestressing anchors. The concentrated forces are gradually distributed over the height and the width of the structure. The distribution of the concentrated forces is done through the disturbance length of de St.-Venant, after which there is a uniform distribution of load. For the anchorage, plate anchorages SD-6805, will be used, the dimensions of which are $180mm \times 150mm$ (figure D.5). The minimum distance from the edge according to the European Technical Approval is equal to: $r_x = 0.5 \cdot a_x + c - 10mm = 0.5 \cdot 320 + 71.5 - 10 = 221.5mm$. [20] The edge distance chosen is $r_{edge} = 237.5mm$ leading to a center to center distance of plates equal to $s = 285mm$. The concentrated force applied on each anchor is equal to $F_p = \sigma_{P_{max}} A_{strand} n_{strand} = 1452 \cdot 150 \cdot 5 = 1089kN$ and is split into two equal forces $F_p/2 = 544.5kN$ with a c.t.c distance equal to $s_1 = 180/2 = 90mm$. These forces gradually spread in the structure over the disturbance length of de St. Venant s_d (the required length to have a uniform load distribution), which is approximately equal to

$$s_d \approx \frac{b}{n} = \frac{1900}{6} = 316.66mm$$

The splitting tensile force can be calculated using D.36 and D.6 and is equal to:

$$T = \frac{F_p}{2}\left(\frac{\frac{s}{2}-\frac{s_1}{2}}{\frac{s_d}{2}}\right) = 544.5\frac{\frac{142.5-90}{2}}{158.3} = 90.29kN \tag{D.36}$$

Multiplane anchorage MA 2311 with additional reinforcement and with helix
with min. centre distances, strand Y1770S7 15.3 / Y1770S7 15.7 / Y1860S7 15.3 / Y1860S7 15.7

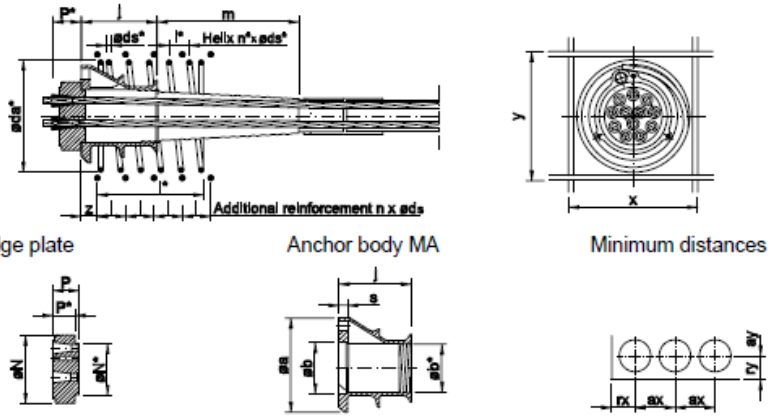

Tendon MA 2311		6805			6807			6809			6812		
Number of strands		**5**			**7**			**9**			**12**		
Strand arrangement													
Wedge plate	ØN	117			130			145			170		
	ØN*	88			96			112			128		
thickness	P	55			60			60			65		
depth	P*	47			52			52			55		
Anchor body MA	Øa	150			170			190			220		
	Øb	90			98			114			130		
	Øb*	80			90			100			120		
height	j	90			100			125			180		
thickness	s	18			18			15			17		
Trumpet length	m	240			210			280			350		
Minimum concrete compressive strength at time of stressing													
$f_{cm,0,cube}$	N/mm²	**25**	**34**	**45**	**25**	**34**	**45**	**25**	**34**	**45**	**25**	**34**	**45**
$f_{cm,0,cyl}$	N/mm²	**20**	**28**	**36**	**20**	**28**	**36**	**20**	**28**	**36**	**20**	**28**	**36**
Minimum centre distance	a_x, a_y	270	235	220	320	280	245	345	305	270	400	350	310
Minimum edge distance	r_x, r_y	0.5 · centre distance + concrete cover – 10 mm											
Helix													
minimum number of turns	n*	4.5	4	4	4	4	4	5.5	5	5	6	7	7
minimum wire diameter	$Ød_s$*	12	12	12	14	14	14	14	14	14	14	14	14
minimum external diameter	$Ød_a$*	205	185	180	240	220	200	270	250	220	320	265	255
	max. i*	45	40	50	50	50	50	50	50	50	50	50	50
	min. l*	270	225	265	255	260	270	335	310	320	360	410	420
Additional reinforcement, Re ≥ 500 N/mm²													
minimum number of layers	n	5	5	5	6	6	6	7	7	7	7	8	8
minimum bar diameter	$Ød_s$	12	12	12	12	12	12	14	14	14	14	14	14
maximum spacing	z	40	40	40	40	40	40	40	40	40	45	45	45
maximum spacing	i	50	45	50	55	50	50	55	55	55	55	50	55
external dimensions	x, y	250	215	200	300	260	225	325	285	250	380	330	290

Dimensions in mm

Figure D.5 Anchorage MA 2311 [20]

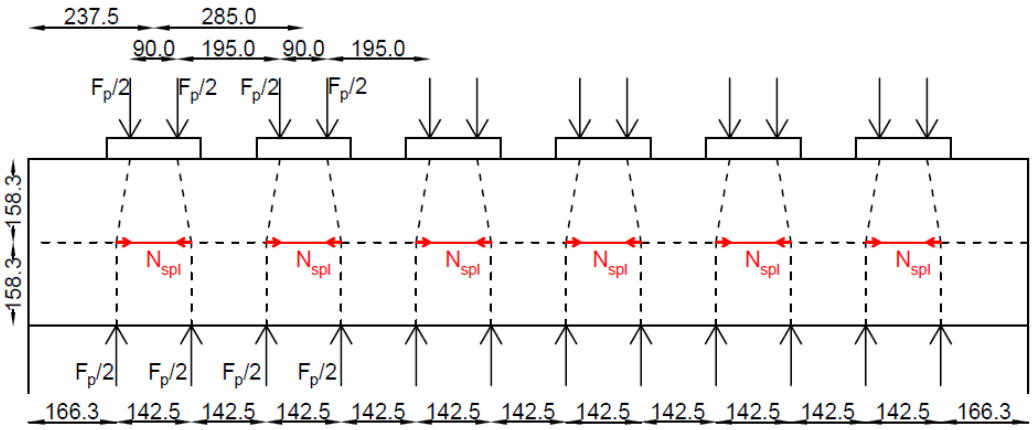

Figure D.6 Strut and tie model over width of bridge

The area of the splitting tensile reinforcement needed may be found from the relation $A_{spl} = T/\sigma_s$, where σ_s is the maximum steel stress allowed. According to chapter 8.10.3 of EN2, if the stress in the reinforcement is limited to 300MPa no check for crackwidth is necessary, therefore the required reinforcement for this direction is equal to:

$$A_{spl} = \frac{90290N}{300\frac{N}{mm^2}} \approx 301mm^2$$

When it comes to the distribution of the concentrated anchorage forces over the height of the bridge deck, the eccentricity of the prestressing force over the height should be taken into account for the determination of the spilling tensile forces. In this case the disturbance length is approximately equal to the height of the bridge cross-section. The maximum total force acting on the cross-section is equal to: $P_{max} = 6 \cdot 1089 = 6534kN$, divided in a pair of equal forces $P_{max}/2 = 3267kN$, and $h_1 = 75mm$. The distribution of stresses when the maximum force is applied is given by:

$$\sigma_{top} = -\frac{P_{max}}{A_c} - \frac{P_{max}e_{sup} \cdot \frac{h}{2}}{I_c} = -26.961MPa$$

$$\sigma_{bot} = -\frac{P_{max}}{A_c} + \frac{P_{max}e_{sup} \cdot \frac{h}{2}}{I_c} = -0.550MPa$$

The stresses will be split into two trapeziums, each one giving a force equal to $P_{max}/2 = -3267kN$. The height of each trapezium is determined by equilibrium:

$$\left[\sigma_{bot} + \left(\sigma_{bot} + \frac{\sigma_{top} - \sigma_{bot}}{h} x_1\right)\right] b \frac{x_1}{2} = -3267 \cdot 10^3 N \Leftrightarrow x_1 = 175.29mm$$

$$x_2 = h - x_1 = 250 - 175.29 = 74.71mm$$

$$\sigma_{x_1} = \sigma_{bot} + \frac{\sigma_{top} - \sigma_{bot}}{h} x_1 = -19.069MPa$$

The forces are applied on the center of mass of each trapezium.

$$y_1 = \frac{\sigma_{bot} \cdot \frac{x_1^2}{2} + (\sigma_{x_1} - \sigma_{bot}) \frac{x_1}{2} \cdot \frac{2x_1}{3}}{(\sigma_{bot} + \sigma_{x_1}) \cdot \frac{x_1}{2}} \Leftrightarrow y_1 = 115.22mm$$

$$y_2 = \frac{\sigma_{x_1} \cdot \frac{x_2^2}{2} + (\sigma_{x_{top}} - \sigma_{x_1}) \frac{x_2}{2} \cdot \frac{2x_2}{3}}{(\sigma_{top} + \sigma\sigma_{x_1}) \cdot \frac{x_2}{2}} \Leftrightarrow y_1 = 39.49mm$$

The splitting tensile force:

$$T_2 = \frac{P_{max}}{2} \left(\frac{x_1 + y_2 - \left(\frac{h}{2} + e_{sup} + \frac{h_1}{2}\right)}{\frac{h}{2}} \right) = 321kN$$

$$T_2 = \frac{P_{max}}{2} \left(\frac{\frac{h}{2} + e_{sup} - \frac{h_1}{2} - y_1}{\frac{h}{2}} \right) = 321kN$$

Therefore the required amount of splitting tensile reinforcement in the vertical direction is equal to:

$$A_{spl,ver} = \frac{321000N}{300\frac{N}{mm^2}} \approx 1070mm^2$$

Orthogonal closed stirrups should be placed in the disturbed zone. If closed stirrups of diameter $\Phi 12$ are used and they need to be distributed over the disturbance length: $h = 250mm$, therefore: $\Phi 12/50$

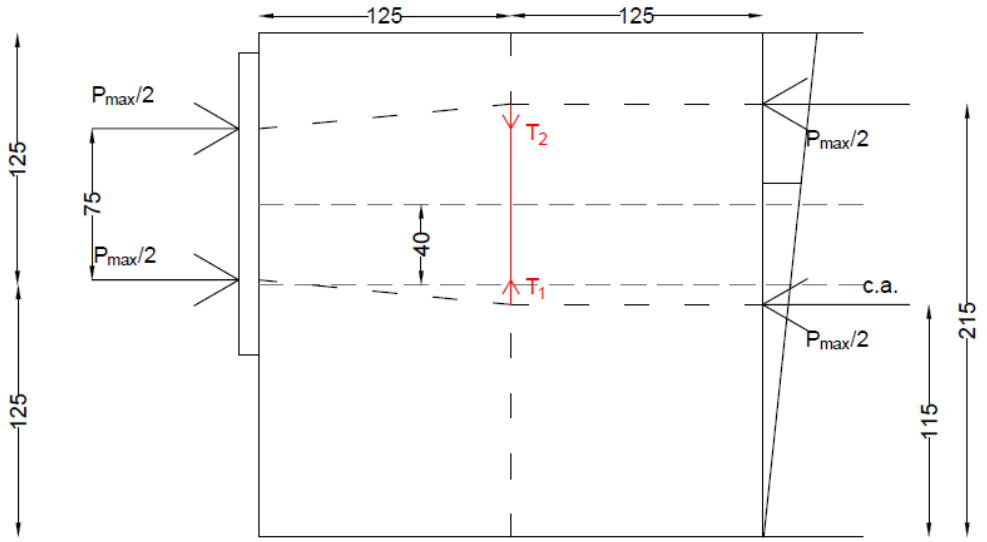

Figure D.7 Strut and tie model over height of bridge